

**MEDNARODNA PODIPLOMSKA ŠOLA JOŽEFA  
STEFANA  
JOŽEF STEFAN INTERNATIONAL POSTGRADUATE  
SCHOOL**

**TIMOTEJ TURK DERMASTIA**

**DIVERSITY, ECOLOGY AND SENSING OF THE TOXIC  
DIATOM *PSEUDO-NITZSCHIA* IN THE GULF OF  
TRIESTE**

**DOCTORAL DISERTATION**

**LJUBLJANA, OCTOBER 2021**

DIVERSITY, ECOLOGY AND SENSING OF  
THE TOXIC DIATOM *PSEUDO-NITZSCHIA*  
IN THE GULF OF TRIESTE

Timotej Turk Dermastia

**Doctoral Dissertation**  
**Jožef Stefan International Postgraduate School**  
**Ljubljana, Slovenia**

**Supervisor:** Assoc. Prof. Patricija Mozetič, National Institute of Biology, Marine Biology Station Piran, Piran, Slovenia

**Co-Supervisor:** Assist. Prof. Andreja Ramšak, National Institute of Biology, Marine Biology Station Piran, Piran, Slovenia

**Evaluation Board:**

Assoc. Prof. Patricija Mozetič, IPS and National Institute of Biology, Ljubljana  
(president),

Prof. dr. Lovrenc Lipej, IPS and National Institute of Biology, Ljubljana,

Prof. dr. Ines Mandić Mulec, Biotechnical Faculty, University of Ljubljana.

MEDNARODNA PODIPLOMSKA ŠOLA JOŽEFA STEFANA  
JOŽEF STEFAN INTERNATIONAL POSTGRADUATE SCHOOL



Timotej Turk Dermastia

DIVERSITY, ECOLOGY AND SENSING OF THE TOXIC  
DIATOM *PSEUDO-NITZSCHIA* IN THE GULF OF  
TRIESTE

**Doctoral Dissertation**

PESTROST, EKOLOGIJA IN DETEKCIJA  
TOKSIČNEGA RODU DIATOMEJ *PSEUDO-NITZSCHIA*  
V TRŽAŠKEM ZALIVU

**Doktorska disertacija**

**Supervisor:** Assoc. Prof. Patricija Mozetič

**Co-Supervisor:** Assist. Prof. Andreja Ramšak

Ljubljana, Slovenia, October 2021

*Mojim najbližjim*



# Acknowledgments

First of all, I would like to thank my supervisor Patricija Mozetič, for giving me the opportunity to conduct this research and for her continued support throughout the process. She opened the world of phytoplankton to me, for which I will be forever grateful.

Next I would like to thank my close colleagues that have physically or theoretically helped this work to come to life with their dedicated work and useful comments and remarks. These include Andreja Ramšak, David Stanković, Janja Francé, Federica Cerino, Alfred Beran, Milijan Šiško, and finally my office mate Ivano Vascotto without whom work life would be measurably more boring and less fruitful. This work would also not have been possible without the help of Petra Slavinec, a dedicated student that was on occasion my left hand, as well as Tihomir Makovec, Tristan Bartole, Matej Marinac, Leon Lojze Zamuda and Marko Tadejević, the technical and support staff at the Marine Biology Station that was collecting samples.

I would like to kindly thank the staff at Microbia Environnement in Banyuls-sur-Mer for their hospitality and cooperation. This includes Elisa Villa, Delphine Guillebault and Fanny Herard.

At last, I would like to thank my family and my partner Naja for their continued support throughout the entire education process and the years of sacrifice that culminated into this work. Without you, this would have never been possible.



# Abstract

This work focuses on a group of diatoms, belonging to the genus *Pseudo-nitzschia*, which is a globally important phytoplankton genus. Some species of the genus produce the toxin domoic acid, which is responsible for shellfish intoxication known as the amnesic shellfish poisoning (ASP). These diatoms have few morphological features that allow us to tell them apart, although more than 50 species are known. This work is the first attempt to discern the diversity of these diatoms in the Gulf of Trieste to which Slovenian waters also belong. Here, species of the genus *Pseudo-nitzschia* are common members of the local phytoplankton community, but we were mostly clueless as to which species occur here and when. This knowledge is important for the study of the ecology of the phytoplankton community but also to understand the potential threats from ASP in the area. Therefore, we first determined the species diversity of the genus using morphological methods, including electron microscopy, and genetic barcoding with three different markers (28S, ITS1 and ITS2, *rbcL*) on environmental isolates that were cultured over a four-year period. Then, we examined the toxicity potential of these cultures using both analytical methods (HPLC, LC-MS/MS) and ELISA assays. We also partnered with a French biotechnological company Microbia Environnement, with whom we developed a colorimetric sandwich-hybridization assay to study and monitor the genus in a more efficient and less costly way. Finally, we introduced the metabarcoding methodology to the study of phytoplankton to analyse the phytoplankton community including *Pseudo-nitzschia* with a state-of-the-art and high-throughput methodology that avoids the human factor in taxonomy and abundance assessment. In total, 9 species along with their seasonal occurrence patterns were identified from October 2016 to October 2020. Ecological associations with these species were also revealed through the study. Three of these species (*P. multistriata*, *P. delicatissima*, *P. galaxiae*) were found to produce domoic acid in culture, with *P. galaxiae* the first time in the Adriatic. The development of the colorimetric assay yielded a set of nucleotide probes used with the assay that work best in easily and efficiently evaluating the status of the *Pseudo-nitzschia* population in the environment. A probe specific for *P. galaxiae* was also found and the assay setup with this probe accurately predicted the population dynamic of this species. Finally, the metabarcoding approach revealed a previously unknown diversity of phytoplankton groups, including a species of *Pseudo-nitzschia* that was not identified from the culturing effort. This work is the first to reveal the diversity and ecology of *Pseudo-nitzschia* in the Gulf of Trieste and one of the most robust to date in the wider Adriatic area, since it combines several morphological and molecular methods, which is essential in a group of organisms, where the concept of species is not well defined. Our work on the colorimetric assay resulted in a new tool that is cost-efficient and can be used in monitoring as well as aquaculture operations to help farmers assess the threat level from potential ASP poisoning of their product. It is also one of the first efforts to employ metabarcoding for phytoplankton in the Adriatic, and to use *rbcL* as a metabarcoding primer for diatoms in the marine environment. The results of this work have greatly improved our understanding of the local phytoplankton community with

globally important implications and findings and will help guide further research into this topic.

# Povzetek

To delo obravnava skupino kremenastih alg (diatomej), ki sodijo v globalno pomemben rod *Pseudo-nitzschia*. Nekatere vrste iz tega rodu proizvajajo toksin domojso kislino, ki je odgovorna za tako imenovano amnezično zastrupitev s školjkami (AZŠ). Te diatomeje nimajo veliko morfoloških značilnosti, na podlagi katerih bi lahko razlikovali vrste med seboj. A kljub temu poznamo več kot 50 vrst. Pričujoče delo je prvi poskus, da ugotovimo, katere vrste so prisotne v Tržaškem zalivu, katerega del je tudi slovensko morje. Tu je *Pseudo-nitzschia* pomemben del fitoplanktonske združbe, a do zdaj vrstne sestave in pojavljanja različnih vrst nismo poznali. To znanje ni pomembno zgolj za raziskave ekologije fitoplanktonske združbe, ampak tudi za razumevanje morebitne nevarnosti zaradi AZŠ. Pomembna naloga je bila pridobitev okoljskih izolatov, ki smo jih vzgojili v kulturah. S pomočjo le-teh smo najprej razčlenili vrstno pestrost rodu s pomočjo morfoloških metod, vključno z elektronsko mikroskopijo, ter genetskega barkodiranja (28S, ITS1 in ITS2, *rbcL*). Nato smo na nekaterih kulturah ugotavljali proizvodnjo domojso kisline s pomočjo analitskih metod (HPLC, LC-MS/MS) in ELISA testov. Povezali smo se tudi s francoskim biotehnološkim podjetjem Microbia Environnement, s katerim smo razvijali kolorimetrični senzor na osnovi hibridizacije, ki omogoča spremljanje in raziskave rodu *Pseudo-nitzschia* učinkoviteje in z manjšimi stroški. Nazadnje, smo v raziskave fitoplanktonske združbe, vključno z rodom *Pseudo-nitzschia*, uvedli sodobno in visoko zmogljivo metodo metabarkodiranja, ki omogoča analize velikega števila okoljskih vzorcev naenkrat brez človeškega faktorja v ocenah številčnosti in vrstne pestrosti združbe. Od oktobra 2016 do oktobra 2020 smo potrdili prisotnost devetih vrst iz rodu *Pseudo-nitzschia* in določili njihovo sezonsko pojavljanje ter ekološke povezave. Tri od teh vrst so se izkazale za toksične v kulturi (*P. multistriata*, *P. delicatissima*, *P. galaxiae*). Za *P. galaxiae* je to prvi zapis o toksičnosti v Jadranu. Med razvojem kolorimetričnega testa smo dobili set nukleotidnih sond, ki omogočajo enostavno in učinkovito spremljanje stanja vrst iz rodu *Pseudo-nitzschia* v okolju, kadar jih uporabimo na dotičnem testu. Našli smo tudi sondo, ki specifično zaznava *P. galaxiae* in je pravilno zaznavala dinamiko populacije te vrste v vzorcih. Nazadnje pa smo z metabarkodiranjem odkrili do zdaj neznano diverzitetno fitoplanktonskih skupin, vključno z vrsto iz rodu *Pseudo-nitzschia*, ki je nismo odkrili in vzpostavili v kulturi. Pričujoče delo je prvo, ki odkriva diverzitetno in ekologijo vrst iz rodu *Pseudo-nitzschia* v Tržaškem zalivu in je tudi eno od najbolj temeljitih v celotni Jadranski regiji, saj združuje številne morfološke in molekularne metode, kar je ključno pri raziskavah organizmov, kjer je koncept vrste slabo definiran. Rezultat našega dela na kolorimetričnem testu je tudi novo orodje, ki je stroškovno učinkovito in ga lahko uporabljamo tako v monitoringu kot tudi v marikulturi za pomoč gojiteljem školjk pri oceni potencialne nevarnosti za AZŠ. Med prvimi smo tudi uporabili metodo metabarkodiranja za analizo fitoplanktonske združbe v Jadranu, in prvi, ki smo v ta namen uporabili marker *rbcL* za metabarkodiranje diatomej v morskem okolju. Rezultati so znatno okrepili naše razumevanje lokalne fitoplanktonske združbe z globalno pomembnimi odkritji in bodo vodili nadaljnje raziskave na tem področju.



# Contents

<b>List of Figures</b>	<b>xvii</b>
<b>List of Tables</b>	<b>xix</b>
<b>Abbreviations</b>	<b>xxi</b>
<b>Glossary</b>	<b>xxiii</b>
<b>Introduction</b>	<b>1</b>
1.1 The Diversity of Marine Phytoplankton .....	1
1.2 The Toxic Microalgae .....	2
1.2.1 What is a HAB and why do we care? .....	2
1.2.2 Factors influencing HAB ecological success.....	4
1.3 Global Research on <i>Pseudo-nitzschia</i> .....	5
1.3.1 Description of the genus .....	5
1.3.2 Domoic acid biochemistry and toxicology .....	9
1.3.3 DA regulation and ecophysiology .....	9
1.4 <i>Pseudo-nitzschia</i> in the Mediterranean and the Adriatic Sea .....	10
1.5 Methodological Overview .....	13
1.5.1 Sampling techniques .....	14
1.5.2 Culturing techniques .....	15
1.5.3 Morphological and imaging techniques.....	16
1.5.4 Molecular methods for identification and quantification of <i>Pseudo-nitzschia</i> - Barcoding and phylogeny.....	17
1.5.5 Hybridization methods in ecology and monitoring .....	19
1.5.6 Metabarcoding.....	22
1.5.7 Toxin analysis .....	24
1.6 Hypotheses and Aims of this Thesis .....	24
<b>2 Materials and Methods</b>	<b>27</b>
2.1 Taxonomy and Seasonal Distribution of <i>Pseudo-nitzschia</i> in the Gulf of Trieste (Chapter 3): .....	27
2.1.1 Sampling.....	27
2.1.2 Culturing.....	28
2.1.3 Phytoplankton counts – the Utermöhl method .....	28
2.1.4 Haemocytometric phytoplankton counts .....	29
2.1.5 Sample preparation for TEM .....	29
2.1.6 Extraction of DNA from cell cultures.....	29
2.1.7 Amplification and sequencing of phylogenetic markers .....	30
2.1.8 Phylogenetic analysis.....	30
2.2 Toxicity Analysis of Selected Strains (Chapter 5) .....	30
2.2.1 Culturing and sampling.....	30

2.2.2	Domoic acid in cultures .....	31
2.2.3	Direct competitive ELISA.....	31
2.2.4	LC-MS and HPLC-UV.....	31
2.2.5	Amplification and sequence analysis of the <i>dabA</i> gene .....	32
2.3	Colorimetric Assays for <i>Pseudo-nitzschia</i> Detection and Quantification (Chapter 4).....	33
2.3.1	Colorimetric assay principle.....	33
2.3.2	Sampling campaign for the colorimetric assay.....	33
2.3.3	Strain selection .....	33
2.3.4	Probe selection and specificity tests.....	34
	Microarray testing .....	34
	First tests on SHA .....	35
	Dilution series with selected probes .....	35
2.3.5	Field samples .....	35
2.4	Metabarcoding of the Phytoplankton Community (Chapter 6) .....	36
2.4.1	Sampling campaign for the metabarcoding analysis .....	36
2.4.2	Extraction of DNA for metabarcoding analysis .....	36
2.4.3	Amplification and preparation of Illumina MiSeq library.....	37
2.4.4	Bioinformatics analysis pipeline for metabarcode resolution.....	37
<b>3</b>	<b>Identification and Ecology of <i>Pseudo-nitzschia</i> in the Gulf of Trieste</b>	<b>39</b>
3.1	Author's Contributions.....	39
<b>4</b>	<b>Toxic Species of <i>Pseudo-nitzschia</i> in the Gulf of Trieste</b>	<b>61</b>
4.1	Summary.....	61
4.2	Results.....	61
4.2.1	Toxicity of individual strains.....	61
4.2.2	Changes in DA concentration in selected cultures.....	62
4.2.3	Phylogeny versus toxicity .....	67
4.2.4	<i>dabA</i> gene screening in toxic and non-toxic strains .....	69
<b>5</b>	<b>Colorimetric Detection of <i>Pseudo-nitzschia</i> in the Environment and in Culture</b>	<b>71</b>
5.1	Summary.....	71
5.2	Results.....	72
5.2.1	Microarray training and preliminary probe screens .....	72
5.2.2	Sandwich-hybridization bioassay .....	72
5.2.3	Dilution-series analysis.....	73
5.2.4	Field sample testing.....	77
<b>6</b>	<b>Phytoplankton Assemblages in the Gulf of Trieste Inferred from Metabarcoding – Case Study of <i>Pseudo-nitzschia</i></b>	<b>81</b>
6.1	Summary.....	81
6.2	Results.....	82
6.2.1	Overview.....	82
6.2.2	18S-V9 Metabarcodes.....	82
	Comparison of non metazoan taxa.....	83
	Dinoflagellates.....	84
	Diatoms (Bacillariophyceae) .....	86
6.2.3	<i>rbcL</i> Results.....	87
	Diatom genera.....	88

Genus <i>Pseudo-nitzschia</i> .....	89
<i>rbcL</i> resequencing .....	91
6.2.4 Comparing Metabarcoding with Traditional Microscopy Monitoring .....	95
Higher level taxonomy .....	95
$\alpha$ -Diversity .....	97
$\beta$ -Diversity .....	99
<b>7 Discussion</b> .....	<b>101</b>
7.1 Research Overview and Highlights .....	101
7.2 <i>Pseudo-nitzschia</i> Species Composition in the GoT .....	102
7.2.1 Ecological preference and seasonal occurrence of different species .....	103
7.2.2 Phylogenies and the relationship of Adriatic strains with other Mediterranean isolates .....	106
7.3 Toxicity of <i>Pseudo-nitzschia</i> in the Gulf of Trieste .....	109
7.3.1 Toxicity and phylogenetic relationships between toxic and non-toxic strains .....	109
7.3.2 <i>dabA</i> gene in selected strains .....	110
7.4 Colorimetric Tools for Monitoring of <i>Pseudo-nitzschia</i> and Management of Aquaculture Sites .....	111
7.5 Monitoring HABs and Phytoplankton Populations – Lessons from Metabarcoding .....	114
7.6 Integrating Molecular and Morphological Data in Ecological Studies at LTER Sites .....	117
<b>8 Conclusions</b> .....	<b>119</b>
<b>Appendix A Permission to Republish</b> .....	<b>121</b>
<b>Appendix B Microarray Probe Signals</b> .....	<b>123</b>
<b>Appendix C Metabarcoding Sample Lists</b> .....	<b>129</b>
C.1 18S Metabarcoding .....	129
C.2 <i>rbcL</i> Metabarcoding .....	130
C.3 <i>rbcL</i> Resequencing .....	131
<b>References</b> .....	<b>133</b>
<b>Bibliography</b> .....	<b>157</b>
<b>Biography</b> .....	<b>159</b>



# List of Figures

Figure 1.3-1 Morphological characters in two <i>Pseudo-nitzschia</i> species.....	7
Figure 1.3-2 <i>Pseudo-nitzschia</i> phylogeny based on ITS2 and morphology as presented in Lim et al. (2018).	8
Figure 1.3-3 Domoic acid 2D structure. Source: PubChem. ....	9
Figure 1.5-1 Sampling devices used in phytoplankton collection: .....	14
Figure 1.5-2 Home-made isolation device with a drawn Pasteur-pipette attached to a suction based system.	15
Figure 1.5-3 The common process flow of genetic data manipulation and analysis.....	18
Figure 1.5-4 Schematic representation of a sandwich-hybridization assay with colorimetric detection.	21
Figure 2.1-1 Sampling stations in the Slovenian part of the Gulf of Trieste. ....	28
Figure 2.1-2 Schematic depiction of a Fuchs-Rosenthal counting chamber (from Neuendorf, 2020).	29
Figure 4.2-1 Change in the content of (A) particulate DA (pDA) (B) dissolved DA (dDA) in <i>P. multistriata</i> strain 119-A4.....	66
Figure 4.2-2 Maximum likelihood trees for three species. ....	68
Figure 4.2-3 Homology modelling of obtained <i>P. multistriata</i> <i>dabA</i> gene sequence.....	70
Figure 5.2-1 Probe specificity and sensitivity results using HYB-A and 50 ng of RNA from each species.	73
Figure 5.2-2 Calibration curves from dilution series for each species-probe pair tested....	75
Figure 5.2-3 Comparison of signal and microscopic counts at station 0DB2 from three probes tested on 2015 environmental samples. ....	78
Figure 5.2-4 Relationship between cell counts of total <i>Pseudo-nitzschia</i> and signals from different probes on environmental samples from 2017 and 2018, different stations.....	79
Figure 5.2-5 Relationship between cell counts of <i>P. cf. galaxiae</i> and signals from different probes on environmental samples from 2017 and 2018, different stations. ....	79
Figure 5.2-6 Comparison of Pn1mod signal and microscopic counts at station 0024.....	80
Figure 6.2-1 Rarefaction curve for 18S-V9 samples cleared of metazoan sequences. Labels represent individual samples. See Appendix B for sample metadata. ....	83
Figure 6.2-2 Relative abundance of non-metazoan higher taxa at two sampling depths at station 00BF (GoT) from March 2019 to February 2020, determined from 18S-V9 metabarcodes.	84
Figure 6.2-3 Relative abundance of dinoflagellate genera (Dinophyceae) at two sampling depths at station 00BF (GoT) from March 2019 to February 2020, determined from 18S-V9 metabarcodes.	86
Figure 6.2-4 Relative abundance of diatom genera (Bacillariophyceae) at two sampling depths at station 00BF (GoT) from March 2019 to February 2020, determined from 18S-V9 metabarcodes.	87
Figure 6.3-1 Relative abundance of diatom genera (Bacillariophyceae) at two different depths at station 00BF (GoT), from April 2019 to February 2020 and an additional October 2020 phytoplankton net sample, determined from <i>rbcL</i> metabarcodes.....	88

Figure 6.3-2 Number of reads for each identified <i>Pseudo-nitzschia</i> species at different bootstrap levels.	90
Figure 6.3-3 Number of reads for each individual species assigned at 50% bootstrap level.	91
Figure 6.3-4 Correspondence analysis (CA) of the different rbcL sequencing projects.....	93
Figure 6.3-5 Genus-wide comparison of assignments of concatenation and resequencing in terms of relative abundance of sequence reads.....	94
Figure 6.3-6 Assignments of <i>Pseudo-nitzschia</i> sequences at the species level with both methods.	95
Figure 6.4-1 Comparison relative abundances of phytoplankton phyla obtained from 18S metabarcoding and phytoplankton counts from March 2019 to February 2020.....	97
Figure 6.4-2 $\alpha$ -diversity indices derived from the taxonomic composition of phytoplankton of different assessment methods.....	98
Figure 6.4-3 Bray-Curtis NMDS ordination of diatom genera in molecular samples.....	99
Figure 6.4-4 Bray-Curtis NMDS ordination of all samples.....	100

## List of Tables

Table 1.4-1 List of species identified in the Adriatic Sea.....	12
Table 2.2-1 Newly designed primers for <i>dabA</i> amplification and sequencing.....	32
Table 2.3-1 Strains and associated GenBank Accession Numbers used in the development of the <i>Pseudo-nitzschia</i> specific SHA. ....	34
Table 4.2-1 Toxicity tests performed on each strain and associated results. ....	63
Table 5.2-2 Limit of detection as ng RNA and cell numbers for each species-probe pair tested.       76	
Table 5.2-3 RNA quota per cell from each extraction performed. ....	77
Table 6.3-1 Bootstrap statistics for each taxon. ....	90
Table 6.3-2 Unique taxa found in the concatenated and resequenced datasets. ....	92
Table 5.2-1 Results of microarray for selected species and probes.....	123



# Abbreviations

AA	... Apical axis
ASP	... Amnesic Shellfish Poisoning
ASV	... Amplicon sequence variant
CTAB	... Cetrimonium bromide
COI	... Cytochrome-c-oxidase subunit 1
DA	... Domoic acid
DSP	... Diarrhetic shellfish poisoning
ELISA	... Enzyme-linked immunosorbent assay
EM	... Electron microscopy
ESP	... Environmental sample processor
HAB	... Harmful algal bloom
HPLC	... High-performance liquid chromatography
ITS	... Internal transcribed spacer
LC/MS	... Liquid chromatography – mass spectrometry
LC/MS-MS	... Liquid chromatography – tandem mass spectrometry
LM	... Light (optical) microscopy
LSU	... Large subunit of the ribosomal RNA
LTER	... Long-term ecological research
NSP	... Neurotoxic shellfish poisoning
OTU	... Operational taxonomic unit
PCR	... Polymerase chain reaction
PSP	... Paralytic shellfish poisoning
SEM	... Scanning electron microscopy
SHA	... Sandwich hybridization assay
SSU	... Small subunit of the ribosomal RNA
TAA	... Trans-apical axis
TEM	... Transmission electron microscopy



# Glossary

16S/18S – Genes coding for the small subunit of the ribosomal RNA in prokaryotes/eukaryotes, respectively.

23S/28S – Gene coding for the large subunit of the ribosomal RNA in prokaryotes/eukaryotes, respectively.

ASV – Amplicon sequence variant. Defines unique sequences obtained through metabarcoding, and filtered through error modelling, to bioinformatically remove variants that were generated through sequencing error. Each sequence should thus represent one genotype.

Biological carbon pump – The biologically mediated transport of carbon from the upper layers of the ocean into the deep and into the sediment.

Contig – Contiguous sequence obtained by merging two overlapping sequence reads.

Demultiplexing – Sequences that are produced by next generation sequencing technologies are indexed by specific nucleotide strings to identify which sequence belongs to which samples. Demultiplexing is a bioinformatic process, where reads with common indices are binned together to represent samples.

Denoising – The bioinformatic process where reads resulting from sequencing errors and artificial contigs (chimeras) are removed, according to an error modelling algorithm.

Environmental Sample Processor – An *in situ* robotic device that can autonomously process water and perform different analysis, based on the setup.

GenBank – Largest public annotated sequence database, curated and maintained by the National Center for Biotechnology information.

Genetic barcoding – Obtaining specific genetic sequences of organisms, based on which species identity can be determined.

Harmful algal bloom (HAB) – A proliferation of certain microalgal taxa which can cause environmental or human health distress.

Metabarcoding – The process of sequencing large pools of amplified DNA (or RNA) from many different targets at once. The amplification products are typically phylogenetic markers or functional genes.

OTU – Operational taxonomic unit. Defines a cluster of sequences usually obtained through metabarcoding, clustered based on a selected cut-off value of similarity (typically 97% or 99%). OTU clusters may include erroneous sequences. Each OTU is represented by one consensus sequence that is based on all sequences in the cluster.

PCR – Polymerase chain reaction. The serial replication of DNA under cycling thermal conditions in the presence of DNA polymerase. The site of replication is determined by nucleotide primers that anneal to opposing ends of the selected product.

Metabarcoding read – A nucleotide sequence produced by next generation sequencing technology.

Ribosomal RNA(rRNA) – Apart from proteins it is the main structural element of ribosomes and is coded in ribosomal DNA (rDNA) in the nucleus. Two main genes code for it – the 16S/18S gene and the 23S/28S gene in prokaryotes/eukaryotes coding for the small ribosomal subunit and the large ribosomal subunit, respectively.

RuBisCo – Ribulose-1,5-bisphosphate carboxylase-oxygenase is an essential enzyme in the photosynthesis chain, responsible for the first step of carbon fixation in the Calvin cycle, catalysing the reaction between Ribulose-1,5-bisphosphate and carbon dioxide, but also oxygen in the case of a reverse reaction.

Sanger sequencing – One of the first available sequencing technologies, where in addition to normal nucleotides (dNTPs), chain-terminating fluorescent or radioactive-labelled dideoxynucleotides (ddNTP) are added to the complementary DNA strand to be sequenced. Each ddNTP is added to a separate reaction, resulting in four different reactions. The different size fragments produced by several chain extension steps in this way are then separated by gel electrophoresis and the fragments inspected by fluorescence or autoradiography to determine the sequence.

Silicate frustule – The casing of diatom cells made from silicon oxide.

# Chapter 1

## Introduction

### 1.1 The Diversity of Marine Phytoplankton

Phytoplankton are a group of organisms that live in both fresh and marine waters. Their role in global biochemical cycles is crucial to the existence of all living beings that inhabit this planet, including us – *Homo sapiens*. Initial estimates suggest that they are responsible for about half of all carbon sequestration and oxygen production in the present climate (Falkowski et al., 1998; Field et al., 1998). Different phytoplankton play different ecological roles in the ecosystem and also use different strategies of energy accumulation, from obligate autotrophy to obligate heterotrophy, with mixotrophy in the middle as the primal state (Mitra et al., 2014, 2016). In general, phytoplankton organisms are also referred to as planktonic microalgae because they represent unicellular organisms that are related to macroalgal groups and even plants through their plastids acquired by primary or secondary endosymbiosis (Falkowski et al., 2004). Although some phyla and classes may contain both microalgae and macroalgae (e.g., green algae, red algae, heterokonts), microalgae are exclusively unicellular organisms with unique ecological and physiological characteristics. The only oxygenic photoautotrophs of the prokaryotic domain Bacteria, i.e., cyanobacteria, are often referred to as microalgae. There are about 4500 morphologically and genetically described microalgal species populating the oceans (Sournia, Chrétiennot-Dinet, Richards, 1991), but the actual number is probably much higher (Guiry, 2012). Indeed, phytoplankton comprise an exceptionally diverse group of species that are represented in two out of three domains of life (bacteria and eukaryotes) while eukaryotic phytoplankton are distributed among several Eukaryote supergroups Archaeplastida, SAR (Stramenopiles, Alveolata, Rhizaria), Excavata, Haptista and Cryptista (Burki et al., 2020). This enormous diversity is reflected in remarkable morphological, genetic, biochemical, and physiological differences which in turn determine their ecology and role in ocean biogeochemistry. The seemingly large number of species competing for the same resources in a homogeneous and coherent environment such as the oceans has often been described as the paradox of the plankton (Hutchinson, 1961). However, the true number of species is very difficult to estimate and detect because they are microscopic organisms inhabiting least explored biome in the world. To perform morphological and genetic analyses on the organisms, cultivation is often necessary, which is a very non-trivial process. New groups and species are constantly being uncovered through the elucidation of phylogenetic relationships between different groups, while high-throughput genetic and advanced imaging techniques that help decipher differences between species and reveal diversity on a large scale have only recently

become available. Results from the global *Tara Oceans* metabarcoding campaign have shown that diversity in the world's oceans is largely underestimated (De Vargas et al., 2015, Malviya et al., 2016). Less than 1% of the 18S rDNA sequences from 150,000 operational taxonomic units (OTUs) were found to be strictly identical to their references, while the revealed diversity of a few studied and inconspicuous groups such as Dictyochophyceae and Chlorarachnea yielded 60 times more OTUs than there are described species (De Vargas et al., 2015). Global metabarcode analyses of diatoms, generally recognized as a well-studied group with about 2000 described morphological species (Sournia et al., 1991), revealed twice the number of OTUs – 4748 (Malviya et al., 2016).

The reason for giving these plain values is that, although it is commonly said that the expected diversity of a group of organisms is much higher than the known diversity, we now have methodological and practical tools to assess this missing diversity. However, high-throughput sequencing approaches have an important caveat – they rely on reference data, usually obtained through the traditional process of sampling, culturing and characterization. And although the large datasets may reveal data deficiencies due to unassigned or poorly assigned sequences, we still do not know which taxa these sequences belong to until they are catalogued using traditional methods that rely on morphological features. This is essentially the basic idea of this work. The aim is to bridge the gap between traditional observational techniques and modern methods of recording and understanding phytoplankton diversity, using the potentially toxic marine diatom genus *Pseudo-nitzschia* as an example.

## 1.2 The Toxic Microalgae

### 1.2.1 What is a HAB and why do we care?

While all phytoplankton species are considered primary producers in a global ecological sense, ecological roles can vary widely among different groups and species. One diverse group that attracts particular attention from scientists, as well as the public, is the mostly planktonic toxin-producing microalgae. Many of these algae are dinoflagellates. There are some representatives of flagellates from the Prymnesiophyceae, Raphidophyceae and Dictyochophyceae and some diatoms (Bacillariophyceae). Toxic microalgae have received increased attention since some are harmful to the environment, human health, and especially to the aquaculture and the fishing industries, particularly but not exclusively when they proliferate and form blooms. There is a wide range of toxins produced by these algae. Those that affect humans can be divided mainly into four groups derived from shellfish poisoning and one group derived from fish poisoning, although new groups of toxins are also being discovered whose consequences are not yet well defined (e.g., yessotoxins). The toxins of Paralytic Shellfish Poisoning (PSP), including the most potent saxitoxin, are produced by several dinoflagellates of the genus *Alexandrium*, *Pyrodinium bahamense*, *Gymnodinium catenatum* and even some cyanobacteria, and cause severe neurological damage that can be fatal in severe cases. Neurotoxic Shellfish Poisoning (NSP) is caused by brevetoxin produced by dinoflagellates of the genus *Karenia* and has neurotoxic effects, but fatal cases have not been reported. Diarrhetic Shellfish Poisoning (DSP) is caused by dinoflagellates of the genera *Dinophysis*, *Phalocroma* and *Prorocentrum*, which produce okadaic acid and the dinophysis toxins DTX-1 and DTX-2. These toxins are protein phosphatase inhibitors and cause severe gastrointestinal pain and

diarrhoea. The only shellfish-borne syndrome not caused by dinoflagellates is the Amnesic Shellfish Poisoning (ASP), which is caused by diatoms of the genus *Pseudo-nitzschia* and few other species from closely related genera (Bates et al., 2018). These diatoms produce domoic acid, a simple but potent neurotoxin that can cause neurotoxicological symptoms and is lethal in severe cases. The last group of toxins that are dangerous to humans are the ciguatoxins, which come from ciguatera fish poisoning (CFP). This syndrome is caused by *Gambierdiscus toxicus*, a benthic dinoflagellate, and the mode acquisition of these toxins is through the consumption of contaminated top predator fish that have acquired the toxins through the food chain. The symptoms of CFP are varied and systemic. Death from CFP is rare, although it can lead to long-term disability. New groups of toxins that affect humans include the azaspiracids (Satake et al., 1998), which are primarily produced by the dinoflagellate *Azadinium spinosum* and cause similar symptoms to DSP. Another group of toxins that have been shown to be toxic *in vitro* are cyclic imines produced by many dinoflagellates including the oceanic *Karenia selliformis*, *Alexandrium ostenfeldii*, *Vulcanodinium rugosum*, the benthic genus *Prorocentrum* and the symbiotic genus *Symbiodinium* (Stivala et al., 2015). However, there is no known toxicosis in humans from these toxins, although the term *Spiroimine Shellfish Poisoning* has already been recorded in the literature (Guéret & Brimble, 2010). Finally, benthic dinoflagellates from the genus *Ostreopsis* are producers, or at least vectors, of the most potent marine biotoxin – palytoxin. This toxin can be aerosolized and can cause severe lung trauma, including pulmonary oedema (Ciminiello et al., 2014). However, the mode of synthesis and trophic transfer for this toxin is not well known, as the toxin is also found in tropical coral of the genus *Palythoa*, although they do not produce it themselves. Some studies even suggest that it may be produced by bacterial genera *Pseudomonas*, *Brevibacterium*, *Actinobacter* and *Vibrio* (Franchini et al., 2010).

Reports of harmful algal blooms (HABs) – defined as a higher than normal abundance of a species, above background levels, that has some harmful effect (Steidinger & Garccés, 2006) and better known as red tides in the marine environment, have increased in frequency and intensity worldwide in recent decades (Anderson, 2014; Fu et al., 2012; Glibert & Burford, 2017). The reasons for this increase are complex and varied, resulting from increases in nutrient concentrations and, in particular, shifts in stoichiometric nutrient ratios in coastal areas (Glibert & Burford, 2017), the introduction of non-indigenous species, changing climatic conditions (Glibert, 2020; Griffith & Gobler, 2020; McCabe et al., 2016) and, what seems to be of high importance, the increased monitoring activities and vigilance, particularly due to the proliferation of marine aquaculture (Hallegraeff et al., 2021). HABs have thus transformed from an occasional nuisance to a persistent threat in some regions of the world, although they invoke closure of beaches, aquaculture facilities and seafood harvesting activities worldwide. It is difficult to quantify the impact of HABs on the economy, although they are measured in hundreds of millions of dollars globally (Hoagland & Scatista, 2006). The unprecedented bloom of *Pseudo-nitzschia* on the western North America coast in 2015 alone resulted in a loss of over \$100 million (Moore et al., 2020; NMFS, 2016). Similarly, *Karenia brevis* causes recurrent blooms in the Gulf of Mexico with major impacts to tourism, fisheries, and recreation measured in millions of dollars, particularly in Florida (Hoagland et al., 2020). Such large-scale HABs have all the hallmarks of natural disasters that affect entire societies (Ritzman et al., 2018). HABs cause considerable distress in populations of marine wildlife. Several mass mortalities of whales, dolphins, sea otters, seabirds, and turtles have been linked to poisoning by microalgal toxins such as domoic acid, brevetoxins and saxitoxins (DeGange & Vacca, 1989; Fire & Dolah, 2012; Flewelling et al., 2005; Geraci, 1989; Hernández et al., 1998; Jessup et al., 2009; Moriarty et al., 2021), while dinoflagellate species such as *Karlodinium*

*veneficum*, *Pfiesteria piscicida*, *Fibrocapsa japonica*, *Heterosigma akashiwo*, *Prymnesium parvum* and also *Karenia brevis* are notorious fish killers. Although large-scale HABs are still quite rare, localized HABs are equally relevant in terms of their impact on the economy, human health, and the environment. The latter is often neglected, because human society tends to view all natural processes through an economic lens and neglects processes that do not directly affect our wallets. Therefore, monitoring programs are essential to ensure a good environmental status but also to minimize the risk of human intoxication. Despite monitoring, this still occurs, especially in less developed regions of the world where there may be no monitoring activities, or there is a lack of risk communication and dissemination to the public. However, the developed world is not immune to the threat, as HABs can develop quickly, they can be localized and go unnoticed. Most importantly, management measures largely address human-produced seafood, while wild-caught and wild-harvested items may be excluded from monitoring programs, depending on local legislation. For example, wild collection of razor clams in the USA West Coast requires a license and is regulated according to ongoing analysis of shellfish toxin concentrations (McCabe et al., 2016; WDFW, 2021). In the Mediterranean, on the other hand, harvesting of seafood is regulated only in some countries and even then, it is usually done through annual licensing and little or no attention is paid to monitoring toxins in wild shellfish or fish and subsequently distributing results to the public (Agius Darmanin & Vella, 2019; Gaudin & De Young, 2007). As a result, consumers willingly take the risk of potentially contaminated seafood when they harvest or they must resort to experts or non-user friendly websites in some cases. We can argue that fewer and fewer people in the developed world participate in these activities, but even then, we must recognize that there is a risk.

### 1.2.2 Factors influencing HAB ecological success

Whether or not the intensification of HABs is anthropogenic, HABs are naturally occurring phenomena in any case. Some of the HAB forming species are important members of phytoplankton communities and their blooms drive microbial food webs through the production of dissolved organic carbon contributing to the biological carbon pump. HAB species may be particularly successful because of their multiple strategies for nutrient accumulation, production of allelopathic substances, or mechanical protection from grazing and grazer avoidance strategies. There is no evidence that harmful algae have higher growth rates compared to their non-harmful counterparts (Glibert et al., 2018). In fact, many of them are slow-growing dinoflagellates that can slowly displace other phytoplankton as the bloom progresses. One strategy to achieve this, for example, is to exploit their ability to use flagella to move around and to form dense and thin layers that can alter the surrounding water chemistry and light penetration, deterring grazers (Glibert et al., 2018). Such layers have been described for many *Dinophysis* species, for example (e.g. Alves-de-Souza et al., 2014; Farrell et al., 2012; Pitcher et al., 2011).

Many HAB dinoflagellates are mixotrophs, *sensu* Mitra et al. (2014), who do not consider osmotrophy – the uptake of dissolved organic substrates, vitamins, and others – to be a distinguishing feature for mixotrophy in protists because it appears to be a ubiquitous strategy among them. For example, diatoms which are exclusively autotrophic still require dissolved vitamins for growth (Croft et al., 2006). Mixotrophy seems to be an advantageous life strategy in environments with unstable nutrient supply or in regions where stoichiometric ratios of nutrient are drastically shifted towards single elements such as nitrogen, as well as in environments where nutrient concentrations or even light saturation are generally low. It is the stoichiometric shifts that are occurring in many areas

around the world and are considered to be the largest contributor to the spread of HABs (Glibert & Burford, 2017). Shifts towards higher nitrogen concentrations relative to other major nutrients such as phosphorus or silicate are occurring in many areas of the world, such as East China Sea and the Mediterranean where large river systems provide nitrogen-enriched effluents that favour the development of HABs. This is largely due to increased urea runoff (Glibert & Burkholder, 2011, 2006). Urea is a form of organic nitrogen that can be utilized by mixotrophs through their efficient urease enzymes, giving them a competitive advantage over species that have little or no urease activity. Given climatic changes, mixotrophs are expected to thrive in a warmer ocean, where nutrient ratios are shifted disproportionately to higher nitrogen concentrations (Glibert, 2020). Fertilization of coastal seas is expected to spread to other regions of the world, especially those that are developing and where fertilizer use is intensifying, in effect increasing the threat of HABs. However, we must always consider these changes in terms of ecosystem functioning and there may be yet unexplored feedbacks and loops that can cause unexpected trophic shifts.

Another possible adaptation that may contribute to the success of HAB species is perhaps the most obvious – toxin production. The adaptive advantage of toxin production is very diverse and, in many cases, not well understood. Rarely does the toxin associated with harmful activity exhibit allelopathic properties to other phytoplankton species, at least not at concentrations found in nature (Granéli & Hansen, 2006). This is true for all species causing human-associated syndromes (DSP, PSP, ASP, NSP), although many of these species exhibit allelopathic properties due to other as yet unidentified compounds – e.g. *Alexandrium* spp., *Pseudo-nitzschia pungens* (Legrand et al., 2003; Tillmann & John, 2002). In contrast, toxins from ichthyotoxic species, such as prymnesins from *Prymnesium parvum*, exhibit allelopathic properties and may give this species a competitive advantage. In any case, toxins produced by microalgae may play other ecological roles. For the toxic diatoms from the genus *Pseudo-nitzschia*, one explanation is that the toxin is a very good chelator of iron and copper, allowing efficient uptake of iron and detoxification of copper during limitation or stress (Maldonado et al., 2002), respectively (more on this in 1.3.3). Iron limitation occurs in 40% of the world’s oceans (Moore et al., 2002) and *Pseudo-nitzschia* and other closely related genera such as *Fragilariopsis* appear to have evolved diverse physiological adaptations to this condition. For example, oceanic members of *Pseudo-nitzschia* and *Fragilariopsis* can store iron, through the protein ferritin, giving them an additional advantage (Marchetti et al., 2009).

Finally, toxins can be used as grazer deterrents. It has been shown that the production of domoic acid (DA) as well as PSP toxins is induced by copepodamides, molecules used for signal transduction between copepods – grazers of phytoplankton (Haroardóttir et al., 2019; Lundholm et al., 2018; Selander et al., 2015). In addition, evidence for grazer deterrence of DA has been found in *Pseudo-nitzschia* and its copepod grazers (Zhang et al., 2021). Although production of these toxins occurs in culture even in the absence of grazer cues, copepodamides tend to dramatically upregulate genes of the domoic acid biosynthetic apparatus and the concentration of toxins.

## 1.3 Global Research on *Pseudo-nitzschia*

### 1.3.1 Description of the genus

*Pseudo-nitzschia* is the focus of this work. As mentioned earlier, several species of this genus produce domoic acid (DA), a potent neurotoxin that at high concentrations causes

severe neurological damage including amnesia and death, hence the name of the syndrome when ingested by contaminated shellfish or other marine invertebrates – Amnesic Shellfish Poisoning (Wright et al., 1989). In the late 1980s, the scientific community was confronted with a novel and potentially lethal toxin produced by these diatoms (Bates et al., 1989). Since the first cases of ASP were revealed, *Pseudo-nitzschia* has received considerable scientific attention worldwide and many new species have been described (Bates et al., 2018). Currently, there are about 60 described species, of which about half have been found to produce DA. This genus is known from all the world's oceans and is a common and often dominant member of phytoplankton communities, particularly in temperate spring and autumn (Trainer et al., 2012). There are both neritic and oceanic members of the genus, all of which are planktonic. They are pennate diatoms with elongated and fusiform valves, typically forming stepped chains. The length or apical axis (AA) varies greatly between species and even between strains: from small 10  $\mu\text{m}$  long valves of *P. galaxiae* and *P. linea* strains to 150  $\mu\text{m}$  long ones of *P. seriata*. The valve width or transapical axis (TAA) is the key feature for light microscopy (LM) identification. Based on this morphological feature, two species groups *sensu* Hasle (1965) have been traditionally distinguished, although this subdivision is not entirely supported (Accoroni et al., 2020). Species in which the TAA is shorter than 3  $\mu\text{m}$  are assigned to the *P. delicatissima* group, while species in which the TAA is larger than 3  $\mu\text{m}$  are assigned to the *P. seriata* group. The TAA of the latter can reach 8  $\mu\text{m}$  in *P. australis* and *P. seriata*, for example. However, the TAA is an arbitrary feature of the species and does not necessarily reflect phylogenetic relationships (Lim et al., 2018). As such, it can also be misleading when drawing ecological inferences from the analysis of environmental samples. Thus the *P. delicatissima* group is further divided into the *P. delicatissima* species complex and the *P. pseudodelicatissima* species complex, which are more phylogenetically representative. LM identification is possible for some species such as *P. multistriata*, otherwise it is very difficult and requires a trained taxonomist's eye and a great understanding of the area from which the cells are obtained. The difficulty of LM identification is also why new species continue to be described and why phylogenetic analyses reveal cryptic species within apparently identical strains. Therefore, methods other than LM must be used to achieve accurate taxonomic and ecological classification.

*Pseudo-nitzschia* species can be identified either by electron microscopy (EM) or by genotyping phylogenetic markers such as the large ribosomal subunit (28S), internal transcribed spacer regions (ITS), the chloroplast-encoded large subunit RuBiSCo gene (*rbcL*) and the mitochondrion-encoded cytochrome-c oxidase gene (COI). Identification with EM, either transmission EM (TEM) or by scanning EM (SEM), is done by comparing the morphometric signature of the silicate frustule, which is presumably unique to each species. The frustule, as in all diatoms, consists of the epitheca and hypotheca, each perforated with poroids that form different patterns, unique to species (Round et al., 1990). The presence of poroids identified the striae: each stria contains one or more rows of poroids, and the unperforated siliceous strip between two striae is called interstria. The most common features measured in EM analysis of *Pseudo-nitzschia* frustules are the valve shape, the overlapping of cells in stepped colonies, the density of fibulae (i.e. number of fibulae in 10  $\mu\text{m}$ ), the density of striae, the presence or absence of the central nodule (an enlarged space between the fibulae, the number and compartmentalization of poroids, and the structure of the valvocopula (see Figure 1.3-1 for visual description of individual characters). In *Pseudo-nitzschia* it has been shown that even with EM analysis species can be misidentified because morphometric characters can be very similar or even identical between different species and strains. Therefore, molecular methods are becoming increasingly important for correct identification.

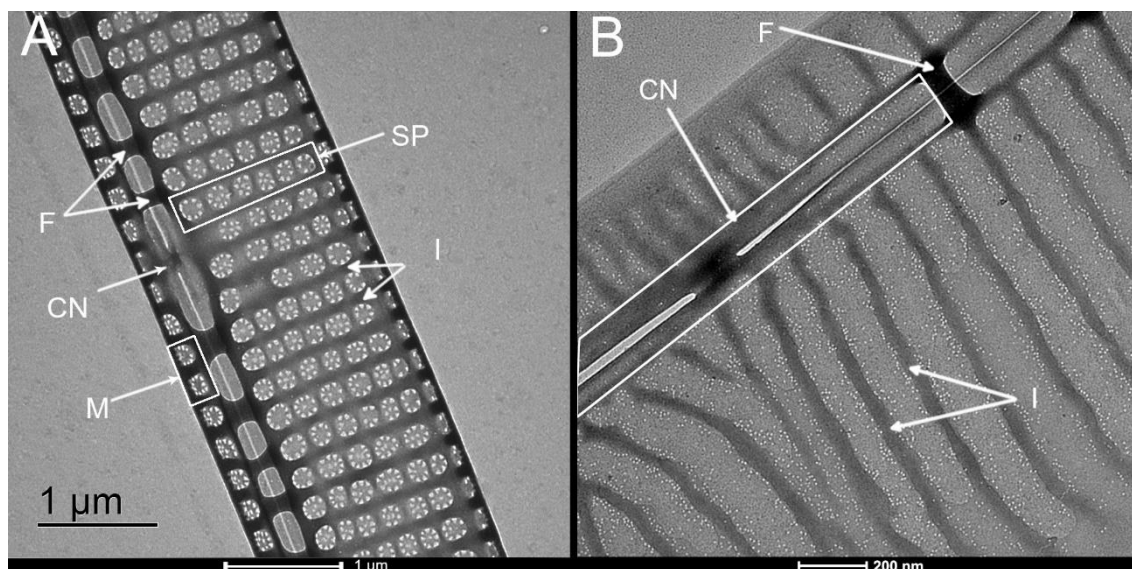


Figure 1.3-1: Morphological characters in two *Pseudo-nitzschia* species. A) *P. calliantha* B) *P. galaxiae*. M – valve manter with associated structure of poroids. CN – central nodule or central interspace. F – fibulae. SP – uniseriate stria with six poroids, with internal compartmentalization into poroid sectors. Notice that in *P. galaxiae* the poroids are not structured and are randomly spaced within the interstitial space. I – interstriae, separating striae.

There is no clear consensus in the scientific community on how many molecular markers should be used for correct identification. The general rule is at least one nuclear-encoded such as 28S or ITS, and one plastid-encoded. The current molecular phylogeny of *Pseudo-nitzschia* identifies six species groups (species complexes) with varying degrees of statistical support depending on the marker (Lim et al., 2018, Figure 1.3-2). This phylogeny does not necessarily reflect the classical systematics based on LM. For example, *P. fraudulenta* and *P. subfraudulenta* have TAA widths greater than 3 µm and are placed in the *P. seriata* complex by LM, but their ultrastructure revealed by EM as well as their genetic markup places them closer to the *P. delicatissima* and *P. pseudodelicatissima* complexes, *sensu* Lim et al. (2018). Correct species identification is important when making ecological inferences. This is because different species can have very different ecological preferences, which are reflected in their seasonal abundance and distribution (Thorel et al., 2017). By placing them in complexes that are phylogenetically and ecologically unjustified, we introduce error and bias into ecological analysis (thoroughly discussed in Chapter 3). Thus, there are multiple levels of species identification from simple LM, to EM, to molecular classification with one or more markers. These data can then be coupled with phenological observations, such as seasonal distribution, short-term abundance changes, advection, transport and phylogeography, as well as ecological parameters ranging from biotic (e.g., phytoplankton community composition) to abiotic (e.g., temperature, salinity and nutrient concentration). The combination of all these data allows us to effectively model species succession and bloom development.



### 1.3.2 Domoic acid biochemistry and toxicology

One of the main features of *Pseudo-nitzschia* diatoms is the production of domoic acid (DA) by some species of the genus. DA (Figure 1.3-3) is a kainic acid and glutamate analogue that binds to membrane-bound kainite receptors and  $\alpha$ -amino-3-hydroxy-5-methyl-4-isoxazolepropionic acid (AMPA) receptors found in certain neuronal cells of the brain (Clayden et al., 2005; Walter et al., 1994). It strongly interferes with glutamate receptors, leading to an uncontrolled build-up of calcium, causing neurons to degenerate (Pulido, 2008). This can lead to swelling, apoptosis, and necrosis of neurons, so severe ASP can have long-term consequences. Severe intoxication can be fatal (Perl et al., 1990). There is also evidence that chronic exposure to low concentrations of the toxin, as is common in tribal subsistence and recreational shellfish harvesting where DA exposure is common, has neurological effects on mice, although these are reversible when exposure is stopped (Lefebvre et al., 2017). There is also evidence that the molecule can cause kidney damage at concentrations considered safe for human consumption (Funk et al., 2014). DA also has several stereoisomers, none of which, apart from 5-epi domoic acid, is as potent as the parent compound (Hallegraeff et al., 2003; Walter et al., 1994). The biosynthesis of DA appears to involve the condensation of two different intermediate precursor units, as demonstrated by isotopic labelling (Ramsey et al., 1998). The first is a terpenoid intermediate geranyl diphosphate (GPP) and the second is the amino acid glutamate (L-Glu) or an analogous intermediate from the Krebs's cycle (Savage et al., 2012). The genetic and enzymatic apparatus that controls the biosynthesis of DA was recently revealed in *P. multiseriata*, apart from a missing isomerase that performs the isomerization from iso-DA to DA (Brunson et al., 2018). The metabolic pathway involves four genes encoding four different enzymes – DabA-DabD. DabA is a magnesium-dependent cyclase that catalyzes the first step of DA synthesis previously suggested by isotopic labelling – the *N*-prenylation of L-Glu with GPP to *N*-geranyl-L-glutamic acid (L-NGG). This compound is then oxidized by DabD to form 7'-carboxyl-L-NGG, which is a substrate for DabC, an  $\alpha$ -ketoglutarate-dependent dioxygenase. This enzyme performs the cyclization of 7'-carboxyl-L-NGG to iso-DA. However, the final isomerization step is not yet known, but it is not carried out by DabB, an unknown protein with an unknown function.

### 1.3.3 DA regulation and ecophysiology

The regulatory and ecological function of DA was partially addressed in section 1.2.2. We have seen that DA can act as a grazer deterrent or as a trace metal chelator, both functions for which there is solid evidence. But several other factors may also influence the regulation of DA production and are summarized in Lelong et al. (2012). These include silicate and phosphate limitation, which upregulates DA production (Bates, 1998), and associated bacterial communities which influence it as well (Kodama et al., 2006). There may also be indirect effects of iron chelation through DA (Sunda, 2006). Under iron-limiting

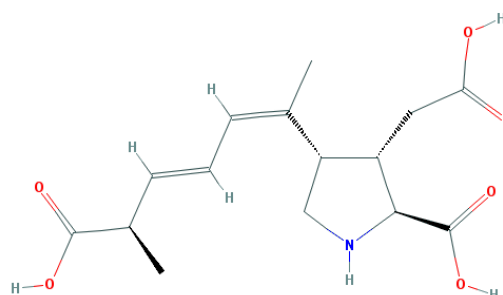


Figure 1.3-3: Domoic acid 2D structure. Source: PubChem.

conditions, silica depletion is higher than nitrate depletion, increasing the Si:N uptake ratio by up to three times (Hutchins & Bruland, 1998). It follows that iron limitation may indirectly increase cellular DA levels by promoting Si-limitation. Paradoxically, toxin-producing *Pseudo-nitzschia* have not been found until recently in regions of high nitrate, low chlorophyll (HNLC), i.e. true oceanic areas, where iron concentrations are typically growth limiting (Bates & Trainer, 2006), although *Pseudo-nitzschia* spp. are common representatives of oceanic phytoplankton communities. However, Silver et al. (2010) have measured and found DA at relatively high concentration alongside high cell counts in HNLC areas in the Pacific where natural or artificial iron enrichment has occurred. This may suggest that the production of DA exists under unfertilized conditions but is below the detection limit because algal growth is minimal.

Toxicity is not characteristic of species but rather of strains or populations. It has been shown in numerous examples that some strains can be toxic while others do not appear to produce DA (Bates et al., 2018 and references therein). This sometimes depends on the geographical region in which the strain was obtained, such as the toxic *P. multistriata* in the Mediterranean (Amato et al., 2010; Pistocchi et al., 2012) and its non-toxic counterpart in New Zealand (Rhodes et al., 2000). However, the current prevailing view is now that all, or at least most, *Pseudo-nitzschia* species are capable of producing DA, but culture or environmental conditions may strongly influence the production of the toxin, even considering that it could be produced in very small amounts that cannot be detected by some toxin detection methods. A way to answer these questions has recently been made possible by the identification of the biosynthetic pathway of the toxin, including the genes and enzymes responsible for the synthesis in *P. multiseriis* (Brunson et al., 2018). Moreover, *Pseudo-nitzschia* are not the only diatoms producing DA, as the toxin has also been found in other, albeit closely related, species – *Nitzschia navis-varingica* (Tan et al., 2016) and *Nitzschia bizertensis* (Smida et al., 2014), while the presence of DA in *Halamphora coffeaeiformis* has been speculated but not confirmed (Bates, 2000). In addition, DA was first found in the Pacific red alga *Chondria armata* (Takemoto et al., 1966) but also in the Mediterranean red alga *Alsidium corralinum*, which has led some researchers to speculate that the acquisition of toxicity from *Pseudo-nitzschia* may be through its epiphytic associations with these algae (Bates, 2000). Although we know that the biosynthetic apparatus is integral to at least *P. multiseriis*, this would imply a form of horizontal gene transfer that might also be mediated by bacteria (Chekan et al., 2020). However, very few analogous sequences of either genes or proteins to the annotated enzymes involved in DA synthesis are available in public databases. Much more work needs to be done on this topic to speculate on the evolutionary origin and function of these genes.

## 1.4 *Pseudo-nitzschia* in the Mediterranean and the Adriatic Sea

*Pseudo-nitzschia* has been the subject of many studies on phytoplankton and HAB ecology worldwide. The Mediterranean Sea, including the Adriatic, is no exception (Mozetič et al., 2019; Zingone et al., 2021). *Pseudo-nitzschia* species are important members of Mediterranean phytoplankton communities, with several species reaching bloom densities of several million cells per litre in many regions (e.g., Northern Adriatic Sea: Ljubešić et al., 2011; Marić et al., 2011; Totti et al., 2019; Central Adriatic Sea: Arapov et al., 2016, 2017; Southern Adriatic Sea: Cabrini et al., 2012; Caroppo et al., 2005; NW Mediterranean: Quijano-Scheggia, et al., 2008; Tyrrhenean Sea: Cerino et al., 2005; Ruggiero et al., 2015).

Several species have been identified in Mediterranean waters and the composition in different areas is similar, although not the same (Bates et al., 2018; Trainer et al., 2012). More species were identified at Mediterranean sites near the Atlantic Ocean, perhaps unsurprisingly due to increased water exchange, than at Central and Eastern Mediterranean sites. Some of the species, such as *P. multistriata*, are suspected to be non-indigenous species that may have been initially introduced to the Gulf of Naples by ballast waters in the 1990s (Zingone et al., 2003) and subsequently detected in other areas of the Mediterranean (Mozetič et al., 2019; Zingone et al., 2021). This is difficult to prove, given the difficulty of identification, but the case is stronger with this species, which is easily identified via LM. The list of extant species is likely to grow longer, given the potential for introduction from human-related activities, as well as climatic and oceanographic changes favouring warm-water species. The Adriatic Sea largely reflects the diversity of *Pseudo-nitzschia* in the Mediterranean, although some species found in Western Mediterranean and Greece, such as *P. brasiliiana* (Moschandrea et al., 2012; Quijano-Scheggia et al., 2010), have not yet been confirmed in the Adriatic Sea. The list of species described and identified so far in the Adriatic, together with information on toxicity, is presented in Table 1.4-1. Ten species have been identified with varying degrees of confidence in terms of the identification methods used.

Toxicity of Mediterranean strains has been demonstrated both in field and in culture (e.g. Orsini et al., 2002; Penna et al., 2013; Pistocchi et al., 2012), but their toxin levels are usually quite low and ASP events are rare (Zingone et al., 2021). DA is almost never detected above threshold levels in shellfish. DA below regulatory levels is sometimes detected in central Adriatic Sea (Arapov et al., 2016; Ciminiello et al., 2005; Ujević et al., 2010), and also in Northern Adriatic, where low levels of DA were detected in shellfish during a bloom of *P. calliantha* (Marić et al., 2011). In another study in the Gulf of Trieste, no relationship was established between toxicity in shellfish and the species present (Honsell et al., 2008). In a 15-year old time series of shellfish monitoring in the Slovenian part of the Gulf of Trieste, did not reveal any single case of DA in shellfish (HAEDAT).

Table 1.4-1: List of *Pseudo-nitzschia* species currently identified in the Adriatic Sea: NM – not measured; IN – indirectly measured. NA – North Adriatic; CA – Central Adriatic; SA – Southern Adriatic. Marked orange is *P. galaxiae*, only tentatively identified with LM; marked blue are species identified only with EM.

Species	Identification method/ Genetic marker	Toxicity	Region	Reference
<i>P. cf. arenysensis</i>	28S, ITS, TEM	NM	NA	Giulietti et al., 2021
<i>P. calliantha</i>	TEM	NM; NM; IN, NM	NA; CA; NA; SA	Lundholm et al., 2003; Burić et al., 2008; Marić et al., 2011; Caroppo et al., 2005
	SEM	Yes	CA	Arapov et al., 2016, 2017, 2020
	ITS	No	NA	Penna et al., 2013
<i>P. delicatissima</i>	28S, ITS, TEM	NM	NA	Giulietti et al., 2021
	TEM	NM	SA	Caroppo et al., 2005
	SEM	NM	CA	Arapov et al., 2017
	ITS	Yes	NA	Penna et al., 2013
<i>P. fraudulenta</i>	28S, EM	No	NA	Pistocchi et al., 2012
	28S, ITS, TEM	NM	NA	Giulietti et al., 2021
	SEM	NM	CA	Arapov et al., 2017
	28S, EM	No	NA	Pistocchi et al., 2012
<i>P. cf. galaxiae</i>	28S, ITS, TEM	NM	NA	Giulietti et al., 2021
	LM	NM	SA; NA	Cabrini et al., 2012; Cerino et al., 2012; Mozetič et al., 2019, Totti et al., 2019
<i>P. multistriata</i>	LM	NM	NA	Mozetič et al., 2019
	28S, EM	Yes	NA	Pistocchi et al., 2012
<i>P. pungens</i>	SEM	NM	CA	Arapov et al., 2016
	ITS	No	NA	Penna et al., 2013
	28S, ITS, TEM	NM	NA	Giulietti et al., 2021
<i>P. subfraudulenta</i>	SEM	NM	CA	Arapov et al., 2016, 2017

<i>P. pseudodelicatissima</i>	SEM	NM	CA	Arapov et al., 2016
<i>P. heimii</i>	TEM	NM	CA	Burić et al., 2008.
<i>P. mannii</i>	ITS	No	NA	Penna et al., 2013
	28S, ITS, TEM	NM	NA	Giulietti et al., 2021

The study of *Pseudo-nitzschia* in the Gulf of Trieste has been mostly limited to data from phytoplankton and HAB monitoring programs. The data obtained in these programs are almost exclusively based on LM and therefore do not allow species distinction but are nevertheless very useful for drawing general ecological conclusions about the occurrence and relationships of the genus with other phytoplankton groups. There are far more data on the general phytoplankton community. Chlorophyll-*a* (Chl *a*) concentration have steadily declined over the last two decades, due to the reduction of seasonal large-diatom blooms in favour of smaller size fractions (Cerino et al., 2019; Mozetič et al., 2010, 2012). There are environmental drivers behind this shift, including reduced river discharge and climatological shifts. Community structure derived from Chl *a* measurements and pigment analyses revealed that large diatom dominated blooms occur in autumn (Talaber et al., 2018) and summer (Mozetič et al., 2012). A smaller seasonal peak also takes place in April and May, although diatoms accounted for only 30% of this bloom. Phosphate is the recognized limiting factor for phytoplankton growth in the Northern Adriatic (Mozetič et al., 2012), especially for larger classes such as diatoms (Talaber et al., 2014). It is therefore not surprising that diatoms tend to bloom during increased river discharge in autumn and spring. Often these blooms are also characterized by the presence of *Pseudo-nitzschia*. For example, the study by Cerino et al. (2019) found that *Pseudo-nitzschia* was present in high abundances in spring, summer, and autumn of certain years, although no species-specific associations were found. A thorough study of the species composition of the area is therefore needed to better understand the ecological conditions of the Northern Adriatic. Although phytoplankton ecology is increasingly considered to be driven by traits (Leonilde et al., 2017; Litchman et al., 2010), such as size and volume, phytoplankton species show a diverse range of adaptations and physiological responses to changing environmental conditions and therefore need to be considered as unique entities rather than groups. Indeed, blooms are often dominated by a single species rather than a species complex, as is also the case of *Skeletonema marinoi* in the Northern Adriatic (Marić Pfannkuchen et al., 2018). Traits are, of course, incredibly important as they define underlying intra- and interspecific variability and thus determine the adaptability of species changing environments.

## 1.5 Methodological Overview

Due to the increased scientific interest in *Pseudo-nitzschia* and HABs in general, the methodology for their study has evolved considerably over the last two decades (Bates et al., 2018). In particular, the spread of large-scale application of polymerase-chain reaction (PCR) has populated public genetic databases with valuable sequence data. These form the basis for phylogeny reconstruction, rapid genetic assay design and high-throughput studies of taxonomic differences and by combining molecular and traditional observation methods to establish ecological preferences of species over large geographic areas. This section discusses the most common methodology used for the study of *Pseudo-nitzschia*, which may also be applied to other diatom and phytoplankton taxa.

### 1.5.1 Sampling techniques

Sampling and collecting microalgae in the field is a relatively simple process. However, the sampling design and how samples are obtained will depend on the purpose of the analysis to be performed. Sampling design can vary considerably if the sampling is research or monitoring orientated (Franks & Keafer, 2003). For example, if one wants to obtain as much material as possible to get an idea of phytoplankton composition and process the material further, the method will be different from the case where one wants to measure cell concentrations of different species in the environment. *Pseudo-nitzschia*, like most other microphytoplankton, can be obtained from environmental samples using fine mesh (20  $\mu\text{m}$ ) phytoplankton nets (**Error! Reference source not found. A**). These nets concentrate the sample by repeated tows, which can be vertical or horizontal, depending on the water layer one wishes to capture. The concentrated sample, which accumulates at the bottom of the net in a purposive collection vessel, can then be drained into holding tanks and the process repeated as many times as desired. The depth and number of net tows need to be considered. The volume of water sieved through the net can be calculated from the volume of the net and the depth. This method cannot distinguish between the presence of phytoplankton at different depths, but it allows sampling of large volumes of water, maximizing the chance of detecting low abundance taxa. This is the reason why it is the method of choice when cultures of toxic algae are to be established. One problem with nets, especially those with small mesh sizes, is that they tend to clog (Franks & Keafer, 2003). This makes them unreliable for quantitative measurements of cell concentrations unless the net is not towed but a known volume of water is pumped through the net (Franks & Keafer, 2003).

Alternative non-concentrating sampling methods include collecting seawater at specific depths, which is usually achieved using remotely operated Niskin bottles arranged in a rosette (**Error! Reference source not found. B**), or by collecting all or part of the water column, i.e., an integrated sample, using a collection hose. Niskin bottles can be used to obtain accurate environmental cell concentrations as well as a vertical profile of phytoplankton, but they are point samples and sampling depths must be defined. The great thing about bottle samples is that they allow replication and simultaneous measurement of water and/or cell properties from the same bottle (Franks & Keafer, 2003). On the other hand, integrated samples give us the phytoplankton composition of the entire water column, but without the detail of its vertical distribution. However, this could be achieved by using segmented tube samplers that have multiple valves placed at different depths. The general disadvantage of tube samplers is that they can only be used at shallow depths.

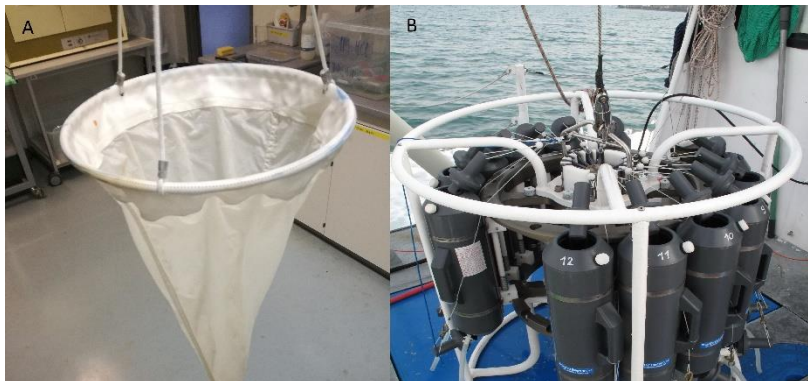


Figure 1.5-1: Sampling devices used in phytoplankton collection: A) 20  $\mu\text{m}$  phytoplankton net with a collection jar at the bottom. B) Oceanographic rosette with an arrangement of 12 Niskin bottles that can be remotely triggered to close at specified depths.

There are several factors to consider when planning phytoplankton sampling. Where does one sample? Are river estuaries, ports, sewage disposal sites representative sampling locations? Does one want to specifically measure or sample at such locations? Ports for example, may be ideal locations to sample for introduced species, that were introduced through ballast water discharge (Anderson, 2009; Hallegraeff, 1998), while eutrophic river mouths are perfect for studying unnatural phytoplankton assemblages and potential epicentres for HAB development. Conversely, if one wishes to capture the relatively pristine natural state, secluded and undisturbed areas of the coast or the open ocean should be considered for sampling. The next issue is the timing and duration of sampling. If seasonal dynamics are to be captured, sampling must be regular and standardized. For exceptional events, such as blooms, the sampling design can be independent. Monitoring programs for HAB forming taxa or shellfish toxin concentrations should also consider sites near aquaculture operations. It is emphasized that for any type of study, environmental factors such as salinity, temperature, nutrient concentrations etc. must be recorded and analysed in accordance with biological sampling (Franks & Keafer, 2003). Finally, an important factor in phytoplankton sampling is depth. In shallow seas such as the Gulf of Trieste, this may not be of such influence, as the seabed is easily accessible. In deeper systems, however, it is important for reasons of time, cost, and sampling quality considerations. Most toxic algae are pelagic species found near the surface, while benthic algae require a different sampling strategy.

### 1.5.2 Culturing techniques

One of the basic requirements in the study of phytoplankton is to obtain enough material to work with. Like microbiological techniques, the need for culturing is essential in phycological studies. The most tedious, but also most reliable way to obtain algal material

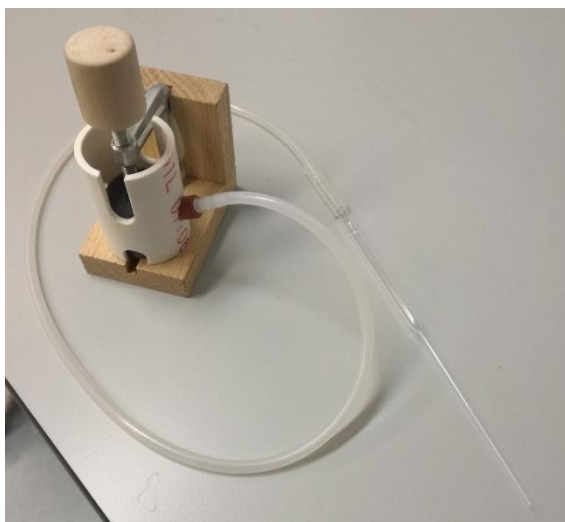


Figure 1.5-2: Home-made isolation device with a drawn Pasteur-pipette attached to a suction-based system.

is to grow environmental isolates. These can be isolated manually using drawn Pasteur pipettes (**Error! Reference source not found.**) by capturing single cells or cell colonies from a sample under a microscope and transferring them serially to observation chambers containing sterile seawater to remove debris, contaminants, and other phytoplankton species. Alternatively, this process can be automated to some degree of success with flow

cytometric cell sorters that recognize cells based on their optical properties and sort them into different compartments. Once the environmental isolates are obtained, they can be grown in cultures, which can then be used for a plethora of different applications and analyses. The research associated with this work required an extensive cultivation process and the establishment of an algal culture bank that took advantage of the manual isolation technique. *Pseudo-nitzschia* species are relatively easy to isolate and grow, but it is extremely difficult to keep them for prolonged periods of time and most cultures die-off after a while – they usually survive for about a year, but some die off much more quickly. The reasons for this are complex, and can include viral or bacterial lysis (Carlson et al., 2016), fungal infections or overgrowth (Hanic et al., 2009), shrinkage of cells as a result of cell division characteristic of diatoms (Round et al., 1990), or simply poor physiological condition of the original isolate.

An important aspect of culturing is also the choice of culture media and culture conditions such as day:night cycle, temperature and irradiance. The literature on this subject is vast and the selection depends on the experimental objectives. Most experiments relate to the production of DA in response to changing culture conditions, which were briefly discussed in 1.3.3. If the purpose of culturing is the accumulation of cellular material rather than experimental manipulation, as was the case in this work, the usual medium for culturing coastal algae is either the F/2 medium (Guillard & Ryther, 1962) or the L1 medium for coastal diatoms (Hallegraeff et al., 2003). Temperature may depend on the study site and the species being cultured, but generally an increase in temperature will result in a higher growth rate until a  $T_{max}$  is reached. Irradiance is typically set at about 70  $\mu\text{mol photon m}^{-2} \text{s}^{-1}$  because diatoms typically prefer turbulent and thus slightly shaded environments.

### 1.5.3 Morphological and imaging techniques

The most basic method for phytoplankton observation is light microscopy (LM). Using the light microscope, a taxonomist can identify phytoplankton cells in fresh or fixed samples, but in many cases is unable to identify the cells to the species level, as in the case of *Pseudo-nitzschia*. Using simple LM techniques, it is also sometimes difficult to distinguish live from dead or senescent cells, even in fresh samples, let alone fixed ones, which is important for predicting threats and for early warning.

Cell counts are important in the case of HABs because thresholds are established for management actions and informing the public of potential threats. There is no single threshold for *Pseudo-nitzschia* cells and it is highly dependent on individual countries, but suggested threshold from the New Zealand monitoring program is 50,000-100,000 cells<sup>-L</sup> (Hallegraeff et al., 2003). The threshold, of course, depends on the exact species and local ecological characteristics of the HAB community. In the Gulf of Trieste, for example, these thresholds are often exceeded in the order of 10<sup>6</sup> cells<sup>-L</sup> (Talaber et al., 2014), but no adverse effects are observed. It is therefore imperative to detect the potentially harmful taxa and quantify their presence to avoid unnecessary closures or false alarms. In the context of imaging this could be achieved by specifically tagging species with fluorescently labelled probes for fluorescent in situ hybridization (FISH). Probes for *Pseudo-nitzschia* FISH have been developed for certain species (Bowers et al., 2017; Medlin & Kegel, 2014; Scholin et al., 1999) and are useful in target species identification under the fluorescent microscope, although most probes developed for particular species tend to cross-react with non-targets (e.g. Barra et al., 2013). Because the original probe designs were based on local populations, they may not work well for populations from other regions of the world (Medlin & Kegel, 2014). Probes that are species-specific and fluorescently labelled allow quantification of species in environmental samples either by LM or by flow cytometry.

A morphological method that can very accurately identify *Pseudo-nitzschia* to species level is electron microscopy, either TEM or SEM. In the case of *Pseudo-nitzschia* and other diatoms this is quite trivial, as the silicate frustule that can withstand an acid wash that removes organic matter from samples. Sample preparation of the sample is similar in both cases, with acid-washed samples loaded either onto carbon coated copper grids for TEM analysis or onto SEM stubs, directly or with additional coating. The sample supports are then dried, usually on air. EM can be used for both environmental samples and cultured material, but for environmental samples some form of concentration is advantageous as natural abundances can be low, while the imaging process uses small sample volumes. The choice of electron microscopy technique in the case of *Pseudo-nitzschia* depends on the preferred method of visualization and, of course, on the infrastructural capabilities of laboratories. Both technologies produce accurate images of the frustule, from which morphometric signatures can be read.

#### 1.5.4 Molecular methods for identification and quantification of *Pseudo-nitzschia* - Barcoding and phylogeny

The basis for molecular study of *Pseudo-nitzschia* is obtaining, or at least having access to, genetic material in either form (DNA or RNA). In the case of cultured material, this is relatively easy, as cultures ensure access to significant amounts of biomass. Cultures are particularly valuable as they can provide a reproducible and reliable source of novel genetic information that can be fed into public databases such as GenBank. This process is extremely important, because many advanced molecular methods that normally skip the cultivation phase depend on these public resources. In this section, we lay out the usual process of molecular analysis and briefly describe the methodology used in this work (Figure 1.5-3).

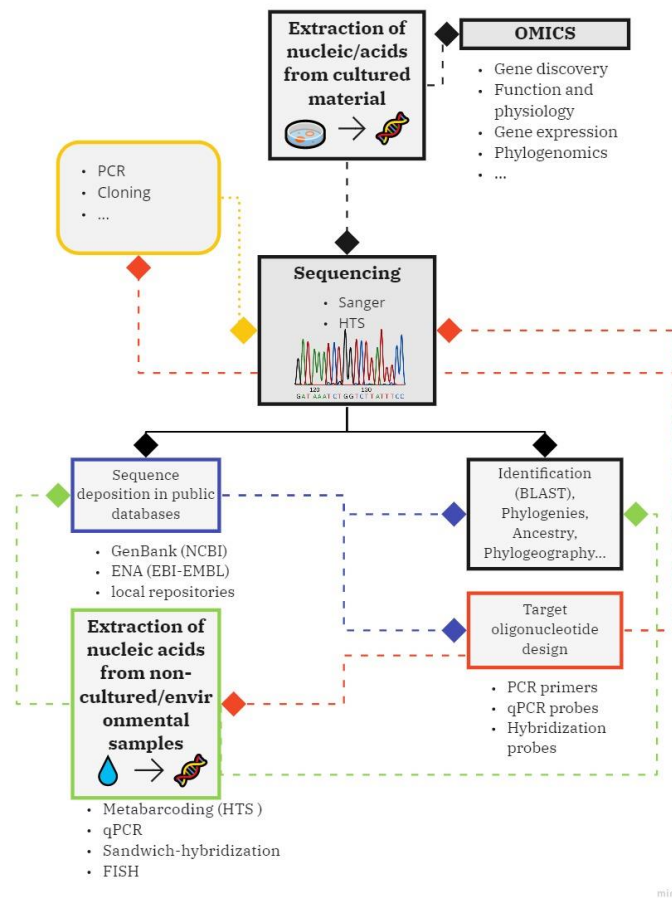


Figure 1.5-3: The common process flow of genetic data manipulation and analysis. Diamonds represent sub-processes from the parent processes, depicted by individual colours.

The full range of methods and technologies that make use of genetic material is vast, and those that fall within the realm of biotechnology, such as genetic manipulation, are not fully addressed here. The basis is the extraction of nucleic acid from cells. In our case, this can be done either from cell cultures or from environmental samples, depending on the purpose of the future work. Extraction can be done in many ways and nowadays most of them are done with commercially available extraction kits. However, to prevent enzymatic degradation of DNA or to avoid contamination with polysaccharides, which is especially problematic with environmental samples manual procedures such as the phenol or CTAB extractions are preferred, respectively.

Cultures are typically used when novel genetic data should be obtained. One of the classical ways of analysis requires specific sections of the genome or transcriptome to be amplified via the polymerase chain reaction (PCR). The choice of primers used in PCR determines what is amplified. The amplicons can be either phylogenetic markers used in species identification, commonly referred to as barcoding, microsatellites used in population and ancestry studies, functional genes, reverse transcripts of mRNA, etc. These amplicons are then sequenced using classical (Sanger sequencing) or state-of-the-art high-throughput sequencing commonly referred to as next-generation sequencing or NGS (e.g., Illumina, Ion Torrent, Nanopore technologies), and their sequences are compared and analysed with

previously published sequences deposited in public databases. These databases are then the source of information for the design of novel oligonucleotide primers and probes that can be used in other applications, including environmental sample-based techniques.

An important aspect of molecular identification of species and unknown strains is phylogenetic analysis. This involves the statistical evaluation of character state changes over time among a set of sequences, where the sequences represent current states. The result of this analysis is a phylogenetic tree. There are several ways to approximate the branching of the phylogenetic tree from sequence data. The simplest is parsimony, where the tree with the fewest changes is considered the best. This is often not the case, as such trees may underestimate the number of character state changes, since backward mutations are as likely as forward mutations. Parsimony is a computationally fast method but is better suited to datasets with less divergence or fewer taxa.

Alternatives to parsimony include maximum likelihood, Bayesian inference, and distance-based methods. The latter are like parsimony, but work with distance matrices obtained from sequence data rather than the sequence data itself. One result of distance-based methods can be phylogenetic networks, such as neighbour-joining or TCS networks (Templeton et al., 1992). Distance-based methods provide a good and fast representation of the data and individual differences between sequences but may not be used as a correct representation of evolutionary relationships.

Maximum likelihood (ML) and Bayesian inference, which were also used in this work, on the other hand, are based on models of DNA evolution. These are Markov models whose inherent assumptions approximate parameters used in phylogenetic analysis, such as base frequencies, probability of mutations, and overall substitution rates. Mutations are defined in DNA evolution as changes in the nucleotide sequence, with transitions ( $A \leftrightarrow T$  or  $C \leftrightarrow G$ ) generally more likely than transversions ( $A, T \leftrightarrow G$  or  $A, T \leftrightarrow C$ ). The correct evolutionary model must be approximated or decided before analysis. Choosing the wrong evolutionary model for your data can lead to bias. Evolutionary models range from simple models, where base frequencies and mutation rates are assumed to be the same for each possible change and the only approximated parameter is the overall substitution rate. An example is the Jukes-Cantor model (Jukes & Cantor, 1969). Complex models estimate more parameters because the base frequencies are allowed to differ and the mutation rates from one base to another can all be different, leading to the approximation of at least ten parameters, which happens in the General time-reversible (GTR) model (Tavare, 1986). There are several models that lie between these two extremes, such as the model of Hasegawa, Kishino and Yano – HKY85 (Hasegawa et al., 1985), which distinguishes between the mutation rates of transitions and transversions and allows for unequal base frequencies, thus approximating six parameters. ML and Bayesian inference are both computationally intensive but provide the best statistical evaluation of the evolutionary past and are needed when inferring evolutionary relationships and speciation.

### 1.5.5 Hybridization methods in ecology and monitoring

In marine phytoplankton monitoring, cell counting is the classical and most used method for estimating phytoplankton abundance. Counting cells using light microscopy provides valuable information on species abundance but may not tell us anything about the condition of the bloom. The latter is desired by the aquaculture industry, water-related businesses, the research-academic sector, and government agencies conducting water quality assessments, among others. Cell counting has both technical as well as financial drawbacks. One hour of microscopy can cost up to 100€, not including the cost of sample preparation, while it can be barely sufficient for the analysis of a single sample, especially when sample preparation is also accounted for. These time and budget constraints also

usually prevent the replication of samples in monitoring programs. Because samples are often fixed in preservatives, dead and senescent cells are hard to distinguish, introducing some bias into the counts. When samples are fresh, viability can often only be determined by staining or digestion assays (Zetsche & Meysman, 2012), which are often not used in routine programs. For all the above reasons, tools that can overcome these problems are being sought. One such option is the use of hybridization methods such as microarrays, sandwich hybridization assays (SHAs), or in the case of imaging techniques fluorescent in-situ hybridization (FISH).

The underlying principle of all hybridization methods is the specific binding of nucleotide probes to the nucleic acids of target organisms. In the case of microarrays and SHAs, the probe is mobilized on a solid support such as a microplate or glass slide, while in the case of FISH the fluorescently labelled probe is introduced into either fixed or living cells where it binds specifically to nucleic acids. Successful binding of the probes is then detected by different approaches. In microarrays, the target nucleic acid is fluorescently labelled, and the signal is read on a microarray slide reader. In SHAs, on the other hand, various detection mechanisms are used, but the most common is colorimetric. In this case, biotinylated capture probes can be bound to solid supports such as microtiter plates, beads, or arrays, followed by the addition of crude lysates containing target nucleic acids, or the direct addition of extracted nucleic acids, which are then hybridized to the capture probe. Digoxigenin (DIG)-labelled signal probes are added to attach to the target and produce hybrids. After the addition of anti-DIG antibodies, usually conjugated with horseradish peroxidase (HRP), the substrate reacts with the enzyme to produce a colorimetric product (Figure 1.5-4). This enzymatic reaction thus colours a substrate in the presence of hybrids and the intensity can be measured on a spectrophotometer.

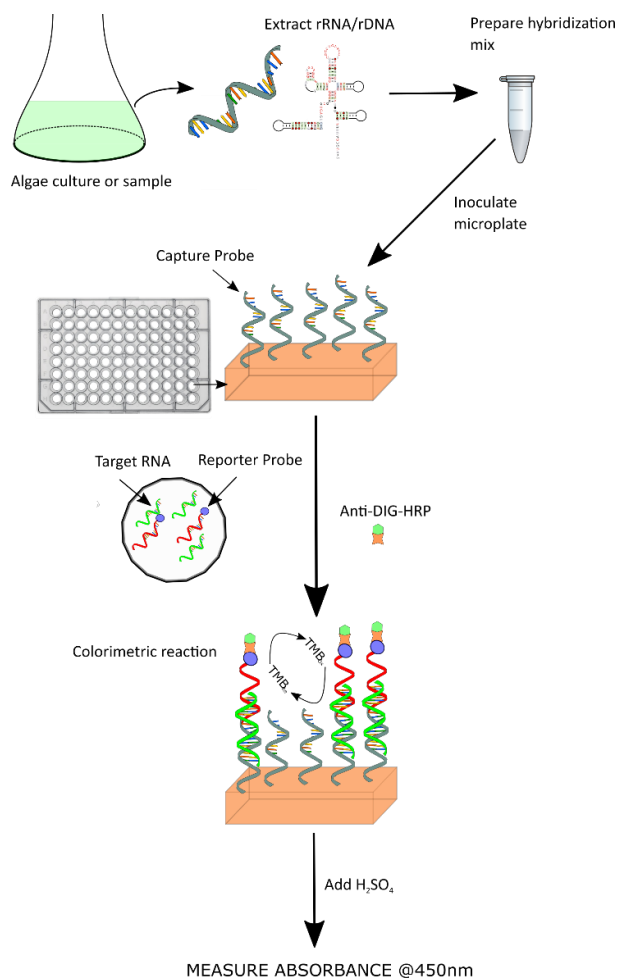


Figure 1.5-4: Schematic representation of a sandwich-hybridization assay with colorimetric detection. The capture probe, target nucleic acid, and reporter probe form a conjugate. The reporter probe is immuno-labelled, in this case with digoxigenin (DIG). After the addition of an antibody-enzyme conjugate (antiDIG-horseradish peroxidase (HRP)), the enzymatic reaction occurs, colouring the substrate of HRP, which in this case is 3,3',5,5'-tetramethylbenzidine (TMB).

Probes targeting *Pseudo-nitzschia* have been previously designed and re-designed (Barra et al., 2013; Bowers et al., 2017; Rhodes et al., 2000; Scholin et al., 1996, 1997, 1999) and have been used in both laboratory and environmental settings, including full automation (Bowers et al., 2018; Greenfield et al., 2006). However, the lack of species monocultures often prevents comprehensive testing of their specificity, while intraspecific genetic variability can lead to errors and difficulties in the testing procedure. In addition, the available cultures are often geographically restricted isolates, located predominantly on the California coast of the United States and the Gulf of Naples in the Mediterranean Sea (Barra et al., 2013; Bowers et al., 2017). Rigorous testing of specificity and cross-reactivity is therefore required, using strains originating from other world regions and including closely related species to validate probes developed *in silico*. The specificity of these probes was often proved to be limited and in many cases leads to unexplained cross-reactivity (Barra et al., 2014). Most probes are based on the nuclear-encoded 28S (LSU) RNA gene and could be modified for both DNA and RNA purposes. The 28S rDNA is incorporated into mature ribosomes and together with the fact that rRNA is short-lived in the environment, this makes it a good proxy for living cells. Increased cellular activity, which may or may not be growth-related, manifests itself in increased rRNA levels (Blazewicz et

al., 2013; Hu et al., 2016; Medlin & Kegel, 2014). While this concept has been used for a variety of applications to date, there are some limitations associated with it, although most have been studied in bacteria (Blazewicz et al., 2013). The limitations may stem from species-specific differences in life-strategies, biases associated with extraction efficiency, and failure to account for the physiological state of cell populations. Increased RNA is also associated with cell activity according to the growth rate hypothesis (Sterner & Elser, 2002). For photoautotrophs, this hypothesis has been proven to be complex with much conflicting evidence from different microalgal groups (Flynn et al., 2010), although it is generally true in some form. The implication of this hypothesis is that cells tend to accumulate ribosomes, where the bulk of the cellular phosphorous is stored, as the growth rate increases. Therefore, by measuring RNA signal on a hybridization-based platform, we can infer cell activity and provide additional information on the state of the bloom. However, the region has a slower evolutionary rate than, for example, the ITS region, which is more suitable for species-specific identification of *Pseudo-nitzschia* species (eg. Lim et al., 2018; Turk Dermastia et al., 2020). Sandwich hybridization probes for ITS have also been developed and shown to be stringent in their specificity (Smith et al., 2012), but the fact that ITS rDNA is not incorporated in mature ribosomes makes this method less suitable for monitoring activity in living cells.

RNA yield naturally increases with increasing cell number. Average nucleic acid concentrations per cell at different stages of growth and stress can be determined in controlled culture experiments (e.g. Medlin & Kegel, 2014), whereas the physiological state of cells is very difficult to measure in environmental samples, rendering conversions from signal to cell numbers complicated. In the study of Medlin and Kegel (2014), the RNA yield of two *Pseudo-nitzschia* species did not seem to change much when the cultures were exposed to stress, but this result cannot be extrapolated to environmental conditions (Dittami & Edvardsen, 2012), which can change greatly over very short periods of time.

### 1.5.6 Metabarcoding

The second pathway of molecular, in our case nucleic acid, analysis depends exclusively on high-throughput or next-generation sequencing (NGS) strategies and exploits the power of Big Data analysis – commonly known as omics technologies. These are cutting-edge tools that rely heavily on bioinformatics and can even be applied to single cells. The results of research in the omics field are far-reaching and include whole genome sequencing projects, studies of gene expression through transcriptome sequencing, construction of phylogenies based on whole genomes (phylogenomics), study of functional ecology with the application of metagenomics in environmental samples, etc. In this work, we have focused on the somewhat more trivial methodology, that of metabarcoding. Here the principle is like that of barcoding described above, with the additional difference that whole communities instead of single cultures are analysed with one or more barcoding markers using NGS and subsequent bioinformatics. Metabarcoding has gained attraction in recent years as it offers several powerful advantages for the natural community analysis compared to traditional methods (Cristescu, 2019; De Vargas et al., 2015; Malviya et al., 2016; Penna et al., 2017; Piredda et al., 2018). These include high throughput, scalability, i.e., large-scale sampling campaigns and analyses are possible and comparable to small-scale ones; interoperability, i.e., datasets can be compiled based on the same bioinformatic pipelines and are thus comparable, while data obtained through counts or observations are always observer-dependent; detection of rare and cryptic taxa; detection of non-indigenous species. On the other hand, this methodology comes with its own problems. First, it depends on reference databases, which are usually not complete, as most marine organisms have never been cultured (Weigand et al., 2019). That said, even those that have been cultured and

barcoded may have considerable genetic diversity resulting in conceptual problems in assigning species or certain taxa. In the microbial ecology of prokaryotes, the consensus is that sequences that are 97% identical are clustered into unique operational taxonomic units (OTUs), which can then be identified based on a consensus reference sequence shared within the OTU. In the microbial ecology of eukaryotes, the 97% cut-off is usually not sufficient since the link between OTUs and species is often unfounded (Callahan et al., 2017; Mysara et al., 2017). OTU clustering was developed to prevent erroneous sequences resulting from sequencing error being identified as real diversity. The development of bioinformatics tools has greatly improved the ability to distinguish erroneous sequence diversity from true diversity and has opened the way for amplicon sequence variant (ASV) analysis, which identified unique sequences and filters out erroneous ones through error modelling. This is now the preferred methodology in metabarcoding analysis, as it also carries the possibility of reusing ASVs in other studies, since ASVs are genetic sequences of real organisms (Callahan et al., 2017). Unfortunately, it still does not solve the problem of missing reference data when taxonomy assignment is the goal. On the other hand, ASVs can artificially inflate diversity, since marker genes may be present in multiple different copies in a single organism, while identical copies may not even be monophyletic (Berry et al., 2017).

Another issue is PCR-bias, since metabarcoding depends on a PCR amplification step that amplifies environmental DNA for the selected metabarcoding marker. Preferential amplification may occur in this step, resulting in a biased community representation (Kelly et al., 2019). For this reason, metabarcoding datasets should be carefully interpreted in terms of abundance or relative abundance. To partially overcome the problem of inconclusive assignment of taxa in a sample, due to the inability of the clustering algorithm to assign sequences to unique taxonomic units, a metabarcoding study can use multiple markers (e.g. Stefanni et al., 2018), which we did in the pilot study presented in Chapter 6. In the Northern Adriatic metabarcoding on phytoplankton communities has only been used only in the Venice Lagoon (Armeli Minicante et al., 2020).

The process of nucleic acid extraction in metabarcoding protocols can be the same as for cultures, but a concentration step is usually required because the abundance of cells in natural environments is much lower than cultures. Concentration can be achieved by filtering large volumes of water through filters with different pore sizes or by ultracentrifugation or concentration membranes. For phytoplankton, these sizes are typically 0.2  $\mu\text{m}$ , 2  $\mu\text{m}$  and 20  $\mu\text{m}$  corresponding to the common phytoplankton size classes (picoplankton: 0.2-2  $\mu\text{m}$ , nanoplankton: 2-20  $\mu\text{m}$  and microplankton: >20  $\mu\text{m}$ ). In coastal environments where the primary productivity is high, one litre of seawater is usually sufficient, but in oligotrophic neritic and oceanic environments, filtration, or concentration of up to 100 L of water may be required.

In terms of metabarcoding markers for phytoplankton studies, the most used markers are the V4 and V9 regions of the small subunit of ribosomal DNA, which are also general markers for eukaryotic metabarcoding. 18S is a well-established eukaryotic marker that has been used in many marine metabarcoding experiments and campaigns, including the global Tara Oceans cruise and the annual Ocean Sampling Day (Bradley et al., 2016; De Vargas et al., 2015; Malviya et al., 2016; Piredda et al., 2017; Stefanni et al., 2018; Tragin et al., 2018). However, other markers need to be tested, since 18S is known for poor resolution species-level resolution in some taxa. Specifically for diatoms, the *rbcL* gene has been proposed in the freshwater domain (Rimet et al., 2016; Vasselon et al., 2017a). In this work, we extend its use to the marine world.

### 1.5.7 Toxin analysis

We will also briefly address the common methods used in the detection of DA. Central to the analysis of DA concentrations is the use of DA standards and reference materials that are prepared by the Canadian Institute for Marine Biosciences (CRMP). The widely used analytical method for the detection of DA is HPLC with UV detection, acknowledged also as a reference method by the EU for shellfish toxicity monitoring (Commission Regulation (EC) No 2074/2005). However, the protocol for this method is designed to detect relatively high concentrations of DA in shellfish tissue, and not for minute concentrations in algae culture (Quilliam, 2003). Therefore, more sensitive methods are used to study the production of DA in cultures or water samples. For example, methods based on derivatisation of samples with fluorescence-reagents and subsequent analysis by HPLC with fluorescence detection can be used to detect trace concentrations of DA (Pocklington et al., 1990). Another sensitive method promising lower detection limits is the liquid chromatography tandem mass spectrometry (LC-MS/MS). It allows for lower concentrations to be detected and quantified, albeit at a much higher analysis price. The simplest methods in terms of operation are different functional assays, including the ELISA immunoassays (e.g. Saeed et al., 2017), which have also been commercialized and are available at several providers. Quality control with such tests is more difficult compared to the analytical methods, although they are reliable and perhaps the most important – they are far more sensitive than the reference method. A comparison of five different commercial tests has revealed that the tests generally underestimate the toxin concentration, while false negatives did occur with two of the tested assays (Johnson et al., 2016).

## 1.6 Hypotheses and Aims of this Thesis

The first objective of the thesis is to thoroughly investigate the species composition and ecology of the genus *Pseudo-nitzschia* in the Gulf of Trieste (NE Adriatic Sea). Many species are present, as several decades of monitoring and observation of the phytoplankton community suggest, although there are no data on exactly which species occur, when they occur, and how they interact with the environment and other organisms. In addition, virtually nothing is known about their toxicity. Therefore, one of the goals is also to find out which species and strains isolated in the Gulf of Trieste can produce DA and whether this toxicity poses a threat to the environment and to human food safety. We assume that at least some species are toxic, as evidence from neighbouring areas indicated the presence of potentially toxic species and DA in shellfish. Lastly, I would like to point out the usefulness of using advanced technologies for monitoring purposes, especially on long-term ecological research (LTER) stations, and developing new ones for this purpose. One of the promising tools that has gained much traction in microbial ecology and biodiversity assessment in recent years is the use of high-throughput sequencing, especially metabarcoding and metagenomics, to analyse microbial communities. I hope to translate this knowledge into preliminary phytoplankton community assessments and compare the results to traditional monitoring methods. In another effort, I will explore the use of simple colorimetric assays based on nucleic acid hybridization and evaluate their performance compared to microscopic counts. As HABs become increasingly widespread and damaging to both the environment and the aquaculture and tourism industries, novel methods for their monitoring and study are needed to ensure safe and productive oceans.

The research hypotheses are:

1. There are many species of *Pseudo-nitzschia* present in the Gulf of Trieste, which were so far unidentified. These species are traditionally, due to the lack of other morphological characteristics visible by light microscopy, grouped into two groups, based on their TAA width.
2. These groups do not reflect the ecological characteristics of the species comprising the groups.
3. Due to the presence of several species of *Pseudo-nitzschia*, including *P. multistriata*, which has already been identified, there is a small but existing risk of ASP in the NE Adriatic Sea.
4. The existing methods of HAB monitoring (including *Pseudo-nitzschia*) are insufficient, and do not meet the requirements of robust environmental status assessment, therefore novel methods need to be introduced into existing monitoring programs.



## Chapter 2

# Materials and Methods

### 2.1 Taxonomy and Seasonal Distribution of *Pseudo-nitzschia* in the Gulf of Trieste (Chapter 3):

#### 2.1.1 Sampling

In the Slovenian part of the Gulf of Trieste (GoT), phytoplankton samples for isolation and cultivation were collected monthly from October 2016 to March 2018 with some additional sampling events in 2019 for cell isolation and monoclonal culture establishment. Five vertical and five horizontal hauls with a 20 µm phytoplankton net were performed at station 0DB2 (13°42'20" E and 45°35'57" N, bottom depth 17 m) next to a mussel farm (Figure 2.1-1). Samples were stored in a darkened glass container and immediately taken to the laboratory where single cell isolations were performed. In addition, integrated samples for phytoplankton counts were collected monthly at station 0DB2 between 2016 and 2019 using a hose sampler and fixed with neutralized formaldehyde (2% final concentration).

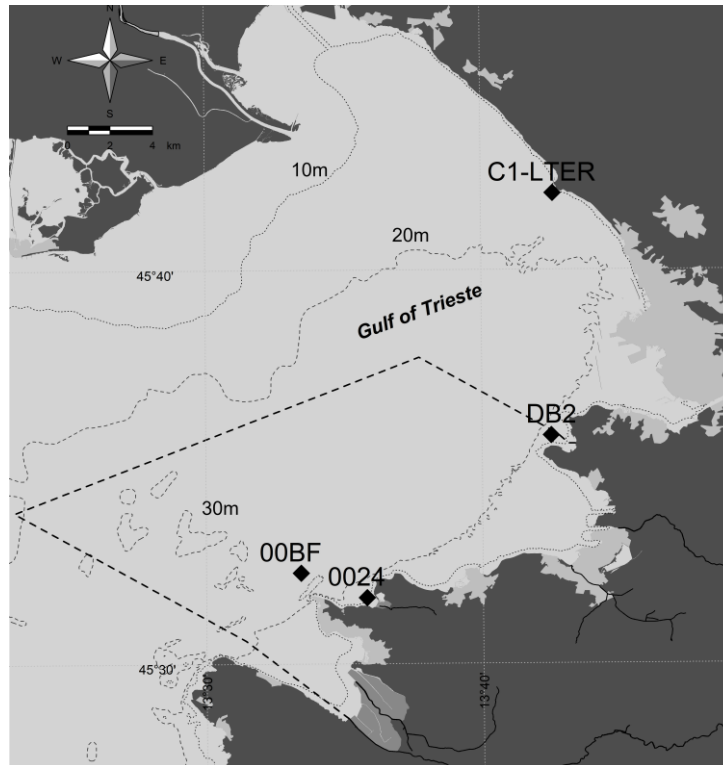


Figure 2.1-1: Sampling stations in the Slovenian part of the Gulf of Trieste. The dashed line represents the border of Slovenian territorial waters.

For the description of a typical seasonal cycle and inter-annual variability of *Pseudo-nitzschia* in the GoT we also considered a 14-year time series of *Pseudo-nitzschia* counts grouped into two species groups, i.e., *seriata* and *delicatissima* group. This time series was obtained at the Italian C1-LTER and included phytoplankton abundance and environmental data like temperature, salinity, and dissolved inorganic nutrients. The time-series was kindly provided by Istituto Nazionale di Oceanografia e di Geofisica Sperimentale (OGS). For details see method section of the article in Chapter 3.

### 2.1.2 Culturing

In this work, cultures were obtained by Pasteur pipette isolation from environmental samples. They were maintained in L1 medium at 20 °C, only when lower growth rates were desired was the temperature lowered to 15 °C, at 70  $\mu\text{mol photon m}^{-2}\text{s}^{-1}$  irradiance and on a 12:12 hour day:night cycle.

### 2.1.3 Phytoplankton counts – the Utermöhl method

Fixed samples were counted using the Utermöhl method (Utermöhl, 1958), in which a known volume of the sample is placed in a sedimentation chamber where it is allowed to settle. Cells were counted along transects of the sedimentation chamber on the inverted microscope Zeiss Axio Observer Z1 (minimum magnification 200x or 400x) and results expressed as cells per litre. This method was used for all phytoplankton counts in environmental samples presented in Chapters 3, 4 and 6.

### 2.1.4 Haemocytometric phytoplankton counts

*Pseudo-nitzschia* cells in cultures were counted using the Fuchs-Rosenthal chamber to assess their abundance, growth, and condition. The Fuchs-Rosenthal chamber is a glass chamber with two grids of 16 squares each covering 1 mm<sup>2</sup> and subdivided into another 16 squares, each covering 0.0625 mm<sup>2</sup>. The chamber also has a known depth of 0.2 mm when covered with a coverslip. The sample is placed in the grid and covered with the coverslip and the excess liquid drains through the channels surrounding the grid (Neuendorf, 2020). This technique was in this thesis to evaluate cell counts prior to DNA extraction and TEM cleaning in Chapter 3, to determine RNA concentrations per cell used in the dilution series in Chapter 4, and to determine total cell counts used in the calculations of toxin quotas per cell in Chapter 5.

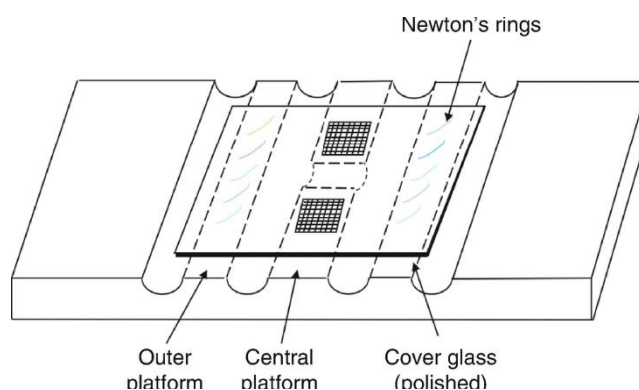


Figure 2.1-2: Schematic depiction of a Fuchs-Rosenthal counting chamber (from Neuendorf, 2020).

### 2.1.5 Sample preparation for TEM

In the article in Chapter 3, we used TEM to examine our culture material for morphological identification of *Pseudo-nitzschia* species. Samples were prepared using a modified method from Hasle & Fryxell, (1970). Briefly, 10 mL of culture were centrifuged, and the supernatant was decanted. Saturated nitric acid (HNO<sub>3</sub>) and sulphuric acid (H<sub>2</sub>SO<sub>4</sub>) were then added to the sample in a ratio of 1:4 and heated to boiling over an open flame under a fume hood. The mixture was boiled until the smoke became white or transparent. The samples were then diluted several times with deionised water (ddH<sub>2</sub>O) and centrifuged to pellet the purified material to remove the acids and stored in a dark place until examination under TEM (Philips CM100). A drop of the well-mixed, purified sample was then placed on a Formvar-coated copper TEM grid (75 or 400 mesh) and allowed to sediment for 5 minutes. The grids were dried and examined under TEM. Species identification based on the silicate frustule characteristics was performed by compiling the morphometrics from several published sources and the original species descriptions (e.g. Amato & Montresor, 2008; Bargu et al., 2002; Cerino et al., 2005; Kim et al., 2015; Lim et al., 2018; Lundholm et al., 2003, 2006).

### 2.1.6 Extraction of DNA from cell cultures

For the studies within this thesis, it was necessary to grow several algal cultures and extract genetic material from them. Most of the DNA extractions were carried out using the

E.Z.N.A. Mollusc DNA kit (Omega Bio-tek) according to the manufacturer guidelines. The kit is primarily designed for the extraction of DNA from organisms with high mucopolysaccharide content, but it has been found from experience that it is also suitable for the extraction of DNA from microalgae. No prehomogenization or disruption of cells prior to extraction is required and yields of DNA are in the range of 1-30 ng/ $\mu$ l, depending on the density and condition of the culture. Typically, DNA was extracted from cultures in the stationary growth phase when cell numbers reached 100,000 – 1,000,000 cells ml<sup>-1</sup> and 10-50 ml of the culture was harvested by centrifugation. The DNA was measured either on the Nanodrop spectrophotometer (Thermo-Fisher Scientific) or the Qubit fluorimeter (Invitrogen).

### 2.1.7 Amplification and sequencing of phylogenetic markers

The selection of phylogenetic markers was based on the availability of sequences in public databases (GenBank) and the availability of phylogenetic benchmarks in the literature. Thus, the regions of internal transcribed spacer I and II (ITS) and the large ribosomal subunit (LSU-28S) of ribosomal RNA, as well as the large subunit of the RuBisCo enzyme (rbcL) encoded in chloroplast DNA were selected for amplification. The primers used were ITS1 and ITS4 (White et al., 1990) for ITS, D1R-F (Nunn et al., 1996) and D3B-R (Scholin et al., 1994) for 28S and DP\_rbcL1/7 for rbcL (Jones et al., 2005). Sanger sequencing was performed at Macrogen Europe Inc. The reason we chose multiple markers for the phylogenetic classification of the cultures obtained in this study is that the markers have different discriminatory power compared to one and other, while plastid-encoded DNA and that encoded in the genome also have different evolutionary rates (Wolfe et al., 1987). In addition, some species are not well represented with sequences in public databases, making classification less reliable. If one brings more markers into the analysis, its robustness and reliability increases. This is especially important with respect to the aim of this work, as no reliable information on the species composition of *Pseudo-nitzschia* species in this part of the Adriatic Sea is available so far.

### 2.1.8 Phylogenetic analysis

The phylogenetic trees presented in the article in Chapter 3 were constructed using Bayesian inference implemented in the software MrBayes (Ronquist et al., 2012). Evolutionary models were evaluated using jModelTest software (Posada, 2008) and compared for each dataset.

## 2.2 Toxicity Analysis of Selected Strains (Chapter 5)

### 2.2.1 Culturing and sampling

Most cultures were maintained in 30 ml Erlenmeyer flasks. Some cultures that were confirmed positive for domoic acid (DA) in preliminary screenings were also cultured in larger volumes (500 ml), where growth and production of DA were continuously monitored. For strains 119-A4 and 119-B3, sampling was performed on days 7, 11 and 13 after inoculation, while for strains MS2 and MS3, the measurements were performed on days 4, 6 and 11 and 4, 5, 6, 7, 11 and 13, respectively. A total of 29 strains from 6 species were tested using different methods and setups.

## 2.2.2 Domoic acid in cultures

Most cultures were tested at a single point in the stationary growth phase. 50  $\mu$ l of the culture was taken in triplicate for enumeration as described in 1.5.3. Then, 10-20 ml of culture was taken in duplicate depending on the cell count. One sample was sonicated on ice at 40 Hz for 1 minute to rupture the cells and release the toxin. This sample was then filtered through a 0.22  $\mu$ m syringe filter (Millipore) to remove debris, and the filtrate was stored at -20 °C. This represented the total DA (tDA). The other sample was centrifuged at 4500rpm for 30min and the supernatant stored was at -20 °C. This represented the dissolved DA portion (dDA). Since the centrifugation process is not perfect, the supernatant was counted again in the Fuchs-Rosenthal chamber to account for the remaining live cells. This was done as follows: The upper layer of the supernatant was counted in duplicate, then a portion of the supernatant was pipetted for analysis, followed by counting the lower layer of the supernatant in duplicate. The cell count in the upper layer and the lower layer was then averaged, assuming a gradual increase in cell number from top to bottom in a centrifuged tube. To obtain the particulate DA concentration (pDA – toxin stored in cells), we subtracted the dDA part from the tDA and divided the resulting concentration by the number of cells in the lysate.

## 2.2.3 Direct competitive ELISA

The main method used to test all cultures examined was the competitive ELISA assay for the detection of domoic acid (Eurofins Abraxis). The cultures were processed according to the manufacturer guidelines. Care was taken to maintain constant temperature, where the plate was prepared, as well as to careful pipetting. The reliability of the procedure was assessed using internal and external controls and standards provided by the kit producer. The absorbance reader (Spark, Tecan) was turned on for a prolonged period (minimum 1 hour) before measuring to settle the light source. This method is approved as a complementary regulatory method by the European Commission (Commission Implementing Regulation (EU) 2019/627). Samples were diluted with the dilution buffer in a 1:25 ratio and diluted further to 1:50 if the signal was still saturated, diluted to 1:10 if the signal was weak/borderline or unquantifiable. Some samples were not reanalysed at higher or lower dilutions and are reported as positive only. Due to discrepancies between some of the conducted methods (LC-MS, HPLC-UV, ELISA), some samples were measured multiple times with ELISA to confirm the presence or absence of toxin.

## 2.2.4 LC-MS and HPLC-UV

Samples that were inconclusive after ELISA screens were also tested by two analytical methods. Samples were analysed 6-12 months after the initial ELISA screens, which may have resulted in some toxin degradation.

The HPLC-UV and the LC-MS/MS analyses were performed by the Institute for Safe Food (Veterinary Faculty of the University of Ljubljana) and the Laboratorio Nazionale di Riferimento per le biotossine marine (Cesatico, Italy), respectively. Determination of the domoic acid content was performed after chromatographic separation on a reversed phase column (C18 reversed phase, 5  $\mu$ m, 250 mm x 4,6 mm) using isocratic conditions (Acetonitrile 5% with TFA 0,1 % v/v). The analysis was performed using a UV-VIS

detector set at 242 nm. The amount of domoic acid was calculated from the external standard. A certified DA standard from NRC-Canada was used to prepare 3 standard solutions used to calibrate the HPLC system.

The LC-MS/MS analyses of domoic acid in extracts were performed using an Agilent UHPLC Infinity II equipped with an Agilent POROSHELL 120 EC C18 2,1 \* 100 mm 2,7  $\mu\text{m}$  -LC column coupled with an Agilent 6460 MS system. A certified DA standard from NRC-Canada was used to prepare 5 standard solutions used to calibrate the LC-MS/MS, system, in MRM mode. The identification of the analyte was based on the monitoring of two product ions of DA ( $m/z$  312 > 266, 312 > 161) by positive ESI (for DA precursor ion  $[M + H]^+$   $m/z$  312). The most abundant fragment, 266 was selected for quantification purpose while the 161 ion was used for qualitative confirmation. For chromatographic separation, the mobile phase of methanol/water and additive ammonium acetate/acetic acid was chosen. 5  $\mu\text{l}$  of the sample was injected in the LC-MS/MS system and a gradient elution lasting for 14 minutes was used to separate the toxins.

## 2.2.5 Amplification and sequence analysis of the *dabA* gene

For the amplification of the *dabA* gene, we first tried with primers published in Brunson et al. (2018) without success. We then designed new primers (Table 2.2-1) based on the alignment of sequences from shotgun sequencing of the *Pseudo-nitzschia multistriata* genome (BioProject: PRJEB9419) and Brunson et al. (2018). Internal sequencing primers were also designed to complete the gene region. Amplification was performed using Phusion HiFi Polymerase (New England Biolabs Inc.) and an annealing temperature of 60  $^{\circ}\text{C}$ , following the manufacturer guidelines for PCR setup. For PCR reactions that resulted in unspecific products, bands of appropriately sized products (~1500bp) were excised from the agarose gels. This was done by running the products at 200V for 30 seconds in pre-cut wells in the gel, followed by 3M sodium acetate and isopropanol precipitation at -20 $^{\circ}\text{C}$  for 1 hour. Precipitates were then washed with 70% ethanol and dissolved in 1x TLE. The products were purified with Exonuclease I and Alkaline Phosphatase – FastAP (Thermo Fisher Scientific). Alternatively, when possible, bands were excised from the gel with a sterile scalpel and the gel purification was performed using the NucleoSpin Gel and PCR Clean-up (Machery-Nagel). Sequence divergence was examined with the NJ and ML methods in R using the phangron (Schliep, 2011) and ape (Paradis & Schliep, 2019) packages implemented in R (R Core Team, 2019). The 3D structure of the predicted proteins was predicted using Phyre2 (Kelley et al., 2015).

Table 2.2-1: Newly designed primers for *dabA* amplification and sequencing.

Primer name	5'-3' Primer-Sequence	Type
DabA_multF	ATGAAATTTGCAACGTCCATTGTC	PCR
DabA_degF	ATGAARTTTGCAACRTCCATYGTC	PCR
N1_R	TCCAAAACGCTTTCATCAA	PCR
N2_R	AACGCTTTCATCAATGGTTTGTGG	PCR
Internal_multistriataF	CGATTGGATGAAGATCCCTTCA	Sequencing
Internal_multistriataR	GCAGAAGTCGACCATCCA	Sequencing

## 2.3 Colorimetric Assays for *Pseudo-nitzschia* Detection and Quantification (Chapter 4)

### 2.3.1 Colorimetric assay principle

Colorimetric hybridization assays were performed in a 96-well microplate format (Figure 1.5-4). The microtiter plates were coated with capture probes targeting 28S rRNA. Each repetition of the assay included a series of positive control (PC) tests in which perfect complementary synthetic RNA was added the wells in different concentrations to obtain the regression coefficients by which all other signals were normalized. The series also included a blank (negative control) that was subtracted as noise from all other signals. The hybridization mix was prepared as follows: A volume of RNA adjusted to the desired concentration, 12.5µl of hybridization buffer, 5µl of the digoxigenin (DIG)-bound signal probe, 1µl bovine serum albumin (BSA), 0.75µl of HRP, and RNA/RNA-se free water to complete the reaction mix to a total of 50µl. All samples, including PC and blank samples, were prepared in duplicates. The samples were then loaded into capture-probe coated microtiter plate wells and hybridized for 1 hour. The microtiter plate was then washed three times with EDTA-based wash buffer, followed by the addition of anti-DIG-HRP to hybridize with the signal probe. After another washing step, TMB was added, and the redox reaction resulted in coloration upon successful hybridization. The reaction was then stopped with sulfuric acid and the signal was measured at 450nm on the spectrometer (Victor, PerkinElmer).

### 2.3.2 Sampling campaign for the colorimetric assay

Environmental sampling was conducted as part of the SMS project (Sensing toxicants in marine water makes sense using bioassays, FP7) from March 2015 to March 2016 and additional sampling associated with this project in 2017 and 2018. Samples were collected at stations 0024 and 0DB2 in the Gulf of Trieste (Figure 2.1-1). At each station, an integrated sample was collected with a hose and the water was divided into two parts. The first part was fixed for cell counting using the Utermöhl method (Utermöhl, 1958; 2.1.3), while the other part was filtered on Whatman GF/F filters. For each litre filtered, 1 mL of ZR lysis buffer (Zymno Research) or in some cases 1 mL of 3% CTAB was added. Samples were then stored at -20 °C until RNA extraction was performed. *Pseudo-nitzschia* cell enumeration was performed by dividing the counted cells into two complexes, namely the *P. delicatissima* complex (TAA width < 3µm) and the *P. seriata* complex (TAA width > 3µm). Where possible, species-specific enumeration was performed as described in Turk Dermastia et al. (2020).

### 2.3.3 Strain selection

Strains were isolated as described in Section 1.5.2 and Chapter 3. The strains used for the specificity tests and calibration are listed in Table 2.3-1. In addition to several *Pseudo-nitzschia* species, the closely related *Cylindrotheca closterium* species was also used as a target for potential unwanted cross-reactions.

Table 2.3-1 Strains and associated GenBank Accession Numbers used in the development of the *Pseudo-nitzschia* specific SHA.

Strain name	Species	28S (Acc. No.)	ITS (Acc. No.)
	<i>Cylindrotheca</i>		
918 – NA1	<i>closterium</i>	MW524151	MK981230
318 – 10	<i>P. calliantha</i>	MW524145	/
817 – A2	<i>P. calliantha</i>	MK682479	MK106650
0BD041219 – B1	<i>P. delicatissima</i>	MW524150	/
318 – 5	<i>P. delicatissima</i>	MK682504	MK106642
218 – B2	<i>P. fraudulenta</i>	MK682506	/
00MA170919 – A2	<i>P. galaxiae</i>	MW524149	MW527387
818 – A1G	<i>P. galaxiae</i>	MK682500	MK690916
00BF190819 – A4	<i>P. mannii</i>	MW524148	/
817 – C1	<i>P. mannii</i>	MK682471	MK106649
MS2 DB2161219	<i>P. multistriata</i>	MW524147	MW527382
131216 – A	<i>P. multistriata</i>	MK682498	/
41217 – A4	<i>P. pungens</i>	MK106645	MK682489
318 – C2	<i>P. pungens</i>	MW524144	MK106643
BD41219 – A2	<i>P. subfraudulenta</i>	MW524146	/

### 2.3.4 Probe selection and specificity tests

#### Microarray testing

The first step in probe selection was to test the RNA on the phytoplankton M.A.R.T.A. microarray (Microbia Environnement) like that used by Barra et al. (2013). Each species was tested on a single array and if the RNA quality and concentration was sufficiently high, the species were tested in duplicates.

For each array, one microgram of total RNA was labelled and purified using ULS™ Fluorescent Label (Kreatech Biotechnology) according to the manufacturer's instructions. The degree of labelling (DoL) was determined by measuring the concentration and incorporation of the dye using a NanoDrop® Spectrophotometer (Thermo Scientific, Wilmington, DE, USA). Samples with DoL values between 1.0–3.0 were processed for hybridization. Labelled RNAs were fragmented by adding 1/10 volume of Fragmentation Buffer (salt buffer) (100 mM ZnCl<sub>2</sub> in 100 mM Tris-HCl, pH 7.0) and incubated at 70 °C for 15 min and immediately cooled to room temperature on ice. The reaction was stopped by adding 1/10 volume of 0.5 M EDTA, pH = 8. Microarray hybridizations were performed according to optimized procedures based on protocols published in Kegel et al. (2011). Briefly, 500 µg of labelled total RNA was mixed with 4X hybridization buffer containing 0.1 µM poly-dA, as a blocking agent and 10 ng of the hybridization control to a final volume of 30 µL. After sample denaturation for 5 min at 95 °C, 7.5 µL of 4X KREAblock (Kreatech Biotechnology) was added as the final blocking reagent. The hybridization mixture was equally distributed to each array and covered with lifter-slips (LifterSlips, Erie Scientific, VWR International, Radnor, PA, USA) before being placed in a SCIENION's sciHYBCHAMBER for 1 h at 65 °C. The slides were washed successively with 2× saline-sodium citrate (SSC)/10 mM EDTA/0.05% SDS for 10 min at room temperature, 0.5× SSC/10 mM EDTA for 10 min at room temperature and 0.2× SSC/10 mM EDTA for 10 min at 50 °C, each in the dark and with agitation.

The best probes were selected based on the normalized signal strength and specificity and served as templates for the design of novel probes that were used in further experiments on the SHA. A total of 9 probes were designed and selected and are under patent protection (Patent number FR 18/58362).

### First tests on SHA

The limit of detection (LOD) and specificity for each species tested, as well as false-positive reactions, were then determined in the SHA based on a 96-well microplate. The key reagent in any hybridization reaction is the hybridization buffer, which determines the stringency conditions of the probe hybridizations. Two different buffers were used during assay development, referred to here as HYB-A and HYB-B (Microbia Environnement), which had very different LODs. Standard curves were generated using complementary synthetic RNA (PCs) to allow for signal normalization. The raw absorbance read was first adjusted for the absorbance of the blank and then normalized by the coefficient of PC regression. Normalization of the signal by the PC coefficient is not necessary but is beneficial, especially when comparing signals from different plates and times.

First, 50 ng of RNA from each species was tested for each selected probe using the less sensitive HYB-A. Based on these tests, we refined our probe selection and chose a 450 nm absorbance value of 0.1 as the cut-off for a positive signal. This value was set based on repeated measurements and the experience of Microbia Environment to separate the signal from the noise. Probes that showed cross-reactivity with the non-target species at 50 ng RNA were disregarded in further experiments, although the non-target species, i.e., *Cylindrotheca closterium*, was retained in the calibration curves to see if there was a positive response at even higher concentrations. The probes that were found to be most specific in terms of species resolution as well as discriminating against negative targets were retained and will be referred to as probes Pn1, Pn1mod, Pn5 and Pn7 in the remainder of the text.

### Dilution series with selected probes

RNA dilution series were then generated; with HYB-A, the dilution series was done in 7 dilution steps – 5 ng, 10 ng, 20 ng, 40 ng, 80 ng, 160 ng, 200 ng using RNA from the *Pseudo-nitzschia* cultures and the probes from the refined selection. With HYB-B, where sensitivity is increased, there were 8 dilution steps - 0.25 ng, 0.5 ng, 1 ng, 2.5 ng, 5 ng, 10 ng, 25 ng and 50 ng. Assay sensitivity and detection limit were defined for each probe-species pair. The average RNA content per cell from all extractions performed was used to calculate cell LODs. The reported LOD values are approximate, as the RNA content per cell changes at different stages of the growth cycle and depends on the extraction efficiency.

### 2.3.5 Field samples

CTAB-extracted environmental RNA from the sampling campaigns was analysed and compared with microscopic counts to determine the reliability and applicability of the designed SHA as a supporting or alternative method for phytoplankton monitoring. We used a variety of strategies to measure the signal. When sufficient RNA was extracted from replicate samples, we averaged the signals and calculated standard deviations. In addition, when RNA concentrations were sufficiently high, we tested samples in 0.3 and 0.6 liters of filtered volume equivalents to see if there was a scaling effect in the assay response. For illustration, for each 1 litre of filtered water, the RNA elution volume was set to 15  $\mu$ l. Therefore, 0.33 litre and 0.66 litre were represented by 5 and 10  $\mu$ l of the eluate, respectively. For the analysis of the environmental samples with probes Pn1 and Pn7, we used the HYB-A protocol, while we used HYB-B with Pn1mod and Pn5 and Pn7. We first

analysed the 2015 samples from station 0DB2 with probes Pn1, Pn1mod, and Pn5, and based on the results we selected the most reliable probe, which was then used in the analysis of the 0024-2015 time-series. Samples collected in 2017 and 2018 were analysed with all probes.

## 2.4 Metabarcoding of the Phytoplankton Community (Chapter 6)

### 2.4.1 Sampling campaign for the metabarcoding analysis

For the metabarcoding campaign, a one-year campaign of monthly sampling was conducted at station 00BF (LTER-SI site) (Figure 2.1-1). Seawater was collected at the sampling stations at 0m and 5m using 10 l Niskin bottles. Part of the samples was destined for cell counting, as described in 2.1.3. For the metabarcoding portion, 1 l of seawater from both depths was filtered in triplicate onto 0.8  $\mu\text{m}$  polycarbonate filters. Samples from April, May and June were also fractionated on 20  $\mu\text{m}$ , 3  $\mu\text{m}$  and 0.8  $\mu\text{m}$  filters, each in triplicate. The filters were frozen and stored at -80 °C. Simultaneous phytoplankton counts were conducted as part of ongoing monitoring activities. Samples were fixed and counted as described in 2.1.3

### 2.4.2 Extraction of DNA for metabarcoding analysis

DNA from environmental samples destined for metabarcoding was extracted in two ways as samples were collected in triplicate. The fractionated samples were pooled so that the 20  $\mu\text{m}$  and 3  $\mu\text{m}$  fractions were combined and the 0.8  $\mu\text{m}$  fraction was separated. After a filter crushing step, where the tubes containing the filters were immersed in liquid nitrogen and crushed into small pieces using a sterile metal spatula, one replicate was analysed using the E.Z.N.A Mollusc DNA kit as described in 2.1.6, while the other two were extracted using the phenol-chloroform extraction procedure as described in the protocol of Angel (2012). 1 ml of 120 mM phosphate buffer (pH 8) and 125  $\mu\text{l}$  of TNS buffer (500 mM Tris base, 100 mM NaCl, 10% SDS) were added to the crushed filters. The cells were then lysed at -80 °C for five freeze-thaw cycles. The mixture was then centrifuged at 20,000  $\times g$  at 4 °C for 3 minutes. The supernatant was collected, and the procedure was repeated. A maximum of 1 ml of supernatant was collected. Then a volume of TE saturated phenol (pH 8) was added and mixed vigorously by vortexing, followed by a centrifugation step at 20,000  $\times g$  at 15 °C for 3 minutes. The upper phase was transferred to a fresh 2 ml tube. The mixture was then purified by adding a volume of phenol/chloroform/isoamyl alcohol (25:24:1), vortexing and centrifuging as described above. The upper phase was then removed again and mixed with a volume of chloroform/isoamyl alcohol (24:1) and repeated twice. The upper phase was then collected in a fresh low-binding DNase/RNase-free microcentrifuge tube. DNA was then precipitated by adding two volumes of PEG precipitation solution (30% polyethylene glycol and NaCl 1.6 M) and 2  $\mu\text{l}$  of glycogen (Thermo Scientific). The tube was mixed by gentle rotation and centrifuged at 20,000  $\times g$  and 4 °C for 60 min. The supernatant was decanted, and the pellet was washed with 1 ml of ice-cold 75% ethanol by inverting the tube several times. The tube was then centrifuged again at 20,000  $\times g$  and 4 °C for 20 min. The ethanol was decanted, and the pellet was dried in a speed-vac for 10 min. The pellet was resuspended in 50  $\mu\text{l}$  of low TLE buffer (pH 8). DNA concentration and quality of both phenol and E.Z.N.A replicates were measured by Nanodrop spectrophotometer and on an agarose gel (1%) by electrophoresis (60 V, 1 h).

### 2.4.3 Amplification and preparation of Illumina MiSeq library

Two markers were selected for metabarcoding, namely the 18S V9 region and a short barcode within the *rbcL* chloroplast gene. Library preparation and sequencing were performed at BMR Genomics srl (Padova, Italy). Sequencing was performed on the Illumina MiSeq platform at 300 cycles (150 pair-end read generation). The primers used for amplification of the 18S gene were 18S\_V9F (TTGTACACACCGCCCGTCGC) and 18S\_V9R (CCTTCYGCAGGTTCACCTAC) (Piredda et al., 2017). Libraries for the *rbcL* barcode were constructed using primers 708F- DEG (CCTTCYGCAGGTTCACCTAC) and R3- DEG (CCTTCTAATTTACWACWACWG), both modified from (Vasselon et al., 2017b). All primers were modified by adding universal Illumina tails, according to the Illumina protocol. All samples were analysed for the generation of visible products on an agarose gel prior to sequencing by PCR. Samples that did not generate products were excluded from sequencing.

### 2.4.4 Bioinformatics analysis pipeline for metabarcode resolution

The sequences provided by BMR genomics were already demultiplexed (each read was assigned to a sample). Sequence denoising and taxonomy assignment were performed using the DADA2 software package (Callahan et al., 2016) embedded in the R software framework (R Core Team, 2019). Reads were filtered and trimmed based on quality score assessment. For both markers, 13 bases of the 5' ends were trimmed, while the length was truncated to 150bp. Error rates were assumed using the implemented DADA2 algorithm and applied to the sample inference step, where unique amplicon sequence variants (ASV) and their relative abundance are derived. Forward (FR) and reverse (RR) reads were then merged. A sequencing problem occurred with the *rbcL* marker and most FRs and RRs did not overlap. We decided to use the `jusConcatenate= TRUE` option where 10 Ns are inserted between FR and RR. This of course introduces some errors and bias, but since the entire contig is then longer than 300bp, this error then results in a discrepancy of about 4% with the reference sequences and can be accounted for. The sequence table obtained was then cleaned of chimeric sequences and finally the taxonomy was assigned. For the 18S marker, we used the PR2 database, version 4.12 (Guillou et al., 2013), while for *rbcL* we used the Rysyt::diatom database, version 9 (Rimet et al., 2016), which we modified by adding local taxa sequences obtained during this work. In addition, we resequenced a subset of the samples for *rbcL* with correct sequencing settings, i.e. 300 Illumina cycles, to evaluate the impact of the concatenation approach on the final results. Comparison was made by visually comparing the taxonomic assignments at the lowest possible level and by correspondence analysis.

Further analyses with the taxonomically assigned tables were performed in the phyloseq package in R (McMurdie & Holmes, 2013), including calculation of  $\alpha$ -diversity indices such as Shannon-Wiener index, Pielou evenness index, and Berger-Parker dominance index, examination of specific taxa, focusing mainly on *Pseudo-nitzschia*, and recovery of species with both markers. We also performed a comparison between metabarcoding and microscopic identification of diatom genera. To compare the methods, ASVs from the metabarcoding analyses that were assigned to the same genus were agglomerated and their read counts per sample were summed. Abundance tables from all three methods (18S, *rbcL*, and counts) were then merged and the proportions of each genus per sample were calculated. The recovery of taxa by each method was assessed and  $\alpha$ - and  $\beta$ -diversities of the molecular and traditional approaches were derived. The three indices used were the Shannon-Wiener diversity index (Shannon, 1948) (Eq. 1, where  $p_i$  is the proportion of the community made up of species  $p_i$ , and  $R$  is the total number of species), the Pielou Evenness

Index (Pielou, 1966) (Eq. 2), and the Berger-Parker Dominance index (Berger & Parker, 1970) (Eq. 3), where  $N$  is the number of all species, and  $N_{max}$  is the abundance of the most abundant species.

Shannon-  
Wiener  
index

$$H = - \sum_{i=1}^R p_i * \ln p_i \quad (\text{Eq.1})$$

Pielou  
Evenness

$$J = \frac{H}{H_{\max}}, H_{\max} = \ln R \quad (\text{Eq.2})$$

Berger-  
Parker  
Dominance

$$D = \frac{N_{\max}}{N} \quad (\text{Eq.3})$$

## Chapter 3

# Identification and Ecology of *Pseudo-nitzschia* in the Gulf of Trieste

### 3.1 Author's Contributions

This article was written in collaboration between researchers from the National Institute of Biology, Marine Biology Station Piran (NIB – MBP) and Istituto Nazionale di Oceanografia e di Geofisica Sperimentale (OGS) in Trieste. The author of this dissertation is the first author of the article and contributed to its realization by performing the following: sampling, cell isolations, culturing, harvesting, DNA extractions, PCRs, TEM purification, TEM visualization and measurements with the help from Magda Tušek Žnidarič, Ph.D., phylogenetic analysis with the initial help of David Stanković, Ph.D. and Andreja Ramšak, Ph.D., ecological analysis with the help of Janja Francé, Ph.D., and Federica Cerino, Ph.D. The author also prepared most of the written text in this article. The author received permission from the publisher to include the article with this paper (Appendix A).



## Ecological time series and integrative taxonomy unveil seasonality and diversity of the toxic diatom *Pseudo-nitzschia* H. Peragallo in the northern Adriatic Sea



Timotej Turk Dermastia<sup>a,d,\*</sup>, Federica Cerino<sup>b</sup>, David Stankovič<sup>a</sup>, Janja Francé<sup>a</sup>, Andreja Ramšak<sup>a</sup>, Magda Žnidarič Tušek<sup>c</sup>, Alfred Beran<sup>b</sup>, Vanessa Natali<sup>b</sup>, Marina Cabrini<sup>b</sup>, Patricija Mozetič<sup>a</sup>

<sup>a</sup> National Institute of Biology, Marine Biology Station Piran, Fornače 41, 6330 Piran, Slovenia

<sup>b</sup> Istituto Nazionale di Oceanografia e di Geofisica Sperimentale – OGS, via Piccardi 54, 34151 Trieste, Italy

<sup>c</sup> National Institute of Biology, Department of Biotechnology and Systems Biology, Večna pot 111, 1000 Ljubljana, Slovenia

<sup>d</sup> International Postgraduate School Jožef Stefan, Jamova cesta 39, 1000 Ljubljana, Slovenia

### ARTICLE INFO

**Keywords:**  
*Pseudo-nitzschia*  
 Morphology  
 Phylogeny  
 Seasonality  
 Time series  
 Adriatic Sea

### ABSTRACT

*Pseudo-nitzschia* H. Peragallo (1900) is a globally distributed genus of pennate diatoms that are important components of phytoplankton communities worldwide. Some members of the genus produce the neurotoxin domoic acid, so regular monitoring is in place. However, the identification of toxic members in routine samplings remains problematic. In this study, the diversity and seasonal occurrence of *Pseudo-nitzschia* species were investigated in the Gulf of Trieste, a shallow gulf in the northern Adriatic Sea. We used time series data from 2005 to 2018 to describe the seasonal and inter-annual occurrence of the genus in the area and its contribution to the phytoplankton community. On average, the genus accounted for about 15 % of total diatom abundance and peaked in spring and autumn, with occasional outbreaks during summer and large inter-annual fluctuations. Increased water temperature and decreased salinity positively affected the presence of some members of the genus, while strong effects could be masked by an unsuitable definition of the species complexes used for monitoring purposes. Therefore, combining morphological (TEM) and molecular analyses by sequencing the ITS, 28S and *rbcL* markers, eight species were identified from 83 isolated monoclonal strains: *P. calliantha*, *P. fraudulenta*, *P. delicatissima*, *P. galaxiae*, *P. mannii*, *P. multistriata*, *P. pungens* and *P. subfraudulenta*. A genetic comparison between the isolated strains and other strains in the Mediterranean was carried out and *rbcL* was inspected as a potential barcode marker in respect to our results. This is the first study in the Gulf of Trieste on *Pseudo-nitzschia* time series from a long-term ecological research (LTER) site coupled with molecular data. We show that meaningful ecological conclusions can be drawn by applying integrative methodology, as opposed to the approach that only considers species complexes. The results of this work will provide guidance for further monitoring efforts as well as research activities, including population genetics and genomics, associated with seasonal distribution and toxicity profiles.

### 1. Introduction

*Pseudo-nitzschia* diatoms are well-recognized and extensively studied components of phytoplankton communities worldwide. The genus comprises 54 described species (Bates et al., 2018; Huang et al., 2019), among which 26 are known to be toxic due to the production of domoic acid (DA), a potent neurotoxin, which can cause harmful effects on human health and marine organisms (Lelong et al., 2012; Trainer et al., 2012).

Precise determination of species identity using light microscopy (LM) is inadequate for most species. Therefore, morphological observations require the use of electron microscopy and even this might not reveal the entire complexity (Amato et al., 2007; Stern et al., 2018a). There are many cases of cryptic and pseudocryptic species within distinct clades and, therefore, genetic tools are used to overcome this problem (Lundholm et al., 2006; Amato et al., 2007; Lelong et al., 2012). Phylogenetic analysis for this genus is performed by analysing the sequence data of several phylogenetic markers. The most commonly

\* Corresponding author.

E-mail address: [timotej.turkdermastia@nib.si](mailto:timotej.turkdermastia@nib.si) (T. Turk Dermastia).

<https://doi.org/10.1016/j.hal.2020.101773>

Received 3 July 2019; Received in revised form 6 January 2020; Accepted 3 February 2020

1568-9883/ © 2020 The Authors. Published by Elsevier B.V. This is an open access article under the CC BY-NC-ND license (<http://creativecommons.org/licenses/by-nc-nd/4.0/>).

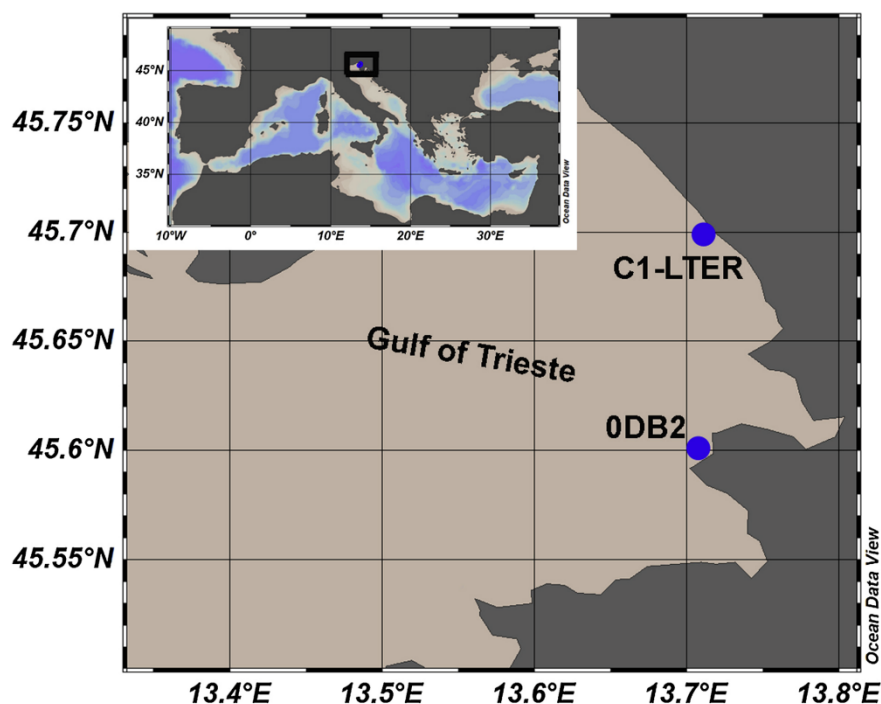


Fig. 1. Map of the study area in the northern Adriatic Sea (Mediterranean Sea) showing the location of the sampling stations (C1-LTER and ODB2).

ones used are: the large ribosomal subunit gene (28S), internal transcribed spacer regions (ITS), plastid encoded genes such as the RuBisCo large subunit (*rbcL*) (e.g. Amato et al., 2007) and mitochondrial encoded *cox1* (Lim et al., 2018). Three large clades have been identified (reviewed in Trainer et al., 2012): *P. seriata*, *P. delicatissima* and *P. pseudodelicatissima*. While the *P. seriata* group is well-resolved, the *P. delicatissima* and *P. pseudodelicatissima* complexes host a large number of cryptic species with new species continuously being described (Bates et al., 2018). In total, 12 new species and one variety have been described since 2012 in the *P. pseudodelicatissima* complex and two new species in the *P. delicatissima* complex (Bates et al., 2018, and references therein; Huang et al., 2019). Integrative taxonomy has proved key in distinguishing species complexes into distinct entities while building the capacity for researchers to gain a better understanding of their studied ecosystems (Orive et al., 2010; Lundholm et al., 2012; Ajani et al., 2013; Huang et al., 2019). This is the first step when threats such as harmful algal blooms (HABs) need to be managed correctly or even forecasted (Fehling et al., 2006; Lane et al., 2009; Anderson et al., 2010; McCabe et al., 2016). Forecasts usually deal with genus or species complex data at best, since this is usually the only long-term data available and is derived from LM counts or automatic samplers (Anderson, 2014). Like-wise, ecological studies from which models are built rely primarily on LM, although novel molecular techniques are constantly being incorporated into long-term ecological research (LTER) management giving us more insight into the complex world of plankton (Stern et al., 2018b; Zingone et al., 2019). By incorporating knowledge and data from detailed morphological and molecular analyses of locally isolated strains into LTER series, valuable information

can be obtained thus rendering the LTER stations more functional (a). Thus, LM data alone, cannot reveal potential threats due to toxic species outbreaks and may miss novel species that show up in regular samplings. Moreover, taxonomists and LTER operators commonly face the lack of prior knowledge due to the incompleteness of curated public and local reference databases. Indeed, in the advent of high-throughput sequencing techniques that are being incorporated into LTER strategies the knowledge of local protist molecular diversity is crucial for the correct and robust clustering of reads (Stern et al., 2018a).

No comprehensive integrated approach combining morphological transmission electron microscopy (TEM) examination and molecular analyses extending over a longer time period has been published so far for the Adriatic, and limited sequence data exist for the area. Existing reports on species diversity and composition rely on TEM data at best (Caroppo et al., 2005; Ljubešić et al., 2011; Marić et al., 2011; Arapov et al., 2016, 2017), while only two studies include genetic data but only for few species (Penna et al., 2013; Pugliese et al., 2017). In this respect, the northernmost region of the Adriatic Sea, the Gulf of Trieste (GoT) has hardly been studied and the true diversity of the genus remains unknown despite decade-long surveys of the phytoplankton community structure in the GoT. Considering the fact that the Gulf is an important fishing and aquaculture area, particularly for mussel farms (Solidoro et al., 2010), which applies to many Adriatic coastal areas, it is essential to assess and identify harmful algal species that can influence these activities. Until now, strains of only two species from the Adriatic have been found to produce DA in cultures, *P. delicatissima* (Penna et al., 2013) and *P. multiseriata* (Pistocchi et al., 2012), albeit at very low concentrations. Monitoring schemes at aquaculture sites along the

eastern coast of the Adriatic Sea report on the occasional presence of DA in shellfish (Ujević et al., 2010; Ljubešić et al., 2011) and phytoplankton net samples (Arapov et al., 2016) during *Pseudo-nitzschia* blooms. However, shellfish toxicity was always below the regulatory limit ( $20 \text{ mg kg}^{-1}$ ; Regulation (EC) 853 of 2004) and the causative agent of toxicity was not identified.

The main aims of this study were to unveil the diversity of the potentially toxic *Pseudo-nitzschia* species in the GoT (Adriatic Sea), by combining morphological analysis and molecular methods over a 2-year study period, and to describe the seasonal occurrence of species or groups in a 14-year long time series. We also wanted to see how this data could be coupled and utilised for LTER management and assessment of the ecological status. Finally, we wanted to re-evaluate the utility of the *rbcl* marker as a potential diatom barcode, proposed recently (Rimet et al., 2016).

## 2. Methods

### 2.1. Study area

The GoT is a shallow coastal area (maximum depth of about 25 m) at the northernmost end of the Adriatic Sea (Fig. 1). Its oceanographic properties are affected by water mass exchanges with the northern Adriatic at the open western boundary, local meteorological conditions that induce a pronounced seasonal seawater temperature cycle (from winter minima of  $5 \text{ }^\circ\text{C}$  to summer maxima  $> 26 \text{ }^\circ\text{C}$ ) and by several freshwater inputs along the northern and southern coastline (Malačić et al., 2006; Cozzi et al., 2012). The Isonzo River is the major source of freshwater and allochthonous nutrients in the GoT, and deeply influences the hydrology, biogeochemistry and productivity of this coastal area (Cozzi et al., 2012). The combination of atmospheric heating of the surface layer and increased freshwater inflow during spring, establishes a pycnocline, which intensifies during summer, while in winter the water column is well-mixed (Malačić, 1991). All these features are ultimately reflected in strong seasonal and inter-annual variability in ecosystem structure and functioning, which primarily includes changes in plankton communities and primary production (Mozetić et al., 1998; Fonda Umani et al., 2007; Talaber et al., 2018).

### 2.2. Cell isolation and cultivation

In the Slovenian part of the GoT, phytoplankton samples for isolation and cultivation were collected monthly from October 2016 to March 2018 with some additional sampling events in 2019. Five vertical and five horizontal hauls were performed at the ODB2 station ( $13^\circ 42' 20'' \text{ E}$  and  $45^\circ 35' 57'' \text{ N}$ , bottom depth 17 m) next to a mussel farm (Fig. 1).

Samples were stored in a darkened glass container and immediately returned to the laboratory where single cell isolations were performed by selecting *Pseudo-nitzschia* cells and washing them repeatedly in  $0.22 \text{ }\mu\text{m}$  filtered seawater until no other phytoplankton species were visibly present. This process was performed using drawn Pasteur pipettes under light microscopy at 100x magnification. Isolated cells were first grown in  $3 \times 4$  Nunclon® culture plates containing  $1/5x$  L1 medium.

After two weeks, the plates were checked for growing cells that were subsequently transferred to autoclaved 50 ml Erlenmeyer flasks containing L1 medium. These flasks were kept at  $20 \text{ }^\circ\text{C}$  on a 12/12 light cycle for growth and subsequent analysis. The cultures were transferred to fresh medium every two weeks.

In the Italian part of the GoT, samples were collected in October 2016 by a vertical haul at the Long-Term Ecological Research station, C1-LTER ( $45^\circ 42' 2.99'' \text{ N}$  and  $13^\circ 42' 36.00'' \text{ E}$ , bottom depth 17.5 m), located 270 m off the coast (<http://nettuno.ogs.trieste.it/ilter/BIO/history.html>). Single *Pseudo-nitzschia* cells were isolated by micropipetting and maintained as described before.

### 2.3. Light and transmission electron microscopy

Cells were measured and photographed using a light microscope (Zeiss Axio Observer.Z1 and LeicaDM2500, Germany) equipped with a digital camera (AxioCam MRC5 and Leica DFC490, Germany).

For TEM observations where only the silicate frustule is observed, cultures were cleaned and prepared using nitric and sulphuric acid to remove organic matter, as described in the Assemble protocol of Percopo and Sarno (<https://www.assemblemarine.org/assets/Uploads/Documents/tool-box/Diatom-Cleaning-with-Nitric-Sulfuric-Acids.pdf>). Briefly, 10 mL of culture was centrifuged for 10 min at 2500 rpm in a glass centrifuge tube, the supernatant was removed and the pellet resuspended in acid at a ratio of 1:1:4 (sample: 65 %  $\text{HNO}_3$ ; 98 %  $\text{H}_2\text{SO}_4$ ). The mixture was placed over a propane flame until it started to boil and the plume turned white/colourless. The mixture was then left to cool down and was serially diluted with MilliQ water followed by centrifugation to remove the residual acid. The prepared samples were subsequently stored at room temperature. A drop of the cleaned material was placed on Formvar-coated copper grids (SPI supplies® 75, 100 and 400 mesh), left to dry overnight and observed using transmission electron microscopy (Philips CM 100 equipped with a Bisocan CCD camera and Olympus Quemesa iTEMon FEI EM208).

### 2.4. DNA extraction, PCR amplification and sequencing

DNA was extracted from cultures in the exponential growth phase, which was established by counting cells in a Fuchs-Rosenthal counting chamber on successive days. The E.Z.N.A. Mollusc DNA (Omega Biotek) and Quick-DNA™ Fungal/Bacterial Miniprep (Zymo Research) kits were used for the extraction process. Different culture volumes (10–50 mL) were centrifuged and the pellet was homogenized using a sterilized hand-held portable homogenizer. The material was then resuspended in the provided buffer with proteinase K. Subsequent steps in DNA extraction followed the producer's guidelines. Polymerase chain reaction (PCR) was performed with a series of primers targeting three gene fragments; namely, the entire transcribed spacer region of the nuclear rDNA (ITS1/5.8S/ITS2), here on ITS, the large ribosomal subunit (28S) gene and the gene encoding the large subunit of the ribulose-1.5-bisphosphate carboxylase/oxidase protein (*rbcl*). PCR amplification was performed by a recombinant *Taq* DNA polymerase (Thermo-Fisher Scientific) or TopTaq polymerase (Qiagen) in a total volume of  $25 \text{ }\mu\text{L}$ . The PCR protocols for the respective gene markers and the

**Table 1**  
PCR protocols and primers.

Enzyme	Marker	Primer set	Primer reference	Protocol				
TF Taq	ITS1-2	ITS1/ITS4	White et al., 1990	1:94 °C 5 min	2: 94 °C 45 s	3: 52 °C 30 s	4: 72 °C 90 s [2–4 35x]	5:72 °C 8min
TF Taq	28S	DIR-E/D3B-R	Nunn et al., 1996 Scholin et al., 1994	1:94 °C 5 min	2: 94 °C 45 s	3: 52 °C 30 s	4: 72 °C 90 s [2–4 35x]	5:72 °C 8min
TopTaq	ITS1-2	ITS-F/ITS-R	Murray et al., 2012	1:94 °C 3 min	2: 94 °C 30 s	3: 52 °C 30 s	4: 72 °C 60 s [2–4 35x]	5:72 °C 10min
TopTaq	28S	DIR-E/D3B-R	Scholin et al., 1994 Nunn et al., 1996	1:94 °C 5 min	2: 94 °C 45 s	3: 52 °C 30 s	4: 72 °C 60 s [2–4 35x]	5:72 °C 10min
TopTaq	<i>rbcl</i>	DP <sub>rbcl</sub> 1/7	Jones et al., 2005	1:94 °C 5 min	2: 94 °C 45 s	3: 52 °C 30 s	4: 72 °C 90 s [2–4 35x]	5:72 °C 10min

corresponding primers that were used are presented in Table 1. In addition, internal primers I1F and I1R were used for sequencing the *rbcl* region for some problematic amplicons (Amato et al., 2007). Sanger sequencing was carried out by Macrogen Inc., using the same primers as for previous amplification (Table 1). Chromatograms were quality checked and assembled in Chromas Pro (v.2.1.8.). The identity of sequences was confirmed with BLASTn service.

### 2.5. Phylogenetic analysis

All available sequences of *Pseudo-nitzschia* species from the GenBank database were aligned with our sequences and included in the final dataset. Sequences were aligned using MAFFT 7 (Katoh and Standley, 2013), applying different strategies depending on the marker. 28S and *rbcl* sequences were aligned using the G-INS-1 progressive method, while both the G-INS-1 progressive method and the FFT-NS-1 iterative method were tested for ITS.

Gene markers (ITS2, 28S and *rbcl*) were analysed separately in order to obtain distinct phylogenies. The ITS2 alignment was 260bp, while phylogenies of 28S and *rbcl* were constructed using 769bp and 1220bp alignments, respectively. The best evolutionary models were selected for each marker in jModelTest (Posada, 2008). The selected model was used for Bayesian inference of phylogenies, using MrBayes v.3.2.6 (Ronquist et al., 2012). For each marker, the analysis was run for 5,000,000 generations in 4 parallel chains and until the average standard deviation had fallen below 0.01. Chain diagnostics were performed in Tracer (v. 1.7.1.; Rambaut et al., 2018) where the estimated sample size (ESS) was confirmed to be above 700 for the LnL parameter and well above 1000 for all other parameters that are estimated in the Markov chain. An additional 312bp-long alignment of *rbcl* sequences was performed and phylogeny reconstructed to compare the species and strain recovery of the proposed *rbcl* diatom barcode (Rimet et al., 2016; Vasselon et al., 2017). Pairwise distances were calculated with MEGA7 (Kumar et al., 2016).

A TCS network (Templeton et al., 1992; Clement et al., 2000) was constructed using the PopArt software package (Leigh and Bryant, 2015) in order to obtain an insight into haplotype differentiation between different *Pseudo-nitzschia* species and strains found in the Adriatic and elsewhere in the Mediterranean Sea. The TCS network was constructed using sequences from the ITS2 and *rbcl* region. For the ITS2 network, we geotagged the sequences according to whether they were found in the GoT (on the Italian and Slovenian side separately), the north-west Adriatic (Pesaro) (Penna et al., 2013; Pugliese et al., 2017), Tyrrhenian Sea (Gulf of Naples, GoN) (several publications), NE Mediterranean (Greek coastal waters) (Moschandrea et al., 2012), NW Mediterranean (Catalan Coast) (Quijano-Scheggia et al., 2008b, 2009), and sequences belonging to strains outside the Mediterranean. Because of the highly divergent nature of ITS2, the alignment used in the phylogenetic tree reconstruction was selected for the most conserved sites using least stringent conditions defined in GBLOCKS (Castresana, 2000), to counteract alignment issues that create masked sites in parsimony networks. Likewise, *rbcl* sequences were geotagged into GoT (Italian and Slovenian side), GoN (Amato et al., 2007; D'Alelio and Ruggiero, 2015), the NW Mediterranean (Elandaloussi et al., unpubl.), and sequences belonging to strains outside the Mediterranean. The geographic location of the sequence was obtained from the location identifier in GenBank where possible.

### 2.6. Environmental characterization and phytoplankton analysis

To describe the typical seasonal cycle and inter-annual variability of *Pseudo-nitzschia* in the GoT, an 14-year long time-series of *Pseudo-nitzschia* grouped into two complexes, i.e. *seriata* and *delicatissima* complex, was considered. Samples were collected monthly from 2005 to 2018 at station C1-LTER (Fig. 1) for both environmental and phytoplankton data. In addition, phytoplankton counts of the two *Pseudo-nitzschia*

complexes were also performed on seawater samples collected at station ODB2 (period 2016–2019) and designated for species isolation and cultivation (see 2.2).

CTD temperature and salinity profiles were obtained with Idronaut Ocean Seven (models 401 and 316) and a SBE 19plus SEACAT multi-parametric probes. Discrete seawater samples were collected with 5-L Niskin bottles at four depths (0.5, 5, 10, 15 m). Dissolved inorganic nutrient concentrations were determined colorimetrically on filtered samples with a Bran + Luebbe Autoanalyzer 3, up to December 2013, and afterwards with a QuAatro (Seal Analytical), according to Hansen and Koroleff (1999).

For phytoplankton analysis, the samples were fixed with prefiltered and neutralized formaldehyde (1.6 % final concentration) (Thronsen, 1978). A variable volume of seawater (10–50 ml) was settled in an Utermöhl chamber depending on cell abundance (Utermöhl, 1958; Zingone et al., 2010). Cells (minimum 200) were counted along transects (1–2) at 400x magnification using inverted microscopes. Additionally, half of the sedimentation chamber was also examined at 200x magnification for more precise identification of less abundant microphytoplankton (> 20 µm) taxa. Species belonging to the *Pseudo-nitzschia* genus were separated into the two complexes distinguished in LM basing, according to cell width: *P. spp. delicatissima* complex (cell width < 3 µm) and *P. spp. seriata* complex (cell width > 3 µm). Additionally, *P. multistriata* and *P. pungens* were identified based on the sigmoid shape of the cell in girdle view and the visibility of striae, respectively. At C1-LTER, *P. cf. galaxiae* was also identified based on thin cell rostrata, while at ODB2, *P. cf. fraudulenta* (composed of *P. fraudulenta* and *P. subfraudulenta*) was identified based on valve dimensions.

### 2.7. Statistical analysis

A non-parametric Spearman rank order correlation was used to assess the relationship among oceanographic parameters and abundance of *Pseudo-nitzschia* complexes. Analysis of Similarity (one-way ANOSIM) was carried out (1000 permutations) to test the significance of similarities in biological features among seasons and years.

Principal Component Analysis (PCA) was performed on a Euclidean distance matrix of selected normalized physical and chemical variables (temperature, salinity and dissolved inorganic nutrients) to characterize and differentiate the seasons. The centroids of the observations of each month were calculated and plotted against the PC1 vs. PC2 combination because they expressed most of the variance of the dataset. Furthermore, the log(X + 1) transformed abundances of *Pseudo-nitzschia* taxa identified with LM were fitted as supplementary variables (vectors) onto the ordination space.

We also conducted a non-metric multidimensional scaling analysis (NMDS) with species abundance data to further inspect potential seasonal patterns and the ordination of species complexes versus specific species in multidimensional space.

All these analyses were performed using the PRIMER software package (v.7).

Finally, the data from ODB2, where isolations took place, was used in a proof-of-concept constrained correspondence analysis (CCA) to demonstrate how feeding molecular data into LTER management can improve research and monitoring. The methodological procedure for this is included in the supplementary data (S4).

The CCA of isolation-currated data was performed using R Statistical Software (R Core Team, 2019) and the “Vegan” package (Oksanen et al., 2019).

## 3. Results

### 3.1. Seasonal cycle and inter-annual variability of environmental properties, phytoplankton community and the *Pseudo-nitzschia* genus

The C1-LTER coastal station was characterized by a strong seasonal

T. Turk Dermastia, et al.

Harmful Algae 93 (2020) 101773

cycle with cold winters ( $9.20 \pm 1.44$  °C, on average) and warm summers ( $22.62 \pm 2.17$  °C, on average) (S1: A). The highest temperature ( $28.34$  °C) of the time series was measured in July 2015. Surface salinity drops that were registered during certain periods of almost each year indicate freshwater inputs of riverine and/or atmospheric origin (S1: B). The most evident and long-lasting persistence of a cooler sub-surface water layer was observed in 2010.

Dissolved inorganic nitrogen (DIN) concentrations, calculated as the sum of ammonium, nitrite and nitrate concentrations, displayed higher values in autumn and winter with increases in spring in some years (S1: C). Elevated concentrations of DIN in the surface layer were particularly evident in years 2009, 2010, 2013 and 2014. Phosphate concentrations showed interannual variability but not a clear seasonality; on average, higher values were recorded in late autumn-early winter and in August (S1: D). Finally, silicate concentrations were generally higher in summer and winter in the deeper part of the water column, while surface peaks were measured in the spring of certain years (S1: E).

Considering the 14-year long phytoplankton time series (2005–2018) of the C1-LTER station, in terms of relative abundance, about 31 % of phytoplankton were represented by diatoms, and *Pseudo-nitzschia* spp. accounted for about 15 % of total diatoms averaged across all samples (Fig. 2). *Pseudo-nitzschia* species were generally present all year round with pronounced autumn blooms occurring annually and reaching 70–80 % of total phytoplankton community abundance. Autumn blooms were characterized by both the *delicatissima* and *seriata* complexes, while occasional spring blooms were due to the *delicatissima* complex (Fig. 3). The *P. delicatissima* complex was the main contributor to the total abundance of the genus, with cell numbers reaching  $2.3 \times 10^6$  cells  $L^{-1}$ , while the *P. seriata* complex showed much lower abundances, rarely exceeding  $10^4$  cells  $L^{-1}$ . There was one extreme event, however, in April 2011 when the *P. seriata* complex reached  $1.4 \times 10^6$  cells  $L^{-1}$  (Fig. 3C). The abundances of both complexes fluctuated at the inter-annual scale; however, these changes did not appear significant in the ANOSIM analysis. The ANOSIM analysis did not show any overall significant difference between years and seasons, except for some years that differed significantly from the others ( $R = 0.11$ ,  $p = 0.01$  and  $R = 0.051$ ,  $p = 0.01$ , respectively).

To summarize the observations from the ecological time series, a PCA was performed. The ordination of samples is largely forced by temperature and salinity that shape PC2 (Fig. 4). The structuring of the complexes demonstrates the seasonal preference of the *seriata* complex for the winter/autumn period and the *delicatissima* complex for the spring/summer period. The latter is also evidenced by the statistically significant although weak correlation coefficient ( $\rho = 0.197$ , Table 2). A statistically significant correlation was also found between salinity and the *seriata* complex, while the whole genus was negatively correlated with silicate and inorganic nitrogen species. The PCA was coupled with data on *P. multistriata*, *P. pungens* and *P. galaxiae*. The structuring

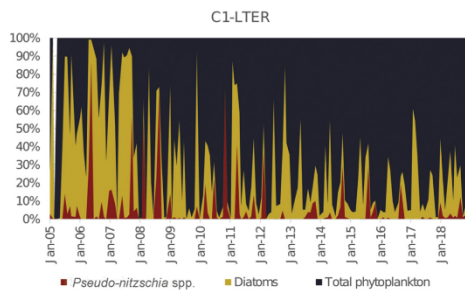


Fig. 2. Percentage abundances of *Pseudo-nitzschia* spp., diatoms and total phytoplankton from 2005 to 2018 at the station C1-LTER in the Gulf of Trieste.

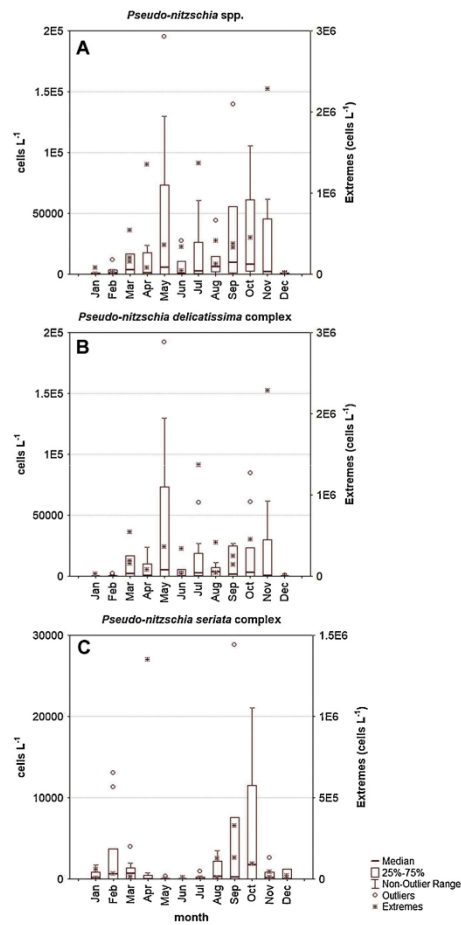


Fig. 3. Seasonal cycle of *Pseudo-nitzschia* spp. (A), *P. delicatissima* complex (B) and *P. seriata* complex (C) at the C1-LTER station in the Gulf of Trieste from 2005 to 2018. In the box plot of cell abundances, the bold line represents the median, the box the 25<sup>th</sup> and 75<sup>th</sup> percentiles of the distribution, the whisker the non-outlier range, the circle the outliers and the stars the extremes.

of *P. multistriata* into even more pronounced winter conditions is self-explanatory but this analysis shows that when reliable single-species data are considered the structure is more apparent than when the species are grouped into complexes that are often phylogenetically and ecologically incorrect, as will be demonstrated in the following section.

### 3.2. Diversity of the genus *Pseudo-nitzschia* in the GoT

Eight species of *Pseudo-nitzschia* were identified from 83 monoclonal strains isolated in the GoT (69 in Slovenian and 16 in Italian waters). Table 3 presents the species that have been identified along with the corresponding identification method and the number of strains within the respective species that have been sequenced or examined with TEM.

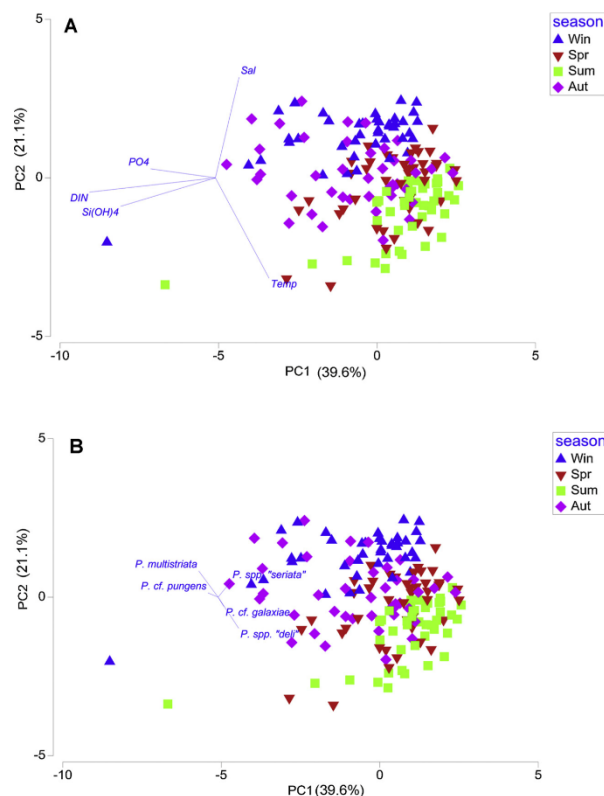


Fig. 4. Principal Component Analysis (PCA) ordination diagram of the selected variables (A). Symbols represent the centroids of the observations in each month. In B, the biological variables are fitted as supplementary variables. Temp: temperature; Sal: salinity; DIN: dissolved inorganic nitrogen; PO<sub>4</sub>: phosphate; Si(OH)<sub>4</sub>: silicate.

Accession numbers of sequenced strains are provided in Supplementary Table 1.

The autumn blooms of the *P. delicatissima* complex were characterized by isolates of *P. calliantha* and *P. mannii*, while the spring blooms of cells assigned to the *P. delicatissima* complex were characterized by isolates belonging to *P. delicatissima*. *P. galaxiae* cells were isolated only in August and September; nevertheless, LM identified cells that could have belonged to these species were also observed in the

spring months. The *seriata* complex was more abundant in late autumn, winter and early spring. Of the species belonging to this complex, *P. multistriata* was isolated only in December and January, *P. subfraudulenta* in October and December, *P. fraudulenta* only in February, and *P. pungens* in December and March. The only species that was isolated in all seasons was *P. calliantha*. The species are described below and their morphometric data are summarized in Table 4. We also provide species-complex fluctuation data overlaid with species

Table 2

Spearman rank correlations among the water column integrated abundances of *Pseudo-nitzschia* taxa with environmental variables at the C1-LTER station for the period 2005–2018.

	Temperature	Salinity	PO <sub>4</sub>	Si(OH) <sub>4</sub>	DIN	NO <sub>2</sub> +NO <sub>3</sub>	<i>P. delicatissima</i> complex	<i>P. seriata</i> complex	<i>Pseudo-nitzschia</i> spp.
Temperature	1								
Salinity	-0.424***	1							
PO <sub>4</sub>	-0.105	0.045	1						
Si(OH) <sub>4</sub>	-0.105	-0.125	0.296***	1					
DIN	-0.374***	-0.234**	0.338***	0.535***	1				
NO <sub>2</sub> +NO <sub>3</sub>	-0.533***	-0.152*	0.244**	0.481***	0.913***	1			
<i>P. delicatissima</i> complex	0.197*	-0.187*	-0.157*	-0.047	-0.095	-0.088	1		
<i>P. seriata</i> complex	-0.059	0.202**	-0.036	-0.116	-0.010	0.004	0.063	1	
<i>Pseudo-nitzschia</i> spp.	0.199**	-0.079	-0.095	-0.189*	-0.172*	-0.159*	0.766***	0.508***	1

**Table 3**

List of species identified in the Gulf of Trieste with information about the number of strains isolated for each species, isolation site and season (I: Italy; S: Slovenian; W: winter; SP: spring; SU: summer; A: autumn), observation methods (LM: light microscopy; TEM: transmission electron microscopy) and sequenced genes (28S, ITS, *rbcL*). For full strain summary see Supplementary Table 1.

Species	Strain number	Location	Season isolated	Methods
<i>P. calliantha</i>	21	I,S	SP,SU,A,W	LM,TEM,ITS,28S, <i>rbcL</i>
<i>P. delicatissima</i>	20	S	SP	LM,TEM,ITS,28S, <i>rbcL</i>
<i>P. fraudulenta</i>	5	S	W	LM,TEM,ITS,28S, <i>rbcL</i>
<i>P. galaxiae</i>	6	S	SU	LM,TEM,ITS,28S, <i>rbcL</i>
<i>P. mannii</i>	14	I,S	SU,A	TEM,ITS,28S, <i>rbcL</i>
<i>P. multistriata</i>	13	S	W	LM,TEM,ITS,28S, <i>rbcL</i>
<i>P. pungens</i>	6	S	SP,W	LM,TEM,ITS,28S, <i>rbcL</i>
<i>P. subfraudulenta</i>	3	I,S	A	LM,TEM,ITS

isolation data for station ODB2 (Fig. 5).

*P. calliantha* Lundholm, Moestrup & Hasle (Fig. 6A-C)

The cells are linear in valve view (Fig. 6A) with the apical axis ranging between 68 and 82  $\mu\text{m}$  and the transapical axis between 1.4 and 2.36  $\mu\text{m}$ . A central larger interspace is present (Fig. 6B). The density of striae and fibulae in 10  $\mu\text{m}$  ranges between 35 and 39 and between 18 and 22, respectively. Each stria contains one row of poroids, with 4–6 poroids in 1  $\mu\text{m}$  (Fig. 6C). Poroids are segmented with 2–12 segments in each poroid, organised in a typical flower-like pattern (Fig. 6C).

*P. mannii* Amato & Montresor (Fig. 6D-F)

The cells resemble those of *P. calliantha*, but are typically longer and wider (Fig. 6D, Table 4). The two species are very hard to tell apart. The structure of the poroids is the only distinct characteristic; in *P. mannii*, they do not display flower-like organisation and are generally less segmented (2–7 sectors per poroid) (Fig. 6E, F).

*P. delicatissima* (Cleve) Heiden (Fig. 6G-I)

The cells are lanceolate in valve view (Fig. 6G) with the apical axis ranging between 20 and 76  $\mu\text{m}$  and the transapical axis between 1.4 and 2.0  $\mu\text{m}$ . A central larger interspace is present (Fig. 6I). The density of striae and fibulae in 10  $\mu\text{m}$  ranges between 35 and 40 and between 18 and 26, respectively. Each stria contains two rows of poroids with 8–12 poroids in 1  $\mu\text{m}$  (Fig. 6I). Poroids are not segmented.

*P. galaxiae* Lundholm & Moestrup (Fig. 7)

Three distinct morphotypes of this species have been identified. In natural samples, the cells were mostly solitary, but the medium

morphotype occasionally formed two-cell chains. The transapical axis of the three morphotypes were similar at the widest part and ranged between 1.3 and 2.8  $\mu\text{m}$ , while the apical axis greatly differed, ranging between 45 and 57  $\mu\text{m}$ , 24 and 40  $\mu\text{m}$  and 8.5 and 11  $\mu\text{m}$  for the largest (Fig. 7 A–E), medium (Fig. 7 J–M) and small (Fig. 7 F–I) morphotypes, respectively. The large morphotype was exclusively tapered towards the rostrate ends, while the medium and small morphotype showed greater variability in this characteristic. We also observed variability in the arrangement of poroids with some cells having them closely arranged along the interstriae (Fig. 7 H), while others having them densely scattered around the striae (Fig. 7E).

*P. pungens* (Grunow ex Cleve) Hasle (Fig. 8A-C)

The cells are linear-lanceolate (Fig. 8A, B). The apical axis ranges between 24 and 121  $\mu\text{m}$  and the transapical axis between 2.4 and 4.2  $\mu\text{m}$ . The central larger interspace is not present. The density of striae and fibulae in 10  $\mu\text{m}$  ranges between 8 and 13 and between 8 and 14, respectively. Each stria contains two rows of unsegmented poroids (2–4/  $\mu\text{m}$ ) (Fig. 8C).

*P. fraudulenta* (Cleve) Hasle (Fig. 8D-F)

The cells are lanceolate (Fig. 8D). The apical axis ranges between 72 and 110  $\mu\text{m}$  and the transapical axis between 4.0 and 6.5  $\mu\text{m}$ . The central larger interspace is present (Fig. 8E). The density of striae and fibulae in 10  $\mu\text{m}$  ranges between 21 and 24 and between 20 and 24, respectively. Each stria contains two rows of poroids (5–6/  $\mu\text{m}$ ), which have several segments (Fig. 8F).

*P. subfraudulenta* Hasle (Fig. 8G-I)

The cells are linear-lanceolate (Fig. 8G). The apical axis ranges between 65 and 106  $\mu\text{m}$  and the transapical axis between 4.3 and 6  $\mu\text{m}$ . The central larger interspace is present (Fig. 8H). The density of striae and fibulae in 10  $\mu\text{m}$  ranges between 23 and 28 and between 12 and 17, respectively. Each stria contains two rows of poroids (5–6/  $\mu\text{m}$ ), which have several segments (Fig. 8I).

*P. multistriata* H.Takano (Fig. 8J-L)

The cells are lanceolate in valve view and sigmoid in girdle view with typically curved apical ends (Fig. 8J). The apical axis ranges between 34 and 60  $\mu\text{m}$  and the transapical axis between 2.2 and 4.0  $\mu\text{m}$ . The central larger interspace is not present. The density of striae and fibulae in 10  $\mu\text{m}$  ranges between 36 and 46 and between 22 and 28, respectively. Each stria contains two rows of unsegmented poroids (5–7/  $\mu\text{m}$ ) (Fig. 8K, L).

**Table 4**

Morphometric measurements of strains isolated in the Gulf of Trieste.

Species	Apical axis ( $\mu\text{m}$ )	Transapical axis ( $\mu\text{m}$ )	CIS	Fibulae in 10 $\mu\text{m}$	Rows of poroids per stria	Poroids in 1 $\mu\text{m}$	Poroids in 1 $\mu\text{m}$	Poroid sectors
<i>P. calliantha</i>	<b>68-88.2</b>	<b>1.4-2.4</b>	+	<b>16-22</b>	<b>33-39</b>	<b>1</b>	<b>4-6</b>	<b>2-12</b>
	<i>77.88 ± 3.67 (91, 6)</i>	<i>2.47 ± 0.9 (86, 6)</i>		<i>19.4 ± 1.4 (48, 6)</i>	<i>36.9 ± 1.5 (48, 6)</i>		<i>4.8 ± 0.5 (53, 6)</i>	<i>7.4 ± 2.3 (62, 4)</i>
<i>P. delicatissima</i>	<b>60-63</b>	<b>1.4-1.9</b>	+	<b>22-26</b>	<b>40-42</b>	<b>2</b>	<b>10-12</b>	
	<i>61.36 ± 0.81 (17, 3)</i>	<i>1.64 ± 0.17 (11, 1)</i>		<i>23.8 ± 1.7 (10, 1)</i>	<i>40.9 ± 1 (10, 1)</i>		<i>11 ± 0.9 (10, 1)</i>	
<i>P. fraudulenta</i>	<b>72-108</b>	<b>4.1-8.3</b>	+	<b>20-24</b>	<b>21-25</b>	<b>1-2</b>	<b>5-7</b>	<b>4-8</b>
	<i>92.4 ± 9.23 (20, 2)</i>	<i>5.87 ± 0.86 (20, 2)</i>		<i>21.6 ± 1.2 (18, 2)</i>	<i>23.1 ± 1 (18, 2)</i>		<i>5.8 ± 0.6 (20, 2)</i>	<i>6.1 ± 1.2 (18, 2)</i>
<i>P. galaxiae</i>	<b>8.5-57.4</b>	<b>1.3-2.8</b>	+	<b>20-30</b>	<b>50-70</b>	<b>many</b>	<b>n.d.</b>	<b>n.d.</b>
	<i>30.96 ± 14.12 (42, 6)</i>	<i>2.01 ± 0.32 (43, 6)</i>		<i>23.8 ± 3.1 (38, 6)</i>	<i>59.6 ± 3.9 (38, 6)</i>			
<i>P. mannii</i>	<b>57-107.7</b>	<b>1.5-2.9</b>	+	<b>14-25</b>	<b>32-39</b>	<b>1</b>	<b>4-6</b>	<b>2-7</b>
	<i>89.93 ± 6.33 (242, 10)</i>	<i>1.98 ± 0.31 (157, 11)</i>		<i>19.6 ± 2 (83, 11)</i>	<i>35.3 ± 1.6 (93, 11)</i>		<i>4.6 ± 0.6 (105, 11)</i>	<i>4.2 ± 1.5 (51, 3)</i>
<i>P. multistriata</i>	<b>30-60</b>	<b>2.4-4.6</b>	-	<b>24-28</b>	<b>34-45</b>	<b>2</b>	<b>7-13</b>	<b>not segmented</b>
	<i>50.15 ± 7.48 (45, 4)</i>	<i>3.35 ± 0.51 (45, 4)</i>		<i>25.3 ± 1.2 (29, 4)</i>	<i>38.7 ± 2.3 (29, 4)</i>		<i>10.7 ± 1.17 (29, 4)</i>	
<i>P. pungens</i>	<b>80-92</b>	<b>2.7-5.9</b>	-	<b>9-13</b>	<b>10-13</b>	<b>2</b>	<b>2-4</b>	<b>not segmented</b>
	<i>86.21 ± 3.66 (24, 3)</i>	<i>3.75 ± 0.96 (24, 3)</i>		<i>11.4 ± 1.2 (10, 1)</i>	<i>11.2 ± 0.9 (10, 1)</i>		<i>2.97 ± 0.45 (35, 1)</i>	
<i>P. subfraudulenta</i>	<b>88.6-134</b>	<b>3.5-6.5</b>	+	<b>13-18</b>	<b>24-25</b>	<b>2</b>	<b>4-6</b>	<b>3-7</b>
	<i>112.16 ± 15.8 (72, 3)</i>	<i>4.57 ± 0.86 (40, 3)</i>		<i>14.9 ± 1.2 (18, 3)</i>	<i>24.2 ± 0.4 (22, 3)</i>		<i>5.1 ± 0.46 (33, 3)</i>	<i>5.2 ± 1.3 (17, 1)</i>

CIS: central interspace. Range of values in bold; means  $\pm$  SD in italics; number of measurements and number of strains measured in parentheses; n.d.: no data.

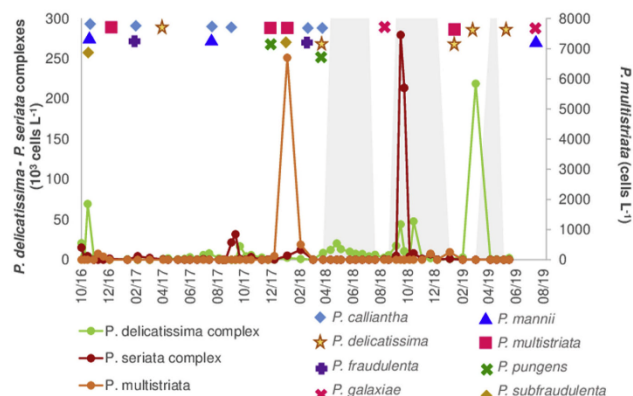


Fig. 5. Temporal distribution of abundances of *Pseudo-nitzschia* taxa identified in LM (lines) at ODB2 station in the Gulf of Trieste from October 2016 to August 2019 and presence of species isolated and identified by molecular analysis (symbols). Grey-shaded areas indicate periods where isolations were not conducted.

### 3.3. Phylogenetic inference based on ITS2, 28S and *rbcl*.

Because the ITS segment is very variable and only ITS2 sequences were available from the Italian strains, we constructed the phylogenies based on the ITS2 marker only, while the entire ITS region was sequenced and the sequences deposited in GenBank. The reconstructed phylogenies grouped our strains into 8 species (Figs. 9–11). We were unable to obtain *rbcl* sequences of *P. subfraudulenta*. The overall average *p*-distances were as follows: 28S: 0.033, *rbcl*: 0.053, ITS2: 0.179. Clearly, ITS2 was the most divergent marker despite having the shortest alignment of all markers used. There were some discrepancies among the different markers, particularly for the *calliantha/mannii* clade. The resolution of the two species concerned is supported by all three markers, but for the *rbcl* phylogeny neither *P. mannii* nor *P. calliantha* clades are sufficiently supported, although the group as a whole is monophyletic with high support. The *rbcl* phylogeny (Fig. 9) constructed in this study comprised of 22 species (40 % of described) of *Pseudo-nitzschia* and included *Fragilariopsis kerguelensis* that, unlike in the 28S phylogeny and the ITS2 phylogeny, clusters outside the *Pseudo-nitzschia* genus. We note that the groups defined by Lim et al. (2018) are well-recovered with monophyletic Groups I, II and III, even though Group II is only represented by *P. calliantha*. *P. fryxelliana*, sister taxa to the *P. fraudulenta* group clusters next to Group IV, which in this case is polyphyletic. The *rbcl* marker was also able to detect intraspecific variation, with the resolution comparable to ITS2 (Fig. 11) and better compared to the 28S marker (Fig. 10).

Intraspecific variation is apparent in the ITS2 and *rbcl* trees for *P. pungens*, *P. delicatissima*, *P. multistriata* and *P. galaxiae*. With 28S, intraspecific variation is detected only in *P. delicatissima* and to a limited extent in *P. galaxiae*, but interestingly not in *P. pungens*, which includes three described varieties. In addition, there is some variation in *P. calliantha*, which has also been revealed in the ITS2 phylogeny. As far as our strains are concerned, there is no pronounced variation between strains of the same species. The only exception is *P. galaxiae*; two strains isolated from the same net tow belong to two different clades in the *rbcl* phylogeny (Fig. 9) as well as in the ITS phylogeny (Fig. 11). On the contrary, although the 28S marker recognizes several clusters (ribotypes) within the *P. galaxiae* group with varying degrees of support (Fig. 10), our two strains fall within the same cluster. The mean *p*-distance (0.021) in the ITS2 marker between *P. galaxiae* strains, including those isolated in this study, is larger than the distances between some species (e.g. the mean distance between *P. sabit* and *P. decipiens* is

0.019). The same is true for the *rbcl* marker where the mean *p*-distance between *P. galaxiae* strains is 0.015, while *P. calliantha* and *P. mannii* are only separated by a mean *p*-distance of 0.006. Strains of *P. galaxiae* and *P. delicatissima* isolated in 2019 were not included in the phylogenetic trees, while only the *rbcl* of the former and both the ITS and *rbcl* of the latter were obtained.

Lastly we would like to point out the phylogenetic tree reconstructed with the 312bp-long *rbcl* barcode region (S3), which shows almost identical recovery of both species and strains compared to the 1220bp-long alignment. The support levels were somewhat lower and the delineation of *P. linea* and *P. americana*, which are very closely related, was not achieved. Otherwise, the barcode performs very well, and even recovers the strain diversity within *P. galaxiae*.

### 3.4. Network analysis and the distribution of Mediterranean *Pseudo-nitzschia* species

The grouping and connections of sequences based on statistical parsimony, coupled with geographical data in TCS networks, are presented in Fig. 12. More sequences were used in this analysis compared to the phylogenetic analysis (392, 258bp for ITS2, and 1111, 1219 for *rbcl*), including the recently described *P. qiana* and *P. chiniana* (ITS2), and the additionally sequenced strains of *P. galaxiae* (*rbcl* only) that we isolated in August and September 2019. There were 68 and 78 parsimony-informative sites in the *rbcl* and ITS2 networks, respectively. The nucleotide diversity in the ITS2 network was much higher than in the *rbcl*. In both networks, the Mediterranean species with haplo and ribotype clusters, without representative Mediterranean strains, are only *P. pungens* (*P. pungens* 2, Fig. 12A; *P. pungens* 2–3, Fig. 12B) and *P. delicatissima* (*P. delicatissima* 2–3, Fig. 12A; *P. delicatissima* 2, Fig. 12B) with the addition of a single *P. multistriata* haplotype of non-Mediterranean origin present in the *rbcl* network. Of course, many species are yet to be found in the Mediterranean Sea, as evidenced by both networks, although some species have already been identified but lack the representative sequence data. Ten species with representative *rbcl* sequences were obtained from Mediterranean strains alone. The *rbcl* dataset is well-represented by Mediterranean strains, with nearly all the species identified in the basin being sequenced for this marker. The only exception is *P. subfraudulenta*. We were also unable to obtain quality *rbcl* sequences for this species. The networks are generally congruent with the Bayesian phylogenies, with considerable substructure seen particularly in Group IV, especially in *P. galaxiae* and *P. delicatissima* in

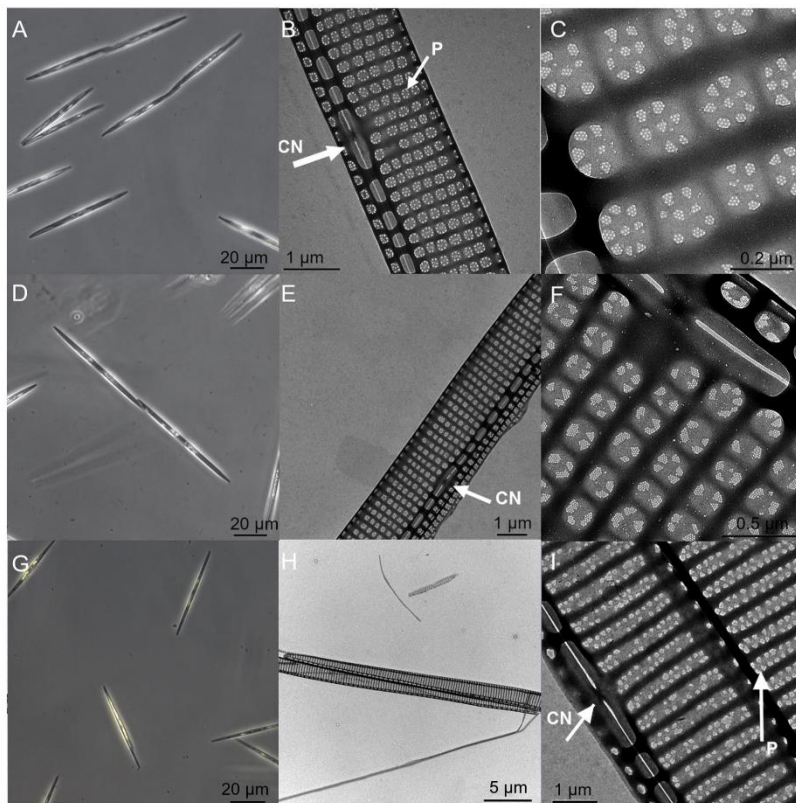


Fig. 6. Micrographs of *Pseudo-nitzschia* species identified in the Gulf of Trieste: *P. calliantha* (A–C), *P. mannii* (D–F), *P. delicatissima* (G–I). (A) Live cells, single and in chains, LM. (B) Central part of the valve showing the presence of the central nodule (CN) and poroid (P) organization (arrows), TEM. (C) Detail of poroid structure, TEM. (D) Girdle view of live cells in chain, LM. (E) Central part of the valve showing the presence of the central nodule (CN, arrow), TEM. (F) Detail of poroids showing the radial arrangement of sectors, TEM. (G) Single live cells, LM. (H) Part of the valve, TEM. (I) Central part of the valve showing the presence of the central nodule (CN) and two rows of poroids (P) (arrows), TEM.

both networks (Fig. 12A, B), as well as the *decipiens/sabit* group in the ITS2 network. Mediterranean strains, including the ones obtained in this study, generally cluster together and constitute a part of the main global haplotypes, with some notable exceptions. The first is the *P. delicatissima* group 1, which contains only Mediterranean strains. Likewise, strains of *P. brasiliensis* from the NE and the NW Mediterranean form distinct haplogroups from the main haplogroup, but also between themselves (Fig. 12A). Other distinct Mediterranean haplotypes are seen in *P. calliantha* with two and *P. arenysensis* with several slightly different strains from the main haplogroup. There is also a haplogroup comprising strains of *P. dolorosa* and *P. cf. delicatissima* from the NE Mediterranean (*P. del. 4*, Fig. 12A), which is probably a cryptic species within the *P. delicatissima* complex. As noted in the previous section, the great diversity within *P. galaxiae* is also reflected at the geographical level, although we lack non-Mediterranean strains for comparison. There is a large haplogroup that comprises strains from GoT, NW and NE Mediterranean coastal waters in the ITS2 network (Fig. 12A), while in the *rbcl* all known haplotypes were recovered in GoN, NE Mediterranean strains group into one haplogroup, and our strains cluster

into 4 haplogroups together with GoN strains (Fig. 12B). Note the additionally sequenced strains isolated from Slovenia, that were not shown in the phylogeny.

#### 4. Discussion

This study introduces an integrated approach combining molecular, ultrastructural and long-term monitoring data to describe the seasonal variation and diversity of *Pseudo-nitzschia* in a shallow gulf in the northern Adriatic Sea. We re-evaluated the power of several markers (28S, ITS2 and *rbcl*) for diatom barcoding and examined the phylogenetic relationships of Mediterranean and non-Mediterranean strains of *Pseudo-nitzschia* in order to fill knowledge gaps for the purpose of future research and surveys.

##### 4.1. *Pseudo-nitzschia* spp. in the GoT and why species complexes don't tell us enough

*Pseudo-nitzschia* species are an important component of the

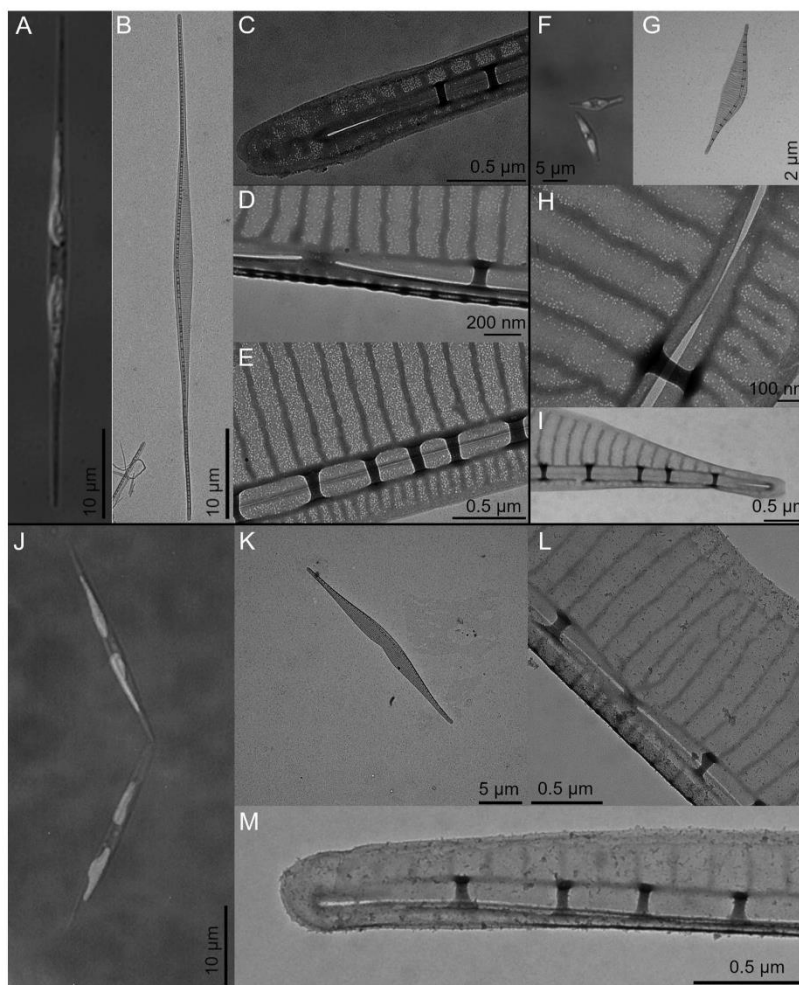


**Fig. 7.** Micrographs of *Pseudo-nitzschia galaxiae* identified in the Gulf of Trieste: large (A–E), small (F–I) and medium (J–M) morphotype. (A) Single live cell, LM, DIC-UV. (B) Valve of a long-sized specimen, TEM. (C) Apical end of a valve, TEM. (D) Central part of a valve with the central nodule, TEM. (E) Detail of a valve showing the typical and scattered poroids, TEM. (F) Live cells, LM, DIC-UV. (G) Valve of a small-sized specimen, TEM. (H) Central part of a valve showing the central nodule and poroids closely arranged along the interstriae, TEM. (I) Apical end of a valve, TEM. (J) Medium-sized specimens, LM, DIC-UV. (K) Valve of a medium-sized specimen, TEM. (L) Central part of a valve with the central nodule, TEM. (M) Apical end of a valve, TEM.

phytoplankton community all over the world (Viličić et al., 2009; Trainer et al., 2012; Bates et al., 2018; Mozetič et al., 2019). In a comparison of the phytoplankton community in port areas across the Adriatic Sea, *Pseudo-nitzschia* species as a whole were found to represent the core of the community in autumn and winter (Mozetič et al., 2019). Our time series analysis showed pronounced autumn blooms taking place annually and comprising up to 80 % of the total phytoplankton communities. Occasional spring blooms were also observed, but they usually represented smaller proportions of the phytoplankton community. Summer-autumn blooms of *Pseudo-nitzschia* are not

surprising and have been documented in many regions including the Adriatic, Mediterranean, NE Atlantic and NE Pacific (Trainer et al., 2002; Mercado et al., 2005; Fehling et al., 2006; Ljubešić et al., 2011) and can represent significant portions of the phytoplankton communities (Quijano-Scheggia et al., 2008a). In our study, the number of cells occasionally reached over  $10^6$  cells  $L^{-1}$ , which is above management thresholds in areas where amnesic shellfish poisoning is a reoccurring problem (Trainer et al., 2002). These numbers are also higher than those reported from other areas in the Mediterranean (Mercado et al., 2005; Quijano-Scheggia et al., 2008a; Marić et al., 2011). However, in

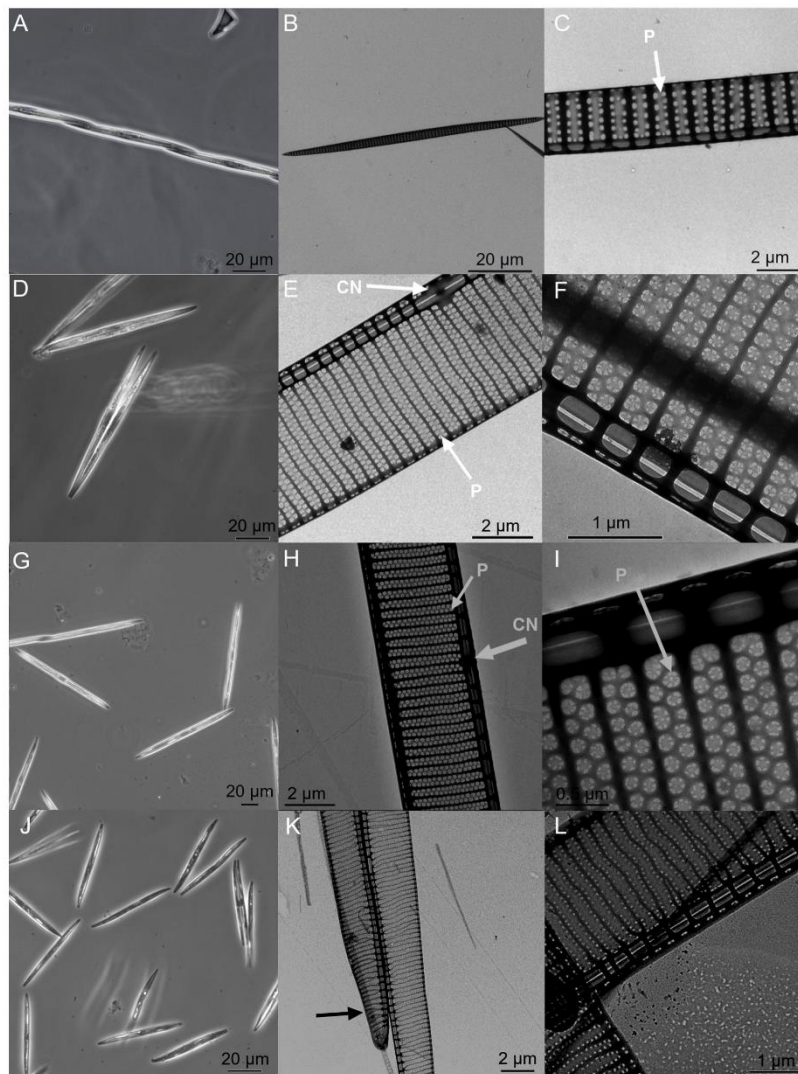


**Fig. 8.** Micrographs of *Pseudo-nitzschia* species identified in the Gulf of Trieste: *P. pungens* (A–C), *P. fraudulenta* (D–F), *P. subfraudulenta* (G–I) and *P. multistriata* (J–L). (A) Live cells in chains, LM. (B) Lanceolate cell, TEM. (C) Central part of the valve showing the poroid (P) organization (arrow), TEM. (D) Single live cells, LM. (E) Central part of the valve showing the presence of the central nodule (CN, arrow) and two rows of poroids (P, arrow), TEM. (F) Detail of poroids, TEM. (G) Single live cells, LM. (H) Central part of the valve showing the presence of the central nodule (CN) and two rows of poroids (P) (arrows), TEM. (I) Detail of poroids (P) (arrow), TEM. (J) Single live cells, LM. (K) The curved apical part of the valve (arrow), TEM. (L) Central part of the valve showing two rows of poroids, TEM.

terms of site management, the number of cells of a given complex is in itself not informative because toxin producers and non-producers can be simultaneously included in the count. The species complexes in the PCA demonstrate some seasonal preference, which is also in accordance with the isolation data, but the observed effects are stronger with the

very reliable *P. multistriata* counts. *P. delicatissima* complex and *P. cf. galaxiae* seem to show the same seasonal preference. This may not be surprising since *P. galaxiae* cells are also included in the complex counts. On the other hand problems of identification cannot be excluded, and *P. cf. galaxiae* most likely constitutes more than one species of the *P.*

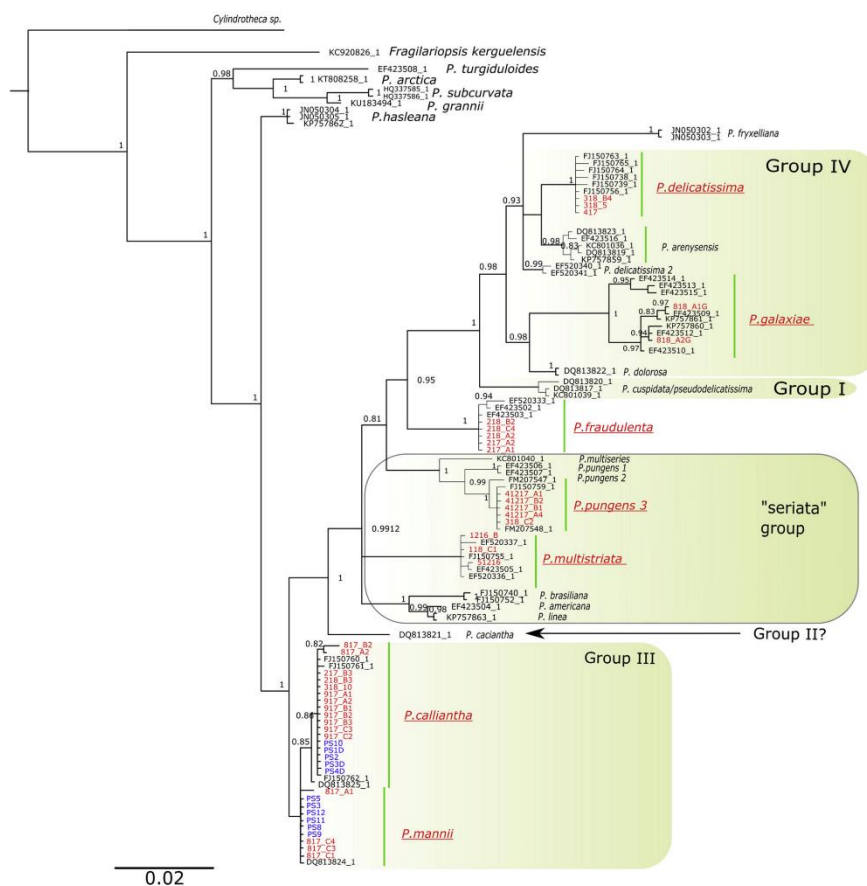


**Fig. 9.** Phylogenetic tree reconstruction using Bayesian inference on the *rbcL* marker GTR + I + G; ngen = 5,000,000. Identical sequences were removed from the tree and only representative strains retained. Species that have our native strains assigned to them are shown in enlarged and underlined red text. Bayesian posterior probabilities (PP) higher than 0.8 are shown on nodes. Strain names coloured in red represent isolates from Slovenia, while those coloured in blue represent isolates from Italy. Green shaded areas correspond to species groups defined by Lim et al. (2018). Group II is only represented by *P. cacintha*. Accession numbers of all of the used sequences are provided in supplementary material (Supplementary Table 2).

*delicatissima* complex, hence the similar ecological preference.

There is contrasting evidence of which environmental conditions promote the blooming of the different species complexes. Particular species may show different affinities to environmental parameters than their representative complexes, and this may be the actual source of the discrepancies between published literature. For example, Thorel et al. (2017) link the occurrence of *P. delicatissima* to low Si:N ratios whereas a negative correlation is observed for the *P. delicatissima* complex in regards to nitrate for the same study region (Downes-Tettmar et al., 2013). In our analysis, the *delicatissima* complex was correlated with high temperatures and lower phosphate concentrations, which could also signify nutrient uptake. Our PCA showed evident partitioning of the two species complexes that was mostly influenced by temperature and salinity; however, no marked seasonality was observed. These results are contradictory to the analysis of Fehling et al. (2006) that shows

a preference of *P. seriata* complex for warmer waters (summer bloom), although the oceanographic conditions in the NE Atlantic are fundamentally different than those of our study area. However, the study area is most likely not the only factor explaining the different patterns of seasonal occurrence. We assume that a great deal of these discrepancies stem from the fact that several species with different ecological affinities are grouped together, and the groups, i.e. the complexes are then treated as single ecological units. Depending on the study area, different species are inherently assigned to the two complexes. Additionally, since cells are assigned to complexes based on valve widths, unnoticed cell division can double the width of the valve thus allowing for incorrect assignment of the complex. Our studied locations hosted at least four species of the *delicatissima* complex. The *seriata* complex is also represented by four species that all occur at similar times of the year, from early autumn to spring. Finally, we did not observe any

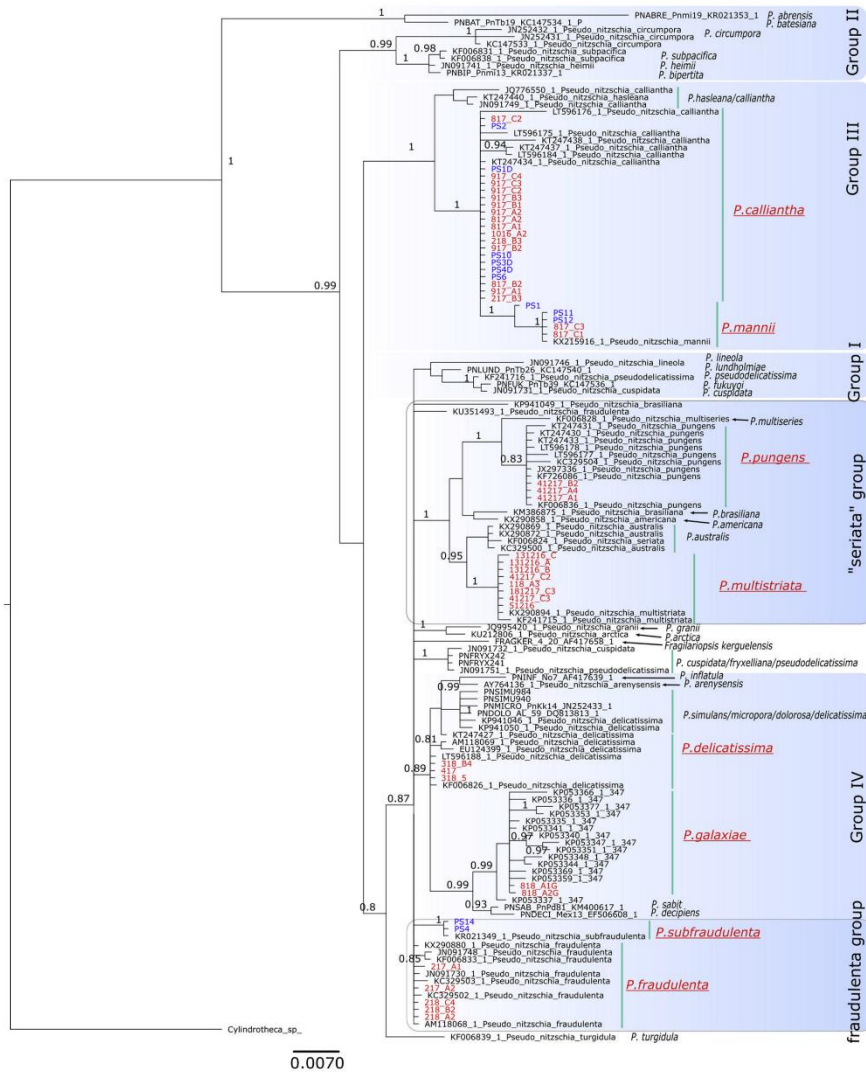


**Fig. 10.** Phylogenetic tree reconstruction using Bayesian inference on the 28S marker GTR + I + G, ngen = 10,000,000. Identical sequences were removed from the tree and only representative strains retained. Species that have our native strains assigned to them are shown in enlarged and underlined red text. Bayesian posterior probabilities (PP) higher than 0.8 are shown on nodes. Strain names coloured in red represent isolates from Slovenia, while those coloured in blue represent isolates from Italy. Blue shaded areas correspond to species groups defined by Lim et al. (2018). Accession numbers of all of the used sequences are provided in supplementary material (Supplementary Table 2).

pronounced seasonality from the NMDS either (S2), although the species complexes separated nicely, whereas the species constituting these complexes and for which data were available had fundamentally different ordinations in the multivariate space. This finding further stresses the importance of knowing the species when ecological explanations are to be drawn.

4.2. Unraveling the complex

To establish a benchmark for regional species diversity and seasonal occurrence, monthly isolations were performed. We concur that this is a stochastic approach that may not capture the entire community present at a given sampling point and is effort-biased. Nevertheless, in the



Fig. 11. Phylogenetic tree reconstruction using Bayesian inference on the ITS2 marker GTR + I + G; ngen = 10,000,000. Identical sequences were removed from the tree and only representative strains retained. Species that have our native strains assigned to them are shown in enlarged and underlined red text. Bayesian posterior probabilities (PP) higher than 0.8 are shown on nodes. Strain names coloured in red represent isolates from Slovenia, while those coloured in blue represent isolates from Italy. Red shaded areas correspond to species groups defined by Lim et al. (2018). Strain names coloured in red represent isolates from Slovenia, while those coloured in blue represent isolates from Italy.

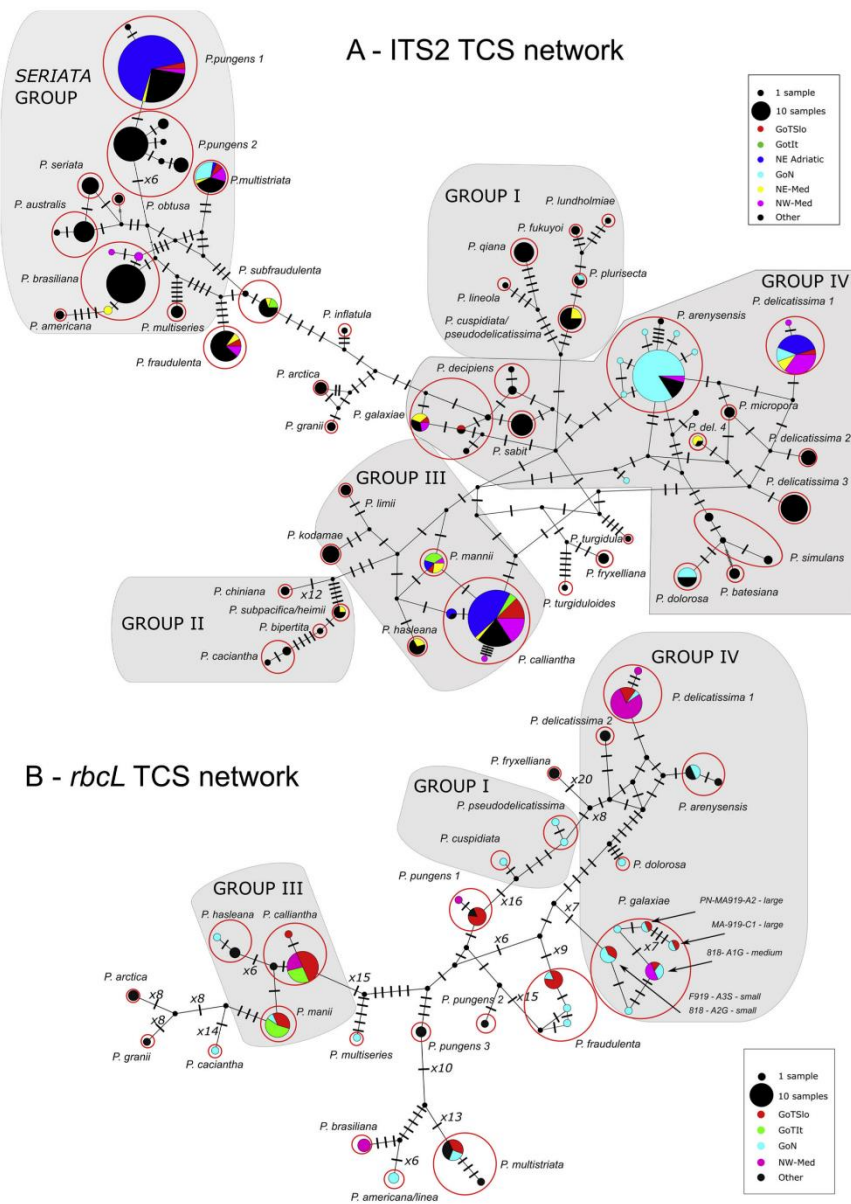


**Fig. 12.** TCS maximum parsimony networks constructed with (A) ITS2; 68 parsimony-informative sites; nucleotide diversity  $\pi = 0.14$  and (B) *rbcL*; 75 parsimony-informative sites; nucleotide diversity  $\pi = 0.04$ . Tick marks on branches represent point mutations. Wherever the number of mutations between two nodes exceeds 5, the number of mutations is written instead. Red circles encompass all present ribo/haplotypes of a given species. Species are grouped according to Lim et al. (2018). The colors of nodes correspond to the geographic origin of the sequence, where all sequences that do not belong to the Mediterranean are colored in black.

survey starting in October 2016 and ending in March 2018 with some additional sampling in August 2018 and 2019 as well as January and February 2019, eight species were identified from 83 isolated strains combining morphological and molecular analyses: *P. calliantha*, *P. delicatissima*, *P. fraudulentula*, *P. galaxiae*, *P. mannii*, *P. multistriata*, *P. pungens* and *P. subfraudulentula*. These species had already been reported from the Adriatic Sea, in studies focusing on this genus (Lundholm et al., 2003; Caroppo et al., 2005; Burić et al., 2008; Marić et al., 2011; Penna et al., 2013; Arapov et al., 2016, 2017). *P. multistriata* and *P. galaxiae* are exceptions because they had been reported in long-term investigations based on LM (Cabrini et al., 2012; Cerino et al., 2012; Mozetič et al., 2019; Totti et al., 2019), but we lack TEM data for both while molecular data exist only for *P. multistriata* (Pistocchi et al., 2012). To our knowledge, this is the first unequivocal report of their presence, confirmed by ultrastructural and molecular evidence. In this study, we identify the Gulf of Trieste as a rich region for *Pseudo-nitzschia*, with eight species identified in a relatively short time. There are more than 16 species described in the GoN with a very long record of *Pseudo-nitzschia* studies (Ruggiero et al., 2015), eight species were recovered from the Bilbao estuary (Orive et al., 2013), 12 were found in a rather extensive area of the Greek coasts (Moschandreu et al., 2012), 10 along the Australian coasts (Ajani et al., 2013), more than 20 were described over the years in the NE Pacific and 22 were recovered by an integrated morphological-HTS approach in a recent study (Stern et al., 2018b).

Each species from a given sampling event has representative morphological image data. In this way we account for potential seasonal morphological variability if the species occurs in multiple seasons, as has been reported for *P. galaxiae* (Cerino et al., 2005). The obvious concern is that morphological variability may also exist within the same sampling event. Conversely to Cerino et al. (2005) we have demonstrated this for *P. galaxiae*. This variability may or may not be captured, depending on the success of isolation and subsequent identification. Morphologically, the isolated species resemble those in type descriptions or in other localities. The larger average size of *P. subfraudulentula* cells is noteworthy; on average, about 10 µm longer than those described in Malaysia (Teng et al., 2013) and almost 60 µm longer than those described in Greece (Moschandreu and Nikolaidis, 2010). Our measurements rely on three strains, two of which were smaller, on average, than the very long one. The morphometric signatures of other species are in line with published data. The only exceptions are the maximum widths of the valve in *P. mannii*, *P. calliantha*, *P. fraudulentula*, *P. pungens* and *P. multistriata*. However, these were outliers in the measurements and could be a consequence of unnoticed cell division, which in effect doubles the measured cell width.

Although the isolation date may not provide clear evidence on seasonal distribution, we have managed to obtain information from various resources, i.e. monitoring data, isolation date and TEM screens of natural samples taken during the monitoring program at the LTER station, in order to provide some insight regarding the seasonal dynamics of certain species. The occurrence of *P. multistriata*, which seems to be limited to December and January, is somewhat in accordance with Ribera d'Alcalà et al. (2004) who report a restricted 3–8 week occurrence of this species in the GoN, albeit in autumn. However, more recent work from this region notes a more widespread seasonal distribution of *P. multistriata* inferred from clone library reconstruction, including a late autumn-winter peak and a high summer peak (Ruggiero et al., 2015). We did not detect this species in summer in any of the samples. *P. delicatissima* was isolated and tentatively identified only in winter-early spring, which is similar to the GoN (Ribera d'Alcalà et al., 2004; Ruggiero et al., 2015), as well as with data from a recent study carried out in the Gulf of Seine (Thorel et al., 2017). The fact that the clonal library study by Ruggiero et al. (2015) detected multiple peaks spread across seasons is not surprising as the resolution of their method is much higher. Interestingly, their study also detected *P. fraudulentula* only in February, which is the only month in two consecutive years

when viable cultures of this species were isolated during our study. *P. fraudulentula* was also found in early-spring cold water samples from other parts of the Mediterranean and the English Channel (Quijano-Scheggia et al., 2008b; Downes-Tettmar et al., 2013). Its sister taxon *P. subfraudulentula* was found in clonal libraries from the Tyrrhenian Sea only in autumn (Ruggiero et al., 2015), which is also in accordance with our isolation data linking this species to the period between October and December. This species is probably responsible for autumn blooms of the *seriata* complex, although this needs to be confirmed by other methods. *P. galaxiae* was isolated at the end of August and September and all three described morphotypes were present, while the morphotypes were found to be time-separated in the GoN (Cerino et al., 2005), even though most types were present in multiple seasons (Ruggiero et al., 2015). It should be noted, however, that small cells that could have belonged to *P. galaxiae* were observed in spring in our study as well, but isolation was not successful. Seasonal occurrence and inter-annual variability of phytoplankton species have been demonstrated to be heavily influenced by their biology. For example, microsatellite genotyping of *P. multistriata* in the GoN showed that two specific populations exist, living in sympatry and readily hybridizing, yet there is a bi-annual interchange of the dominant population (Tesson et al., 2014). This change is governed by their reproductive cycles that are influenced by cell size reductions and the existence of cell size optima for reproduction (D'Alelio et al., 2010). Thus, it may well be that the three distinct morphotypes of *P. galaxiae* that we found in the same spatio-temporal window are distinct populations at different stages of their life cycles that occur and bloom sympatrically in the ecological optimum for this species. These notions should be examined in light of the ability of the different *P. galaxiae* morpho-genotypes to reproduce, although increasingly smaller cells seem to lose this ability (D'Alelio et al., 2009). Genetically distinct sympatric or parapatric populations of planktonic protists have also been widely documented elsewhere, with varying degrees of hybridization, e.g. *Pseudo-nitzschia pungens* (Casteleyn et al., 2010), *Alexandrium fundysense*, *A. minutum* (Casabianca et al., 2011; Richlen et al., 2012), *Skeletonema marinoi* (Godhe and Härnström, 2010). The reason for genetic differentiation could be due to oceanographic features such as in *S. marinoi* or life-cycle characteristics such as resting stage formation or parasitism, as in *A. fundysense*. While there is no such apparent force in the Tyrrhenian Sea, Tesson et al. (2014) speculate that a meta-population model would explain the persisting existence of two or more interbreeding populations. Significant seasonal variability may have been missed by our study, since isolation data does not provide sufficient resolution of the community, unless effort is significantly increased (Bowers et al., 2018). Thus, to fully understand the seasonal profile of *Pseudo-nitzschia*, dedicated species-oriented techniques such as sandwich-hybridization, ARISA, qPCR or high-throughput sequencing, and where possible TEM/SEM screens of natural samples, should be used. For example, Bowers et al. (2018) have shown that by applying a species-oriented approach using a multitude of molecular and traditional techniques, a much better understanding of bloom dynamics is gained compared to the consideration of species complex data alone.

#### 4.3. Phylogenies and the relationship of Adriatic strains with other Mediterranean isolates

While genetic characterization is crucial for correct identification of species and strains in the *Pseudo-nitzschia* genus, the selection of markers can sometimes lead to ambiguous results. The reason for this is the differential evolution rate among phylogenetic markers and perhaps even lineages, which emphasizes the importance of selecting multiple markers (Patwardhan et al., 2014). The majority of the strains that were sequenced in our study are associated with at least one genetic marker. Only *P. subfraudulentula* from the Slovenian part of the GoT constitutes an exception. In the phylogenetic analysis, we focused on the recently published phylogenies of Lim et al. (2018) in order to compare our trees

and evaluate the power of the *rbcl* marker on a novel set of species, to our knowledge the most inclusive to date.

The groups defined in Lim et al. (2018) were all recovered in the ITS2 and 28S phylogenies although the tree structure is slightly different, which could be the consequence of strain selection, the fact that only Bayesian inference was used in this study, and the fact that the alignment of ITS2 was not guided by secondary structure. Groups were also recovered by *rbcl*, although Group II was only represented by *P. cacialantha*. The *rbcl* marker compared to *cox1* used in Lim et al. (2018) has a better discriminative power, leading to a tree with greater support, although the overall *p*-distances are somewhat shorter. These were in agreement with Lim et al. (2018), with ITS2 showing the largest distances, followed by *rbcl* and 28S. The *rbcl* alignment was the longest of all three. Proper identification of species, using the molecular approach alone is somewhat problematic as can be seen in the relationship between *P. manni* and *P. calliantha*. Phylogenetically, *P. manni* and *P. calliantha* are closely related and form a well-supported common clade according to all genetic markers. While in our analysis, one taxon was always parent to the other, the phylogenetic trees of Lim et al. (2018) place them as sister species. Moreover, according to the *rbcl*, the distance between the two taxa was smaller than the distance between strains of *P. galaxiae*, and also the separation between the two taxa was not supported by high posterior probability (PP). Nevertheless, *P. manni* has been successfully delineated from *P. calliantha* based on mating experiments and morphology (Amato and Montresor, 2008). However, it should be noted that prior to our study that recorded 15 different sequences, only one sequence of *P. manni* was publicly available for *rbcl*.

In our case, the *rbcl* marker proved to be very versatile with high amplification success. The suitability of a 540-bp *rbcl* barcode has been evaluated in the past as regards the ability to distinguish *Pseudo-nitzschia* species (MacGillivray and Kaczmarek, 2011). The authors noted that the evaluated fragment is suitable especially in a dual-barcode system with ITS2, since they were unable to distinguish certain biologically distinct species (e.g. *P. calliantha* and *P. manni*). Recently, a curated database for diatom *rbcl* barcodes was established based on a 312bp *rbcl* fragment (Rimmet et al., 2016). Although the initial focus was on freshwater diatoms, many marine species are included and the use of the database in metabarcoding applications for monitoring the ecological status of water has been demonstrated (Vasselon et al., 2017). To illustrate the utility of this barcode, we produced a phylogenetic analysis based on this fragment. The recovery of the taxa was indeed almost identical to the 1220bp alignment (S3). This evaluation was done *in silico*; therefore, the entire amplification and sequencing process should be repeated using the selected barcode primers. The barcode should also be evaluated against a larger set of marine diatoms to fully understand its potential. So far, significantly less *Pseudo-nitzschia* species are sequenced for *rbcl* compared to ITS and 28S, but there are more compared to *cox1*. Of course, there is a relationship between the number of sequences and the variation detected but *rbcl* alignment had by far the least sequences and thus its discriminative power is apparent. 28S generally showed high amplification success in our study, but with much lower species resolution compared to ITS and *rbcl*. ITS is technically the most problematic, as it exists in multiple repeats in the genome, which could potentially be heterogenic (Orsini et al., 2004). This could impair PCR or result in unreadable sequences. Indeed, the amplification and sequencing success with this marker was the lowest, even though its discriminative power is the best.

While we detected some intraspecific variation among our strains this was limited. Only strains of *P. galaxiae*, which appears to be a species of great morphological as well as genetic variability (Cerino et al., 2005; D'Alelio and Ruggiero, 2015), are obviously different, as confirmed by this study. Interestingly, the two strains isolated from the same net sample and reported here, share a very similar 28S allele (Fig. 10), but have different ITS2 copies (Fig. 11) and cluster into different chloroplast haplogroups in the *rbcl* phylogeny (Fig. 9). Strain

818-A2 (small morphotype) even forms a unique branch in ITS2. The study by Cerino et al. (2005) examined the different morphotypes only with 28S and did not find significant differences between them, but it was noted that the morphotypes indeed differ in ITS (Ruggiero et al., 2015) while large differences in *rbcl* were also revealed although they were not backed by morphological data (D'Alelio and Ruggiero, 2015). Thus, it may well be that *P. galaxiae* is a species complex as was tentatively proposed before by Ruggiero et al. (2015). In the *rbcl* network, where recently isolated strains of *P. galaxiae* were also included, additional haplotypes were revealed, complementing those previously described elsewhere in the Mediterranean (*P. galaxiae* cluster, Fig. 12B). The discrepancies between nuclear and plastid markers have been documented for other species of *Pseudo-nitzschia* as well. In *P. delicatissima*, Amato et al. (2007) demonstrated that the examined strains possessed two distinct *rbcl* haplotypes but had only one LSU and ITS genotype. These strains were able to interbreed successfully, and the authors postulated that different *rbcl* haplotypes can occur within single interbreeding populations. In *Pseudo-nitzschia*, inheritance of chloroplasts is bi-parental and recombination between chloroplasts was recorded for this genus including *P. galaxiae* (D'Alelio and Ruggiero, 2015). To further reveal the relationship of *P. galaxiae* strains in the Adriatic and in general, additional morphological and genetic studies should be conducted, including microsatellite genotyping, as well as a study of ITS2 secondary structure, which seems to be a good proxy for mating capability (Amato et al., 2007).

The genetic diversity among the Mediterranean strains is somewhat better captured with ITS2 compared to *rbcl*, which is not surprising given the number of sequences available (412 and 111, respectively). Furthermore, in the *rbcl* network, we observed that many species are only represented by Mediterranean strains; therefore, it is difficult to draw conclusions about genetic difference within and between the Mediterranean and other global regions. However, it should be reminded that the alignment used in the ITS2 network reconstruction was shorter since it was amended with gBlocks to aid alignment and remove gappy regions. Furthermore, strains may differ in one marker but be identical in another as was shown for *P. calliantha*, where strains differed in ITS1 but were identical in 5.8S-ITS2 (Lundholm et al., 2012). Some *Pseudo-nitzschia* species such as *P. pungens* are known cosmopolites, although it has been shown that distinct geographical partitioning backed by both morphological and genetic data exists for this species, where only one group out of three is in fact cosmopolitan (Casteleyn et al., 2010). This is also evident in our analysis with Mediterranean strains belonging to the globally distributed Clade I, and the geographically restricted clades II and III without Mediterranean members. A similar case is observed with *P. delicatissima* with two non-Mediterranean clades, although this species complex is less resolved and the two groups could well represent cryptic species. In contrast, *P. brasiliensis* showed different haplogroups in ITS2 with a larger non-Mediterranean cluster and two Mediterranean ones. The differences between Catalan, Greek and other non-Mediterranean strains of *P. brasiliensis* have already been discussed in Moschandreou et al. (2012). Finally, species represented by unique haplogroups that also include Mediterranean strains, including *P. multistriata*, *P. fraudulenta*, *P. manni*, *P. hasleana*, *P. subpacifica*, *P. pseudodelicatissima/cuspidata* and *P. plurisetata* could reflect a lack of sequencing effort on the one hand and the absence of crypticism within these species on the other.

#### 4.4. Integrating molecular and morphological data for better management of LTER sites

Traditional methods such as light microscopy are often insufficient to uncover cryptic protist diversity, yet this is the most common method used for long-term monitoring for analyses of plankton community structure. While knowing the exact species or even ecotypes of a certain species may not be the goal of such monitoring, we should be more careful when potentially toxic species are concerned (Bickford

et al., 2007). The most notable example is perhaps the *Alexandrium tamarense* species complex, comprised of five species of which only some are producers of saxitoxin, and cannot be distinguished using light and even electron microscopy (John et al., 2014). Similarly, it was shown that distinct genetic varieties of *Akashiwo sanguinea* assume different ecological niches, but are morphologically undistinguishable (Luo et al., 2017). In *Pseudo-nitzschia*, HAB and LTER monitoring usually recovers only species complexes defined by valve width. Although morphological traits can be proxies for ecological preference as was shown in freshwater diatoms (Potapova and Hamilton, 2007), we are not aware of any research that shows valve width defines ecological preference in *Pseudo-nitzschia*. We thus question the serviceability of this data in terms of LTER site management and explore what can be gained from dedicated molecular surveys such as the one presented here. Incorporating molecular knowledge into LTER strategies allows for a better understanding of the local ecosystem and leads to better management (Stern et al., 2018b). Such efforts also help to build local reference databases of both sequence and biological data that can be then referred to in high-throughput sequencing studies, which are more reliable and robust (Stern et al., 2018a). Our data shows that the *P. delicatissima* complex, which we now know comprises of at least four species (*P. delicatissima*, *P. calliantha*, *P. mannii* and *P. galaxiae*), preferentially occurs in summer and spring conditions, while the *seriata* complex (comprising of *P. multistriata*, *P. pungens*, *P. fraudulentula* and *P. subfraudentula*) peaks in autumn. Until the current study was conducted, only species complex data and data on *P. multistriata* were available in the GoT. The three-year campaign of strain isolation followed by characterization and backtracking to LM data allowed us to understand the community much better and also enabled us to identify more species under LM because we now know which species can be expected at different times of the year. To demonstrate this, a proof-of-concept CCA analysis was conducted (S4 B) where we used the isolation data of each sampling event to quality check the count data (see S4 A for methodology). Backtracking was only done for the *seriata* complex because tentative counts of species that are grouped into this complex exist for LM, whereas the *delicatissima* complex is always reported as it is because the species are almost impossible to tell apart even with prior knowledge. *P. galaxiae* is an exception; its cells show some distinct features such as thin rostrae, while the small morphotype is also distinguishable. Nevertheless, the smaller morphotype often impedes detection due to its size and resembles many small planktonic and benthic diatoms, while the larger morphotype can from our experience be confused with *P. delicatissima*. The CCA showed the preference of *P. multistriata* and *P. pungens* for saltier, colder waters with higher concentrations of silicate and DIN, which represent typical winter conditions, while *P. fraudulentula* was associated with quite different conditions. Although, the number of samples in this analysis is small, we can see that the respective species complex of the aforementioned species ordinate differently than the species itself. Therefore, any discrepancies between species complex and species affinities to environmental conditions reported in Thorel et al. (2017) and previously discussed in this work, may not be surprising. We are convinced that decomplexing of the *P. delicatissima* complex would yield similar results, since we know that different species occur in different temporal windows. We believe our work feeds well into the framework of molecular data integration in routine monitoring proposed by Stern et al., 2018, and is thus an example of good practice, even though the resolving power of our method was not the strongest. Many molecular tools can be used to gain better species resolution and seasonal profiles (e.g. qPCR: Andree et al., 2011; microarray: Smith et al., 2012; various SHA and FISH techniques: Orozco et al., 2016; Medlin and Orozco, 2017; Bowers et al., 2018), although the feasibility to use them in routine monitoring is often impaired due to budgetary and staff limitations. Yet, we must be careful when drawing conclusions on the affinities of different species to environmental conditions, since bloom phenology and species succession also depends on species interactions, nutrition and parasitism (Gleason

et al., 2015; D'Alelio et al., 2019). Further studies and models of the seasonal distribution of individual species, including inter-annual difference, will help fill the knowledge gaps and help elucidate the ways in which species dominance and blooming relates to environmental and ecosystem conditions.

To conclude, we have demonstrated that by combining the molecular and morphological toolkit more reliable information on species diversity and seasonality can be established, which greatly improves monitoring strategies while enabling further ecological analyses.

#### Funding

The authors acknowledge the financial support from the Slovenian Research Agency (research core funding No. P1-0237 and program for young researchers, in accordance with the agreement on (co) financing research activities), the Friuli Venezia Giulia Region (L.R. 15/2005) and the Slovenian Environment Agency.

#### Declaration of Competing Interest

The authors declare that they have no known competing financial interests or personal relationships that could have appeared to influence the work reported in this paper.

#### Acknowledgments

The authors wish to thank Paolo Bertoncin (Department of Life Science, University of Trieste) for technical assistance with TEM. Station C1-LTER is part of the national and international Long Term Ecological Research network (LTER-Italy, LTER-Europe, ILTER). The authors would like to thank Bruno Cataletto, Cinzia Comici, Edvino Cociancich, Miljan Šiško and Tihomir Makovec for sampling and performing CTD measurements, Martina Kralj for nutrient data and Daniela Fornasaro and Miljan Šiško for phytoplankton data. The authors thank Valentina Torboli (Department of Life Science, University of Trieste) and the staff of the Laboratory for Evolutionary Ecology (Centre for Marine Research, Ruđer Bošković Institute) in Rovinj, Croatia for providing some ITS and 28S sequences of the Italian strains. Finally, we thank three anonymous reviewers who have helped to substantially improve this manuscript with their insight and suggestions.[CG]

#### Appendix A. Supplementary data

Supplementary material related to this article can be found, in the online version, at doi:<https://doi.org/10.1016/j.hal.2020.101773>.

#### References

- Ajani, P., Murray, S., Hallegraeff, G., Lundholm, N., Gillings, M., Brett, S., Armand, L., 2013. The diatom genus *Pseudo-nitzschia* (Bacillariophyceae) in New South Wales, Australia: morphotaxonomy, molecular phylogeny, toxicity, and distribution. *J. Phycol.* 49, 765–785. <https://doi.org/10.1111/jpy.12087>.
- Amato, A., Montresor, M., 2008. Morphology, phylogeny, and sexual cycle of *Pseudo-nitzschia mannii* sp. nov. (Bacillariophyceae): a pseudo-cryptic species within the *P. pseudodelicatissima* complex. *Phycologia* 47, 487–497. <https://doi.org/10.2216/07-92.1>.
- Amato, A., Koolstra, W.H.C.F., Levaldi Ghiron, J.H., Mann, D.G., Pröschold, T., Montresor, M., 2007. Reproductive isolation among sympatric cryptic species in marine diatoms. *Protist* 158, 193–207. <https://doi.org/10.1016/j.protis.2006.10.001>.
- Anderson, D., 2014. HABs in a changing world: a perspective on harmful algal blooms, their impacts, and research and management in a dynamic era of climatic and environmental change. In: *Harmful Algae 2012 Proc. 15th Int. Conf. Harmful Algae Oct. 29 - Novemb. 2, 2012. CECO, Chang, Gyeongnam, Korea. Int. Conf. Harmful Algae (15th 2012 Chang, Gyeongnam, Kore. 2012. pp. 3–17.*
- Anderson, C.R., Sapiano, M.R.P., Prasad, M.B.K., Long, W., Tango, P.J., Brown, C.W., Murtugudde, R., 2010. Predicting potentially toxicogenic *Pseudo-nitzschia* blooms in the Chesapeake Bay. *J. Mar. Syst.* 83, 127–140. <https://doi.org/10.1016/j.jmarsys.2010.04.003>.
- Andree, K.B., Fernández-Tejedor, M., Elandaloussi, L.M., Quijano-Scheggia, S., Sampedro,

T. Turk Dermastia, et al.

Harmful Algae 93 (2020) 101773

- N., Garcés, E., Camp, J., Diogène, J., 2011. Quantitative PCR coupled with melt curve analysis for detection of selected *Pseudo-nitzschia* spp. (Bacillariophyceae) from the northwestern Mediterranean Sea. *Appl. Environ. Microbiol.* 77, 1651–1659. <https://doi.org/10.1128/AEM.01978-10>.
- Arapov, J., Ujević, I., Pfannkuchen, D.M., Bakrač, A., Gladan, Z.N., Marasovic, I., 2016. Domoic acid in phytoplankton net samples and shellfish from the krka river estuary in the central Adriatic Sea. *Mediterr. Mar. Sci.* 17, 340–350. <https://doi.org/10.12681/mms.1471>.
- Arapov, J., Skejić, S., Bužanić, M., Bakrač, A., Vidjak, O., Bojanić, N., Ujević, I., Gladan, Z.N., 2017. Taxonomical diversity of *Pseudo-nitzschia* from the Central Adriatic Sea. *Phycol. Res.* 65, 280–290. <https://doi.org/10.1111/prec.12184>.
- Bates, S.S., Hubbard, K.A., Lundholm, N., Montresor, M., Leaw, C.P., 2018. *Pseudo-nitzschia*, *Nitzschia*, and domoic acid: new research since 2011. *Harmful Algae* 1–41. <https://doi.org/10.1016/j.hal.2018.06.001>.
- Bickford, D., Lohman, D.J., Sodhi, N.S., Ng, P.K.L., Meier, R., Winker, K., Ingram, K.K., Das, I., 2007. Cryptic species as a window on diversity and conservation. *Trends Ecol. Evol. (Amst.)* 22, 148–155. <https://doi.org/10.1016/j.tree.2006.11.004>.
- Bowers, H.A., Ryan, J.P., Hayashi, K., Woods, A.L., Marin, R., Smith, G.J., Hubbard, K.A., Doucette, G.J., Mikulski, C.M., Gellene, A.G., Zhang, Y., Kudela, R.M., Caron, D.A., Birch, J.M., Scholin, C.A., 2018. Diversity and toxicity of *Pseudo-nitzschia* species in Monterey Bay: perspectives from targeted and adaptive sampling. *Harmful Algae* 78, 129–141. <https://doi.org/10.1016/j.hal.2018.08.006>.
- Burić, Z., Viličić, D., Mihalčić, K.C., Carić, M., Kralj, K., Ljubešić, N., 2008. *Pseudo-nitzschia* blooms in the Krka river estuary (eastern Adriatic sea). *Diatom Res.* 23, 51–63. <https://doi.org/10.1080/0269249X.2008.9705736>.
- Cabrini, M., Fornasaro, D., Cossarini, G., Lipizer, M., Virgilio, D., 2012. Phytoplankton temporal changes in a coastal northern Adriatic site during the last 25 years. *Estuar. Coast. Shelf Sci.* 115, 113–124. <https://doi.org/10.1016/j.eccs.2012.07.007>.
- Caroppo, C., Congesti, R., Braccini, L., Albertano, P., 2005. On the presence of *Pseudo-nitzschia calliantha* Lundholm, Moestrup et Hasle and *Pseudo-nitzschia delicatissima* (Cleve) Heisterkamp in the Southern Adriatic Sea (Mediterranean Sea, Italy). *J. Plankton Res.* 27, 763–774. <https://doi.org/10.1093/plankt/fbi050>.
- Casabianca, S., Penna, A., Pecchioli, E., Jordi, A., Basterretxea, G., Vernesi, C., 2011. Population genetic structure and connectivity of the harmful dinoflagellate *Alexandrium minutum* in the Mediterranean Sea. *Proc. R. Soc. B Biol. Sci.* 279, 129–138. <https://doi.org/10.1098/rspb.2011.0708>.
- Castelijn, G., Leliart, F., Bäckeljaug, T., Debeer, A.E., Kotaki, Y., Rhodes, L., Lundholm, N., Sabbe, K., Vyverman, W., 2010. Limits to gene flow in a cosmopolitan marine planktonic diatom. *Proc. Natl. Acad. Sci. U. S. A.* 107, 12952–12957. <https://doi.org/10.1073/pnas.1001380107>.
- Castresana, J., 2000. Selection of conserved blocks from multiple alignments for their use in phylogenetic analysis. *Mol. Biol. Evol.* 17, 540–552. <https://doi.org/10.1093/oxfordjournals.molbev.a026334>.
- Cerino, F., Orsini, L., Sarno, D., Dell'Aversano, C., Tartaglione, L., Zingone, A., 2005. The alternation of different morphotypes in the seasonal cycle of the toxic diatom *Pseudo-nitzschia galaxiaca*. *Harmful Algae* 4, 33–48. <https://doi.org/10.1016/j.hal.2003.10.005>.
- Cerino, F., Bernardi Aubry, F., Coppola, J., La Ferla, R., Maimone, G., Socal, G., Totti, C., 2012. Spatial and temporal variability of pico-, nano- and microphytoplankton in the offshore waters of the southern Adriatic Sea (Mediterranean Sea). *Cont. Shelf Res.* 44, 94–105. <https://doi.org/10.1016/j.csr.2011.06.006>.
- Clement, M., Posada, D., Crandall, K.A., 2000. TCS: a computer program to estimate gene genealogies. *Mol. Ecol.* 9, 1657–1659. <https://doi.org/10.1046/j.1365-294x.2000.01020.x>.
- Cozzi, S., Falconi, C., Comici, C., Čermelj, B., Kovac, N., Turk, V., Giani, M., 2012. Recent evolution of river discharges in the Gulf of Trieste and their potential response to climate changes and anthropogenic pressure. *Estuar. Coast. Shelf Sci.* 115, 14–24. <https://doi.org/10.1016/j.eccs.2012.03.005>.
- D'Alenio, D., Ruggiero, M.V., 2015. Interspecific plastidial recombination in the diatom genus *Pseudo-nitzschia*. *J. Phycol.* 51, 1024–1028. <https://doi.org/10.1111/jpy.12350>.
- D'Alenio, D., Amato, A., Kooistra, W.H.C.F., Proccacini, G., Casotti, R., Montresor, M., 2009. Internal Transcribed Spacer Polymorphism in *Pseudo-nitzschia* multistriata (Bacillariophyceae) in the Gulf of Naples: Recent Divergence or Intraspecific Hybridization? *Protist* 160, 9–20. <https://doi.org/10.1016/j.p.2008.07.001>.
- D'Alenio, D., d'Alcalá, M.R., Dubroca, L., Sarn, D., Zingone, A., Montresor, M., 2010. The time for sex: a biennial life cycle in a marine planktonic diatom. *Limnol. Oceanogr.* 55, 106–114. <https://doi.org/10.4319/l.2010.55.1.0106>.
- D'Alenio, D., Hay Mele, B., Libralato, S., Ribera d'Alcalá, M., Jordán, F., 2019. Rewiring and indirect effects underpin modularity reshuffling in a marine food web under environmental shifts. *Ecol. Evol.* <https://doi.org/10.1002/eec3.5641>.
- Downes-Tettmar, N., Rowland, S., Widdicombe, C., Woodward, M., Llewellyn, C., 2013. Seasonal variation in *Pseudo-nitzschia* spp. and domoic acid in the Western English Channel. *Cont. Shelf Res.* 53, 40–49. <https://doi.org/10.1016/j.csr.2012.10.011>.
- Fehling, J., Davidson, K., Bolch, C., Tett, P., 2006. Seasonally of *Pseudo-nitzschia* spp. (Bacillariophyceae) in western Scottish waters. *Mar. Ecol. Prog. Ser.* 323, 91–105. <https://doi.org/10.3354/meps323091>.
- Fonda Umami, S., Del Negro, P., Larato, C., De Vittor, C., Cabrini, M., Celio, M., Falconi, C., Tamberlich, F., Azam, F., 2007. Major inter-annual variations in microbial dynamics in the Gulf of Trieste (northern Adriatic Sea) and their ecosystem implications. *Aquat. Microb. Ecol.* 46, 163–175. <https://doi.org/10.3354/ame046163>.
- Gleason, F.H., Jephcott, T.G., Küpper, F.C., Gerphagnon, M., Sime-Ngando, T., Karpov, S.A., Guillou, L., van Ogtrop, F.F., 2015. Potential roles for recently discovered chytrid parasites in the dynamics of harmful algal blooms. *Fungal Biol. Rev.* 29, 20–33. <https://doi.org/10.1016/j.fbr.2015.03.002>.
- Godhe, A., Hämström, K., 2010. Linking the planktonic and benthic habitat: genetic structure of the marine diatom *Skeletonema marinoi*. *Mol. Ecol.* 19, 4478–4490. <https://doi.org/10.1111/j.1365-294X.2010.04841.x>.
- Hansen, H.P., Koroleff, F., 1999. Determination of nutrients, in: *Methods of Seawater Analysis: Third, Completely Revised and Extended Edition*. Wiley-VCH Verlag GmbH, Weinheim, Germany, pp. 159–228. <https://doi.org/10.1002/9783527613984.ch10>.
- Huang, C.X., Dong, H.C., Lundholm, N., Teng, S.T., Zheng, G.C., Tan, Z.J., Lim, P.T., Li, Y., 2019. Species composition and toxicity of the genus *Pseudo-nitzschia* in Taiwan Strait, including *P. chiniana* sp. nov. and *P. qiana* sp. nov. *Harmful Algae* 84, 195–209. <https://doi.org/10.1016/j.hal.2019.04.003>.
- John, U., Litaker, R.W., Montresor, M., Murray, S., Brosnahan, M.L., Anderson, D.M., 2014. Formal revision of the Alexandrium tansanense species complex (Dinophyceae) taxonomy: the introduction of five species with emphasis on molecular-based (rDNA) classification. *Protist* 165, 779–804. <https://doi.org/10.1016/j.protis.2014.10.001>.
- Katoh, K., Standley, D.M., 2013. MAFFT multiple sequence alignment software version 7: improvements in performance and usability. *Mol. Biol. Evol.* 30, 772–780. <https://doi.org/10.1093/molbev/mst010>.
- Kimur, S., Stecher, G., Tamura, K., 2016. MEGA7: molecular evolutionary genetics analysis version 7.0 for bigger datasets. *Mol. Biol. Evol.* 33, 1870–1874. <https://doi.org/10.1093/molbev/msw054>.
- Lane, J.Q., Raimondi, P.T., Kudela, R.M., 2009. Development of a logistic regression model for the prediction of toxicogenic *Pseudo-nitzschia* blooms in Monterey Bay. *California. Mar. Ecol. Prog. Ser.* 383, 37–51. <https://doi.org/10.3354/meps07999>.
- Leigh, J.W., Bryant, D., 2015. POPART: full-featured software for haplotype network construction. *Methods Ecol. Evol.* 6, 1110–1116. <https://doi.org/10.1111/2041-210X.12410>.
- Lelong, A., Hégarat, H., Soudant, P., Bates, S.S., 2012. *Pseudo-nitzschia* (Bacillariophyceae) species, domoic acid and amnesic shellfish poisoning: revisiting previous paradigms. *Phycologia* 51, 168–216. <https://doi.org/10.2216/11-37.1>.
- Ljubešić, Z., Bosak, S., Viličić, D., Borojević, K.K., Marić, D., Godrijan, J., Ujević, I., Pešarec, P., Dakovac, T., 2011. Ecology and taxonomy of potentially toxic *Pseudo-nitzschia* species in Lim Bay (north-eastern Adriatic Sea). *Harmful Algae* 10, 713–722. <https://doi.org/10.1016/j.hal.2011.06.002>.
- Lundholm, N., Moestrup, Ø., Hasle, G.R., Hoef-Emden, K., 2003. A study of the *Pseudo-nitzschia pseudodelicatissima/cuspidata* complex (Bacillariophyceae): What is *P. pseudodelicatissima*? *J. Phycol.* 39, 797–813. <https://doi.org/10.1046/j.1529-8817.2003.02031.x>.
- Lundholm, N., Moestrup, Ø., Kotaki, Y., Hoef-Emden, K., Scholin, C., Miller, P., 2006. Inter- and intraspecific variation of the *Pseudo-nitzschia delicatissima* complex (Bacillariophyceae) illustrated by rRNA probes, morphological data and phylogenetic analyses. *J. Phycol.* 42, 464–481. <https://doi.org/10.1111/j.1529-8817.2006.00211.x>.
- Lundholm, N., Bates, S.S., Baugh, K.A., Bill, B.D., Connell, L.B., Léger, C., Trainer, V.L., 2012. Cryptic and pseudo-cryptic diversity in diatoms with descriptions of *Pseudo-nitzschia hasleana* sp. nov. and *P. fryxelliana* sp. nov. *J. Phycol.* 48, 436–454. <https://doi.org/10.1111/j.1529-8817.2012.01132.x>.
- Luo, Z., Yang, W., Leaw, C.P., Pospelova, V., Billen, G., Liow, G.R., Lim, P.T., Gu, H., 2017. Cryptic diversity within the harmful dinoflagellate *Akashiwo sanguinea* in coastal Chinese waters is related to differentiated ecological niches. *Harmful Algae* 66, 88–96. <https://doi.org/10.1016/j.hal.2017.05.008>.
- MacGillivray, M.L., Kozmaraska, I., 2011. Survey of the efficacy of a short fragment of the rbcL gene as a supplemental DNA barcode for diatoms. *J. Eukaryot. Microbiol.* 58, 529–536. <https://doi.org/10.1111/j.1550-7408.2011.00585.x>.
- Malačić, V., 1991. Estimation of the vertical Eddy Diffusion Coefficient of heat in the Gulf of Trieste (Northern Adriatic). *Oceanol. Acta* 14, 23–32.
- Malačić, V., Celio, M., Čermelj, B., Bussani, A., Comici, C., 2006. Interannual evolution of seasonal thermohaline properties in the Gulf of Trieste (northern Adriatic) 1991–2003. *J. Geophys. Res. Ocean* 111. <https://doi.org/10.1029/2005JC003267>.
- Marić, D., Ljubešić, Z., Godrijan, J., Viličić, D., Ujević, I., Prečali, R., 2011. Blooms of the potentially toxic diatom *Pseudo-nitzschia calliantha* Lundholm, Moestrup et Hasle in coastal waters of the northern Adriatic Sea (Croatia). *Estuar. Coast. Shelf Sci.* 92, 323–331. <https://doi.org/10.1016/j.eccs.2011.01.002>.
- Mccabe, R.M., Hickey, B.M., Kudela, R.M., Lefebvre, K.A., Adams, N.G., Bill, B.D., Gulland, F.M.D., Thomson, R.E., Cochlan, W.P., Trainer, V.L., 2016. An unprecedented coastwide toxic algal bloom linked to anomalous ocean conditions. *Research Letter* 366–376. <https://doi.org/10.1002/2016GL070023>.
- Medlin, L.K., Orozco, J., 2017. Molecular techniques for the detection of organisms in aquatic environments, with emphasis on harmful algal bloom species. *Sensors (Switzerland)* 17. <https://doi.org/10.3390/s17051184>.
- Mercedo, J.M., Ramírez, T., Cortés, D., Sebastián, M., Vargas-Yáñez, M., 2005. Seasonal and inter-annual variability of the phytoplankton communities in an upwelling area of the Alborán Sea (SW Mediterranean Sea). *Sci. Mar.* 69, 451–465. <https://doi.org/10.3989/scimar.2005.69n4451>.
- Moschandreou, K.K., Nikolaidis, G., 2010. The genus *Pseudo-nitzschia* (Bacillariophyceae) in Greek coastal waters. *Bot. Mar.* 53, 159–172. <https://doi.org/10.1515/BOT.2010.014>.
- Moschandreou, K.K., Baxevanis, A.D., Katikou, P., Papaefthimiou, D., Nikolaidis, G., Abatzopoulos, T.J., 2012. Inter- and intra-specific diversity of *Pseudo-nitzschia* (Bacillariophyceae) in the northeastern Mediterranean. *Eur. J. Phycol.* 47, 321–339. <https://doi.org/10.1080/09670262.2012.713998>.
- Mozetić, P., Fonda Umami, S., Cataletto, B., Malej, A., 1998. Seasonal and inter-annual plankton variability in the Gulf of Trieste (Northern Adriatic), in: *ICES Journal of Marine Science*. Narnia 711–722. <https://doi.org/10.1006/jmsc.1998.0396>.
- Mozetić, P., Cangini, M., Francić, J., Bastianini, M., Bernardi Aubry, F., Bužanić, M., Cabrini, M., Cerino, F., Čalić, M., D'Adamo, R., Drakulović, D., Finotto, S., Fornasaro, D., Grilli, F., Kraus, R., Kužat, N., Marić Pfannkuchen, D., Ninčević Gladan, Z., Pompei, M., Rotter, A., Servadei, I., Skejić, S., 2019. Phytoplankton diversity in

- Adriatic ports: lessons from the port baseline survey for the management of harmful algal species. *Mar. Pollut. Bull.* <https://doi.org/10.1016/j.marpolbul.2017.12.029>.
- Oksanen, J., Blanchet, F.G., Friendly, M., Kindt, R., Legendre, P., McGilgan, D., Minchin, P.R., O'Hara, R.B., Simpson, G.L., Solymos, P., Stevens, M.H.H., Szocs, E., Wagner, H., 2019. *Vegan: Community Ecology Package*.
- Orive, E., Laza-Martínez, A., Seoane, S., Alonso, A., Andrade, R., Miguel, I., 2010. Diversity of pseudo-nitzschia in the southeastern bay of biscay. *Diatom Res.* **25**, 125–145. <https://doi.org/10.1080/0269249X.2010.9705834>.
- Orive, E., Pérez-Acua, L., David, H., García-Etxebarria, K., Laza-Martínez, A., Seoane, S., Miguel, I., 2013. The genus *Pseudo-nitzschia* (Bacillariophyceae) in a temperate estuary with description of two new species: *Pseudo-nitzschia plurisetica* sp. nov. and *Pseudo-nitzschia abrensis* sp. nov. *J. Phycol.* **49**, 1192–1206. <https://doi.org/10.1111/jpp.12130>.
- Orozco, J., Villa, E., Manes, C.L., Medlin, L.K., Guillebault, D., 2016. Electrochemical RNA biosensors for toxic algal species: enhancing selectivity and sensitivity. *Talanta* **161**, 560–566. <https://doi.org/10.1016/j.talanta.2016.08.073>.
- Orsini, L., Proccacini, G., Sarno, D., Montresor, M., 2004. Multiple rDNA ITS-types within the diatom *Pseudo-nitzschia delicatissima* (Bacillariophyceae) and their relative abundances across a spring bloom in the Gulf of Naples. *Mar. Ecol. Prog. Ser.* **271**, 87–98. <https://doi.org/10.3354/meps271087>.
- Patwardhan, A., Amit, R., Ray, S., 2014. Molecular markers in phylogenetic Studies-A review. *J. Phylogenetics Evol. Biol.* **2**, 1–9. <https://doi.org/10.4172/2329-9002.1000131>.
- Penna, A., Casabianca, S., Perini, F., Bastianini, M., Riccardi, E., Pigozzi, S., Scardi, M., 2013. Toxic *Pseudo-nitzschia* spp. in the northwestern Adriatic Sea: characterization of species composition by genetic and molecular quantitative analyses. *J. Plankton Res.* **35**, 352–366. <https://doi.org/10.1093/plankt/fbs093>.
- Pistocchi, R., Guerrini, F., Pezolesi, L., Riccardi, M., Vanucci, S., Giminiello, P., Dell'Aversano, C., Forino, M., Fattorusso, E., Tartaglione, L., Milandri, A., Pompei, M., Cangini, M., Pigozzi, S., Riccardi, E., 2012. Toxin levels and profiles in microalgae from the North-Western Adriatic Sea - 15 Years of studies on cultured species. *Mar. Drugs*. <https://doi.org/10.3390/md10010140>.
- Posada, D., 2008. jModelTest: phylogenetic model averaging. *Mol. Biol. Evol.* **25**, 1253–1256. <https://doi.org/10.1093/molbev/mtn083>.
- Potapova, M., Hamilton, P.B., 2007. Morphological and ecological variation within the *Achnanthes minutissimum* (Bacillariophyceae) species complex. *J. Phycol.* **43**, 561–575. <https://doi.org/10.1111/j.1529-8817.2007.00332.x>.
- Pugliese, L., Casabianca, S., Perini, F., Andreoni, F., Penna, A., 2017. A high resolution melting method for the molecular identification of the potentially toxic diatom *Pseudo-nitzschia* spp. in the Mediterranean Sea. *Sci. Rep.* **7**, 4259. <https://doi.org/10.1038/s41598-017-04245-z>.
- Quijano-Scheggia, S., Garcés, E., Flo, E., Fernandez-Tejedor, M., Diogène, J., Camp, J., 2008a. Bloom dynamics of the genus *Pseudo-nitzschia* (Bacillariophyceae) in two coastal bays (NW Mediterranean Sea). *Sci. Mar.* **72**, 577–590. <https://doi.org/10.3989/scimar.2008.72n3577>.
- Quijano-Scheggia, S., Garcés, E., Sampedro, N., Van Lenning, K., Flo, E., Andree, K., Fortuño, J.M., Camp, J., 2008b. Identification and characterisation of the dominant *Pseudo-nitzschia* species (Bacillariophyceae) along the NE Spanish coast (Catalonia, NW Mediterranean). *Sci. Mar.* **72**, 343–359. <https://doi.org/10.3989/scimar.2008.72n2343>.
- Quijano-Scheggia, S.I., Garcés, E., Lundholm, N., Moestrup, Ø., Andree, K., Camp, J., 2009. Morphology, physiology, molecular phylogeny and sexual compatibility of the cryptic *Pseudo-nitzschia delicatissima* complex (Bacillariophyta), including the description of *P. Arenysensis* sp. nov. *Phycologia* **48**, 492–509. <https://doi.org/10.2216/08-21.1>.
- R Core Team, 2019. *R: A Language and Environment for Statistical Computing*.
- Rambaut, A., Drummond, A.J., Xie, D., Baele, G., Suchard, M.A., 2018. Posterior summarization in bayesian phylogenetics using tracer 1.7. *Syst. Biol. (Stevenage)* **67**, 901–904. <https://doi.org/10.1093/sysbio/syy032>.
- Ribera d'Alcalá, M., Conversano, F., Corato, F., Licandro, P., Mangoni, O., Marino, D., Mazzocchi, M.G., Modigh, M., Montresor, M., Nardella, M., Saggiomo, V., Sarno, D., Zingone, A., 2004. Seasonal patterns in plankton communities in a pluriannual time series at a coastal Mediterranean site (Gulf of Naples): an attempt to discern recurrences and trends. *Sci. Mar.* **68**, 65–83. <https://doi.org/10.3989/scimar.2004.68n165>.
- Richlen, M.L., Erdner, D.L., McCauley, L.A.R., Liberal, K., Anderson, D.M., 2012. Extensive genetic diversity and rapid population differentiation during blooms of *Alexandrium fundyense* (Dinophyceae) in an isolated salt pond on cape cod, MA, USA. *Ecol. Evol.* **2**, 2588–2599. <https://doi.org/10.1002/eec3.373>.
- Rimet, F., Chaumel, P., Keck, F., Kernarrec, L., Vasselon, V., Kahler, M., Franc, A., Bouchez, A., 2016. R-Syst: Diatom: an Open-access and Curated Barcode Database for Diatoms and Freshwater Monitoring. Database 2016, baw016. <https://doi.org/10.1093/database/baw016>.
- Ronquist, F., Teslenko, M., van der Mark, P., Ayres, D.L., Darling, A., Höhna, S., Larget, B., Liu, L., Suchard, M.A., Huelsenbeck, J.P., 2012. MrBayes 3.2: efficient Bayesian phylogenetic inference and model choice across a large model space. *Syst. Biol.* **61**, 539–542. <https://doi.org/10.1093/sysbio/sys029>.
- Ruggiero, M.V., Sarno, D., Barra, L., Kooistra, W.H.C.F., Montresor, M., Zingone, A., 2015. Diversity and temporal pattern of *Pseudo-nitzschia* species (Bacillariophyceae) through the molecular lens. *Harmful Algae* **42**, 15–24. <https://doi.org/10.1016/j.hal.2014.12.001>.
- Smith, M.W., Maier, M.A., Suci, D., Peterson, T.D., Bradstreet, T., Nakayama, J., Simon, H.M., 2012. High resolution microarray assay for rapid taxonomic assessment of *Pseudo-nitzschia* spp. (Bacillariophyceae) in the field. *Harmful Algae* **19**, 169–180. <https://doi.org/10.1016/j.hal.2012.07.003>.
- Solidoro, C., Del Negro, P., Libralto, S., Malaku Canu, D., 2010. Sostenibilità Della Mitilicoltura Triestina. Istituto Nazionale di Oceanografia e di Geofisica Sperimentale-OGS.
- Stern, R., Moore, S.K., Trainer, V.L., Bill, B.D., Fischer, A., Botten, S., 2018a. Spatial and temporal patterns of *Pseudo-nitzschia* genetic diversity in the North Pacific Ocean from the Continuous Plankton Recorder survey. *Mar. Ecol. Prog. Ser.* **606**, 7–28. <https://doi.org/10.3354/meps12711>.
- Stern, R., Kraberg, A., Bresnan, E., Kooistra, W.H.C.F., Lovejoy, C., Montresor, M., Morán, X.A.G., Not, F., Salas, R., Siano, R., Vault, D., Amaral-Zetter, L., Zingone, A., Metfies, K., 2018b. Molecular analyses of protists in long-term observation programmes - Current status and future perspectives. *J. Plankton Res.* **40**, 519–536. <https://doi.org/10.1093/plankt/fby035>.
- Talaber, I., Francé, J., Flander-Putrlje, V., Mozetič, P., 2018. Primary production and community structure of coastal phytoplankton in the Adriatic Sea: insights on taxon-specific productivity. *Mar. Ecol. Prog. Ser.* **604**, 65–81. <https://doi.org/10.3354/meps12721>.
- Templeton, A.R., Crandall, K.A., Sing, C.F., 1992. A cladistic analysis of phenotypic associations with haplotypes inferred from restriction endonuclease mapping and DNA sequence data. III. Cladogram estimation. *Genetics* **132**, 619–633.
- Teng, S.T., Leaw, C.P., Lim, H.C., Lim, P.T., 2013. The genus *Pseudo-nitzschia* (Bacillariophyceae) in Malaysia, including new records and a key to species inferred from morphology-based phylogeny. *Bot. Mar.* **56**, 375–398. <https://doi.org/10.1515/bot-2012-0194>.
- Tesson, S.V.M., Montresor, M., Proccacini, G., Kooistra, W.H.C.F., 2014. Temporal changes in population structure of a marine planktonic diatom. *PLoS One* **9**, 1–23. <https://doi.org/10.1371/journal.pone.0114984>.
- Thorel, M., Clauquin, P., Schapira, M., Le Gendre, R., Riou, P., Goux, D., Le Roy, B., Raimbault, V., Deton-Cabanillas, A.F., Bazin, P., Kienz-Bouchart, V., Fauchot, J., 2017. Nutrient ratios influence variability in *Pseudo-nitzschia* species diversity and particulate domoic acid production in the Bay of Seine (France). *Harmful Algae* **68**, 192–205. <https://doi.org/10.1016/j.hal.2017.07.005>.
- Thronsdon, J., 1978. Preservation and storage. In: Sournia, A. (Ed.), *Phytoplankton Manual*. UNESCO, Paris, pp. 69–74.
- Totti, C., Romagnoli, T., Accoroni, S., Coluccelli, A., Pellegrini, M., Campanelli, A., Grilli, F., Marini, M., 2019. Phytoplankton communities in the northwestern Adriatic Sea: interdecadal variability over a 30-years period (1988–2016) and relationships with meteorological drivers. *J. Mar. Syst.* **193**, 137–153. <https://doi.org/10.1016/j.jmarsys.2019.01.007>.
- Trainer, V.L., Hickey, B.M., Horner, R.A., 2002. Biological and physical dynamics of domoic acid production off the Washington coast. *Limnol. Oceanogr.* **47**, 1438–1446. <https://doi.org/10.4319/lo.2002.47.5.1438>.
- Trainer, V.L., Bates, S.S., Lundholm, N., Thessen, A.E., Cochlan, W.P., Adams, N.G., Trick, C.G., 2012. *Pseudo-nitzschia* physiological ecology, phylogeny, toxicity, monitoring and impacts on ecosystem health. *Harmful Algae* **14**, 271–300. <https://doi.org/10.1016/j.hal.2011.10.025>.
- Ujević, I., Ninčević-Gladan, Ž., Roje, R., Skejić, S., Arapov, J., Marasović, I., 2010. Domoic acid - a new toxin in the croatian adriatic shellfish toxin profile. *Molecules* **15**, 6835–6849. <https://doi.org/10.3390/molecules15106835>.
- Utermöhl, H., 1958. Zur Vervollkommnung der quantitativen phytoplankton-methodik. *Sil Commun.* **1953-1996** 1953–1996 (9), 1–38. <https://doi.org/10.1080/05384680.1958.11904091>.
- Vasselon, V., Rimet, F., Topolczaj, K., Bouchez, A., 2017. Assessing ecological status with diatoms DNA metabarcoding: scaling up on a WFD monitoring network (Mayotte island, France). *Ecol. Indic.* **82**, 1–12. <https://doi.org/10.1016/j.ecolind.2017.06.024>.
- Viličić, D., Djakovac, T., Burić, Z., Bosak, S., 2009. Composition and annual cycle of phytoplankton assemblages in the northeastern Adriatic Sea. *Bot. Mar.* <https://doi.org/10.1515/BOT.2009.004>.
- Zingone, A., Totti, C., Sarno, D., Cabrini, M., Caroppo, C., Giacobbe, M.G., Lugliè, A., Nuccicci, C., Social, G., 2010. *Fitoalga: metodiche di analisi quali-quantitative*. In: Social, G., Buttino, I., Cabrini, M., Mangoni, O., Penna, A., Totti, C. (Eds.), *Metodologie Di Studio Del Plancton Marino. Manuali E Linee Guida* 56/2010. ISPRA SIBM, Rome, pp. 213–237.
- Zingone, A., D'Alcalá, M., Mazzocchi, M.G., Montresor, M., Sarno, D., Balestra, C., Cannavacciuolo, M., Casotti, R., Conversano, F., Di Capua, I., Iudicone, D., Margiotta, F., Passarelli, A., Percopo, L., Ribera d'Alcalá, M., Saggiomo, M., Saggiomo, V., Tramontano, F., Zazo, G., 2019. Time series and beyond: multifaceted plankton research at a marine Mediterranean LTER site. *Nat. Conserv.* **34**, 273–310. <https://doi.org/10.3897/natureconservation.34.30789>.



## Chapter 4

# Toxic Species of *Pseudo-nitzschia* in the Gulf of Trieste

### 4.1 Summary

In this chapter we will present the results of toxicity tests on individual cultures of *Pseudo-nitzschia* to determine potential threats in GoT from ASP. In the Northern Adriatic Sea there are virtually no cases of ASP, but DA occasionally occurs in shellfish samples. So far, three species – *P. delicatissima*, *P. multistriata* and *P. calliantha* -have been identified as producers of DA in the Adriatic. In this study we analysed 33 strains of five *Pseudo-nitzschia* species isolated from the Northern Adriatic Sea in the Gulf of Trieste and reconfirm the presence of DA in *P. multistriata* and *P. delicatissima*, and detect for the first time in the Adriatic DA in *P. galaxiae*. We couple our data with genetic relationships of toxic and non-toxic strains based on ITS sequences, which suggest that toxicity is not related to phylogeny in *P. multistriata* and *P. delicatissima*, but may very well be in *P. galaxiae*. In this species, morphological evidence is also provided to further accentuate the notion that *P. galaxiae* is a species complex. Finally, we examined for the first time the sequence structure of the *dabA* gene in *P. multistriata*, which is thought to be involved in the biosynthesis of DA. The work pertaining to this chapter has been submitted for publication to the *Phycologia* journal.

### 4.2 Results

#### 4.2.1 Toxicity of individual strains

26 strains of *Pseudo-nitzschia* species were tested for DA content. Table 4.2-1 shows the toxicity results for each strain tested. The method with the lowest LOD was the ELISA method with a LOQ of 0.5 ng/mL of DA. HPLC-UV had a LOQ of 2 ng/mL and LC-MS/MS had a LOQ of 0.8 mg/L. Some strains were confirmed to be toxic by ELISA test only, while they did not prove positive by HPLC-UV or LC-MC/MS methods. This prompted us to retest these samples with ELISA at lower dilutions to confirm the presence or absence of DA. Most retests resulted in concentrations below LOQ, except for the *P. galaxiae* strain B3S pDA, where the concentration was still above the quantification levels. There were also many borderline strains that had concentrations below 0.5 ng/mL (LOQ), but we could not rule out their toxicity as the absorbance was lower than the negative

standards, indicating some competitive binding in the ELISA. *P. galaxiae* strain BAT2 and B2S also showed peculiar results, as the dDA fraction resulted in higher measured concentrations than the pDA fraction. In the repeated analysis both pDA and dDA were <LOQ for B2S, while for BAT2 the concentration of pDA was higher than dDA, although we could not quantify it again because pDA was above quantification. We could not confirm any toxin production in *P. manni* and *P. subfraudulenta* and *P. calliantha* strains, although some results did point to minute concentrations below the LOQ in the ELISA assay.

#### 4.2.2 Changes in DA concentration in selected cultures

For *P. multistriata* strains 119-A4, MS2 and MS3 and *P. delicatissima* strain 119-B3, we performed toxin analyses in different growth phases. We observed a decreasing trend of per cell toxin quota with increasing cell density in 119-A4 (Figure 4.2-1 A), while dDA increased slightly only on the last day of measurements (Figure 4.2-1 B). We can see that the first (initial) screen yielded a similar cell count to Day 11, but a completely different concentration for both the pDA and dDA fractions. While the pDA fraction was lower compared to Day 11, the dDA fraction was much higher. This could be due to the age of the culture and the fact the culture was already in stationary phase at the initial screening, while it had not yet reached stationary phase at day 11 of the experiment. Unfortunately, the measurements of DA present in the MS2 and MS3 cultures were not reliable enough to obtain graphs of DA content change. This is also since in the initial ELISA screens, the dDA fractions were higher than the total fractions, while the concentrations in the retest were below quantification, possibly due to sample degradation. Similarly, after the initial confirmation of toxicity in *P. delicatissima* strain 119-B3, we did not confirm any DA production in the continuous sampling experiment. The concentration of DA was probably very low in this case, as the HPLC-UV method could not detect DA even in the initial screening.

Table 4.2-1: Toxicity tests performed on *Pseudo-nitzschia* species reporting results for each tested strain. The toxicity range was obtained from different tests of the same culture. NA – not available; </> quant – below/above quantification; o – DA presence could not be reliably determined. Point sampling refers to a single sampling during the stationary growth phase. Continuous sampling refers to several sampling points during different stages of growth.

Species	Strain	Sampling frequency	Partition tested	Test method	Result	DA concentration	ELISA retest
<i>P. delicatissima</i>	219 A1	point	pDA	ELISA	-		
	219 A2	point	pDA	ELISA	-		
	219 A3	point	pDA	ELISA	-		
	219 B1	point	pDA	ELISA	-		
	219 B2	point	pDA	ELISA	-		
	219 B3	point	pDA	ELISA	-		
	219 B4	point	pDA	ELISA	-		
	119 A2	point	pDA	ELISA	-		
	119 A3	point	pDA	ELISA	-		
	119 B3	point & continuous	pDA and dDA	ELISA&HPLC-UV	+ (ELISA)	1.5 fg/cell	<quant
	119 C1	point	pDA and dDA	ELISA&HPLC-UV	+ (ELISA)	NA	<quant
	119 C4	point	pDA	ELISA	-		
<i>P. multistriata</i>	119 A4	point & continuous	pDA and dDA	ELISA&HPLC-UV	+ (Both)	pDA: 16-114 fg/cell; dDA: 6-257 ng/mL	
	119 C3	point	pDA and dDA	ELISA&HPLC-UV	+ (Both)	pDA: 121-160 fg/cell; dDA: 30-80 ng/mL	

	MS2	Point & continuous	pDA and dDA	ELISA; HPLC-UV; LC-MS/MS	+	pDA: 0-32.8 fg/cell; dDA: 20 ng/mL	<quant
	MS3	Point & continuous	pDA and dDA	ELISA; HPLC-UV; LC-MS/MS	+	pDA: 1.42-20.7 fg/cell; dDA: 14.6-38.5 ng/mL	<quant
<i>P. galaxiae</i> – large morphotype	MA-919-C1	point	pDA and dDA	ELISA&HPLC-UV	-		
	MA-919-A2	point	pDA and dDA	ELISA&HPLC-UV	-		
	F919 - C2L	point	pDA and dDA	ELISA&HPLC-UV	-		
<i>P. galaxiae</i> – medium morphotype	F919-B1M	point	pDA and dDA	ELISA&HPLC-UV	-		
	BAT2	point	pDA and dDA	ELISA&HPLC-UV	o (ELISA)	dDA: 13 ng/mL	<quant
<i>P. galaxiae</i> – small morphotype	B3S	point	pDA and dDA	ELISA&HPLC-UV	+	dDA: 5-24.8 ng/mL; pDA >quant	>quant
	B2S	point	pDA and dDA	ELISA&HPLC-UV	o (ELISA)	dDA: 12.6 ng/mL	<quant
<i>P. mannii</i>	BF-819-B2	point	pDA and dDA	ELISA&HPLC-UV	-		
	BF-819-A4	point	pDA and dDA	ELISA&HPLC-UV	-		
	BD-919-A3	point	pDA and dDA	ELISA&HPLC-UV	-		

	PNF_1020_5	point	pDA and dDA	ELISA	o	<quant
<i>P. subfraudulenta</i>	PNF_1020_1	point	pDA and dDA	ELISA	-	
<i>P. calliantha</i>	PNF_1020_2	point	pDA and dDA	ELISA	o	<quant

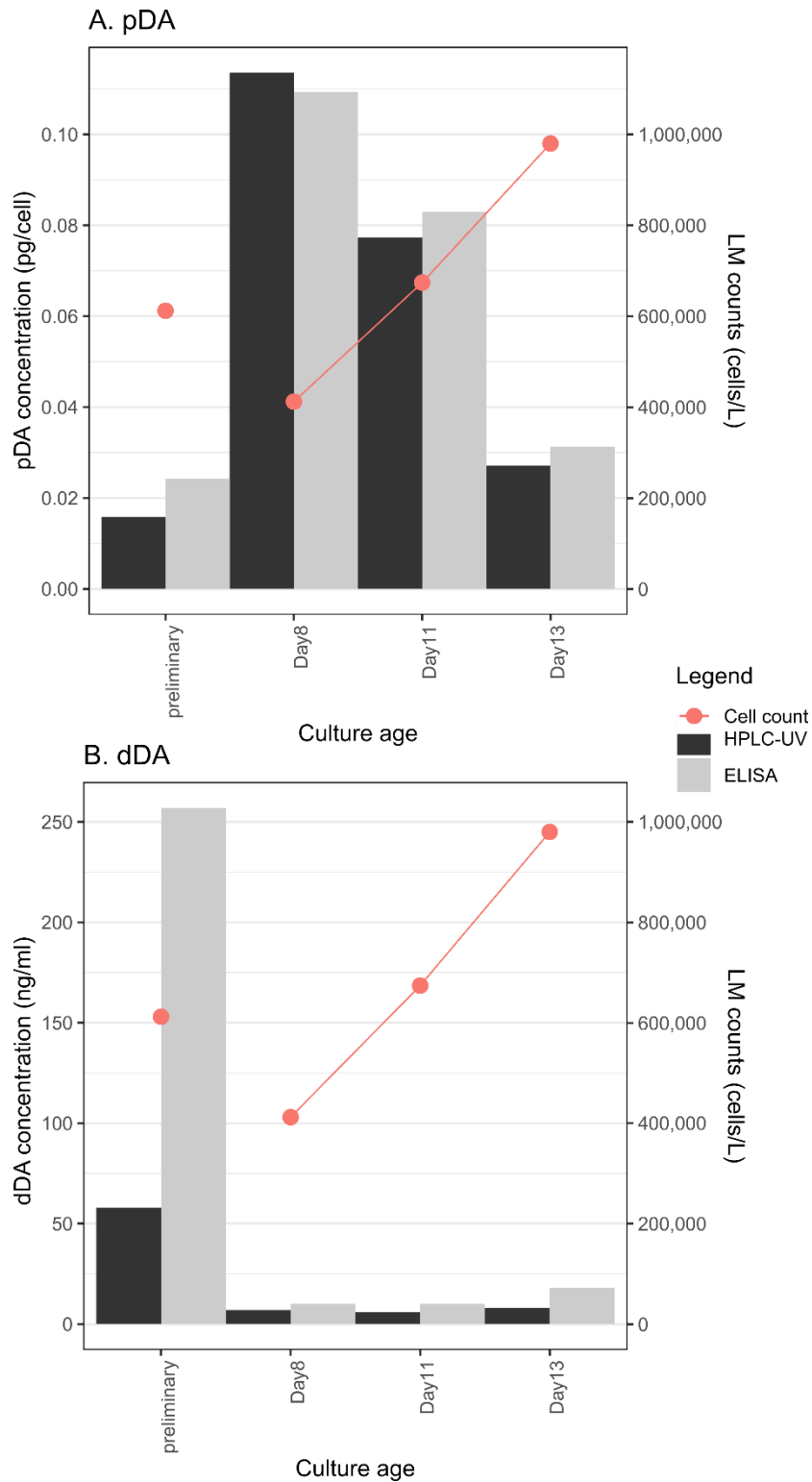


Figure 4.2-1: Change in the content of (A) particulate DA (pDA) (B) dissolved DA (dDA) in *Pseudo-nitzschia multistriata* strain 119-A4. The preliminary measurement was performed in another experiment at the stationary phase (Day 14).

### 4.2.3 Phylogeny versus toxicity

Our phylogenetic analysis based on ITS sequences of the selected strains showed that there is no clear phylogenetic relationship with toxicity within *P. delicatissima* and *P. multistriata* (Figure 4.2-2 A, C). The only toxic strain of *P. delicatissima* that we could identify from the literature (Pn100-07A2) from Maine, USA, had high bootstrap support, but we saw different toxicity profiles in our strains, all of which were phylogenetically identical. On the other hand, there was some evidence that toxicity in *P. galaxiae* is somewhat related to the strain in question (Figure 4.2-2 B). We also support this with morphological data, as the strains that we identified as toxic (FB2S and FB3S) belong to the small morphotype of *P. galaxiae*, while the strains that were negative for DA belong to the medium and large morphotypes. Strain BAT2, which was tentatively identified as toxic, belongs to the larger morphotype, although it had a peculiar bat-like morphology. The *P. galaxiae* tree also showed the highest support for branching obtained by bootstrapping the tree space, while the trees for *P. multistriata* and *P. galaxiae* showed little ITS variability among the selected strains, despite broad geographical representation.

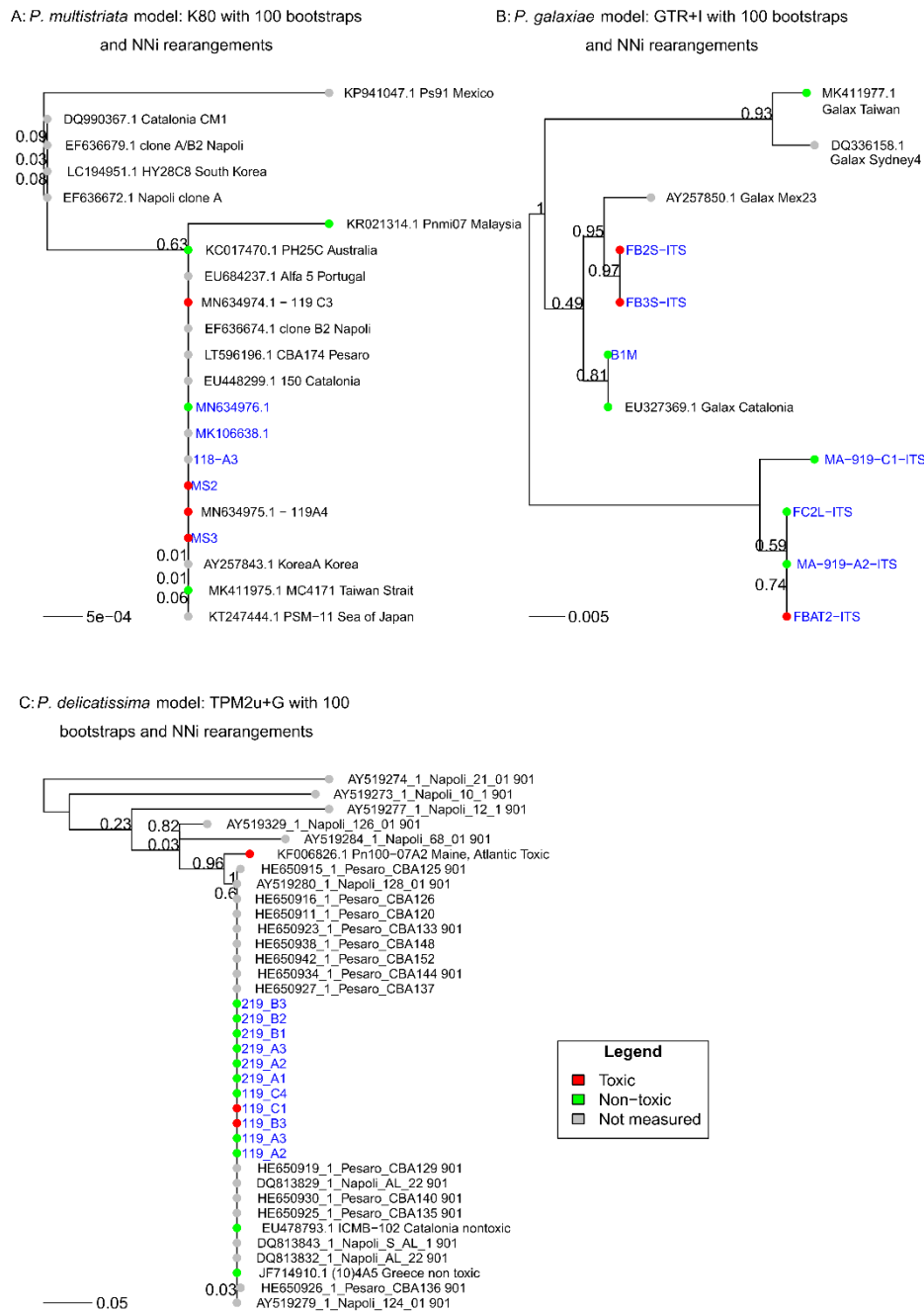


Figure 4.2-2: Maximum likelihood trees for three species. Blue-coloured strains represent those used in this study.

#### 4.2.4 *dabA* gene screening in toxic and non-toxic strains

*Pseudo-nitzschia multistriata* *dabA* gene sequences were obtained using the custom primers from four different *P. multistriata* strains. The amplified product was maximum 1372bp long and contained the intronic region that was removed from the sequences following alignment with the existing two published sequences (MH202990.1 – *P. multiseriis*; CAACVS010000654.1 – *P. multistriata* genomic). The product obtained is a partial gene sequence because amplification with primers designed in Brunson et al. (2018) did not yield a specific product, thus primers had to be designed internally. The sequences obtained were highly conserved with only a few ambiguous sites (16 on a 1372bp long fragment ~ 1%), but these were all on degenerate codon positions and had thus no effect on the amino acid sequence. The sequences all aligned well with the sequence obtained from the *P. multistriata* genome project (Basu et al., 2017), but this was not perfect as it contained undefined sites resulting in a translated amino acid sequence with multiple stop codons. The published sequence of *P. multiseriis* (MH202990) is 84% identical to the sequences of our *P. multistriata* strains, while the translated sequences show 89% similarity to the DabA protein from *P. multiseriis*, with significant structural similarity as identified by homology modelling in Phyre2 (Figure 4.2-3). This highlights the functionality of the *P. multistriata* enzyme in the production of DA. However, our attempt to amplify the *dabA* gene in other species of *Pseudo-nitzschia* using the same primers was unsuccessful. Some of the amplifications yielded several non-specific products, while others yielded no product. Excision and sequencing of these products resulted in unknown sequences or sequences of prokaryotic origin following BLAST that do not fall into the category of terpene synthases, such as the DabA enzyme. Thus, the primers are not *dabA*-specific. Although we cannot rule out the possibility that the genetic machinery to produce DA is absent in strains that have been shown to be non-toxic, we would expect the gene to be present at least in strains that have been confirmed to be toxic by our analysis. Screening of *P. delicatissima* strains 219-A1 (non-toxic) and 119-C1 (toxic) revealed several amplicons, including one of the correct size, but no readable sequences could be obtained without cloning, which was not performed.



## Chapter 5

# Colorimetric Detection of *Pseudo-nitzschia* in the Environment and in Culture

### 5.1 Summary

In recent years, much research in the field of harmful and toxic microalgae has focused on the development of rapid and reliable systems for the detection of harmful species and their toxic products in marine and freshwater environments. While there have been considerable improvements in the detection of toxins in various matrices, the identification and quantification of species producing these toxins remains problematic, particularly for species that are not easily identified under the light microscope (LM). In Chapter 3, we showed that *Pseudo-nitzschia* is a genus that is difficult to distinguish under LM, requiring further analysis by electron microscopy or molecular methods. We have identified species occurring in the Gulf of Trieste using an integrated approach of both morphological and molecular methods, but this process is tedious for routine use and requires a considerable investment of time. This chapter presents work carried out by the author of this thesis during his research stay in Banyuls-sur-Mer in France, where he collaborated with Microbia Environnement, a spin-off company of the Oceanological Observatory of in Banyuls-sur-Mer. The aim of the collaboration was to develop and test a solid support-based sandwich hybridization assay (SHA) for the detection and assessment of cell activity of harmful algae in the marine environment. The collaboration focused primarily on *Pseudo-nitzschia* and the cultures we established during this work.

By experimenting with RNA from cultured material, we tested several different probes for specificity for different *Pseudo-nitzschia* species in a microplate-based colorimetric RNA ELISA assay. The goal was to achieve low RNA detection limits and to generate calibration curves with RNA dilution series for several different species. Selected probes were then used on environmental samples collected to test the performance of the assay compared to traditional monitoring techniques in terms of: (i) time and cost, (ii) specificity and detection limits, (iii) replicability, (iv) potential for monitoring and bloom prediction, (v) measurement of cell activity. The results show a very good coherence between colorimetric signal and microscopic counts. Preliminary data shows the cell activity measurements from RNA signal can even anticipate blooms, which is an invaluable result, as it can greatly improve shellfish aquaculture management. The assay is simple to use and offers higher

sample throughput and replication and a much faster analysis time compared to traditional monitoring.

The assay could become a new tool for phytoplankton monitoring by aquaculture operators in the future. Aquaculture is one of the fastest growing food industries and as it expands and grows, approaches to ensuring food safety must also evolve to meet the demands of the growing sector. The results of the development and testing of the *Pseudo-nitzschia* assay, presented here, have been submitted for publication in an international peer-reviewed journal.

## 5.2 Results

### 5.2.1 Microarray training and preliminary probe screens

Experiments with the M.A.R.T.A microarray (Microbia Environment) provided information on the reactivity of various probes to *Pseudo-nitzschia* and *Cylindrotheca* RNA. RNA extraction with buffer containing CTAB and labelling were performed on six species. The amount of labelled RNA was insufficient to perform an array on *P. pungens*, while *P. mannii* was not tested due to cost considerations and was omitted due to the close phylogenetic relationship to *P. calliantha*. Duplicate arrays were only performed on *P. delicatissima*. During the initial screening of suitable probes spotted on the microarray, five probes were selected based on the mean signal-to-noise ratio calculated from the blank signals (see Appendix B). Probes specific for the RNA of our isolated strains from the Northern Adriatic were identified: Probe specific for *P. fraudulenta* (PcaciD02\_25\_dT), *P. calliantha* (Pcal1D01\_25\_dT) and *P. galaxiae* (PgalaD02\_25\_dT), among the species tested. The probe for *P. fraudulenta* originally targeted to *P. cacciantha* (PcaciD02\_25\_dT) had a low signal response to *P. fraudulenta*. The other probes that were selected were a probe that was semispecific for *P. multistriata* (PmulaD0325), and a genus-wide specific probe (PsnGS02\_25). Note that some probes are labelled as “with hierarchy”. This essentially means that if you have a sequence of probes under the hierarchy that respond, you can determine which species is present in the sample, even if that probe hybridizes with many species. These probes have been used as templates for the design of novel probes used in the SHA.

### 5.2.2 Sandwich-hybridization bioassay

The first step of testing the SHA was performed with the HYB-A buffer, which is less sensitive and requires higher RNA concentrations to detect targets. Therefore, the selection of probes for subsequent specificity and environmental testing may have been biased towards more sensitive probes that showed a more genus-wide response. The results for each species and probe are shown in Figure 5.2-1. The initial tests after HYB-A were performed using 50 ng of RNA from the target species extracted using the QuickRNA protocol (Zymo Research), which is much faster than the CTAB protocol, although it provides lower quality RNA. However, the quality is sufficient for analysis on the SHA. Time of the analysis (TOA) is essential in this regard, as the aim of the assay is to provide rapid and reliable answers to the status of the harmful algal population in the environment.

While Pn1 gave the strongest signals, it showed a slight cross-reaction with the *Cylindrotheca* strain tested, albeit below the threshold line. We decided to keep this probe in a dilution series for further analysis to check for cross-reactivity at higher concentrations. Pn1mod was also a good candidate for genus-wide detection, although it did not meet thresholds at 50 ng RNA for some species, notably *P. fraudulenta*, *P. delicatissima* and *P.*

*manni*, but still warranted further investigation in a dilution series. The probe Pn7 showed some specificity for *P. galaxiae*, which is not surprising since it was derived from the *P. galaxiae*-specific probe (PgalaD02\_25\_dT) tested on the microarray. Finally, Pn5 was also chosen as a relatively low-sensitivity probe to compare it with more sensitive probes in environmental samples. We can see that many probes that did not meet the threshold were excluded from further testing, even though the threshold is not absolute, and the low sensitivity protocol was used here. For example, Pn9 showed relatively good response to *P. delicatissima* and *P. fraudulenta* but did not reach the threshold and there is a possible cross-reaction with *Cylindrotheca* strain suspected from the signal. The RNA concentration used for the initial screening was nevertheless high and we aimed for highly sensitive probes that can detect minute cell concentrations in environmental samples, increasing the power of the assay compared to more traditional techniques such as microscopy counting.

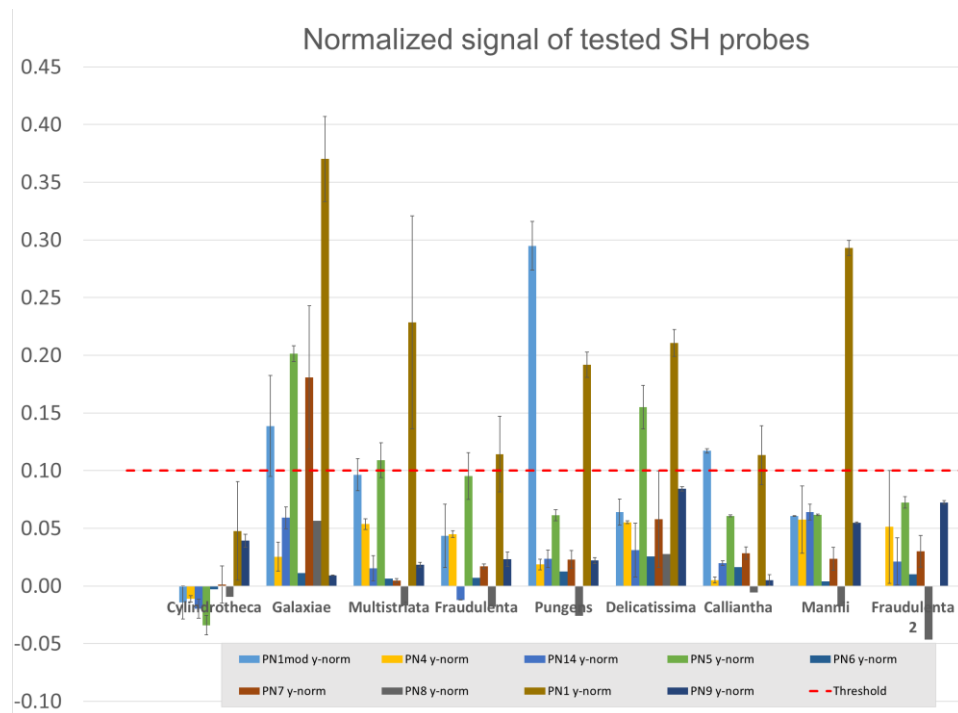


Figure 5.2-1: Probe specificity and sensitivity results using HYB-A and 50 ng of RNA from each species. The threshold is set at 0.1. Signals below this threshold may still indicate some hybridization with target probes as the threshold is not absolute.

### 5.2.3 Dilution-series analysis

Dilution series analysis revealed different responses of the probes to RNA from different species, but none of the probes tested were truly species-specific (

Figure 5.2-2). We did not obtain calibration curves with HYB-B and Pn1, while Pn1mod and Pn5 were tested with HYB-B only. We saw that when this buffer is used, the detection limits of RNA could be lowered by about tenfold compared to Pn1 and Pn7 tested with HYB-A. The most sensitive probe used in this study was Pn1mod, with steep calibration curves at low RNA concentrations, with signal saturation starting at 25-50 ng of RNA (50 ng data points were removed from the plot to show proper calibration). The only exception was *P. subfraudulenta*, where the RNA was likely degraded as it was extracted from an aging culture. We observed that none of the probes tested were truly species specific, but

there was a difference in reactivity between them. Pn7 was the most specific, although the reaction curves with HYB-A for *P. galaxiae* and *P. delicatissima* were quite comparable. A significant response was also observed for *P. fraudulenta*. Sensitivity was not drastically improved with HYB-B and Pn7, except for *P. galaxiae* and *P. fraudulenta*, where the increase was about tenfold, because tenfold lower RNA concentrations were used in the HYB-B tests.

The main reason why we chose to use RNA dilutions instead of cell dilutions in the calibration assays was that the LODs depend strongly on the average RNA ratio per cell. The cellular LODs given in Table 5.2-1 for each species-probe pair are approximations and were determined from the average ratios per cell that we obtained from the extractions performed (Table 5.2-2). This is because the RNA ratios in different extractions differed by as much as tenfold for some species. (e.g., *P. delicatissima*, *P. galaxiae*, *P. fraudulenta*). This bias may be due to several factors, including unreliable cell counts (applies only to *P. galaxiae*; due to small size, many cells may have been neglected in the counting chamber), physiological state of cultures (probably the case for *P. fraudulenta*), and extraction bias. The difference in cell detection limits relative to RNA detection limits is also a consequence of the different cell biovolumes. The morphological species complex of *P. seriata*, which also includes *P. multistriata*, *P. pungens* and *P. fraudulenta*, has a biovolume up to tenfold higher than the morphological species complex of *P. delicatissima* which contains *P. galaxiae*, *P. calliantha*, *P. mannii* and *P. delicatissima* (Olenina, 2006). Higher biovolume should translate into more ribosomes stored in cells (Godhe et al., 2008). For example, *P. fraudulenta* had the highest average per cell RNA quota in our extractions, which is not surprising since its cells are the largest among those tested. This species is the least reactive to Pn1 (

Figure 5.2-2), but because of this property, LOD is the lowest in terms of cell number for this species (Table 5.2-1). It is therefore very difficult to extrapolate RNA content to cell number unless several factors such as those described above are considered, while many more calibration tests would need to be performed with cultures at different growth stages. Pn1mod and Pn5 have very low and similar LODs for all species except *P. calliantha* and *P. subfraudulenta*, which are detected at 1 ng and 25-50 ng, respectively, with Pn5.

This result shows that active cells can be detected in environmental samples at low abundances comparable to the detection limits of microscopy. It should be noted that the LODs reported here are absolute, whereas the abundance in environmental samples depends on the volume filtered or examined. Thus, the significance of the assay is also affected by from the sampling protocol used. Different specificity of probes for the targeted species may result in competitive binding of RNA in mixed samples, with the most specific RNA binding most competitively, although exclusion is most likely not possible. Only with Pn7 was the specificity to *P. galaxiae* high enough that we could expect *P. galaxiae* RNA to hybridize preferentially to this probe in the presence of other species RNA, which will be shown later with field samples.

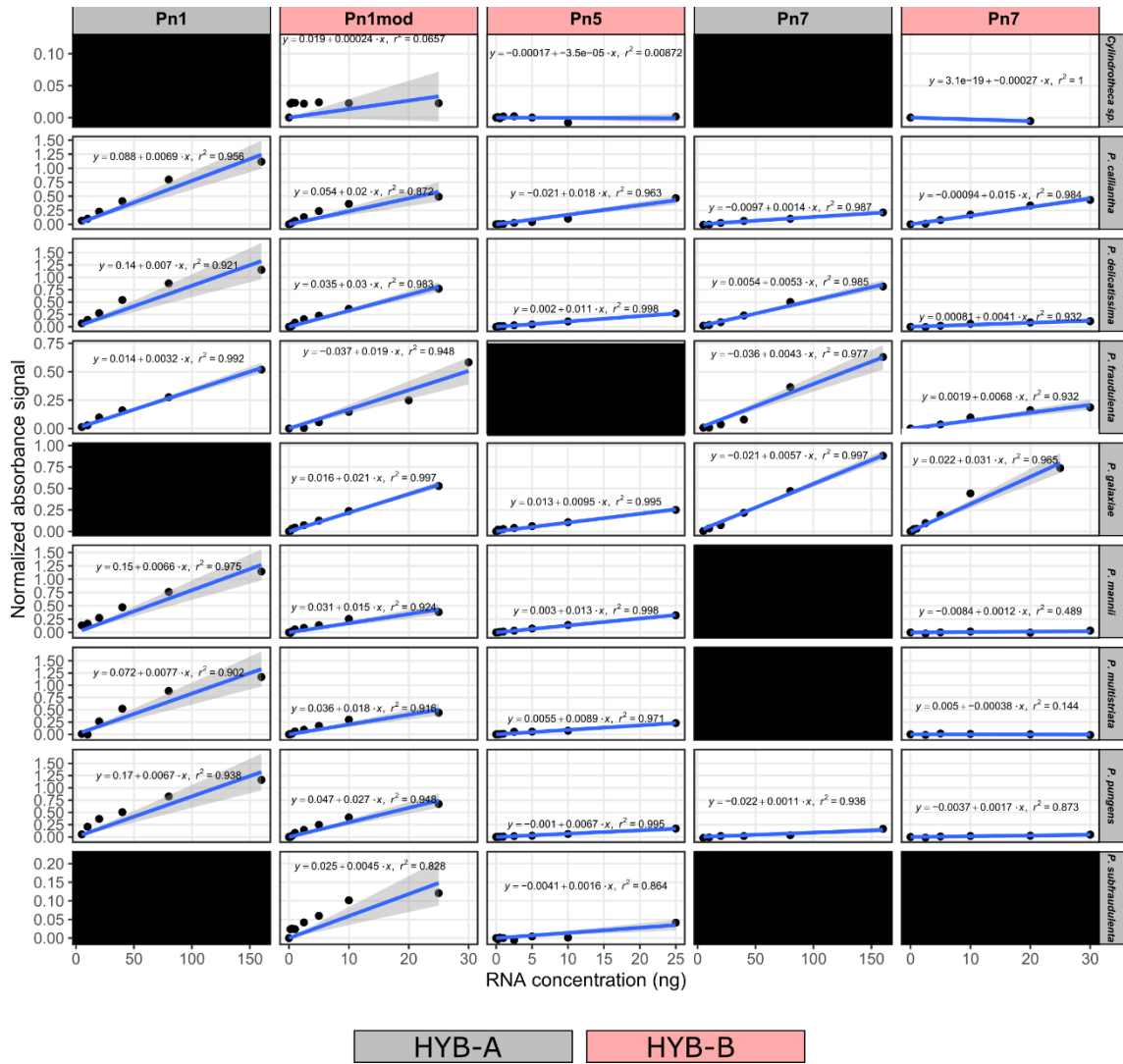


Figure 5.2-2: Calibration curves from dilution series for each species-probe pair tested. Note that the scales on both axes are different, depending on the buffer used and the sensitivity of the probe for different species.

Table 5.2-1: Limit of detection as ng RNA and cell numbers for each species-probe pair tested. NT = not tested, /= could not be determined.

HYB-B	LOD (ng)	LOD (cell)	LOD (ng)	LOD (cell)	LOD (ng)	LOD (cell)	LOD (ng)	LOD (cell)
	<i>PN1</i>		<i>PN1mod</i>		<i>PN5</i>		<i>PN7</i>	
<i>P. mannii</i>	/		0.5	1010	0.5	1010	/	/
<i>P. calliantha</i>	/		0.25	920	1	3679	2.5-5	9000-18000
<i>P. multistriata</i>	/		0.5	1104	0.5	1104	/	/
<i>P. pungens</i>	/		0.5	537	0.5	537	5-10	5000-10000
<i>P. delicatissima</i>	/		0.5	645	0.25	322	5-10	6500-13000
<i>P. galaxiae</i>	NT		0.25	558	0.25	558	0.25-0.5	558-1116
<i>Cylindrotheca closterium</i>	NT		/	/	/	/	/	/
<i>P. subfraudulenta</i>	NT		2.5-5	/	25-50	/	NT	NT
<i>P. fraudulenta</i>	/		5	2621	NT	NT	5	2500
HYB-A		<i>in thousands</i>						<i>in thousands</i>
<i>P. mannii</i>	<5	10	NT		NT		NT	
<i>P. calliantha</i>	<5	18	NT		NT		20-40	74-147
<i>P. multistriata</i>	10-20	22-44	NT		NT		NT	
<i>P. pungens</i>	<5	5	NT		NT		80-160	86-172
<i>P. delicatissima</i>	<5	6	NT		NT		10-20	13-26
<i>P. galaxiae</i>	NT		NT		NT		5	11
<i>Cylindrotheca closterium</i>	NT		NT		NT		NT	
<i>P. subfraudulenta</i>	NT		NT		NT		NT	
<i>P. fraudulenta</i>	5	2.5	NT		NT		20-40	10-20

Table 5.2-2: RNA quota per cell from each extraction performed. Data for *Pseudo-nitzschia subfraudulenta* is not available as the culture was in a poor condition and therefore only the recovery of RNA was the aim.

	RNA (pg/cell)			
Species	Ext. 1	Ext. 2	Ext. 3	Average
<i>P. mannii</i>	0.61725	0.613928	0.254207	0.495128
<i>P. calliantha</i>	0.166767	0.41605	0.23272	0.271846
<i>P. multistriata</i>	0.5596	0.477147	0.321936	0.452894
<i>P. pungens</i>	0.648903	1.2086	0.933235	0.930246
<i>P. delicatissima</i>	1.75045	0.292593	0.283704	0.775582
<i>P. galaxiae</i>	0.8086	0.087272	/	0.447936
<i>P. fraudulenta</i>	3.24125	0.573733	/	1.907492
<i>P. subfraudulenta</i>	/			
<i>Cylindrotheca closterium</i>	5.740			

#### 5.2.4 Field sample testing

The proof-of-concept comparison between the environmental time series of the microscopic counts and the assay signal analysis was performed as part of the experimental portion of the assay development. The most informative comparison of probes tested in the microplate format comes from station 0DB2 for the 2015 time series (Figure 5.2-3), as the majority of probes were tested on these samples. From Figure 5.2-3 we can draw a few observations. When cell abundances were very low, the Pn1mod probe retained less background noise compared to Pn5 and Pn1. Thus, Pn1mod captures population dynamics best, although the signals showed some nonlinear fluctuation during the "bloom" period when cell numbers fluctuated at high numbers. During this period, the signals from probes Pn5 and Pn1 showed similar trends, although the magnitude was ten times higher for Pn1. The above threshold signals of Pn1 when cell numbers were low can be attributed to negative targeting, as we saw that even *Cylindrotheca*, which is not as closely related to *Pseudo-nitzschia* as *Fragilariopsis* or *Nitzschia* species, responded to this probe (Figure 5.2-1). Based on these results, we concluded that Pn1mod was the most reliable probe and was used in the analysis of the data from 0024, 2015 (Figure 5.2-6). The samples were tested in two volume equivalent dilutions, however the strength of the signal in the 0.66 L dilution was visibly higher by a factor of two in only one case, as in the other samples both signals were either too low or too high. We see that although the cell counts were similar to 0DB2, there was a fundamental difference in the response of the assay just prior to the blank period when no samples were collected. At this point, the cell counts were very low, but the signal was saturated. This could indicate a pre-bloom phase where cells are not numerous but very active and producing large amounts of ribosomes, which is reflected in the signal.

In the case of the 2017-2018 dataset, we did not have enough data points to be analysed in terms of a meaningful time series, so we analysed it as a correlation between cell abundance and signal. Pn1mod showed the best correlation between abundance and signal, while Pn1 and Pn5 showed similar performance (Figure 5.2-4). The signal from Pn1 showed the strongest absolute signal, as seen in the 2015 data. On the other hand, we saw no correlation with Pn7, which was expected due to the specificity of this probe. We further emphasised this by analysing the limited dataset of counts of *P. cf. galaxiae*, for which this probe was found to be most specific (**Error! Reference source not found.**). In analysing the 2017-2018 samples, we also measured the effect of volume on the resulting signal response. Although we did not filter different volumes, which would be the correct way to assess this scaling, we were able to pseudo-replicate this by applying different amounts of RNA to the sensor, corresponding to the elution volumes of the extraction. Cell abundance in the correlation analysis was also adjusted to match the volume equivalents of RNA added to the sensor. To test the specificity of Pn7 resulting from the calibration curve analysis, we also applied the probe to the samples associated with *P. cf. galaxiae*. We must emphasise that in most cases these may also contain counts of *P. delicatissima*, to which this probe also responds. **Error! Reference source not found.** shows the relationship between various probe signals and *P. cf. galaxiae*. The Pn7 probe showed a very specific response to *P. cf. galaxiae*, while there was no obvious relationship between the signal from Pn1mod and Pn5 and abundance. Pn1, on the other hand, also responded to *P. cf. galaxiae*, although the relationship was much weaker compared to Pn7 and it could also have been a false positive response due to the presence of other diatoms.

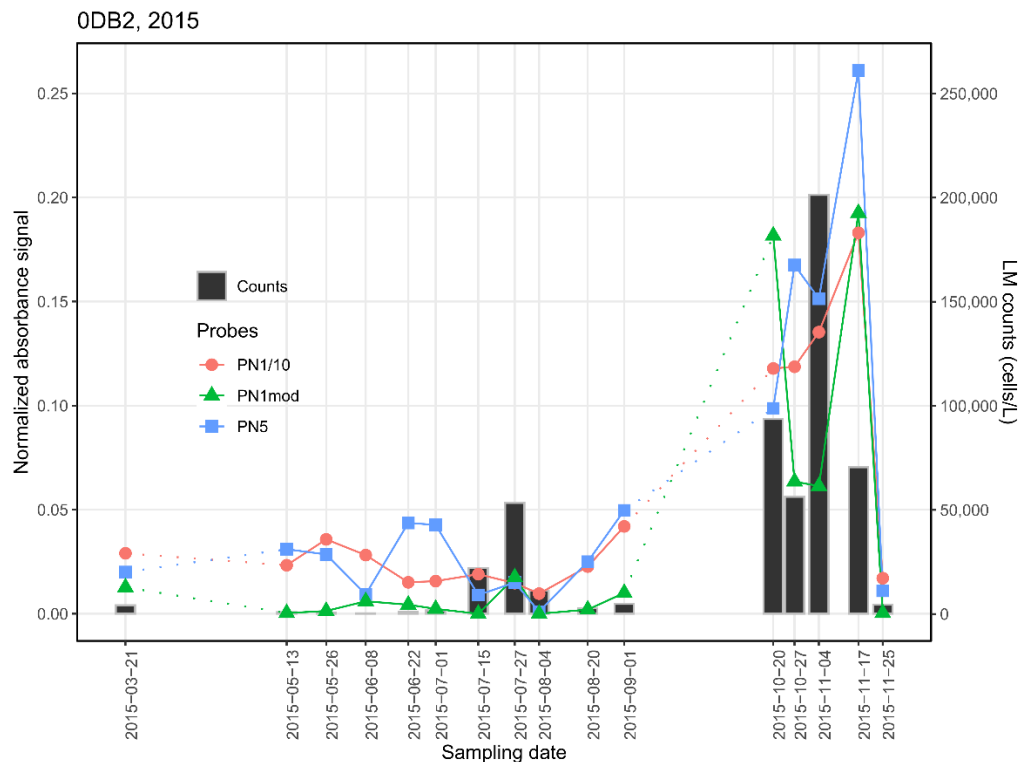


Figure 5.2-3: Comparison of signal and microscopic counts at station 0DB2 from three probes tested on 2015 environmental samples.

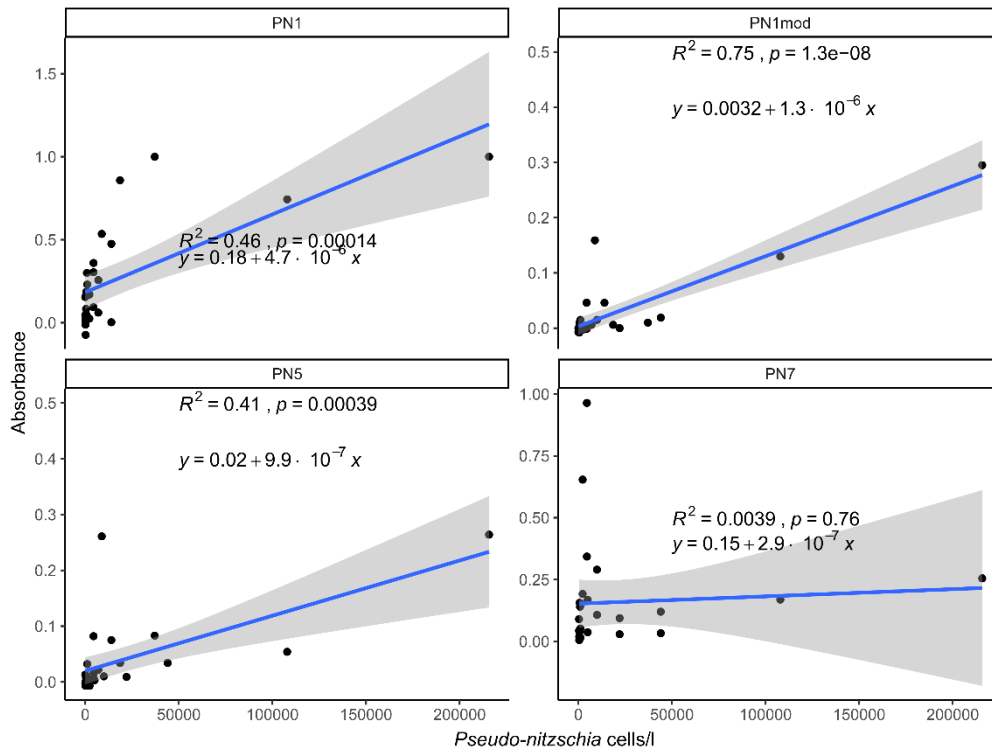


Figure 5.2-4: Relationship between cell counts of total *Pseudo-nitzschia* and signals from different probes on environmental samples from 2017 and 2018, different stations.

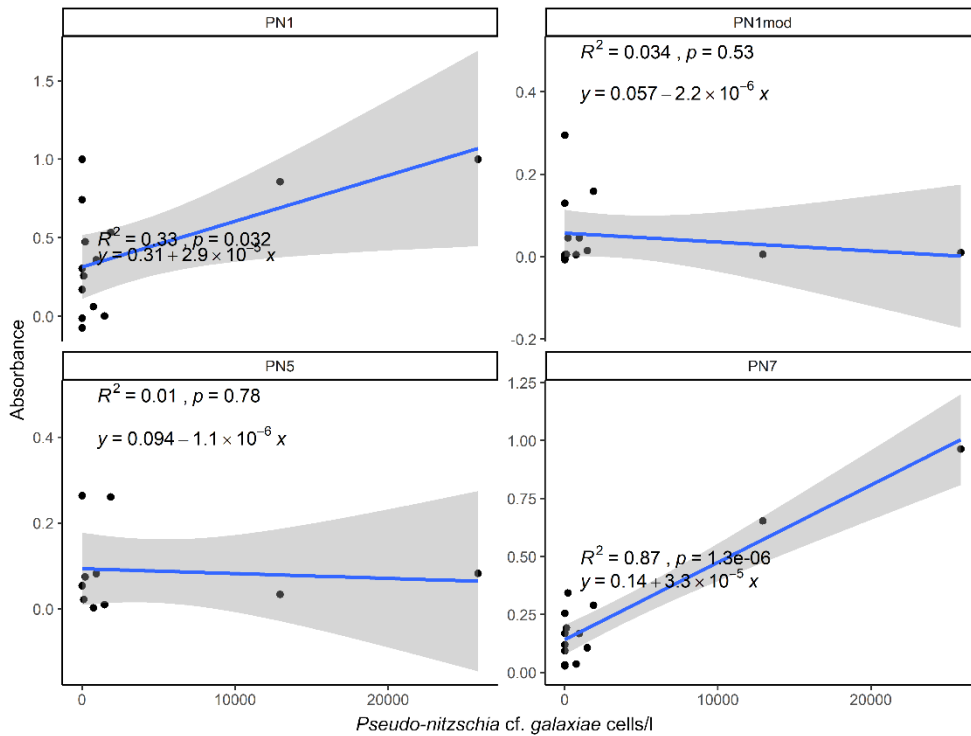


Figure 5.2-5: Relationship between cell counts of *P. cf. galaxiae* and signals from different probes on environmental samples from 2017 and 2018, different stations.

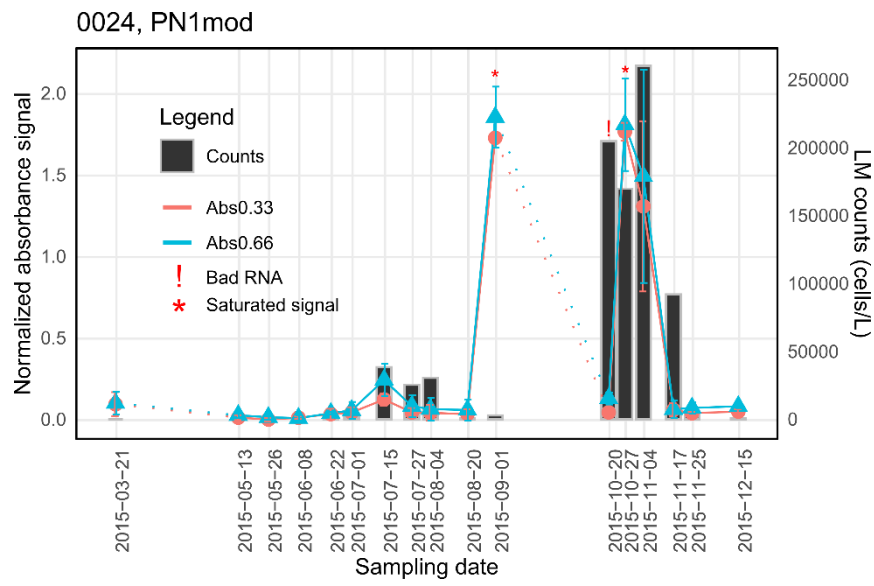


Figure 5.2-6: Comparison of Pn1mod signal and microscopic counts at station 0024.

## Chapter 6

# Phytoplankton Assemblages in the Gulf of Trieste Inferred from Metabarcoding – Case Study of *Pseudo-nitzschia*

### 6.1 Summary

In this chapter we present the results of the metabarcoding study, which aimed to reveal phytoplankton biodiversity previously hidden by applying traditional techniques due to their morphological similarity, rarity or misidentification. The approach we took was to amplify the environmental DNA with the 18S-V9 region marker, which is commonly used in such studies but is not entirely suitable for identifying taxa below the genus level because the resolution of this marker at the species level is poor. Since the main study organisms in this work are diatoms of the genus *Pseudo-nitzschia*, we therefore decided to also amplify the *rbcL* marker, which has been shown to be very good at distinguishing diatom species, even when using a small section of the *rbcL* gene (see Chapter 3). To our knowledge, this is also the first study to use *rbcL* as a metabarcoding marker for marine diatoms. Another aim of this study was to gather information on whether and to what extent this technique is comparable to the traditional phytoplankton monitoring methods that have been used at our institute and are also the gold standard worldwide. We focused only on diatom genera that can be identified by all three methods, but also due to the primers used in PCR amplification of the *rbcL* region, diatom sequences are preferentially amplified, which provides a good comparison to the 18S-V9 region. In the results we particularly focus on dinoflagellates and diatoms as the most represented groups in phytoplankton monitoring data. Our approach indeed reveals a hidden diversity in both groups including genera and species that seem to prevail in certain periods, but are rarely recorded in microscopic counts. Such examples are the nanodiatom *Minidiscus* and *Pseudo-nitzschia galaxiae* which seem to dominate the winter community. Several potentially harmful dinoflagellates were also recorded, including *Karlodinium*, *Karenia*, *Alexandrium* and *Takayama*. The *rbcL* marker was online used for the analysis of the diatom community, and the resulting abundance tables are comparable to 18S-V9, although the individual taxa recovery is much higher. Based on *rbcL* we could identify eight species, all previously recorded, except for a handful of sequences belonging to the *Pseudo-nitzschia americana/linea* complex. There

was a clear prevalence of sequences belonging to *Pseudo-nitzschia galaxiae*, and more specifically to the small morphotype, although this was not supported with high bootstrap. The comparison of the two metabarcoding markers in terms of diatom genera assignment revealed very congruent results, but when we compared the assignments to abundance data from microscopy these were rarely comparable, except in months when certain genera such as *Chaetoceros* and *Cyclotella* dominated the community.

## 6.2 Results

### 6.2.1 Overview

A total of 36 samples were collected monthly from March 2019 to February 2020 at two different depths, 0 m and 5 m. A phytoplankton net sample was also collected in October 2020 for sequencing. While most samples were filtered on 0.8  $\mu\text{m}$  polycarbonate filters, the April, May, and June 2019 samples also included fractionation of water samples on 20  $\mu\text{m}$ , 2  $\mu\text{m}$ , and 0.8  $\mu\text{m}$  filters. These fractionated samples were later used for sequencing when the non-fractionated samples did not produce visible PCR products. This was the case for the April and May samples with both 18S and *rbcL* barcodes. Otherwise, we obtained good amplicons for the entire year with 18S, while we were unable to obtain sequences from March and October 2019 with *rbcL*.

### 6.2.2 18S-V9 Metabarcodes

Read quality was consistently high and only trimmed to ensure maximum read quality. Two samples yielded a read count below the threshold and were therefore discarded from further analysis. The average number of reads per sample was approximately  $50,000 \pm 16000$  reads. Roughly 1.5 million non-chimeric contigs were obtained with this marker and about half of these belonged to metazoan organisms and were filtered out of further analyses. Chimeric contigs accounted for only 2% of all merged sequences. Rarefaction curves were generated and show saturation at about 10,000 reads (Figure 6.2 1). We see that there is a large difference in recovered diversity between samples, but this may also reflect environmental heterogeneity.

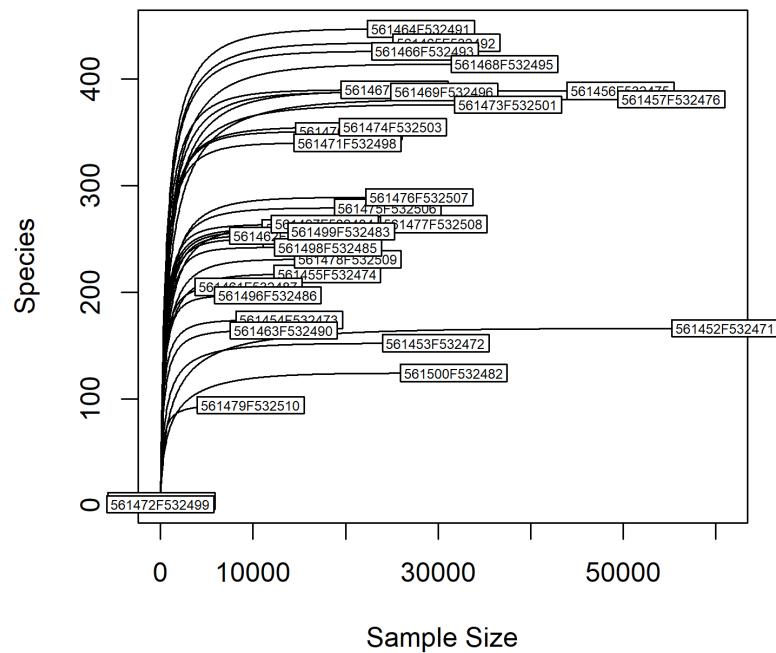


Figure 6.2-1: Rarefaction curve for 18S-V9 samples cleared of metazoan sequences. Labels represent individual samples. See Appendix B for sample metadata.

#### Comparison of non metazoan taxa

Analysis of the non-rarefied dataset shows that the predominant non-metazoan class of organisms in our samples was dinoflagellates, except in the March samples where a bloom of diatoms (seen as a large proportion of Ochrophyta) was recorded (Figure 6.2 2). Diatoms occurred in varying relative abundances throughout the study in each case. Haptophytes, which include coccolithophorids and other non-calcareous haptophytes (e.g., Prymnesiales), were also relatively abundant in spring and early summer. Winter communities appeared to be most even in class distribution with equal numbers of chlorophytes, ciliophorans, cryptophytes and ochrophytes and a greater proportion of dinoflagellates. Other predominantly zooplanktonic classes did not represent significant proportions of abundance in the reads, except in the October sample where these accounted for a fairly large proportion of opalozoans, which in this case also included inconspicuous flagellates such as *Cafeteria roenbergensis* and *Pseudobodo tremulans* (data not shown), but consisted largely of unidentified marine Stramenopiles – MAST group (Massana et al., 2014).

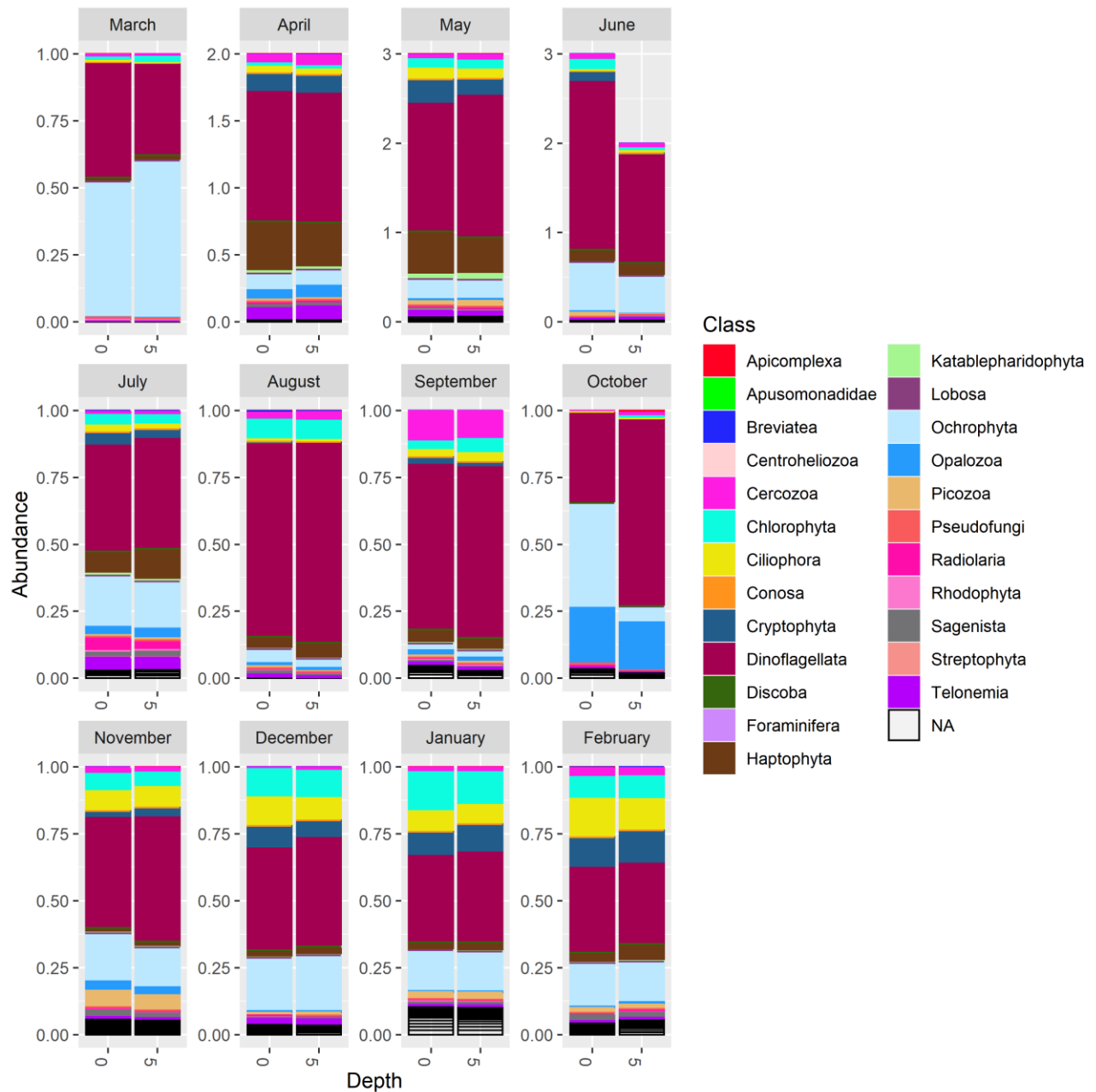


Figure 6.2-2: Relative abundance of non-metazoan higher taxa at two sampling depths at station 00BF (GoT) from March 2019 to February 2020, determined from 18S-V9 metabarcodes. Note that in some cases the total proportions add up to more than 1. This is because in some months there was more than one sample at each depth and the bars represent the sum of all individual samples.

### Dinoflagellates

When we dive deeper into specific taxonomic groups, the diversity becomes even more apparent. Although we focus on diatoms in this chapter, a survey of the genera of dinoflagellates (class Dinophyceae) is an interesting representation of biodiversity that is not captured in traditional monitoring (Figure 6.2 3). In the following figure, we have removed from the proportional representation unresolved or unclassified genera that represented most sequences assigned to dinoflagellates. Forty-eight genera of dinoflagellates were recovered, some of which were never or very rarely recorded in phytoplankton counts.

In most cases the two depths did not differ much in composition, perhaps the only noticeable difference being in the March and October samples. From the data it appears that the bloom of certain genera was not very pronounced, however there was a large spike in the relative abundance of *Heterocapsa* in June, which was also recorded with morphological counts. Other genera that "bloomed" include *Tripes* in September and October and *Karlodinium* in November and December. *Alexandrium* represented more than 20% of the sequences in April, May, and October. The potentially harmful genus *Dinophysis*, which often lead to closures of shellfish farms in the region, showed no significant increase in relative abundance except in the 5-meter sample in October. This result is an exact mirror image of the phytoplankton counts, which recorded 1000 *Dinophysis fortii* cells at 5 m and none at 0 m, increasing confidence in our method (data not shown). The large proportions of *Karlodinium* in November and December are also quite significant, as this genus was never recorded in microscopy monitoring.

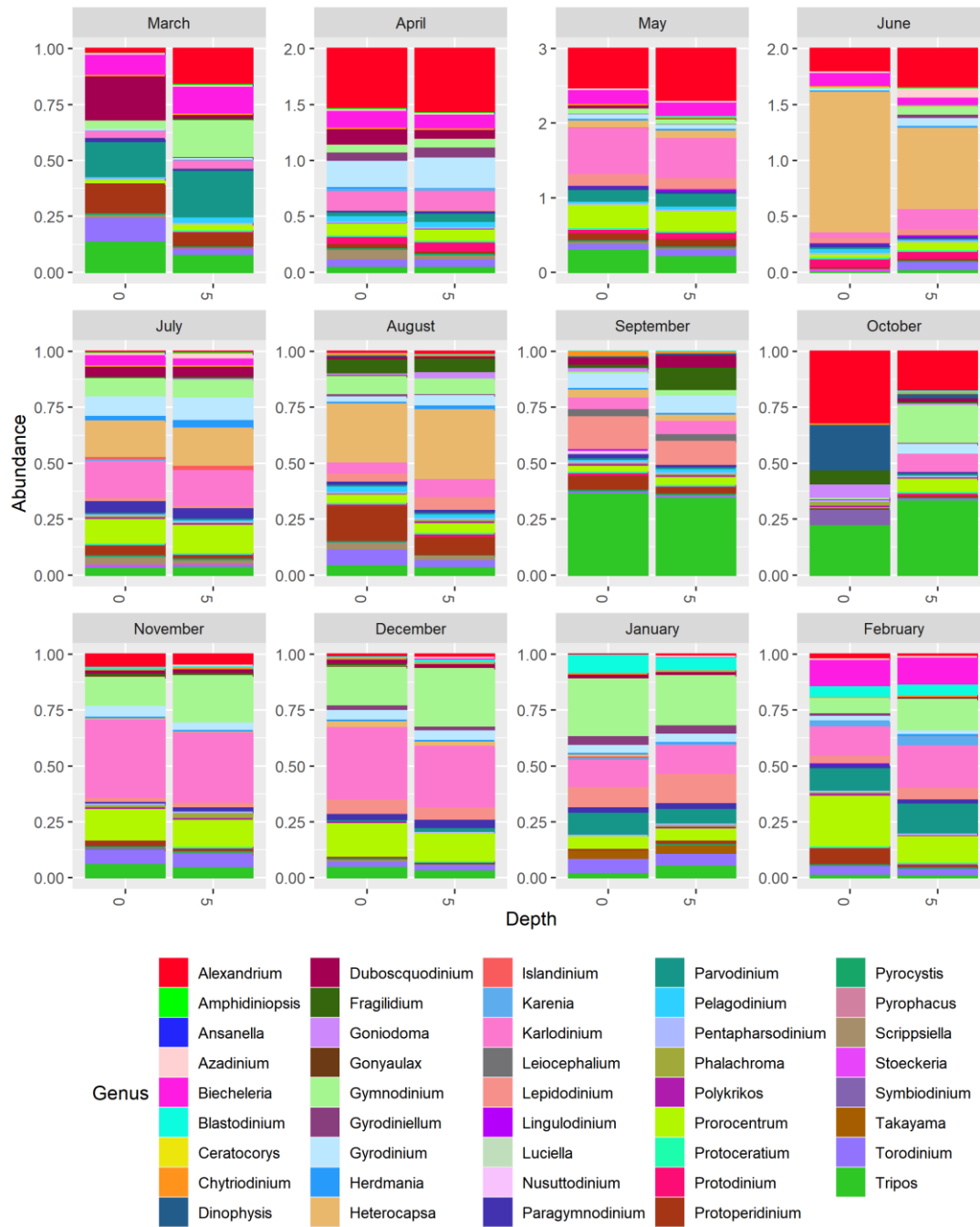


Figure 6.2-3: Relative abundance of dinoflagellate genera (Dinophyceae) at two sampling depths at station 00BF (GoT) from March 2019 to February 2020, determined from 18S-V9 metabarcodes.

### Diatoms (Bacillariophyceae)

Finally, let us consider the taxonomic composition of diatoms obtained with the 18S-V9 marker. A total of 18 genera were found, which is quite a low number, mainly because some common genera such as *Guinardia*, *Thalassiosira* or *Nitzschia* were missing. We observed a very clear seasonal succession in these samples, from a *Chaetoceros*-dominated community in spring, followed by a small *Cyclotella*-dominated community in summer. The autumn samples were more even, with an increase in smaller taxa such as *Thalassiosira* in November and December compared to the month of October. *Pseudo-nitzschia* also

occupied a larger proportion in autumn, gradually increasing towards the winter months. In December and January, the small diatom *Minidiscus* occupied a significant relative abundance. This diatom was not recorded in phytoplankton counts. To better understand the diatom diversity and make a direct comparison, we resorted to the *rbcL* marker.

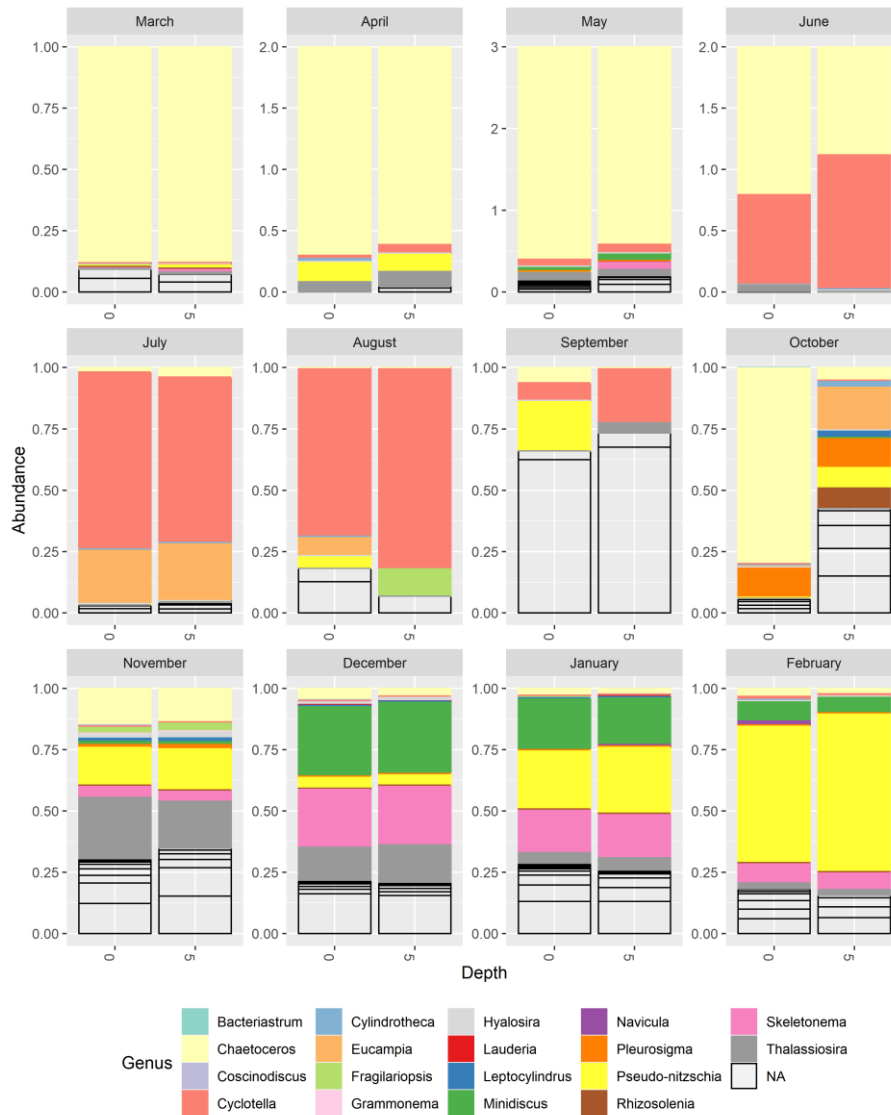


Figure 6.2-4: Relative abundance of diatom genera (Bacillariophyceae) at two sampling depths at station 00BF (GoT) from March 2019 to February 2020, determined from 18S-V9 metabarcodes.

### 6.2.3 *rbcL* Results

Sequencing of the *rbcL* marker resulted in a higher number of reads per sample and more recovered ASVs compared to the 18S-V9 method. This is not surprising considering that the marker was twice as long, and that the region is less conserved compared to 18S-V9. Removal of chimeras resulted in a much smaller dataset of contigs – only about 30% of contigs were retained. Initially, forced merging was thought to be a possible reason for this, but resequencing of some samples where a good read total was obtained resulted in a very similar percentage of non-chimeric sequences, so this was a consequence of the data. The reference database used in this analysis contained a limited amount of non-diatom

sequences and so it was not surprising that many sequences were not classified according to the taxonomy assignment in DADA2. We then extracted only those sequences that had a genus assignment to compare with the 18S-V9 and phytoplankton count data. The March and October samples are missing from the dataset because these samples did not yield visible PCR products. We included the October 2020 sample, which was collected with a phytoplankton net and therefore the comparison to other samples is uncertain.

### Diatom genera

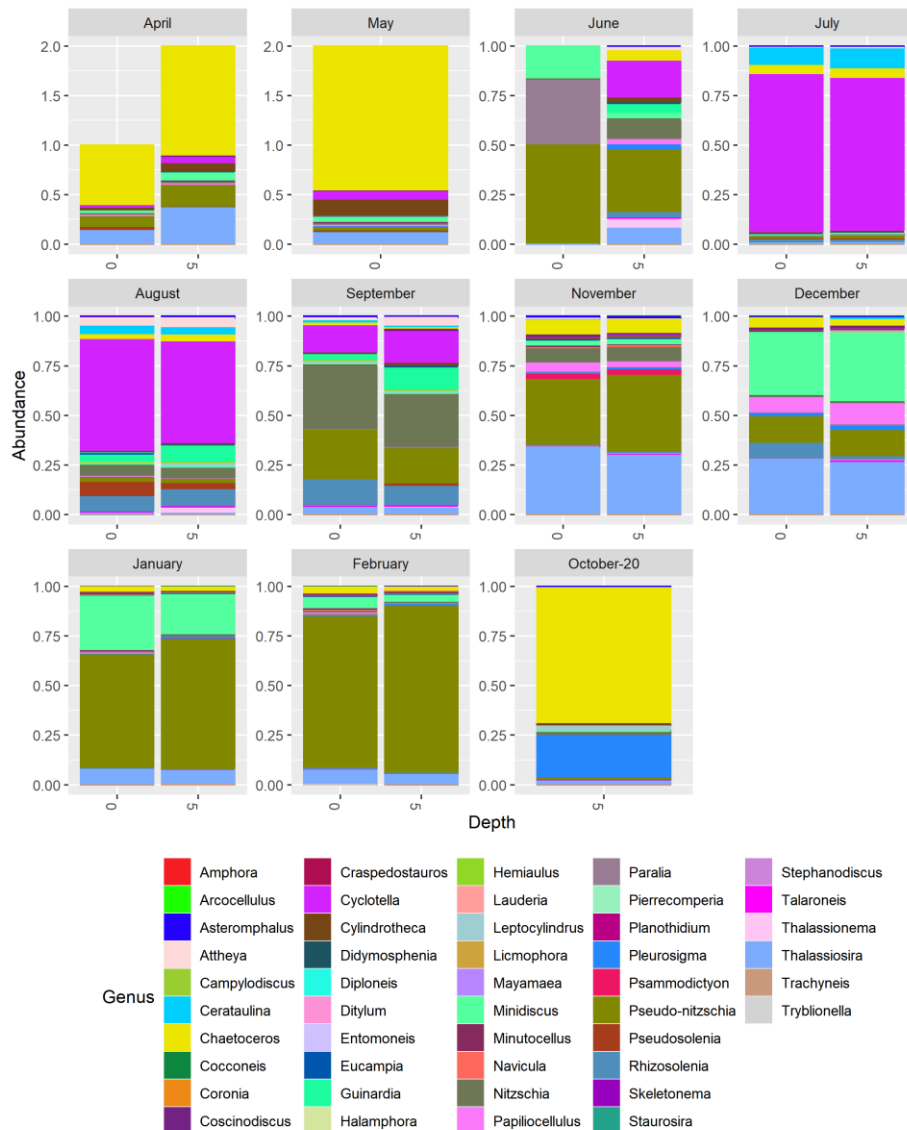


Figure 6.2-5: Relative abundance of diatom genera (Bacillariophyceae) at two different depths at station 00BF (GoT), from April 2019 to February 2020 and an additional October 2020 phytoplankton net sample, determined from *rbcL* metabarcodes. The June samples must be viewed with caution, as the number of reads in these samples was extremely low.

The *rbcL* marker detected 46 genera, many more than 18S (Figure 6.2-4). Many pennate benthic taxa such as *Attheya*, *Amphora*, *Coronia* and others were also found. However, the

general pattern in terms of relative abundance was very similar between markers. *rbcL* also detected the early spring bloom of *Chaetoceros* and the transition to *Cyclotella*-dominated summer communities. Winter blooms of genera such as *Minidiscus*, *Thalassiosira* and *Pseudo-nitzschia* were also recognised. Strikingly, almost half of the diatom sequences recorded in September belonged to the genus *Nitzschia*. Looking at the September reads from 18S-V9, we observed that they had a large proportion of missing sequences (Figure 6.2-4), which could well belong to *Nitzschia*. We should note that the June samples had a very low number of reads and should therefore be viewed with caution. It can be seen from the surface sample (June-0 m, 561484F532521) that the diversity was unusually low.

### Genus *Pseudo-nitzschia*

We also examined the taxonomic composition of the genus *Pseudo-nitzschia*, as shown by sequencing of the *rbcL* marker (Figure 6.2-6, Figure 6.2-7). This genus is the focus of this thesis and so we wanted to know how well the composition matched the data we have seen in other chapters of this thesis. The results were surprising to some degree. We observed that most species revealed in the integrated taxonomic approach described in Chapter 3 also appeared in the metabarcoding dataset. There were exceptions, however, namely the conspicuous absence of *P. calliantha*, which seemed to be a central species in our earlier work, and the absence of *P. multistriata*. Instead, there was a large prevalence of *P. galaxiae* and specifically of the small morphotype. The large number of *P. galaxiae* sequences in January and February was surprising mainly because *Pseudo-nitzschia* is rarely detected in such high proportions in these months. Other species found in larger proportions were *P. fraudulenta*, *P. subfraudulenta* and *P. delicatissima*. Species that were assigned but with a very low number of reads and low bootstrap support included *P. pungens* and *P. manni*. Interestingly, two other species, namely *P. linea* and *P. americana*, were also assigned with a total of 7 reads and low bootstrap support value (Table 6.2-1). The bootstrap value under which a taxon was still assigned was initially set to 50%. When we compared the assignment results for each taxon, we saw those sequences belonging to the *P. galaxiae* complex having quite low bootstrap scores on average (Table 6.2-1). In Figure 6.2-6-B, this is evidenced by the higher proportion of unassigned taxa. *P. fraudulenta*, *P. subfraudulenta*, and *P. delicatissima* were assigned with the highest probability, which can also be seen in the bootstrap assignment comparison. The phylogeny also showed that the genetic diversity within the sequences classified as *P. galaxiae* at 50% bootstrap support was enormous (data not shown). Thus, it is unclear whether these sequences represent *P. galaxiae*, although we showed in Chapter 3 that this species complex has the highest genetic variability among all *Pseudo-nitzschia* species.

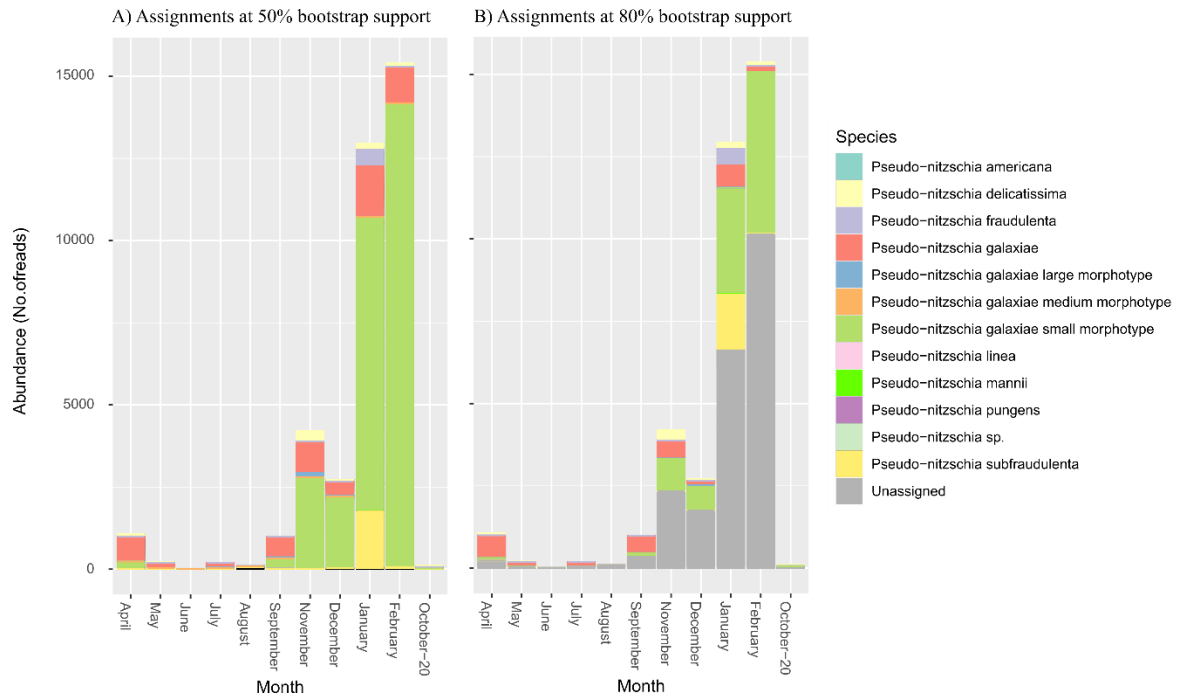


Figure 6.2-6: Number of reads for each identified *Pseudo-nitzschia* species at different bootstrap levels.

Table 6.2-1: Bootstrap statistics for each taxon.

Taxon	Mean	SD	Min	Max
<i>Pseudo-nitzschia americana</i>	53.00	NA	53	53
<i>Pseudo-nitzschia delicatissima</i>	98.26	3.14	89	100
<i>Pseudo-nitzschia fraudulentula</i>	92.35	10.45	68	100
<i>Pseudo-nitzschia galaxiae</i>	79.09	12.59	50	100
<i>Pseudo-nitzschia galaxiae large morphotype</i>	75.04	12.64	53	95
<i>Pseudo-nitzschia galaxiae medium morphotype</i>	68.20	17.48	52	96
<i>Pseudo-nitzschia galaxiae small morphotype</i>	76.67	11.33	51	98
<i>Pseudo-nitzschia linea</i>	53.00	1.41	52	54
<i>Pseudo-nitzschia mannii</i>	74.75	10.31	60	84
<i>Pseudo-nitzschia pungens</i>	57.60	5.94	51	66
<i>Pseudo-nitzschia sp.</i>	62.00	NA	62	62
<i>Pseudo-nitzschia subfraudulenta</i>	90.62	10.06	74	100

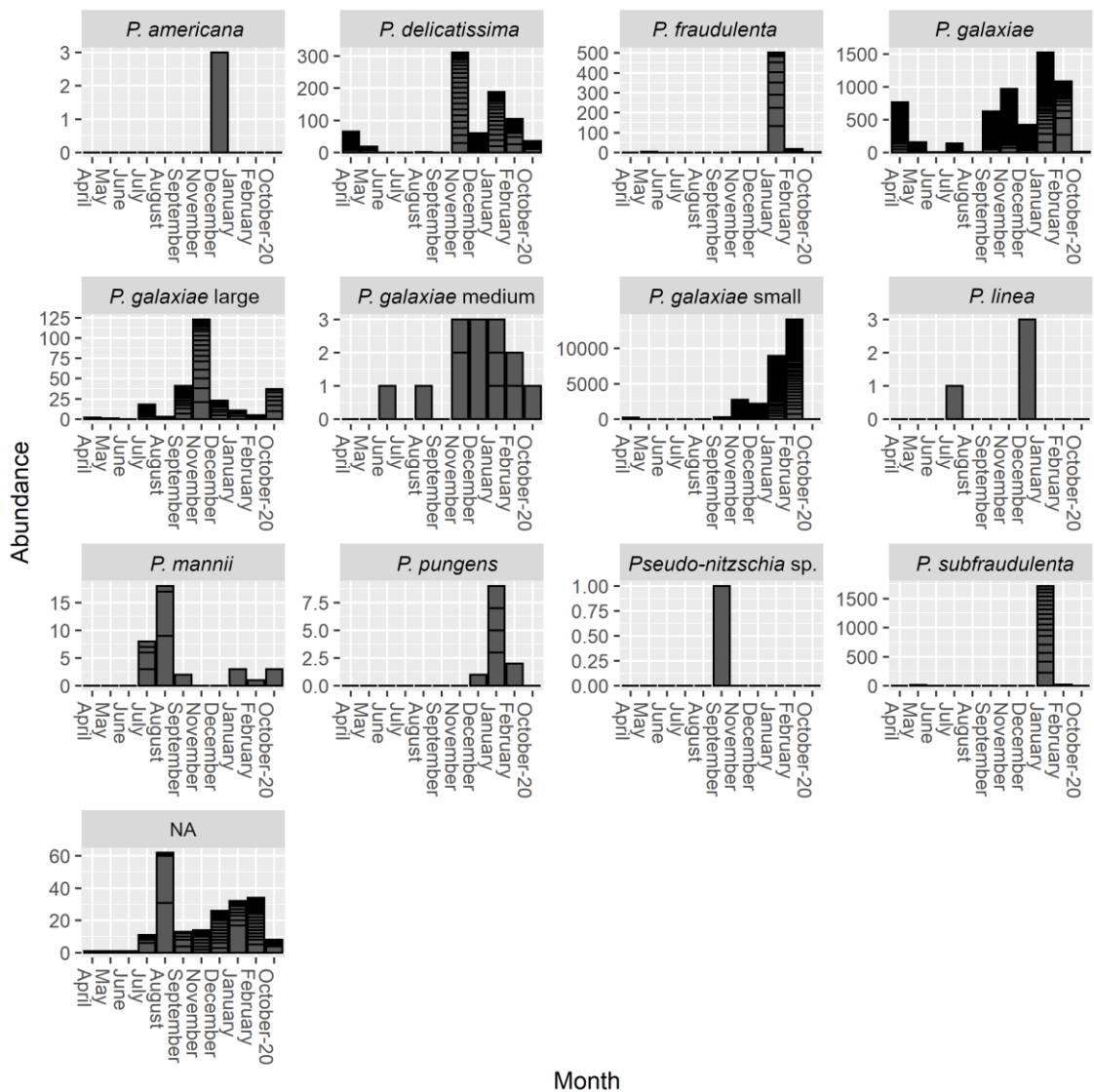


Figure 6.2-7: Number of reads for each individual species assigned at 50% bootstrap level. Each bar represents an ASV.

### *rbcL* resequencing

To assess the effect of concatenating non-overlapping forward and reverse reads, we performed a resequencing project in which a subset of samples under 300 Illumina cycles were resequenced to achieve sufficient overlap. The resequencing project resulted in a higher sequencing depth, with 1557259 raw reads, corresponding to 141569 reads per sample. This was roughly double the depth of the previous run, which also gave us the opportunity to assess the effect of sequencing depth on the final taxonomic composition. While slightly fewer taxa were recovered using the concatenation method, taxonomic recovery at the lowest identified level was generally very similar, as shown by the canonical analysis (CA) (Figure 6.2-8). The lowest taxonomic level was species in most cases, but also the genus level in some cases. The September samples differed the most, regardless of the method. Looking at the taxonomic composition of the samples identified to genus level, we found that the differences were quite small (Figure 6.2-9). In the concatenated dataset, slightly more genera were found, as well as multiple species (Table 6.2-2), but generally unique taxa are found in each dataset.

Table 6.2-2: Unique taxa found in the concatenated and resequenced datasets.

Genera		Species	
Concatenated only	Reseq only	Concatenated only	Reseq only
<i>Amphora</i>	<i>Climaconeis</i>	<i>Attheya longicornis</i>	<i>Climaconeis</i> cf. <i>lorenzii</i>
<i>Arcocellulus</i>	<i>Cymatosira</i>	<i>Attheya</i> sp.	<i>Haslea nipkowii</i>
<i>Attheya</i>		<i>Chaetoceros calcitrans</i>	<i>Haslea ostrearia</i>
<i>Coronia</i>		<i>Coronia</i> sp.	<i>Psammodictyon</i> sp.
<i>Craspedostauros</i>		<i>Craspedostauros</i> sp.	<i>Pseudo-nitzschia calliantha</i>
<i>Didymosphenia</i>		<i>Didymosphenia dentata</i>	<i>Staurosira pinnata</i>
<i>Diploneis</i>		<i>Diploneis</i> cf. <i>smithii</i>	
<i>Mayamaea</i>		<i>Diploneis</i> sp.	
<i>Pierrecomperia</i>		<i>Entomoneis paludosa</i>	
<i>Planothidium</i>		<i>Entomoneis pulchra</i>	
<i>Tracheneis</i>		<i>Halamphora ghanensis</i>	
		<i>Mayamaea permitis</i>	
		<i>Navicula ramosissima</i>	
		<i>Nitzschia dissipata</i>	
		<i>Nitzschia gracilis</i>	
		<i>Nitzschia nanodissipata</i>	
		<i>Nitzschia volvendirostrata</i>	
		<i>Pierrecomperia catenuloides</i>	
		<i>Psammodictyon panduriforme</i>	
		<i>Pseudo-nitzschia americana</i>	
		<i>Pseudo-nitzschia linea</i>	
		<i>Pseudo-nitzschia mannii</i>	
		<i>Pseudo-nitzschia pungens</i>	
		<i>Staurosira shiloi</i>	
		<i>Thalassiosira minuscula</i>	
		<i>Thalassiosira oestrupii</i>	
		<i>Thalassiosira pseudonana</i>	

It is also worth reviewing the differences in *Pseudo-nitzschia* classification between the two projects (Figure 6.2-10). Only one additional species occurred in the resequenced data, *P. calliantha* in the October 2020 net sample, while the other assignments appeared very similar. However, *P. americana*, *P. linea*, *P. pungens*, and *P. mannii* did not occur in the resequenced data. From the figures in Figure 6.2-10, the difference in sequencing depth is very clear, as the resequencing projects recovered about twice as many sequences, except for the December samples (Figure 6.2-10). However, the proportions were very similar, so we can say that the concatenation method did not introduce many errors. Thus, we can use the whole time series from the concatenation project to compare the results with the 18S and morphological data.



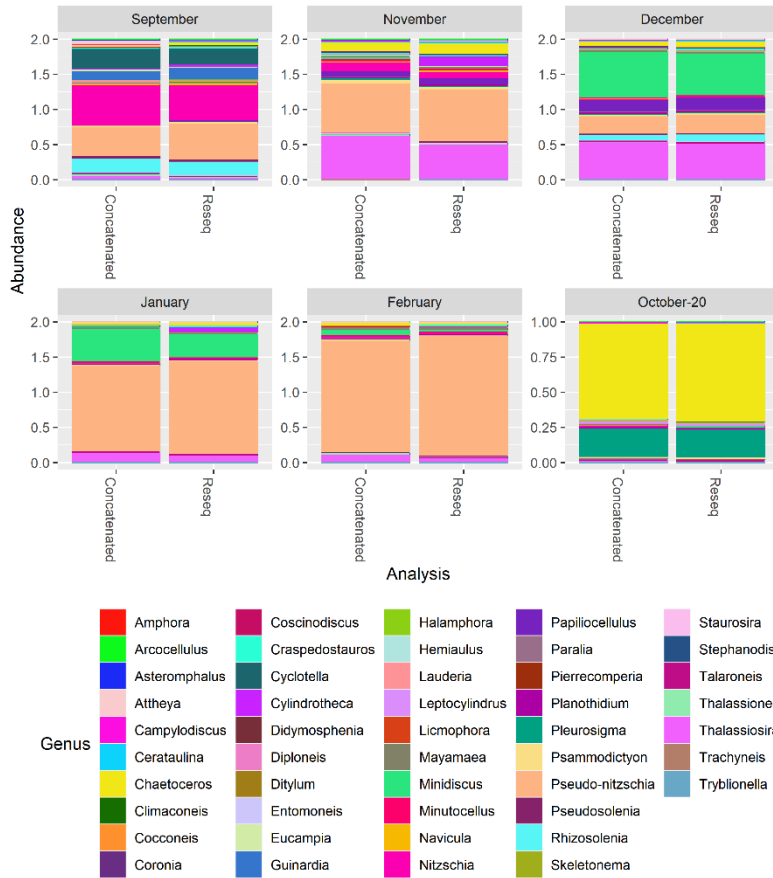


Figure 6.2-9: Genus-wide comparison of assignments of concatenation and resequencing in terms of relative abundance of sequence reads.

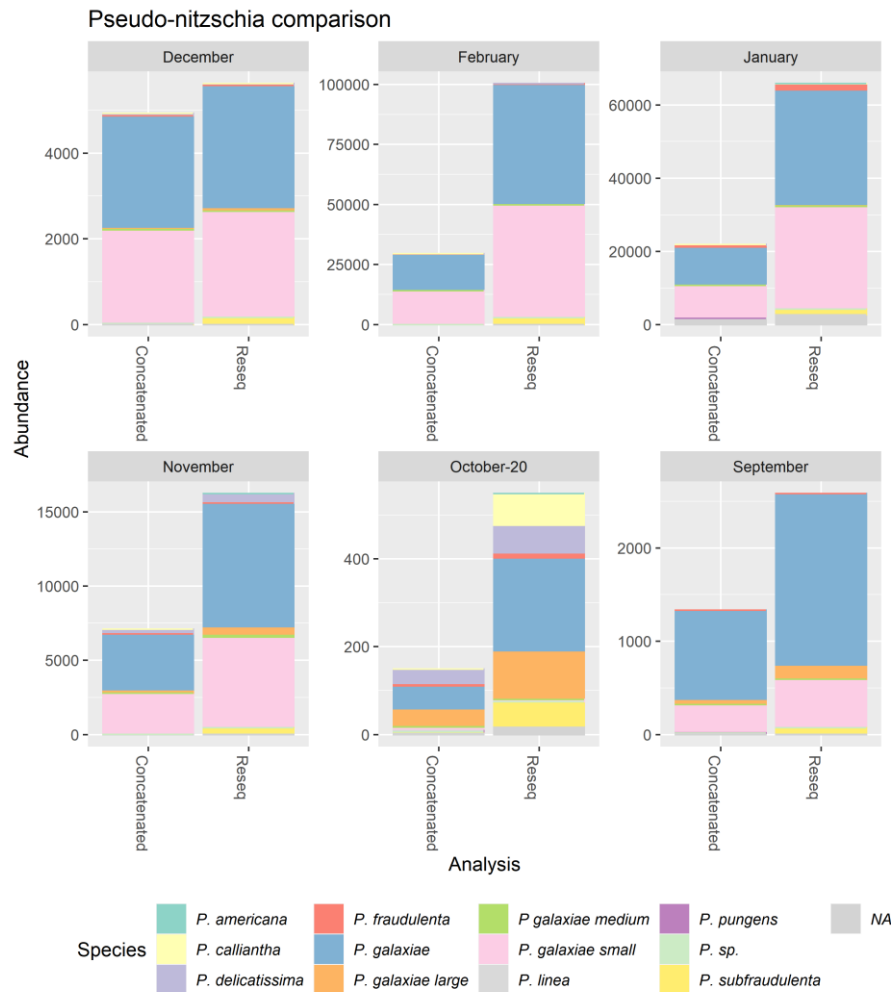


Figure 6.2-10: Assignments of *Pseudo-nitzschia* sequences at the species level with both methods.

## 6.2.4 Comparing Metabarcoding with Traditional Microscopy Monitoring

### Higher level taxonomy

Phytoplankton counts under the microscope of a known seawater volume provide absolute abundance, and are therefore independent of size and possible amplification biases associated with metabarcoding. Here we present only differences at the phytoplankton

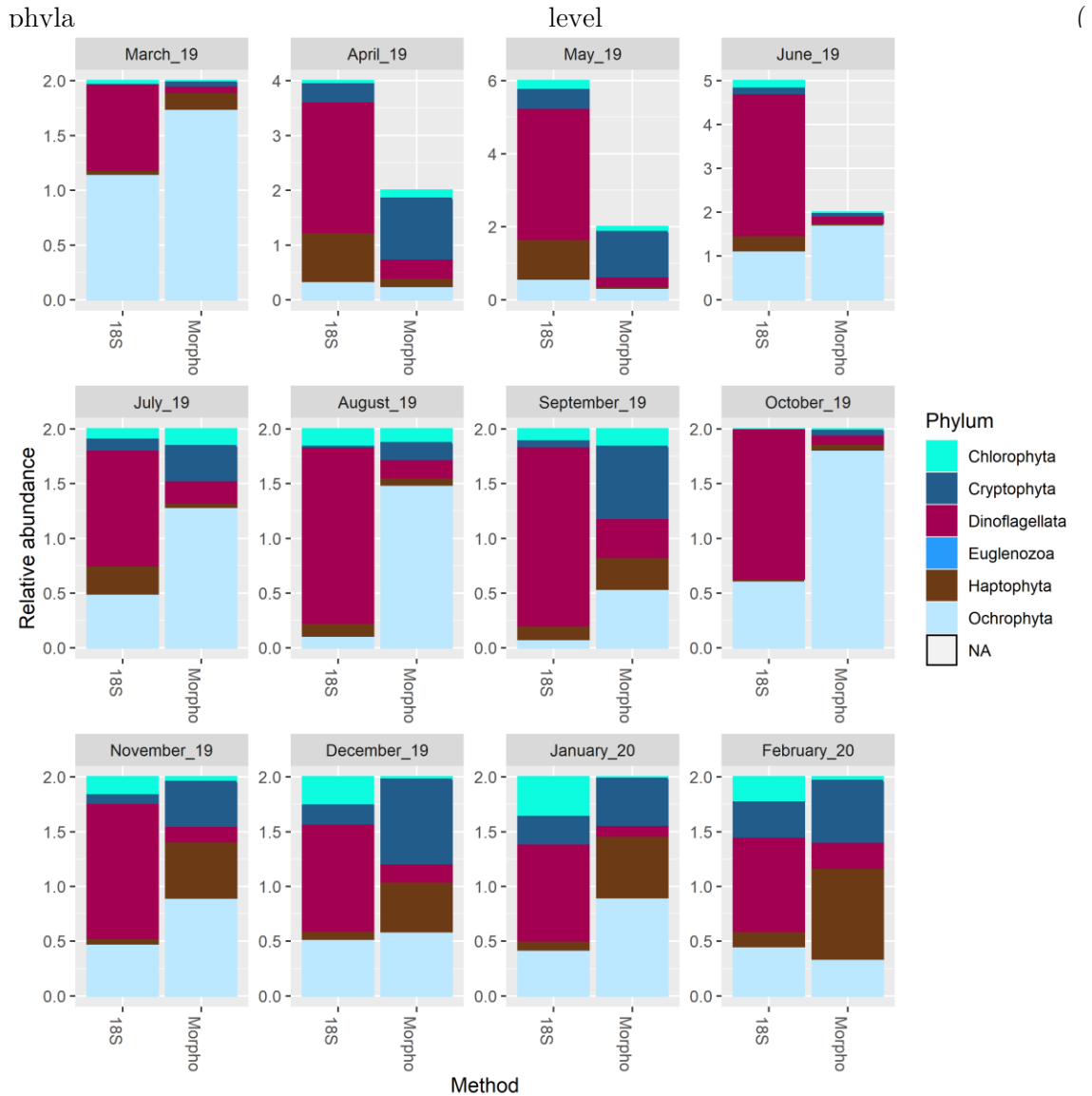


Figure 6.2-11). This figure represents relative abundances that depend on the number of samples analysed explaining the discrepancy between morphological and 18S methods in the April, May, and June samples. The differences between the 18S metabarcoding results and the phytoplankton counts are clear. The metabarcoding method clearly favoured dinoflagellates over other smaller groups such as haptophytes and cryptophytes, which are more abundant in the results of microscopy counts. Ochrophytes, which are predominantly represented by diatoms, also occupied different relative abundances except in samples from winter and early spring, where the two methods seemed mostly comparable. Chlorophytes were the only group that accounted for a comparable proportion of relative abundance throughout the study. It is important to remember that we were comparing two different biological entities which may have affected the results. The first is the number of genetic sequences, while the other is the cell number of a given taxon. These are related, but the relationship is not clear.

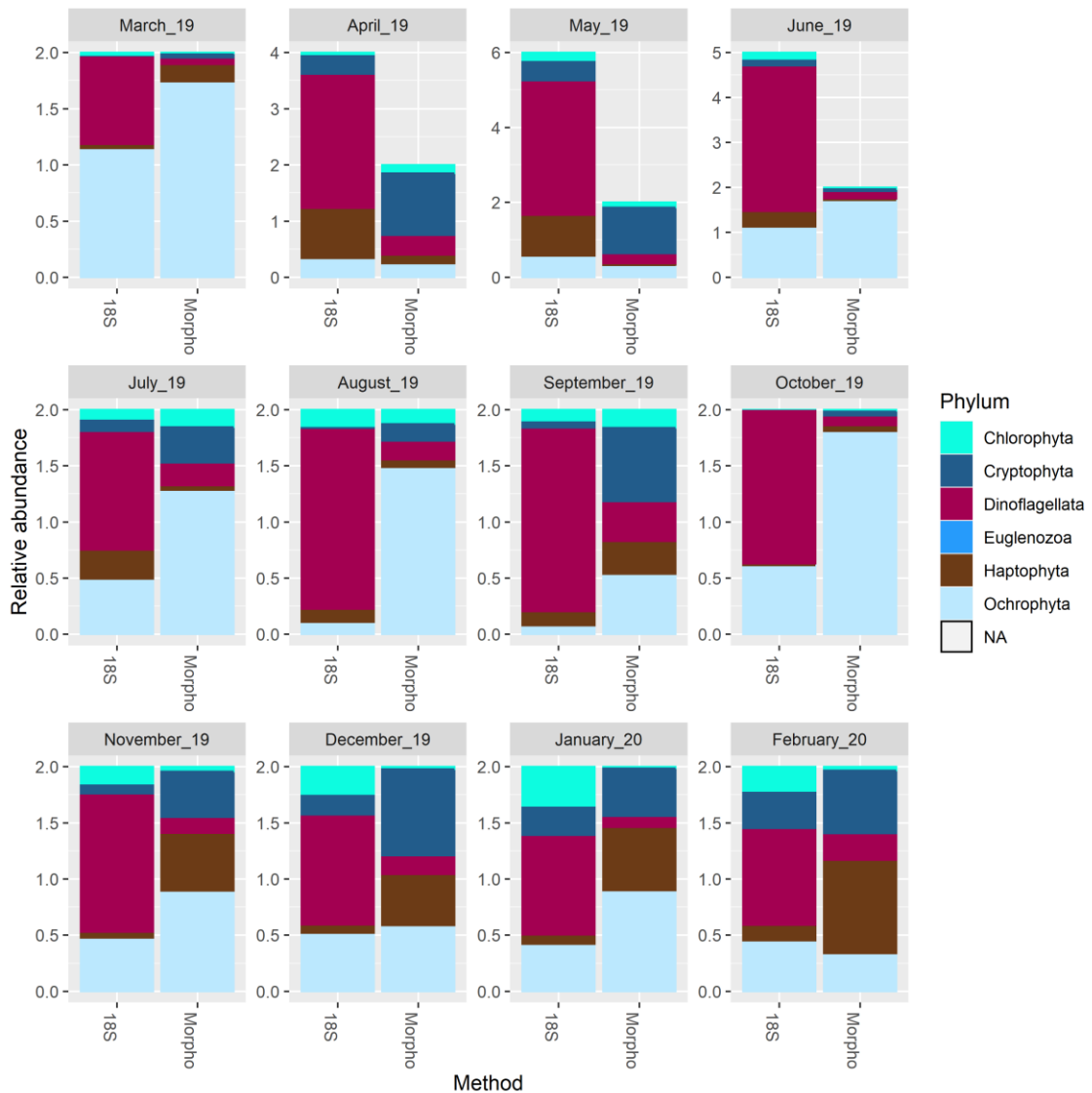


Figure 6.2-11: Comparison relative abundances of phytoplankton phyla obtained from 18S metabarcoding and phytoplankton counts from March 2019 to February 2020. Most relative abundances add up to 2, which is due to the summation of relative abundances from two depth samples. Where the result is more than 2, more samples were used.

### $\alpha$ -Diversity

To compare the morphological approach with the two metabarcoding markers, we focused on diatom genera, as diatoms were the group that was better represented in all datasets. First, we focused on the  $\alpha$ -diversity measures. In Figure 6.2-12, we compared four different  $\alpha$ -diversity indices. The trend lines were drawn by applying local regression smoothing. We have already seen that in terms of metabarcoding, the *rbcL* marker recovered more genera than 18S, while the datasets were comparable especially in terms of dominant taxa. On the other hand, 18S had similar observed species richness as the traditional morphological approach. All indices showed an increase in taxonomic richness towards the autumn-winter period, with this increase being most pronounced for *rbcL*, while the lowest richness was observed in summer. This was also reflected in the Shannon-Wiener diversity index, which was highest in September for *rbcL*, in December for 18S and in October for the

morphological approach. The Berger-Parker dominance index and the Pielou-Evenness index were, not surprisingly, inversely proportional, but here there was more discrepancy between the molecular and morphological methods. However, minima and maxima were reached at roughly the same time periods with all three methods. The community appeared to be the most diversified in September-October, and in November with 18S. A clear difference between the molecular and morphological methods occurred in January and February, where the dominance index increased for both 18S and *rbcL*, while it decreased for the morphological data. The molecular methods had similar trend lines, although there was quite a discrepancy, especially when we looked at the dominance index at the beginning of the observation period. The October 20 observation must be viewed with caution, as the sampling method in the molecular sample was completely different from the rest, while the morphological approach remained the same.

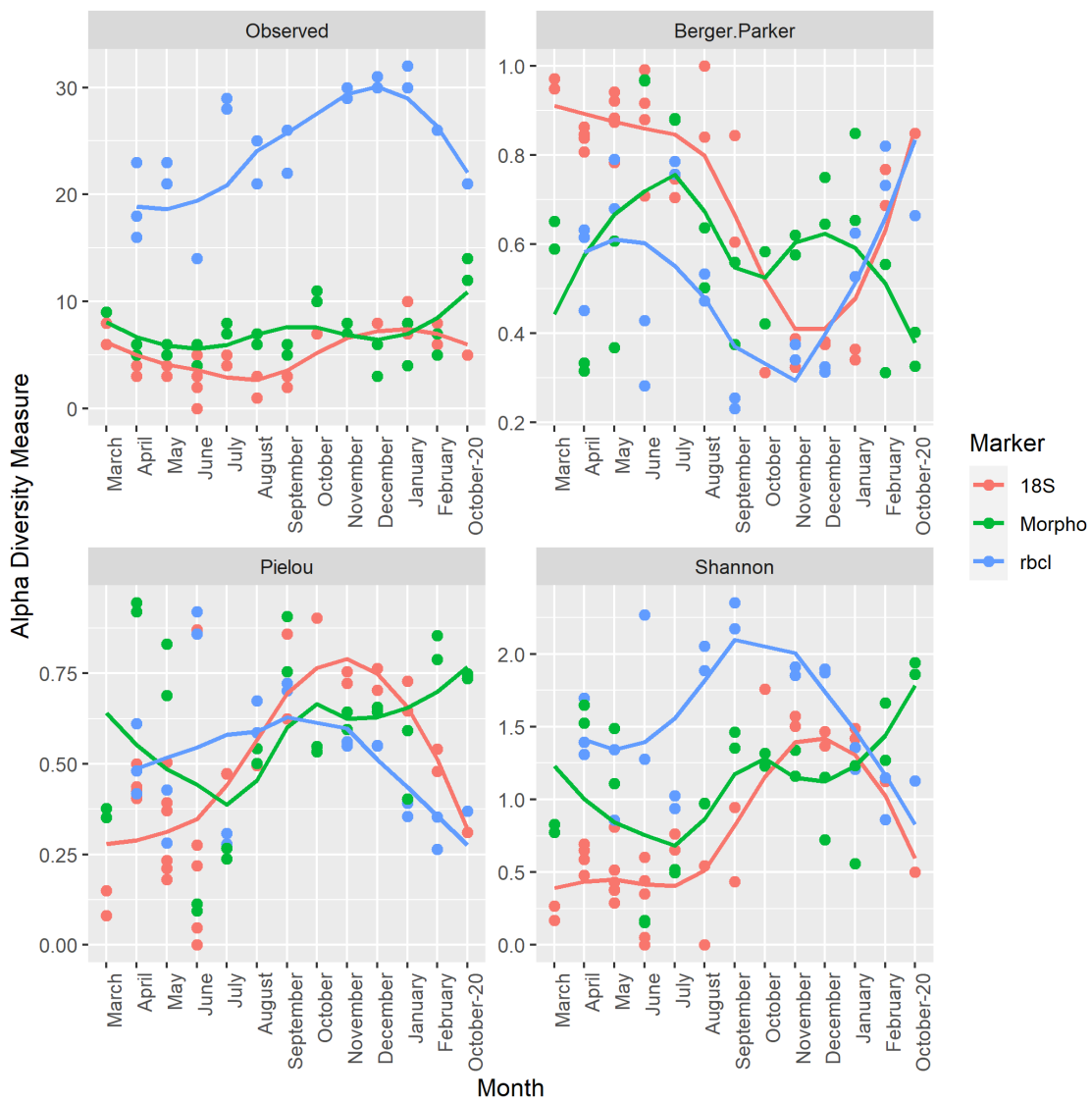


Figure 6.2-12:  $\alpha$ -diversity indices derived from the taxonomic composition of phytoplankton of different assessment methods. Trend lines were calculated by local regression smoothing. Index codes: Observed = raw taxonomic richness; Berger.Parker = Berger-Parker dominance index; Pielou = Pielou evenness index; Shannon = Shannon-Wiener diversity index.

## $\beta$ -Diversity

To compare the different datasets, we performed a Bray-Curtis distance analysis and a non-metric multidimensional scaling ordination, again using diatom genera as an example. First, we look at the comparison of only the molecular data, which is more uniform and directly comparable because the methodology of data collection was similar. We observed that there was a very strong seasonal clustering of samples for both molecular markers (Figure 6.2-13). The only samples that were more scattered outside of these clusters were those in the transition periods. This was most evident in the 18S-June samples obtained in different parts of the month (See Appendix B), with the later sample tending towards the summer cluster. Nevertheless, these samples were the least reliable for both molecular markers, since the read number was very low. The October-20 samples belonged to the spring cluster, but as mentioned earlier, the October 20 sample was a phytoplankton net sample from a different year, and therefore this positioning could be related to this fact.

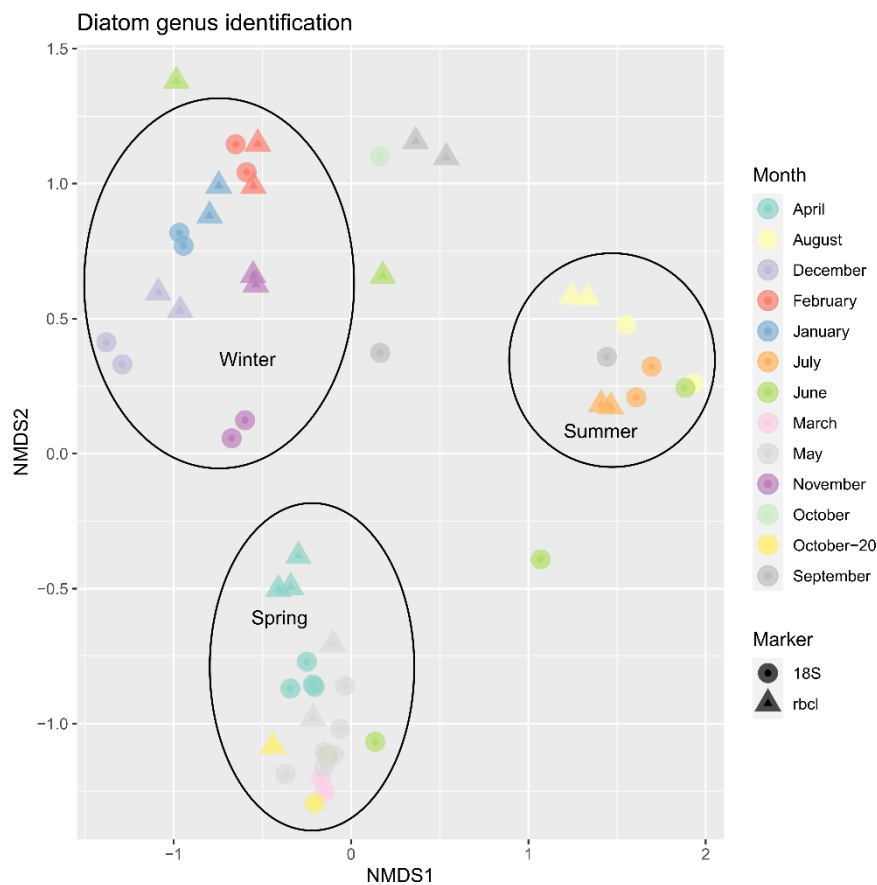


Figure 6.2-13: Bray-Curtis NMDS ordination of diatom genera in molecular samples.

When we added the morphological dataset to the analysis, we saw that an additional cluster composed of only microscopy samples appeared (Figure 6.2-14). This cluster consisted of winter/spring samples. One of the reasons for this could be that small diatoms such as *Minidiscus* and *Thalassiosira* were rarely or never recorded in phytoplankton counts, whereas molecular analyses revealed that they made up significant proportions of the community in these months (see 0 and 0). In the months when these genera were not present in the molecular dataset (March, June, July, September, October, November), the morphological and molecular approaches were more comparable. Interestingly, the October 20 community was like the October 19 community based on the morphological data,

whereas it was very different based on the 18S data. However, we must reiterate that the sampling method was not the same.

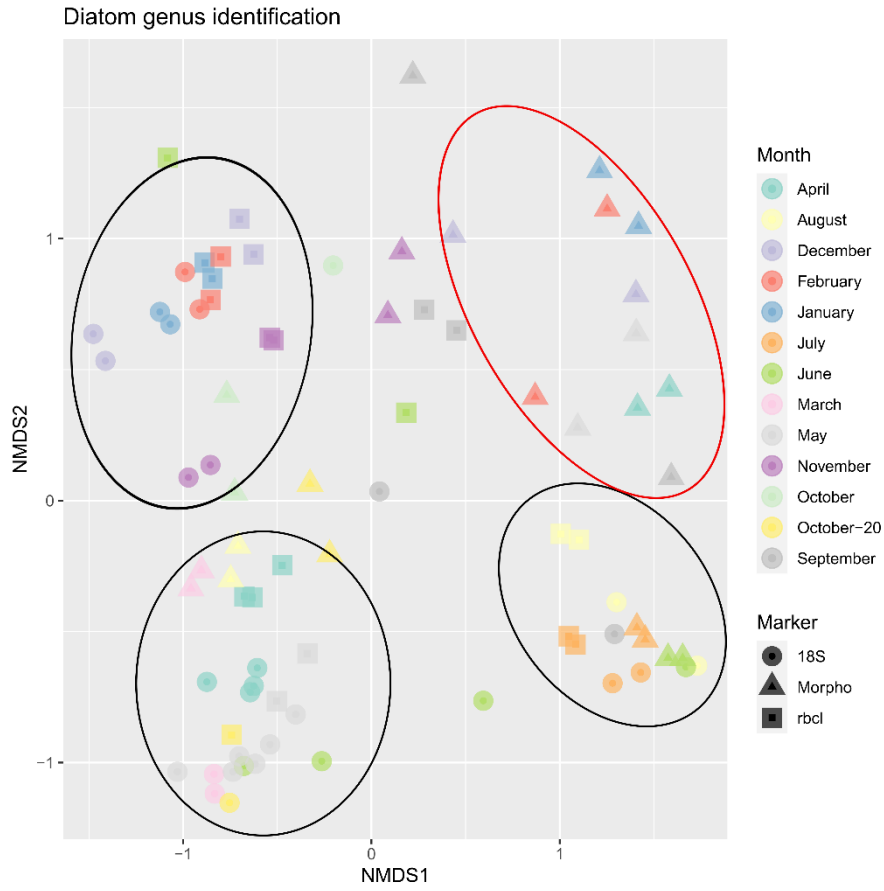


Figure 6.2-14: Bray-Curtis NMDS ordination of all samples.

## Chapter 7

# Discussion

### 7.1 Research Overview and Highlights

- A thorough and robust molecular and morphological assessment of the species composition and seasonal occurrence of the genus *Pseudo-nitzschia* in the Gulf of Trieste.
- Discovery of three toxic species: *P. multistriata*, *P. delicatissima* and *P. galaxiae* and sequencing *dabA* gene of *P. multistriata*.
- First metabarcoding study of phytoplankton community composition in the region, and first evaluation of the *rbcL* marker for metabarcoding marine diatom communities.
- Development and testing of a calorimetric sandwich-hybridization assay used to track and predict trends in population size of *Pseudo-nitzschia*.

To study the harmful diatom genus *Pseudo-nitzschia*, we initially used classical phytoplankton study techniques involving strain collection, culturing, and morphological observation. This was then extended and combined with molecular, ultrastructural, and long-term observational data to describe the seasonal variation and diversity of *Pseudo-nitzschia* in the Gulf of Trieste. In Chapter 3, we re-evaluated the performance of several phylogenetic markers (28S, ITS2 and *rbcL*) for diatom barcoding and examined the phylogenetic relationships of Mediterranean and non-Mediterranean strains of *Pseudo-nitzschia* to fill knowledge gaps for future research and surveys. Aside from obtaining one of the most thorough and robust assessments of species composition and occurrence in the area to date, this work provided us with two important insights. The first is that the commonly distinguished morphological groups, i.e., the *Pseudo-nitzschia delicatissima* species group and the *Pseudo-nitzschia seriata* species group, recognized as ecological units in many phytoplankton studies (e.g., Ajani et al., 2021; Fehling et al., 2006; Thorel et al., 2017), are in fact polyphyletic (Lim et al., 2018), with a different seasonal distribution and, above all, dependent on regional species composition. This misclassification is most likely the source of different ecological conclusions about the seasonality and ecological preference of different species complexes (Downes-Tettmar et al., 2013; Fehling et al., 2006; Thorel et al., 2017), as different species can have completely different ecological preferences even within simple organisms. The other finding related to phylogeny and barcoding is that the *rbcL* gene is a very good predictor of species divergence and can detect minute differences between strains and species that other commonly used markers such as 18S and 28S often miss. This was later illustrated by the metabarcoding study, where *rbcL* appeared to be

far superior in terms of species and genus recovery, although there was more difficulty in obtaining good quality amplicons.

The results of the toxicity analysis revealed some toxic members of the genus even among the strains we isolated in the GoT. The toxic species, apart from *P. galaxiae*, were already known in the wider region, and we showed that for *P. delicatissima* and *P. multistriata* toxicity is not related to phylogeny, while for *P. galaxiae* there is some evidence that smaller morphotypes are toxic while the larger ones are not. We have also successfully amplified the *dabA* gene in *P. multistriata*, further demonstrating the ability of our strains to produce the toxin, while amplification of the gene in other species proved difficult and would require further efforts in primer design, while it is possible that the gene is absent in the non-toxic strains (Chekan et al., 2020; Lema et al., 2019).

Finally, our collaboration with Microbia Environnement produced valuable and far-reaching results in the form of a working bioassay for monitoring and detecting *Pseudo-nitzschia* in the marine environment. Although species specificity could not be achieved, the assay is still very useful for general assessment of the status of *Pseudo-nitzschia* populations, especially when scattered and large-scale sampling needs to be performed.

## 7.2 *Pseudo-nitzschia* Species Composition in the GoT

*Pseudo-nitzschia* species are an important component of the phytoplankton community worldwide (Bates et al., 2018; Mozetič et al., 2019; Trainer et al., 2012; Viličić et al., 2009). The underlying aim of this work was to increase the knowledge of *Pseudo-nitzschia* in the Northern Adriatic Sea in our study area in the Gulf of Trieste by clarifying taxonomic uncertainties and phylogenetic relationships of *Pseudo-nitzschia* species complexes, assessing the toxic potential of North Adriatic isolates, and proposing modern tools for monitoring population size and species diversity. To answer the most pressing questions about the ecology, taxonomy and occurrence of the genus, the approach had to be multifaceted to cover the full complexity of these diatoms. To establish the morphological and genetic benchmark of the occurring species, a series of cell isolations were performed over several years. This is a classical method in phytoplankton research and has been applied locally and globally in several *Pseudo-nitzschia* studies (Ajani et al., 2013; Arapov et al., 2017; Bates et al., 1989; Cerino et al., 2005; Marić et al., 2011; Scholin et al., 1996). To obtain seasonal data, monthly cell isolations were performed. This is a stochastic approach that may not capture the entire community present at a given sampling point and is effort-biased, but we extended this effort with the metabarcoding survey in a later year to supplement these data. Nonetheless, during the isolation campaign that began in October 2016 and ended in March 2018, with some additional sampling in August 2018 and January, February and August 2019, eight species were identified from 83 isolated strains, combining morphological and molecular analyses: *P. calliantha*, *P. delicatissima*, *P. fraudulenta*, *P. galaxiae*, *P. manni*, *P. multistriata*, *P. pungens* and *P. subfraudulenta*. These species have been previously reported from the Adriatic Sea (Lundholm et al., 2003; Caroppo et al., 2005; Burić et al., 2008; Marić et al., 2011; Penna et al., 2013; Arapov et al., 2016, 2017). *P. multistriata* and *P. galaxiae* are an exception, as they have been reported in long-term studies based on LM (Cabrini et al., 2012; Cerino et al., 2012; Mozetič et al., 2019; Totti et al., 2019), but we lacked TEM data for both, while molecular data exist only for *P. multistriata* (Pistocchi et al., 2012). To our knowledge, this is the first unequivocal report of the presence of *P. multistriata* and *P. galaxiae* confirmed by ultrastructural and molecular evidence. Except for *P. multistriata*, our metabarcoding study also confirmed the presence of these species with the addition of the *P. americana/linea* species complex. These diatoms were previously found as epiphytes on cells of *Chaetoceros* sp. and do not

exhibit the typical *Pseudo-nitzschia* morphology (Lundholm et al., 2002). Therefore, they have been rarely identified under the microscope. *P. linea* was also previously found in the Mediterranean Sea, particularly on the Catalan coast and in the Gulf of Naples (Quijano-Scheggia et al., 2010; Ruggiero et al., 2015).

Morphologically, most isolated species resembled those in type descriptions or at other localities. Of note is the large average length of the cells of *P. subfraudulenta* (112  $\mu\text{m}$ ), which are on average about 10  $\mu\text{m}$  longer than those described in Malaysia (Teng et al., 2013) and almost 60  $\mu\text{m}$  longer than those described in Greece (Moschandreu & Nikolaidis, 2010). Our measurements were based on three strains, two of which were on average shorter than the very long one. The morphometric signatures of the other species are consistent with the published data. The only exception was the valve width in *P. manni*, *P. calliantha*, *P. fraudulenta*, *P. pungens* and *P. multistriata*, which could be larger than previously reported. However, these were outliers in the measurements and could be a result of unnoticed cell division that effectively doubles the measured cell width.

Based on these results, we can conclude that the Gulf of Trieste is a region with a high *Pseudo-nitzschia* diversity, where nine species have been identified in a relatively short time. In contrast, in a recent study in the Northern Adriatic Sea, which also followed a similar integrated morphological-molecular approach, only 6 species were found (Giulietti et al., 2021). In the Gulf of Naples with a very long record of *Pseudo-nitzschia* studies, more than 16 species have been already reported (Ruggiero et al., 2015), eight species have been recovered from the Bilbao estuary (Orive et al., 2013), 12 have been found in a rather extensive area along the Greek coasts (Moschandreu et al., 2012), 10 along the Australian coasts (Ajani et al., 2013), more than 20 have been described in the NE Pacific over the years and 22 were recovered through an integrated morphological-HTS approach in a recent study (Stern et al., 2018a).

### 7.2.1 Ecological preference and seasonal occurrence of different species

In the case of organisms that are difficult to identify at the species level by light microscopy, they are usually reported as spp. or grouped into species complexes based on some common traits. Phytoplankton trait biology is a growing field and studies show that phytoplankton communities can be classified and analysed based on a selection of morphological traits such as size, volume and shape (Francé et al., 2021; Litchman et al., 2010; Potapova & Hamilton, 2007). Grouping of different *Pseudo-nitzschia* based on valve width into two species complexes – *P. delicatissima* species group (TAA width < 3  $\mu\text{m}$ ) and *P. seriata* species group (TAA width > 3  $\mu\text{m}$ ), is a common practice. Although this trait-based classification may work in terms of phytoplankton community functioning, it is unreliable and flawed when making predictions about HAB threat or the ecological preferences of individual species. A consequence of this approach is also that different areas of the world may harbour different species within these complexes, making comparisons and conclusions impossible. In addition, it was recently demonstrated that the arbitrary limit of 3  $\mu\text{m}$  is unreliable, since some *P. pungens* cells that are classified into the *P. seriata* group have shorter TAA widths (Accoroni et al., 2020).

Using only the time series count data presented in the PCA of the published article from Chapter 3 (Turk Dermastia et al., 2020, Fig. 4), we see that the species groups showed some seasonal preference, which is also consistent with the isolation data, but the observed effects were stronger in the highly reliable *P. multistriata* counts. The *P. delicatissima* group and *P. cf. galaxiae* appeared to show the same seasonal preference. This may not be surprising since *P. galaxiae* cells are also included in the *P. delicatissima* group counts. We

saw in the metabarcoding data that *P. galaxiae* was virtually present all year round, with a significant peak in winter (Figure 6.2-7). This finding was surprising because in previous years the prevalence of this species was not recorded, nor was it recorded in 2019-2020 when the metabarcoding survey was conducted. The morphological diversity of the species, and the cryptic nature of particularly small morphotypes could be the reason for this species being overlooked in the LM counts. The *P. seriata* complex showed a preference towards winter conditions, and this was confirmed by both isolation data and metabarcoding, in which *P. fraudulenta*, *P. subfradulenta*, *P. pungens* and *P.americana/linea* were all found only in winter months. In this sense, metabarcoding complements the isolation and time-series data and indeed confirms that these species are winter-specialists in our region. These results are contradictory to the analysis of Fehling *et al.* (2006) who show a preference of the *P. seriata* complex for warmer waters (summer bloom), although the oceanographic conditions in the NE Atlantic (56°30' N) are fundamentally different from those of our study area. However, the study area is most likely not the only factor explaining the different patterns of seasonal occurrence. We suspect that much of this discrepancy is due to the fact that multiple species with different ecological affinities are grouped together and the groups, or complexes, are then treated as individual ecological units. Depending on the study area, different species are naturally assigned to the two complexes. Because cells are assigned to complexes based on valve widths, unnoticed cell division can double the valve width, leading to incorrect assignment of the complex, in addition to the fact that the TAA width is not reliable (Accoroni *et al.*, 2020). There is conflicting evidence about to which environmental conditions promote the blooming of the different species complexes. Individual species may show a different affinity for environmental parameters than their representative complexes, and this may be the real source of the discrepancies in the published literature. For example, Thorel *et al.* (2017) associated the occurrence of *P. delicatissima* complex with low Si:N ratios, while a negative correlation was observed for the *P. delicatissima* complex with respect to nitrate for the same study region (Downes-Tettmar *et al.*, 2013). In our analysis, the *P. delicatissima* complex was correlated with high temperatures and lower phosphate concentrations, which could also indicate nutrient uptake. Thorel *et al.* (2017) found this complex to be correlated with low Si:N ratios, which was not the case in our study. Our PCA showed a clear partitioning of the two species complexes, which was mainly influenced by temperature and salinity; however, no pronounced seasonality was observed (Turk Dermastia *et al.*, 2020, Fig. 4). Clearly grouping species into complexes when drawing ecological conclusions is problematic and may obscure the true mechanisms of species seasonality. Therefore, one of the goals of this work was also to decipher these species complexes and define which species are most likely to occur at different times of the year and, most importantly, whether the isolated strains are toxic.

Our time-series analysis revealed pronounced autumn blooms of *Pseudo-nitzschia* that occur annually and occasionally account for up to 80% of the total phytoplankton abundance (Turk Dermastia *et al.*, 2020, Fig. 2). Occasional spring blooms were also observed, but they usually represented smaller proportions of the phytoplankton community. Metabarcoding analysis revealed a somewhat different picture. While *Pseudo-nitzschia* dominance was highest during the winter months, diatoms rarely represented significant proportions of the phytoplankton community compared to the microscopy count data (Turk Dermastia *et al.*, 2020, Fig. 2). The dominant species was also different, as in the analysed time-series the bloom was mainly attributed to *P. calliantha* and *P. mannii*, whereas in our metabarcoding dataset the dominant species was *P. galaxiae*. Summer-autumn blooms of *Pseudo-nitzschia* are not surprising and have been documented in many regions, including the Adriatic, Mediterranean and NE Atlantic and NE Pacific (Fehling

et al., 2006; Ljubešić et al., 2011; Mercado et al., 2005; Trainer et al., 2002) and may represent significant proportions of the phytoplankton communities (Quijano-Scheggia, Garcés, Flo, et al., 2008). In a comparison of the phytoplankton community in port areas across the Adriatic Sea, *Pseudo-nitzschia* species were found to represent the core of the community in autumn and winter (Mozetič et al., 2019). In our time-series, the number of *Pseudo-nitzschia* abundances occasionally exceeded  $10^6$  cells L<sup>-1</sup>, which is markedly above the management thresholds in areas where Amnesic Shellfish Poisoning is a recurring problem (Trainer et al., 2002). These numbers are also higher than those reported from other areas in the Mediterranean Sea (Marić et al., 2011; Mercado et al., 2005; Quijano-Scheggia, Garcés, Flo, et al., 2008). Each species from a given sampling event has representative morphological image data. In this way, we accounted for possible seasonal morphological variability if the species occurred in multiple seasons, as it has been reported for *P. galaxiae* (Cerino et al., 2005) and as has also been demonstrated by the metabarcoding analysis (Figure 6.2-6). The obvious concern is that morphological variability may also exist within the same sampling event. In contrast to Cerino et al. (2005), we demonstrated this for *P. galaxiae* by performing multiple isolations of morphologically and genetically distinct *P. galaxiae* strains at identical time points. This was later also confirmed in metabarcoding although bootstrap supports to individual morphotypes were on average very low, and we could not explicitly associate ASVs to morphological properties.

LM counts, isolation dates, TEM screens of natural samples taken during the monitoring programme at the LTER station and finally metabarcodes provided some insight into the seasonal dynamics of *Pseudo-nitzschia* species, independently of their grouping into species complexes. The occurrence of *P. multistriata*, which appears to be restricted to early winter (December, January), is somewhat consistent with Ribera d'Alcalà et al. (2004), who reported a restricted 3-8 week occurrence of this species in the Gulf of Naples, albeit in autumn. However, recent work from the same area indicated a more widespread seasonal distribution of *P. multistriata* inferred from clone library reconstruction, including a late autumn-winter peak and a high summer peak (Ruggiero et al., 2015). We did not detect this species in any of the summer samples, and the species was not present in the year-round metabarcoding study. We can say that this species does not represent a threat to the ecosystem and shellfish industry due to its low abundance and sporadic occurrence, although we confirmed it is a DA producer. *P. delicatissima* was isolated and tentatively identified only in winter/spring, which is consistent with the Gulf of Naples (Ribera d'Alcalà et al., 2004; Ruggiero et al., 2015) and with data from a study in the Gulf of Seine (Thorel et al., 2017). The fact that the clonal library study by Ruggiero et al. (2015) detected multiple peaks distributed across seasons is not surprising, as the resolution of their method is much higher than ours. Metabarcoding, which has a similar resolution to clonal libraries, also confirmed the presence of *P. delicatissima* in autumn but its absence in summer. Interestingly, in the study by Ruggiero et al. (2015), *P. fraudulenta* was also found only in February, which is the only month in two consecutive years in which viable cultures of this species were isolated during our study and in which we detected *P. fraudulenta* metabarcoding reads. *P. fraudulenta* has also been found in early spring cold-water samples from other parts of the Mediterranean Sea and in the English Channel (Downes-Tettmar et al., 2013; Quijano-Scheggia, Garcés, Sampedro, et al., 2008). Its sister taxon *P. subfraudulenta* was found in clonal libraries from the Tyrrhenian Sea only in autumn (Ruggiero et al., 2015), which is also consistent with our isolation data and metabarcoding linking this species to the period between October and December. This species was likely responsible for the occasional autumn blooms of the *P. seriata* complex, which was also detected in the resequenced samples of the *rbcL* metabarcoding analysis,

where this species was always present, albeit with low relative abundances. *P. galaxiae* was isolated in late August and September and all three described morphotypes were present together. They were found to be temporally separated in the Gulf of Naples (Cerino *et al.*, 2005), although each morphotype was also found in multiple seasons (Ruggiero *et al.*, 2015). However, it should be noted that in our study small cells that could have belonged to *P. galaxiae* were also observed in spring, but isolation was not successful. Metabarcoding indeed confirmed the presence of this species throughout the year, except in summer, while sequences that were assigned to different morphotypes were found in the same sample in agreement with our isolation data.

What exactly are the morphotypes of *P. galaxiae* and whether *P. galaxiae* is indeed a species complex remains to be determined. The seasonal occurrence and interannual variability of phytoplankton species have been shown to be strongly influenced by their biology. For example, microsatellite genotyping of *P. multistriata* in the Gulf of Naples showed that two specific populations exist, that live in sympatry and hybridize readily, but there is a semi-annual alternation of the dominant population (Tesson *et al.*, 2014). This alternation is determined by their reproductive cycles, which are influenced by the reduction of cell size and the existence of cell size optima for reproduction (D’Alelio *et al.*, 2010). Thus, it may be hypothesized that the three morphotypes of *P. galaxiae* that we found in the same spatiotemporal window represent distinct populations at different stages of their life cycle that occur and bloom sympatrically at the ecological optimum for this species. These ideas should be examined in light of the ability of the different morphogenotypes of *P. galaxiae* to reproduce sexually, although the smaller sized cells may be unable to reproduce altogether. This was shown with *P. multistriata* where increasingly smaller cells seem to lose the ability to reproduce (D’Alelio *et al.*, 2009). Genetically distinct sympatric or parapatric populations of planktonic protists have also been widely documented elsewhere, with varying degrees of hybridization, e.g. *Pseudo-nitzschia pungens* (Casteleyn *et al.*, 2010), *Alexandrium fundysense*, *A. minutum* (Casabianca *et al.*, 2011; Richlen *et al.*, 2012), *Skeletonema marinoi* (Godhe & Härnström, 2010). The reason for genetic differentiation could be oceanographic features as in *S. marinoi* or life-cycle features such as the formation of resting stages or parasitism as in *A. fundysense*. While there is no such obvious force in our case, Tesson *et al.* (2014) speculated that a meta-population model would explain the persistence of two or more interbreeding populations.

### 7.2.2 Phylogenies and the relationship of Adriatic strains with other Mediterranean isolates

While genetic characterization is crucial for the correct identification of species and strains in the *Pseudo-nitzschia* genus, marker selection can sometimes lead to ambiguous results. This is because of the different evolutionary rates between phylogenetic markers and perhaps even lineages, highlighting the importance of selecting multiple markers (Patwardhan *et al.*, 2014). In the phylogenetic analysis presented in the published article in Chapter 3, we focused on the recently published phylogenies of Lim *et al.* (2018) to compare our trees and evaluate the performance of the *rbcL* marker on a new set of species, which to our knowledge is the most comprehensive to date.

The groups defined in Lim *et al.* (2018) were all recovered in the ITS2 and 28S phylogenies. The tree structure diverged slightly, which could be the result of (i) strain selection, (ii) the fact that only Bayesian inference was used in this study, and (iii) the fact that the alignment of ITS2 was not guided by secondary structure (Turk Dermastia *et al.*, 2020, Figs. 10,11). The groups were also recovered by *rbcL*, although Group II was

represented only by *P. caciantha* (Turk Dermastia et al., 2020, Fig. 9). The *rbcL* marker has better discriminatory power compared to the COI used in Lim et al. (2018), resulting in a tree with greater support, although the overall *p*-distances are slightly smaller. This agreed with Lim et al. (2018), with ITS2 showing the largest distances, followed by *rbcL* and 28S. The *rbcL* alignment was the longest of the three. Correct identification of species using the molecular approach alone is somewhat problematic, as can be seen in the relationship between *P. mannii* and *P. calliantha*. Phylogenetically, *P. mannii* and *P. calliantha* are closely related and form a well-supported common clade according to all genetic markers. While in our analysis, one taxon was always parent to the other, the phylogenetic trees of Lim et al. (2018) placed them as sister species. Moreover, according to the *rbcL* phylogeny, the distance between the two taxa was smaller than the distance between the strains of *P. galaxiae*, and the separation between the two taxa was not supported by high posterior probability (0.85). Nevertheless, *P. mannii* was successfully separated from *P. calliantha* based on mating experiments and morphology (Amato & Montresor, 2008). However, it should be noted that prior to our study in which 15 different sequences were included, only one sequence of *P. mannii* was publicly available for *rbcL* (AL-101, DQ813824.1). 28S generally showed high amplification success in our study, but with much lower species resolution compared to ITS and *rbcL*. ITS was technically the most problematic because it occurs in multiple repeats in the genome that could potentially be heterogeneous (Orsini et al., 2004). This could interfere with PCR or lead to unreadable sequences if not cloned and then sequenced. Indeed, amplification and sequencing success was lowest with this marker, although its discriminatory power is the best.

In our case, the *rbcL* marker proved to be very versatile with high amplification success. The suitability of a 540 bp *rbcL* barcode has been evaluated in the past in terms of its ability to distinguish *Pseudo-nitzschia* species (MacGillivray & Kaczmarska, 2011). The authors noted that the evaluated fragment was particularly suitable in a dual barcode system with ITS2, as they were unable to distinguish certain biologically distinct species (e.g., *P. calliantha* and *P. mannii*). Recently, a curated database for diatom *rbcL* barcodes was established based on a 312 bp *rbcL* fragment (Rimet et al., 2016). Although the initial focus was on freshwater diatoms, many marine species are included and the use of the database in metabarcoding applications for monitoring the ecological status of aquatic environments has been demonstrated (Vasselon et al., 2017b). In our metabarcoding analysis this database was further modified, and local strains were added to ensure robustness and stringency of the results. This includes the addition of morphologically classified *P. galaxiae* and *P. subfraudulenta*, which were sequenced for *rbcL* for the first time. *In silico* evaluation of the 312 bp barcode revealed that the taxa recoveries were nearly identical to the 1220 bp alignment. This gave us the confidence to extend the use of this marker to the metabarcoding field, which proved to be efficient. Although some samples could not be amplified, those that were amplified gave comparable results to classical 18S-V9 metabarcoding, with significantly more taxa recovered.

Among the strains isolated, we detected some intraspecific variations, but they were limited. Only strains of *P. galaxiae*, which appears to be a species with high morphological as well as genetic variability (Cerino et al., 2005; D'Alelio & Ruggiero, 2015), were obviously different. As seen in the metabarcoding analysis, genetic variability within *P. galaxiae* was also highest, although other species such as *P. delicatissima*, *P. fraudulenta* and *P. subfraudulenta* also expressed a number of ASVs greater than expected from the sequence data of our isolates (Figure 6.2-7), of which sequences were more conserved. This could potentially be an effect of sequencing error that was not accounted for by the error modelling (Nearing et al., 2018). Overestimation of genetic diversity by ASV methodology is widespread and could be further reduced by implementing sequence similarity networks

(Forster et al., 2019). On the other hand, the coverage of metabarcoding is much higher compared to isolation and barcoding, so this variability is reasonably expected. This is better illustrated by our *P. galaxiae* isolates, where strains 818-A1G and 818-A2G shared a very similar 28S allele but had different ITS2 copies and clustered into different chloroplast haplogroups in the *rbcL* phylogeny. Strain 818-A2G (small morphotype) even formed a distinct branch in the ITS2 phylogeny. The study by Cerino *et al.* (2005) examined the different morphotypes only with 28S and found no significant differences between them. However, further studies by the same research group remarked that the morphotypes indeed differed in ITS (Ruggiero *et al.*, 2015), while large differences in *rbcL* were also uncovered, although not supported by morphological data (D'Alelio & Ruggiero, 2015), similarly to what was revealed by our metabarcoding data. Thus, this reinforces the hypothesis previously tentatively suggested by Ruggiero *et al.* (2015) – that *P. galaxiae* is a species complex.

Nuclear and chloroplast-encoded genes can have large discrepancies, and this has also been documented for *Pseudo-nitzschia*. In *P. delicatissima*, Amato *et al.* (2007) showed that the strains studied expressed two different *rbcL* haplotypes but had only one LSU and ITS genotype, which could be a result of concerted rDNA evolution. These strains were able to successfully interbreed, and the authors postulated that two distinct *rbcL* haplotypes occurred within these single cross populations. In our metabarcoding study, several co-occurring *P. delicatissima* ASVs were detected, reinforcing this hypothesis. In *Pseudo-nitzschia*, chloroplast inheritance is bi-parental and recombination between chloroplasts has been recorded for this genus including *P. galaxiae* (D'Alelio & Ruggiero, 2015). To further reveal the relatedness of *P. galaxiae* strains in the Adriatic Sea and in general, additional morphological and genetic studies should be conducted, including microsatellite genotyping as well as an investigation of ITS2 secondary structure, which seems to be a good proxy for mating ability (Amato *et al.*, 2007).

Genetic diversity among Mediterranean strains was slightly better captured by ITS2 than by *rbcL*, which is not surprising given the number of sequences available (412 and 111, respectively). Moreover, in the *rbcL* network, we observed that many species are represented only by Mediterranean strains (Turk Dermastia et al., 2020, Fig. 12); therefore, it is difficult to draw conclusions about genetic differences within and between the Mediterranean and other global regions. Some *Pseudo-nitzschia* species, such as *P. pungens*, are known to be cosmopolitan, although it has been shown that a distinct geographic division exists for this species, supported by both morphological and genetic data, with only one of three groups being truly cosmopolitan (Casteleyn et al., 2010). This is also evident from our analysis with both markers with Mediterranean strains belonging to the globally distributed clade I and the geographically restricted clades II and III without Mediterranean members (Turk Dermastia et al., 2020, Fig. 12). A similar case is observed for *P. delicatissima* species with two non-Mediterranean clades, although this species complex is less resolved and the two groups may well represent cryptic species, as also recently suggested (Giulietti et al., 2021). In contrast, *P. brasiliiana* showed different haplogroups in ITS2 with one major non-Mediterranean and two Mediterranean clusters. The differences between Catalan, Greek, and other non-Mediterranean strains of *P. brasiliiana* were previously discussed in Moschandreu et al. (2012). Finally, species represented by distinct haplogroups that include Mediterranean strains, including *P. multistriata*, *P. fraudulenta*, *P. mannii*, *P. hasleana*, *P. subpacific/heimii*, *P. pseudodelicatissima/cuspidata*, and *P. plurisecta*, may reflect a lack of sequencing effort on the one hand and the lack of crypticism within these species on the other.

## 7.3 Toxicity of *Pseudo-nitzschia* in the Gulf of Trieste

### 7.3.1 Toxicity and phylogenetic relationships between toxic and non-toxic strains

The results of the toxicity analyses complemented previous studies from the NW Adriatic Sea, in that the mildly toxic strains of *P. delicatissima* and *P. multistriata* strains are also present in the NE Adriatic Sea. Toxicity levels of *P. delicatissima* were slightly higher ( $\sim 1.5 \text{ fg cell}^{-1}$ ) than those reported in the NW Adriatic –  $0.006\text{-}0.040 \text{ fg cell}^{-1}$  (Penna et al., 2013), although it became clear to us during this study that many factors can affect the concentration per cell, including sample preparation, counting error, condition of the culture and others associated with DA production (reviewed in Lelong et al., 2012). This was particularly evident in the continuous sampling experiment of *P. multistriata* strain 119-A4, where the initial screens differed greatly from the concentration measured during the experiment. *P. delicatissima* from the Northern Adriatic is nevertheless a mildly toxic species that can reach bloom abundances, especially in spring, although data from shellfish monitoring do not detect any DA in shellfish during this period (Jožica Dolenc, personal communication). *P. multistriata*, on the other hand, appears to have a higher cell quota of DA compared to *P. delicatissima*, also higher than *P. multistriata* strains from the NW Adriatic (Pistocchi et al., 2012), but comparable to some from the Gulf of Naples (Orsini et al., 2002). However, this species rarely proliferates to blooms with high abundance and has been detected only in winter months (Chapter 3). We consider the ratios per cell unreliable because of inconsistencies in some measurements of pDA. Namely, in some cases, dDA concentrations were higher than tDA concentrations, resulting in negative values for pDA. For this reason, we had to re-analyse using a different method, in this case LC -MS/MS. Unfortunately, the LC -MS/MS detection limit of  $2 \text{ mg/L}$  was too low to detect DA in our samples, which could also be due to the fact that the samples were not specifically prepared for the LC -MS/MS tests, i.e., not stored in aqueous methanol. In addition, the replicate tests were performed on samples stored six months to over a year after the initial ELISA screens, which may have resulted in some toxin degradation (Smith et al., 2006; Wang et al., 2012). Despite these shortcomings, we can report toxic strains of *P. galaxiae* for the first time in the Adriatic Sea. This discovery is preliminar, as no toxicity could be confirmed by chromatographic methods, although repeated ELISA screens confirmed the presence of DA in at least one strain (B3S) (Table 4.2-1). DA was found only in small and medium morphotypes of the species and even among these only in the dissolved partition at the first test. This was unexpected, as the total partition included the dissolved DA, and we would expect the toxin to be present in both. We attributed this to procedural errors and therefore repeated the ELISA with these samples, which resolved this discrepancy somewhat, at least for strain B3S. Toxicity of *P. galaxiae* strains could also be related to their phylogeny as shown in Figure 4.2-2. Both strains of the smaller morphotype showed DA production, while only one strain of the larger morphotype was found to be toxic. This could reinforce the hypothesis that *P. galaxiae* is indeed a species complex, but further tests are needed. Conversely, the similarity of the sequences of *P. delicatissima* and *P. multistriata* in terms of toxicity suggests that toxicity is irrelevant to the phylogeny in these two cases and may support the previously discussed idea that the physiological state of the culture determines whether DA production is detected. Although there was a toxic strain of *P. delicatissima* with high bootstrap support that was different from ours, we also know that some of the Adriatic strains from Pesaro used in the phylogenetic analysis are toxic (Penna et al., 2013). These clusters are on the same branch of the ITS tree as our strains, but we could not tell from the literature which of them are toxic. Finally, the

possible detection of DA in *P. calliantha*, although below ELISA quantification, would need to be inspected further, because of procedural problems during the assay. It would not be surprising, however, as DA was recently found in Adriatic *P. calliantha* strains (Arapov et al., 2020), although it has been previously suspected (Arapov et al., 2016; Marić et al., 2011). On the other hand, the indication that even some *P. mannii* strains may also be toxic is surprising, as this species has not previously been confirmed to be toxic (Amato & Montresor, 2008; Bates et al., 2018). However, the apparent very low concentration could be a result of methodological error and should not be taken for certain.

### 7.3.2 *dabA* gene in selected strains

For the first time since the discovery of the DA biosynthetic pathway (Brunson et al., 2018), we were able to amplify the *dabA* gene in a species other than *P. multiseriis*. Although the *dabA* sequence of *P. multistriata* was deposited in GenBank by genome sequencing (Basu et al., 2017), which allowed us to design primers, we filled in the missing sites in the genome sequence that made it untranslatable. The secondary structure of the protein appears to be conserved between *P. multistriata* and *P. multiseriis*, although the nucleotide sequence is only 84% identical, which may contribute to the fact that the primers used did not amplify the gene in other species tested. *P. multistriata* and *P. multiseriis* are closely related, while *P. calliantha*, *P. mannii*, *P. galaxiae* and *P. delicatissima* are more distantly related (Lim et al., 2018). For the strains for which good products were not obtained, the reason could be a missing gene or poor primers. If it is due to the latter, further genomic and transcriptomic experiments need to be performed in other *Pseudonitzschia* species to populate the reference databases, which will facilitate the design of more universal *dabA* primers. These genes can now be searched for in other species, although our preliminary data show that the genetic as well as amino acid sequence differences between, for example, *P. multiseriis* and *P. multistriata* *dabA* genes are quite large and that this may not be a trivial task. Recently, a transcriptomic study showed that only *dabA* and *dabD* of the *dabABCD* cluster were expressed in DA producing *P. pungens*, and only *dabD* was found in *P. fraudulenta* transcripts. In contrast, *P. australis* expressed all four genes (Lema et al., 2019). In the future, these transcriptomes could be mined to obtain sequence data and design new primers. However, there is also the possibility that the gene cluster is completely absent from the genome of some species or strains that are indeed non-toxic (Bates et al., 2018), although such an explanation is unlikely as it would suggest either multiple deletions or insertions of the gene through the evolutionary history of the genus. Such a mechanism could imply either horizontal gene transfer, which is a viable explanation for the occurrence of DabA analogues in red algae (Chekan et al., 2020), or ongoing hybridization, which has, however, been demonstrated in the genus (Casteleyn et al., 2009; Tesson et al., 2013).

There is an idea that measuring the copy number of genes involved in the synthesis of DA, e.g., by qPCR, could be key to accurately predicting the threat of ASP. Now, however, the proper design of probes is hampered by the lack of sequences from different species and could perhaps only be developed for *P. multiseriis* and now with our data for *P. multistriata*. We acknowledge that there are other genes involved in the biosynthesis of DA (Brunson et al., 2018; Haroardóttir et al., 2019) that we did not examine in this work and that may prove to be more conserved and thus better targets for such efforts. However, the scope of this work focused on the toxicity profiles of NE Adriatic strains, and we envision that this work will open novel possibilities for the research on gene expression and discovery of genes involved in DA synthesis.

## 7.4 Colorimetric Tools for Monitoring of *Pseudo-nitzschia* and Management of Aquaculture Sites

Although sandwich-hybridization probes for *Pseudo-nitzschia* have existed for nearly 25 years (Scholin et al., 1996) and their usefulness has been demonstrated in several publications (e.g. Scholin et al., 1997; Medlin and Kegel, 2014; Bowers et al., 2017), there is still room for improvement in the serviceability and utility of assays exploiting this concept. One reason is that most probes have been developed and tested on strains from a few localities (i.e., NE Pacific and Tyrrhenian Sea) and the other is the lack of rigorous testing on unwanted targets as well as in environmental samples. Here, we used strains from the Northern Adriatic and tested them on a series of newly developed probes (Patent number FR 18/58362). In total, four probes from an initial set of 10 were thoroughly examined, both in terms of species specificity and performance on environmental samples.

All probes tested showed a general agreement with microscopic counts, although these two data sets measure two different properties and reliable conversion factors have not been obtained and were not sought for at this stage. We attempted to convert the signal to cell numbers (data not shown), but the discrepancies between the count data and converted values obtained by applying the regression formula from the dilution series were higher than 10%, which is the limit reported in Medlin and Kegel (2014). Several limitations must be taken in account here, namely the species-unspecific response of the assay, which complicated the conversion of signal to cell number, and the lack of data on the RNA content of the species tested at different conditions and growth stages. However, even if these data were available and the assays were more specific, it would be difficult to extrapolate these data to environmental conditions in a way that would be cost and time efficient, which is the main purpose of this assay. In fact, our assay detects the amount of RNA, which is a proxy for cell activity, and therefore we must consider the count and assay data as two completely independent data sets. Based on the results from the dilution series and initial environmental sample analysis (Figure 5.2-2, Figure 5.2-3), we can say that Pn1mod was the most accurate and specific for detecting *Pseudo-nitzschia* in environmental samples. Therefore, we tested this probe on another set of environmental samples. In Figure 5.2-6, we see that there was a significant spike in assay reactivity on September 1, 2015, while the number of cells remained at very low values. Unfortunately, there was a large gap between September 1<sup>st</sup>, 2015, and the next measurement on October 20<sup>th</sup>, 2015 to get a clear picture of what happened in between. *Pseudo-nitzschia* blooms have been common in the NE Adriatic during this time period (Ljubešić et al., 2011; Mozetič et al., 2019; Turk Dermastia et al., 2020). We speculate that in our case the assay detected the onset of a bloom event before it was detected in microscopic counts. If the assay did indeed detect an increase in cellular activity before there was an increase in cell counts, the applicability of the assay for early warning is thus well demonstrated. There is strong evidence from unpublished tests of Microbia Environnement that this is indeed the case.

We have demonstrated the practicality of the microplate assay for measuring the activity of *Pseudo-nitzschia* cells either in culture or in the environment. The concept of the method is not new and builds on years of experience and knowledge of sandwich-hybridization probes for the detection of *Pseudo-nitzschia*. Our work is a continuation of some European projects that have sought to develop sensors for the detection and monitoring of harmful algae (MIDTAL – Microarrays for the detection of toxic algae, SMS – Sensing toxicants in marine waters makes sense using biosensors). Most of the work has been done with microarrays (e.g. Edvardsen et al., 2013; Medlin & Kegel, 2014), which are impractical for large-scale daily use due to high cost, longer sample turnaround times and

lower throughput, although they are better at species identification and also quantification (Barra et al., 2013). A microplate assay similar to ours for the detection of *Alexandrium*, *Pseudo-nitzschia* and several other harmful algae was demonstrated by Diercks et al. (2008a, 2008b). Their assay had a similar implementation time to ours (approximately 3 h per 96-well plate and within 1 day of sampling) but showed unsatisfactory detection limits (280 ng RNA or 10 000 *Alexandrium* cells/L; not available for *Pseudo-nitzschia*) and has not been tested with environmental samples. We see that the LODs of our assay, which are below 1000 cells or 0.25 ng RNA for some species-probe pairs are drastically lower, improving the applicability of the assay. Thus, the LODs are comparable or even better than microscopic counting, implying that the assay can be used as an early warning tool to assess cell activity in a population and anticipate blooms (Figure 5.2-6). Although Pn5 probe showed a more linear response to increasing synthetic RNA concentrations compared to Pn1mod, we found that Pn1mod was still a better probe for genus-wide detection as the signals were generally stronger compared to Pn5. Additionally, as seen in the environmental series (Figure 5.2-3), Pn5 produced a higher signal in the absence of *Pseudo-nitzschia* cells compared to Pn1mod. We cannot explain this noise because the probe did not react with the *Cylindrotheca* strain used in this study, although it may have reacted with other untested targets, including untested *Pseudo-nitzschia* species that may be present in the area but have not yet been identified. *Pseudo-nitzschia* often blooms in autumn with other diatom species in the Mediterranean, including *Cylindrotheca closterium* (Cabrini et al., 2012; Quijano-Scheggia, Garcés, Flo, et al., 2008; Ribera d'Alcalà et al., 2004), and they may be the cause of the strong signal with this probe in the absence of *Pseudo-nitzschia*. Additionally, it must be emphasized that the signal of Pn1 in Figure 5.2-3 was reduced tenfold for clarity reasons. Thus, the signal was about tenfold higher than in Pn1mod and Pn5, but for time series analysis it is the change in signal that matters, not the absolute signal value.

Part of our phytoplankton count data also included *P. galaxiae* counts, although this is not entirely reliable as *P. galaxiae* is a species that is difficult to identify by light microscopy. It occurs in various morphological forms, some of which are very small and virtually undetectable, while the larger morphotypes are very similar to *P. delicatissima* (Cerino et al., 2005; Turk Dermastia et al., 2020). Not surprisingly, given that the two species are closely related (Lim et al., 2018), some cross-reactivity with *P. delicatissima* was also suspected in this first phase of testing of the Pn7 probe. This limited dataset however exhibited strong correlation between *P. cf. galaxiae* counts and Pn7 assay signal. This is a promising step in developing the assay for species-specific detection. The next interesting goal is to test this probe on the samples collected during the metabarcoding campaign, which revealed a high prevalence of *P. galaxiae*. During this campaign, parallel samples were taken for colorimetric assay analysis, opening the possibility of testing these samples with the Pn7 probe and seeing if it picks up a strong signal when the relative abundance of *P. galaxiae* is high.

The main drawback of our assay is the fact that signal amplitude varies from test to test and that there are currently no good standardization methods that would ensure repeatability. The other caveat is that none of the probes we tested, excluding Pn7, are truly species-specific, and for the moment the assay is a good tool for monitoring cell activity alongside other methods that may be better suited for species-specific detection. It is also very useful when many samples need to be analysed to assess threat risk. If strong signals are detected, managers can be directed to in-depth analysis of only those samples, saving money and time. Following the first objective of this study, we compared the results of both cell numbers and assay signal. Our results showed that cell counts, and absorbance values were not interchangeable, but they were complementary and can be used as a

preliminary proxy for each other. Cell counts are absolute values, but they often do not detect dead and senescent cells and thus may overestimate toxicity threat (Zetsche & Meysman, 2012), especially after the bloom peak. Additionally, cell counts may miss the warning signals of a developing bloom. On the other hand, absorbance may be affected by extraction efficiency and possible non-target binding, although the probes are generally good for detecting *Pseudo-nitzschia* and did not respond to *Cylindrotheca*, the closely related species we tested. The results of the colorimetric assay necessarily involve an additional level of biological complexity compared to simple cell counts, which is the most advantageous property of the assay. However, the methods are complementary, as it appears that the performance of one and the other changes over the course of the bloom. RNA levels tend to increase prior to the bloom event, when cells become more active, allowing us to predict and identify early warning signs of a bloom event. This concept has been explored mainly in studies of bacterial activity (Blazewicz et al., 2013), but has also been used in microarray screening of harmful phytoplankton (Edvardsen et al., 2013; Smith et al., 2012). Therefore, we argue that the signal derived from our assay provides a stronger indication of the direction of bloom progression, although it appears to be less reliable in the post-bloom peak phase. This could be because when cells begin to die due to resource depletion, a certain number of cells remain very active and benefit from the death of their counterparts, thus maintaining the bloom. Another explanation, although unlikely, could be that some RNA is retained in the environment or in dead cells, affecting signal strength in the post-peak period. Recently, some experiments have shown that invertebrate RNA can remain in the environment for up to 13 hours (Wood et al., 2020), when the organisms are removed, while it can persist for much longer given the right conditions (Cristescu, 2019). This is in contrast to the widely accepted notion that RNA is unstable, which is supported by *in vitro* assays, although eRNA monitoring has already shown its strength in assessing live and active assemblages (e.g. Pochon et al., 2017). The post bloom peak period is therefore the most problematic for both colorimetric detection and cell counting because of uncertainties regarding RNA stability and because immediately after the bloom the proportion of dead and senescent cells in counts is greatest. However, we argue that given that the sampling windows were much longer than 13 hours – two weeks on average – even if RNA were more stable than expected, this should not greatly alter the signal output from living cells and would contribute to only a small fraction of the overall signal, making the RNA hybridization technique preferable to counts in assessing the living fraction of the community. While the experiments of Wood et al. (2020) were performed on invertebrates that continuously excrete cells and RNA, very little RNA excretion likely occurs in the case of protists, with most eRNA likely coming from dead cells and possibly extracellular vesicles (Cristescu, 2019). Finally, the actual fluctuation in live cell abundance, and thus the measured RNA concentration that comes directly from cells – i.e. not from eRNA – is also highly dependent on external factors such as prey and nutrient availability and advection processes (Jørgensen & Andersen, 2007). However, this also applied to cell counts.

How useful can our assay be in terms of aquaculture management? Aquaculture is the fastest growing food industry in the world (FAO, 2018). Shellfish production is an important component of this industry, especially in the core producers of the EU, Spain, Italy and France (Massa et al., 2017). The more the industry grows, the more is at stake. HABs pose a particular risk to the industry as they are very difficult to predict, can affect production over long periods of time, and involve costs for monitoring and safety measures. This is where we come in by developing a bioassay that has the potential to significantly reduce monitoring costs while providing valuable new data that sheds a different light on the state of the bloom. HAB Monitoring systems that rely on genetic information to detect algae are usually implemented on expensive systems, such as the Environmental Sample

Processor (ESP), which can monitor *Pseudo-nitzschia australis* through an automated ELISA immunoassay (Greenfield et al., 2006), or are by-products of specific research activities and rarely meet the end user. This is not ideal for small and highly dispersed aquaculture operations that want to ensure a good and safe product while limiting costs. *Pseudo-nitzschia*-related closures of mussels are not common in European waters, but with the changing climate and possible bioinvasion or anthropogenic introduction, this scenario is not excluded. On the other hand, *Pseudo-nitzschia* can cause significant economic and ecological problems in other areas of the world – e.g. the west coast of the USA (McCabe et al., 2016). Our assay significantly shortens the time from sample collection to potential warning to farmers or environmental agencies, compared to traditional monitoring techniques that involve a required 24h sample settling period. The assay can and has already been modified for other targets that may currently be more relevant in the European context. In parallel with this work, the assay has been developed for *Dinophysis* species, which are responsible for most European shellfish farm closures, including in Slovenia. This assay has also been used with oyster farmers in France, with very good response, as it limits the time from sampling to warning and thus the economic loss to farmers.

## 7.5 Monitoring HABs and Phytoplankton Populations – Lessons from Metabarcoding

Above (Chapter 6), we demonstrated the utility of a metabarcoding approach to monitor and assess phytoplankton community composition in the marine environment. Traditionally, this has been done by counting phytoplankton cells under a light microscope using the Utermöhl method (Section 2.1.3). These counts have been the gold standard in environmental assessments by government agencies and research institutes for decades. However, the method has its drawbacks, namely dependence on a skilled observer, i.e., the taxonomist counting the cells, the inability to distinguish cryptic or inconspicuous taxa, the insensitivity to rare taxa, and the low sample throughput. The latter may not be important when the number of samples to be assessed is small but becomes critical when large areas or transects need to be covered. Metabarcoding addresses all the above issues, but also brings some problems of its own. First, it is PCR-dependent. PCR may preferentially amplify some targets while others may not or may be amplified at a lower rate (Kelly et al., 2019). Next, taxonomic assignment relies on reference databases that do not cover all genetic diversity because most organisms have never been cultured and sequenced (Weigand et al., 2019). Thus, assignment may be ambiguous or, in some cases, not possible at all, as it is very likely that metabarcoding in a new environment will yield a wide range of novel sequences. A conceptual problem also arises in translating sequence data into taxonomic richness at the species level. What is a genetic species and up to what point are dissimilar sequences considered a species?

The selection of markers in our study, 18S-V9 region and *rbcL*, was based on previous practice in marine plankton metabarcoding and novelty. 18S is a well-established eukaryotic marker that has been used in many metabarcoding experiments and campaigns including the global Tara Oceans cruise and the annual Ocean Sampling Day (Bradley et al., 2016; De Vargas et al., 2015; Malviya et al., 2016; Piredda et al., 2017; Stefanni et al., 2018; Tragin et al., 2018). In this sense, 18S data are useful for a general overview of the phytoplankton community structure and for global comparisons, while they lack the species-specific robustness that may be sought. We saw this in our results (compare Figure 6.2-4 and Figure 6.2-5), especially for diatom genera, as 18S could not distinguish between

them in many cases. However, the power of 18S was shown in the analysis of higher taxonomic levels of phytoplankton as well as in the abundance of different phytoplankton groups that the marker could detect, but probably with an inflated abundance of dinoflagellates. This inflation could be the result of preferential amplification of dinoflagellate DNA, resulting in a relative abundance that is likely not the true representation of the community. We have seen in the count data (Figure 6.2-11) that cryptophytes and haptophytes rather than dinoflagellates occupy larger proportions of the total abundance. These organisms are small and provide little DNA, but can be very abundant, resulting in high proportions of the total phytoplankton cell count. Thus, this discrepancy could also be the result of method differences. Perhaps a better way to compare the results of morphological and genetic methods would be to have data on the biomass or biovolume of different phytoplankton groups (Godhe et al., 2008; Leonilde et al., 2017; Olenina, 2006), although these data are rarely available. Dinoflagellate rDNA from 18S-V9 metabarcoding was previously examined for agreement with actual abundances of organisms in mock samples, and it was found that the percentages found were quite variable (Guo et al., 2016). The authors found that the *actin* gene that is actively translated is a better representative of the community. In this work, this was complemented by the *rbcL* gene, but for diatoms. Nevertheless, potentially harmful dinoflagellates such as *Karlodinium* or *Takayama* were found in our metabarcoding data, which are rarely or never recorded in phytoplankton monitoring.

To overcome the challenge of correct species assignment, which is often not possible with 18S, we resorted to the *rbcL* marker for diatom analysis. In Chapter 3, we showed that *rbcL* is a robust marker for identifying *Pseudo-nitzschia* species, whereas it has previously been used for metabarcoding freshwater diatoms (Vasselon et al., 2017a). To our knowledge, this is the first study to do the same in the marine environment, although the principle is the same. The primers used to generate the *rbcL* amplicons were diatom-specific, although many other non-diatom amplicons were generated. In order to assign a taxonomy to these sequences, a completely new reference database would need to be constructed, which was beyond the scope of this work, and therefore these sequences will not be analysed for the time being. At this point, it is important to discuss the flawed sequencing protocol for *rbcL* amplicons, which did not include enough cycles, resulting in non-overlapping forward and reverse reads. The solution of forced merging, which introduced multiple unidentified nucleotide bases between the forward and reverse reads, is not ideal, but since the error introduced is consistent across all sequences because they are all truncated at the same base, the taxonomic assignment should not have been drastically different from the expected. This was indeed confirmed by resequencing a subset of samples using a modified protocol. The concatenation data yielded slightly more unique taxa (Table 6.2-2), which could be a consequence of the concatenation process introducing more errors into the assignments. Therefore, it is possible that many of the assigned genera were in fact artefacts, but fortunately they did not represent the majority of the data (Figure 6.2-9). The diatom community was generally very comparable between the concatenated and resequenced data sets, as also shown by the correspondence analysis performed at the lowest level of taxonomic assignment available (Figure 6.2-8). This result gave us confidence to use the concatenated dataset from the entire sampling period for comparison with the morphological and 18S data.

Focusing now on the diatom genera, and in particular on *Pseudo-nitzschia*, we can confidently conclude that *rbcL* is the most reliable marker in the identification and classification of this group. This is not surprising since the primers were designed to selectively amplify diatom DNA and the differentiation rate of the *rbcL* gene is higher compared to 18S. Nevertheless, both 18S and *rbcL* identified dominant taxa, while seasonal patterns were equally well detected (Figure 6.2-13). What is particularly interesting when

comparing the molecular data with the microscopic count dataset is the recovery of small diatom taxa such as *Minidiscus* and *Thalassiosira*. Particularly *Minidiscus* was previously identified as globally overlooked in phytoplankton counts, while their biomass and abundance potential has been captured in other metabarcoding studies (Arsenieff et al., 2020; Leblanc et al., 2018). Our work adds to these findings, as *Minidiscus* in particular was never recorded in our cell count datasets, although it can represent up to a quarter of the diatom community in certain winter months, as indicated by the metabarcoding study. The morphological and molecular data sets complemented each other when the dominant taxa were large and recognizable diatoms, whereas they seemed to differ markedly in more complex samples dominated by smaller and less conspicuous taxa. One reason for such marked differences could also be related to the selective amplification of some taxa by the molecular methods, resulting in an overrepresentation of the DNA of some taxa relative to the others and their apparent dominance in a sample that was not detected in the phytoplankton count (Guo et al., 2016). Many genera that appeared in the *rbcL* dataset were benthic taxa, which is not surprising since most diatom species are benthic and their presence in planktonic datasets with low read counts has also been demonstrated in other diatom metabarcoding studies (Piredda et al., 2018). Indeed, benthic genera are also represented in our data with a low read count. Reads assigned to *Pseudo-nitzschia* resulted in eight species, which are fewer than those collected using the integrated approach in Chapter 3. However, the metabarcoding study covered only one year, whereas the integrated study spanned four years. The prevalence of *P. galaxiae*, which was not previously recorded in phytoplankton monitoring, is particularly surprising. The high number of reads in January and February assigned to the small morphotype of this species when the bootstrap level was set to 50% may indicate that these small cells were missed in the phytoplankton counts, although it remains uncertain whether, due to the low bootstrap support, these reads actually represent the small morphotype. Furthermore, it was not possible to directly translate the number of reads into the actual abundance of the species, although a high number of reads may indicate a high DNA content. Fixed phytoplankton samples from the periods with the greatest differences between records should be carefully rechecked to determine if certain taxa, such as *Minidiscus* and *P. galaxiae*, have indeed been overlooked or assigned to a different taxon.

Apart from the metabarcoding study in the Venice Lagoon by Armeli Minicante et al. (2020), this study represents the first attempt to metabarcode the phytoplankton community in the coastal region of the NE Adriatic. Moreover, it is the first to use *rbcL* as a metabarcoding marker in the marine environment. We used a non-fractionated approach for filtration of the water samples, as the target group was diatoms, for which size fractionation is neither informative nor advisable, as their cells may rupture or clog filters during filtration, leading to inaccurate representation of the different size fractions (Piredda et al., 2018). The main objective was to complement the studies of *Pseudo-nitzschia* presented in other chapters of this thesis, to see if more species can be found with powerful high-throughput methods. As a conclusion, no new species were found, apart from the *P. americana*/*P. lineata* species complex, which could not be further identified. A surprising dominance of *P. galaxiae* was noted, which was not previously observed in the integrative taxonomic approach used in Chapter 3, nor in the years of phytoplankton monitoring by phytoplankton counts. The latter appears to provide very different phytoplankton abundance data sets compared to the two molecular methods we used, except when very dominant or blooming taxa are present. It is particularly inferior in terms of biodiversity estimates when small and inconspicuous taxa are involved, which has now been consistently noted by metabarcoding studies worldwide (Leblanc et al., 2018; Malviya et al., 2016; Piredda et al., 2017). The next step will be to dive deeper into the taxonomy of discovered ASVs, especially for the *rbcL* dataset, as the Ribosomal Database project

naïve Bayes classifier method implemented in DADA2 (Wang et al., 2007) and developed specifically for rDNA may lose resolution for distant taxa due to mutation saturation. Therefore, a BLAST approach may be more appropriate (Stefanni et al., 2018). Similarly, we will investigate whether the distribution and abundance of *Pseudo-nitzschia* ASVs is rooted in any of the ecological parameters to decompose species complexes, as discussed in 7.2. We believe that this work will further deepen our study of the coastal ecosystem of the NE Adriatic and further fuel questions about the seasonal and ecological dynamics of the phytoplankton community.

## 7.6 Integrating Molecular and Morphological Data in Ecological Studies at LTER Sites

Traditional methods such as light microscopy are often insufficient to reveal the actual diversity of cryptic protists, yet this is the most commonly used method for long-term monitoring to analyse plankton community structure. Although knowing the exact species or even ecotypes of a particular species is beneficial to ecological studies feeding from LTER data, these data are often not available and simplifications need to be made. However, we should be more cautious when dealing with potentially toxic species (Bickford et al., 2007). Perhaps the most notable example is the *Alexandrium tamarense* species complex, which consists of five species, only some of which produce saxitoxin, and cannot be distinguished by either light or electron microscopy (John et al., 2014). Similarly, different genetic varieties of *Akashiwo sanguinea* have been shown to occupy different ecological niches but are morphologically indistinguishable (Luo et al., 2017). In *Pseudo-nitzschia*, only species complexes roughly defined by valve width are usually determined by HAB and LTER monitoring programmes. Although morphological traits can be proxies for ecological preference, as has been shown in freshwater diatoms (Potapova & Hamilton, 2007), we are not aware of any studies showing that valve width defines ecological preference in *Pseudo-nitzschia*, as most attempts to do so yield contradictory results. In addition, valve width limits discriminating the two groups are arbitrarily defined, and some cells of certain species may not meet the threshold to be assigned to either group (Accoroni et al., 2020). We therefore question the usefulness of these data in relation to LTER site management and explore what can be gained from specific molecular studies such as those presented in this paper. Incorporating molecular knowledge into LTER strategies provides a better understanding of the local ecosystem and leads to better management (Stern et al., 2018b). Such efforts also help build local reference databases of sequence and biological data that can then be relied upon in high-throughput sequencing studies that are more reliable and robust (Stern et al., 2018a). Our data show that the *P. delicatissima* group, which we now know consists of at least four species (*P. delicatissima*, *P. calliantha*, *P. manni* and *P. galaxiae*), occurs preferentially in summer and spring, whereas the *P. seriata* group (comprising of *P. multistriata*, *P. pungens*, *P. fraudulenta* and *P. subfraudulenta*, *P. americana/linea*) peaks in autumn. Until the current study was conducted, only species complex data and data on *P. multistriata* were available in the Gulf of Trieste. The three-year strain isolation campaign followed by characterization and tracing to LM data and the one-year metabarcoding campaign allowed us to understand the community much better and to identify more species at LM because we now know which species to expect at different times of the year. Using the toxicity data, we understand which time periods are potentially problematic in terms of domoic acid, although mussel monitoring data has not shown any threshold exceedances to date (in <http://haedat.iode.org>). We believe that our work fits well within the framework proposed by Stern *et al.* (2018b) for integrating

molecular data into routine monitoring and is thus an example of good practise. Furthermore, our methodology can be improved by integrating the developed colorimetric assay into monitoring strategies, which would greatly simplify the process. Many molecular tools can be used to obtain better species resolution and seasonal profiles (e.g. qPCR: Andree et al., 2011; microarray: Smith et al., 2012; various SHA and FISH techniques: Orozco et al., 2016; Medlin & Orozco, 2017; Bowers et al., 2018), although the feasibility of their use in routine monitoring is often compromised due to budget and personnel constraints. Nevertheless, we must be cautious when drawing conclusions about the affinities of different species to environmental conditions, since bloom phenology and species succession also depend on species interactions, nutrition, and parasitism (D'Alelio et al., 2019; Gleason et al., 2015). Further studies and models of the seasonal distribution of individual species, including interannual differences, will help fill in the knowledge gaps and clarify the ways in which species dominance and blooming relates to environmental and ecosystem conditions. Many opportunities have opened up with this dissertation and there will be opportunity for great new discoveries based on the knowledge and expertise we have gained through this process.

## Chapter 8

# Conclusions

This work provides a comprehensive insight into the diversity, ecology, occurrence of the potentially toxic diatom genus *Pseudo-nitzschia* in the Gulf of Trieste, and novel tools for detecting *Pseudo-nitzschia* species, with far-reaching implications for other harmful and non-harmful phytoplankton taxa in this and other world regions. Using a unique set of morphological and molecular tools, we have unravelled the previously unknown diversity of the genus, which is now known to comprise at least 9 species – *P. americana*/*P. linea*, *P. calliantha*, *P. delicatissima*, *P. fraudulenta*, *P. galaxiae*, *P. mannii*, *P. multistriata*, *P. pungens*, *P. subfraudulenta*. Furthermore, a surprising morphological as well as genetic diversity of the species *P. galaxiae* was found, which might indicate that this species is indeed a species complex consisting of several different species. This will need to be proven in further mating experiments and analysis of secondary rRNA structures. The metabarcoding study also revealed a great deal of genetic diversity in this species, as well as others that could not be assigned to any known species with a high degree of statistical certainty. The seasonality of the different species was also investigated. We found that the greatest diversity occurred during the winter months, especially among species morphologically belonging to the *P. seriata* species complex, i.e., species with the frustule width greater than 3  $\mu\text{m}$ . Spring and autumn communities are typically dominated by one or two species, *P. delicatissima* and *P. calliantha* or *P. mannii*, respectively. Metabarcoding revealed a year-round prevalence of *P. galaxiae* in 2019 and early 2020, which was not recorded during phytoplankton counts and should be reassessed by examining fixed samples. An increase in reads of this diatom was observed especially in January and February. In general, the metabarcoding approach revealed patterns of phytoplankton diversity not previously recorded, but consistent with similar studies from other world regions. For example, the presence of nanodiatoms, which are often not recorded in phytoplankton counts but may represent large portions of the phytoplankton biomass. Three species – *P. delicatissima*, *P. galaxiae*, *P. multistriata* – were found to produce the domoic acid toxin. The results of some toxin analyses suggested that *P. calliantha* and *P. mannii* might also have produced the toxin, but the results were not conclusive enough to state this with certainty. We also succeeded in amplifying the gene *dabA* in several strains of *P. multistriata*, for the first time in a species other than the one in which it was discovered – *P. multiseriata*. We also attempted to amplify the gene in other species, particularly *P. delicatissima* and *P. galaxiae* strains that produced DA in our experiments, but this attempt was unsuccessful, perhaps due to the non-universality of the primers. *P. multistriata* and *P. multiseriata* are indeed more closely related than *P. multiseriata* and *P. delicatissima* or *P. galaxiae*. Further work on finding universal primers will help us understand how the biosynthetic apparatus of *Pseudo-nitzschia* evolved, whether it is

universal to all species, including those that do not appear to produce the toxin, or whether perhaps species that do not produce the toxin have defunct or missing genes. Finally, by testing the colorimetric sandwich-hybridization sensor on a series of newly developed nucleotide probes, we have generated a novel tool that is as good or better for monitoring *Pseudo-nitzschia* in the environment. This tool was developed based on the Northern Adriatic *Pseudo-nitzschia* strains and thus represents an advancement in respect to similar tools that were exclusively tested on DNA from Pacific strains. In addition, the sensor is RNA-based, thus capturing the active or living part of the community and is thus a better representation of cell activity than plain cell counts. By combining the theory of the increase in RNA concentration prior to the propagation of the bloom and the use of the assay in environmental samples, we were able to obtain early warning predictions of the development of the bloom. This is very useful for aquaculture operators, who can save their product or harvest it early before potential product contamination occurs. The company Microbia Environnement, with whom we collaborated, already has working solutions for other harmful phytoplankton groups using the same principle which are used in French aquaculture farms. Further work with the assay will improve its specificity and allow better standardization and possibly even produce conversion factors from signal to cell numbers. For this, however, species-specific probes will need to be developed.

# Appendix A

## Permission to Republish

### Timotej Turk Dermastia

---

From: Christopher Gobler <christopher.gobler@stonybrook.edu>  
 Sent: Tuesday, March 2, 2021 7:04 PM  
 To: Timotej Turk Dermastia  
 Subject: Re: Enquiry: Permission for manuscript publication in doctoral thesis

You may proceed

--

Christopher J. Gobler, Ph.D.  
 Endowed Chair of Coastal Ecology and Conservation School of Marine and Atmospheric Sciences Director, New York State Center for Clean Water Technology Stony Brook University

On Tue, Feb 23, 2021 at 8:11 AM <timotej.turkdermastia@nib.si> wrote:

>

> The following enquiry was sent via the Elsevier Journal website:

>

> -- Sender --

> First Name: Timotej

> Last Name: Turk Dermastia

> Email: timotej.turkdermastia@nib.si

>

> -- Message --

> Dear Professor Gobler,

>

> I am writing you to ask for permission to attach my paper Ecological time series and integrative taxonomy unveil seasonality and diversity of the toxic diatom *Pseudo-nitzschia H. Peragallo* in the northern Adriatic Sea (<https://doi.org/10.1016/j.hal.2020.101773>) published in *Harmful Algae*, to my doctoral thesis. If you are not the right address for this kind of permissions, please refer me to the relevant person.

>

> Sincerely,

> Timotej Turk Dermastia

>

>

> --

> This email was sent to you by Timotej Turk Dermastia

> (timotej.turkdermastia@nib.si) via the Elsevier Journal Editor

> contact form at

> <https://www.journals.elsevier.com:443/harmful-algae/editorial-board/ch>

> ristopher-gobler Elsevier B.V., Radarweg 29, 1043 NX Amsterdam, The

> Netherlands. Reg. No. 33156677.

>

> Elsevier is not responsible for the content of this email, and anything written in this email does not necessarily reflect the views or opinions of Elsevier. Please note that neither the email address nor name of the sender have been verified.



## Appendix B

### Microarray Probe Signals

Table 7.6-1: Results of microarray for selected species and probes. Signals are normalized and only signals above threshold levels are shown. Highlighted probes were considered in further probe development.

Probe	Target Species	<i>P. delicatissima</i>	<i>P. fraudulenta</i>	<i>P. multistriata</i>	<i>P. galaxiae</i>	<i>P. caliantha</i>	<i>Cylindrotheca sp.</i>
PcaciD01_25_dT	<i>Pseudo-nitzschia caliantha</i> (with hierarchy)						
PcaciD02_25_dT	<i>Pseudo-nitzschia</i> spp.		0.87				
PcaciD04_25_dT=Pca ciausD04_25_dT							
Pcal1D01_25_dT	<i>Pseudo-nitzschia</i> spp.					3.05	
Pcaldel2D03_25_dT			0.66		1.19	2.60	

PcaldelD03_25_dT	<i>Pseudo-nitzschia delicatissima</i> Clade2 (with hierarchy)		0.84		1.15	1.40	1.05
PcalfrauD04_25_dT	<i>Pseudo-nitzschia</i> spp.	2.85	1.02	1.16	1.19	3.59	1.06
PcaserausD02_25_dt= PcaserausmultD02_25_dT		0.93	0.83	1.01	1.20	3.62	
PcaserausD03_25_dT	<i>Pseudo-nitzschia calliantha</i> (with hierarchy)	1.11	0.78			3.47	
Pdel1D01_25_dT=Pdel1mulaausgal2D01_25_dT			0.70	1.04			
Pdel3A_25_dT=Pdel3ausA_25_dT			0.62	0.60	1.20	1.54	
Pdel3B_25_dT	<i>Pseudo-nitzschia delicatissima</i> Clade3 (with hierarchy)						
Pdel4D01_25_dT	<i>Pseudo-nitzschia</i> spp.		0.65	0.85	1.19	1.36	
Pdel4D02_25_dT=Pdel4gal2ausD01_25_dT			0.60				
Pdel4D0325_dt=Pdel4gal2ausD03_25_dT			0.74		1.20	1.91	1.03
PdeliD02_25_dT	<i>Pseudo-nitzschia</i> spp.				1.20		

PfraucalD02_25_dT	<i>Pseudo-nitzschia</i> spp.	0.85	0.79	0.96	0.90	3.66	0.93
PgalaD01_25_dT	<i>Pseudo-nitzschia</i> spp.				1.17	0.81	
PgalaD02_25_dT	<i>Pseudo-nitzschia</i> <i>galaxiae</i> (with hierarchy)				1.20		
PgalaD04_25_dT	<i>Pseudo-nitzschia</i> spp.				1.20	1.44	
Pman2D02_25_dT	<i>Pseudo-nitzschia</i> <i>manii</i>		0.65			3.41	
Pman2D03_25_dT	<i>Pseudo-nitzschia</i> spp.		0.77		1.19	3.41	1.05
Pman2D05_25_dT	<i>Pseudo-nitzschia</i> spp.		0.63			3.65	
PmanD01_25_dT	<i>Pseudo-nitzschia</i> spp.						
PmulacalD02_25_dT	<i>Pseudo-nitzschia</i> spp.			1.15		3.53	
PmulaD0325_dt=Pm laausD03_25_dT				1.15	0.62		
PmulausD01_25_dT	<i>Pseudo-nitzschia</i> <i>multistriata</i> (with hierarchy)		0.69	1.15			
PmultcalD01_25_dT	<i>Pseudo-nitzschia</i> spp.		0.96		1.20	2.83	
PmultcalD03_25_dT	<i>Pseudo-nitzschia</i> spp.					1.88	

PmultcalD04 25_dt=PmultcalausD0 4_25_dT				0.98	1.20	4.26
PmultD02 _25_dT=PmultausD0 2_25_dT					0.94	2.19
PmultS01_25_dT=P multausS01_25_dT		0.69	0.95	0.88	1.20	3.28
PpdeD01_25_dT	<i>Pseudo-nitzschia</i> spp.		0.71			
PpdeD02_25_dT	<i>Pseudo-nitzschia</i> <i>pseudodelicatissima</i> (with hierarchy)				1.20	0.91
PpungcalD02_25_dt= PpungcalmultausD02_ 25_dT			1.05		1.21	2.79
PpungcalD0425_dt=P pungcalausD04_25_d T			0.90	0.87	1.20	2.28
PpungcalS01_25_dT	<i>Pseudo-nitzschia</i> spp.		1.05			1.08
PsercalD01_25_dT	<i>Pseudo-nitzschia</i> spp.		0.71	1.12	1.20	2.14
PSN + some FragS_25_dT	<i>Pseudo-nitzschia</i> spp.		0.97	1.15	1.18	3.69
PSN no pungens_25_dT	<i>Pseudo-nitzschia</i> spp.		0.62		0.92	
PSN+FRAGS02- 25new_dT	<i>Pseudo-nitzschia</i> spp.	2.61	0.92	1.15	1.19	4.05

PsnGS01_25_dT	<i>Pseudo-nitzschia</i> spp.						
PsnGS02_25_dT	<i>Pseudo-nitzschia</i> spp.	2.09	0.99	1.15	1.20	3.64	



## Appendix C

# Metabarcoding Sample Lists

### C.1 18S Metabarcoding

Sample code	Date	Filter	Depth (m)	Raw reads
561452F532471	11-Mar-19	0.8 $\mu\text{m}$	0	70088
561453F532472	11-Mar-19	0.8 $\mu\text{m}$	5	60172
561454F532473	18-Apr-19	20 + 3 $\mu\text{m}$ fraction	0	47459
561455F532474	18-Apr-19	20 + 3 $\mu\text{m}$ fraction	5	51073
561456F532475	18-Apr-19	0.8 $\mu\text{m}$ fraction	0	63903
561457F532476	18-Apr-19	0.8 $\mu\text{m}$ fraction	5	71747
561475F532506	06-May-19	0.8 $\mu\text{m}$	0	59924
561476F532507	06-May-19	0.8 $\mu\text{m}$	5	53513
561477F532508	06-May-19	0.8 $\mu\text{m}$ fraction	0	60051
561478F532509	06-May-19	0.8 $\mu\text{m}$ fraction	5	47260
561458F532479	06-May-19	20 + 3 $\mu\text{m}$ fraction	0	77665
561459F532480	06-May-19	20 + 3 $\mu\text{m}$ fraction	5	57423
561474F532503	04-Jun-19	0.8 $\mu\text{m}$ fraction	5	54481
561473F532501	04-Jun-19	0.8 $\mu\text{m}$ fraction	0	53124
561472F532499	13-Jun-19	0.8 $\mu\text{m}$	0	384
561460F532481	19-Jun-19	0.8 $\mu\text{m}$	0	374
561500F532482	19-Jun-19	0.8 $\mu\text{m}$	5	56183
561499F532483	17-Jul-19	0.8 $\mu\text{m}$	0	59867
561497F532484	17-Jul-19	0.8 $\mu\text{m}$	5	59076
561498F532485	20-Aug-19	0.8 $\mu\text{m}$	0	59777
561496F532486	20-Aug-19	0.8 $\mu\text{m}$	5	45797
561461F532487	17-Sep-19	0.8 $\mu\text{m}$	0	40544
561462F532488	17-Sep-19	0.8 $\mu\text{m}$	5	43159
561463F532490	16-Oct-19	0.8 $\mu\text{m}$	5	39243
561464F532491	21-Nov-19	0.8 $\mu\text{m}$	0	45369
561465F532492	21-Nov-19	0.8 $\mu\text{m}$	5	53264
561466F532493	16-Dec-19	0.8 $\mu\text{m}$	0	48854
561467F532494	16-Dec-19	0.8 $\mu\text{m}$	5	47104
561468F532495	15-Jan-20	0.8 $\mu\text{m}$	0	70159
561469F532496	15-Jan-20	0.8 $\mu\text{m}$	5	62480
561470F532497	02-Feb-20	0.8 $\mu\text{m}$	0	46981

561471F532498	02-Feb-20	0.8 $\mu\text{m}$	5	41452
561479F532510	14-Oct-20	NET	integrated	53856

## C.2 *rbcL* Metabarcoding

Sample code	Date	Filter	Depth (m)	Raw reads
561480F532513	18-Apr-19	20 + 3 $\mu\text{m}$ fraction	0	38393
561481F532514	18-Apr-19	20 + 3 $\mu\text{m}$ fraction	5	36566
561482F532516	18-Apr-19	0.8 $\mu\text{m}$ fraction	5	45775
561483F532519	06-May-19	20 + 3 $\mu\text{m}$ fraction	0	50208
561494F532548	06-May-19	0.8 $\mu\text{m}$ fraction	0	45961
561484F532521	19-Jun-19	0.8 $\mu\text{m}$	0	225
561501F532522	19-Jun-19	0.8 $\mu\text{m}$	5	370
561502F532523	17-Jul-19	0.8 $\mu\text{m}$	0	39788
561503F532524	17-Jul-19	0.8 $\mu\text{m}$	5	43103
561504F532525	20-Aug-19	0.8 $\mu\text{m}$	0	50387
561505F532526	20-Aug-19	0.8 $\mu\text{m}$	5	53219
561506F532527	17-Sep-19	0.8 $\mu\text{m}$	0	51759
561485F532528	17-Sep-19	0.8 $\mu\text{m}$	5	45236
561486F532531	21-Nov-19	0.8 $\mu\text{m}$	0	36366
561487F532532	21-Nov-19	0.8 $\mu\text{m}$	5	42827
561488F532533	16-Dec-19	0.8 $\mu\text{m}$	0	50158
561489F532534	16-Dec-19	0.8 $\mu\text{m}$	5	67262
561490F532535	15-Jan-20	0.8 $\mu\text{m}$	0	67835
561491F532536	15-Jan-20	0.8 $\mu\text{m}$	5	59191
561492F532537	02-Feb-20	0.8 $\mu\text{m}$	0	50177
561493F532538	02-Feb-20	0.8 $\mu\text{m}$	5	43827
561495F532550	14-Oct-20	NET	integrated	38453

### C.3 *rbcL* Resequencing

Sample code	Date	Filter	Depth (m)	Raw reads
723820F710998	17-Sep-19	0.8 $\mu\text{m}$	0	100899
723821F710999	17-Sep-19	0.8 $\mu\text{m}$	5	105447
723822F711000	21-Nov-19	0.8 $\mu\text{m}$	0	135333
723823F711001	21-Nov-19	0.8 $\mu\text{m}$	5	141845
723824F711002	16-Dec-19	0.8 $\mu\text{m}$	0	27288
723825F711003	16-Dec-19	0.8 $\mu\text{m}$	5	183453
723826F711004	15-Jan-20	0.8 $\mu\text{m}$	0	186480
723827F711005	15-Jan-20	0.8 $\mu\text{m}$	5	181016
723828F711006	02-Feb-20	0.8 $\mu\text{m}$	0	164157
723829F711007	02-Feb-20	0.8 $\mu\text{m}$	5	143107
723830F711008	14-Oct-20	NET	integrated	188234



## References

- Accoroni, S., Giuliotti, S., Romagnoli, T., Siracusa, M., Bacchiocchi, S., & Totti, C. (2020). Morphological variability of *Pseudo-nitzschia pungens* clade i (Bacillariophyceae) in the northwestern adriatic sea. *Plants*, *9*(11), 1–20. <https://doi.org/10.3390/plants9111420>
- Ajani, P. A., Murray, S., Hallegraeff, G., Lundholm, N., Gillings, M., Brett, S., & Armand, L. (2013). The diatom genus *Pseudo-nitzschia* (Bacillariophyceae) in New South Wales, Australia: Morphotaxonomy, molecular phylogeny, toxicity, and distribution. *Journal of Phycology*, *49*(4), 765–785. <https://doi.org/10.1111/jpy.12087>
- Ajani, P. A., Verma, A., Kim, J. H., Woodcock, S., Nishimura, T., Farrell, H., Zammit, A., Brett, S., & Murray, S. A. (2021). Using qPCR and high-resolution sensor data to model a multi-species *Pseudo-nitzschia* (Bacillariophyceae) bloom in southeastern Australia. *Harmful Algae*, *108*(August), 102095. <https://doi.org/10.1016/j.hal.2021.102095>
- Alves-de-Souza, C., Varela, D., Contreras, C., de La Iglesia, P., Fernández, P., Hipp, B., Hernández, C., Riobó, P., Reguera, B., Franco, J. M., Diogène, J., García, C., & Lagos, N. (2014). Seasonal variability of *Dinophysis* spp. and *Protoceratium reticulatum* associated to lipophilic shellfish toxins in a strongly stratified Chilean fjord. *Deep-Sea Research Part II: Topical Studies in Oceanography*, *101*, 152–162. <https://doi.org/10.1016/j.dsr2.2013.01.014>
- Amato, A., Kooistra, W. H. C. F., Levialdi Ghiron, J. H., Mann, D. G., Pröschold, T., & Montresor, M. (2007). Reproductive Isolation among Sympatric Cryptic Species in Marine Diatoms. *Protist*, *158*(2), 193–207. <https://doi.org/10.1016/j.protis.2006.10.001>
- Amato, A., Lüdeking, A., & Kooistra, W. H. C. F. (2010). Intracellular domoic acid production in *Pseudo-nitzschia multistriata* isolated from the Gulf of Naples (Tyrrhenian Sea, Italy). *Toxicon*, *55*(1), 157–161. <https://doi.org/10.1016/j.toxicon.2009.07.005>
- Amato, A., & Montresor, M. (2008). Morphology, phylogeny, and sexual cycle of *Pseudo-nitzschia mannii* sp. nov. (Bacillariophyceae): a pseudo-cryptic species within the *P. pseudodelicatissima* complex. *Phycologia*, *47*(5), 487–497. <https://doi.org/10.2216/07-92.1>
- Anderson, D. M. (2009). Approaches to monitoring, control and management of harmful algal blooms (HABs). *Ocean and Coastal Management*, *52*(7), 342–347.

- <https://doi.org/10.1016/j.ocecoaman.2009.04.006>
- Anderson, D. M. (2014). HABs in a changing world: a perspective on harmful algal blooms, their impacts, and research and management in a dynamic era of climactic and environmental change. *Harmful Algae 2012: Proceedings of the 15th International Conference on Harmful Algae: October 29 - November 2, 2012, CECO, Changwon, Gyeongnam, Korea / Editors, Hak Gyoon Kim, Beatriz Reguera, Gustaaf M. Hallegraeff, Chang Kyu Lee, M., 2012, 3–17.* <http://www.ncbi.nlm.nih.gov/pmc/articles/PMC4667985/>
- Andree, K. B., Fernández-Tejedor, M., Elandaloussi, L. M., Quijano-Scheggia, S., Sampedro, N., Garcés, E., Camp, J., & Diogène, J. (2011). Quantitative PCR coupled with melt curve analysis for detection of selected *Pseudo-nitzschia* spp. (Bacillariophyceae) from the northwestern Mediterranean Sea. *Applied and Environmental Microbiology*, *77*(5), 1651–1659. <https://doi.org/10.1128/AEM.01978-10>
- Arapov, J., Skejić, S., Bužančić, M., Bakrač, A., Vidjak, O., Bojanić, N., Ujević, I., & Gladan, Ž. N. (2017). Taxonomical diversity of *Pseudo-nitzschia* from the Central Adriatic Sea. *Phycological Research*, *65*(4), 280–290. <https://doi.org/10.1111/pre.12184>
- Arapov, J., Ujevic, I., Pfannkuchen, D. M., Godrijan, J., Bakrac, A., Gladan, Z. N., & Marasovic, I. (2016). Domoic acid in phytoplankton net samples and shellfish from the krka river estuary in the central Adriatic Sea. *Mediterranean Marine Science*, *17*(2), 340–350. <https://doi.org/10.12681/mms.1471>
- Arapov, J., Ujević, I., Straka, M., Skejić, S., Bužančić, M., Bakrač, A., & Gladan, Ž. N. (2020). First evidence of domoic acid production in *Pseudo-nitzschia calliantha* cultures from the central Adriatic Sea. *Acta Adriatica*, *61*(2), 135–144.
- Armeli Minicante, S., Piredda, R., Finotto, S., Aubry, F. B., Acri, F., Pugnetti, A., & Zingone, A. (2020). Spatial diversity of planktonic protists in the lagoon of venice (LTER-Italy) based on 18s rDNA. *Advances in Oceanography and Limnology*, *11*(1), 35–44. <https://doi.org/10.4081/aiol.2020.8961>
- Arsenieff, L., Le Gall, F., Rigaut-Jalabert, F., Mahé, F., Sarno, D., Gouhier, L., Baudoux, A. C., & Simon, N. (2020). Diversity and dynamics of relevant nanoplanktonic diatoms in the Western English Channel. *ISME Journal*, *14*(8), 1966–1981. <https://doi.org/10.1038/s41396-020-0659-6>
- Bargu, S., Koray, T., & Lundholm, N. (2002). First Report of *Pseudo-nitzschia calliantha* Lundholm, Moestrup & Hasle 2003, a New Potentially Toxic Species from Turkish Coasts. *E.U. Journal of Fisheries & Aquatic Sciences*, *19*(3–4), 479–483.
- Barra, L., Ruggiero, M. V., Chen, J., & Kooistra, W. H. C. F. (2014). Specificity of LSU rRNA-targeted oligonucleotide probes for *Pseudo-nitzschia* species tested through dot-blot hybridisation. *Environmental Science and Pollution Research*, *21*(1), 548–557. <https://doi.org/10.1007/s11356-013-1953-x>
- Barra, L., Ruggiero, M. V., Sarno, D., Montresor, M., & Kooistra, W. H. C. F. (2013). Strengths and weaknesses of microarray approaches to detect *Pseudo-nitzschia* species in the field. *Environmental Science and Pollution Research*, *20*(10), 6705–6718. <https://doi.org/10.1007/s11356-012-1330-1>

- Basu, S., Patil, S., Mapleson, D., Russo, M. T., Vitale, L., Fevola, C., Maumus, F., Casotti, R., Mock, T., Caccamo, M., Montresor, M., Sanges, R., & Ferrante, M. I. (2017). Finding a partner in the ocean: molecular and evolutionary bases of the response to sexual cues in a planktonic diatom. *New Phytologist*, *215*(1), 140–156. <https://doi.org/10.1111/nph.14557>
- Bates, S. S. (1998). Ecophysiology and metabolism of ASP toxin production. *NATO ASI SERIES G ECOLOGICAL SCIENCES*, *41*, 405–426.
- Bates, S. S. (2000). Domoic-acid-producing diatoms: Another genus added! In *Journal of Phycology* (Vol. 36, Issue 6, pp. 978–983). John Wiley & Sons, Ltd. <https://doi.org/10.1046/j.1529-8817.2000.03661.x>
- Bates, S. S., Bird, C. J., de Freitas, A. S. W., Foxall, R., Gilgan, M., Hanic, L. A., Johnson, G. R., McCulloch, A. W., Odense, P., Pocklington, R., Sim, P. G., Smith, J. C., Subba Rao, D. V., Todd, E. C. D., Quilliam, M. A., Walter, J. A., & Wright, J. L. C. (1989). Pennate Diatom *Nitzschia pungens* as the Primary Source of Domoic Acid, a Toxin in Shellfish from Eastern Prince Edward Island, Canada. *Canadian Journal of Fisheries and Aquatic Sciences*, *46*(February 2017), 1203–1215. <https://doi.org/10.1139/f89-156>
- Bates, S. S., Hubbard, K. A., Lundholm, N., Montresor, M., & Leaw, C. P. (2018). *Pseudo-nitzschia*, *Nitzschia*, and domoic acid: New research since 2011. *Harmful Algae*, *79*, 1–41. <https://doi.org/10.1016/j.hal.2018.06.001>
- Bates, S. S., & Trainer, V. L. (2006). The Ecology of Harmful Diatoms. In *Ecology of Harmful Algae* (pp. 81–93). Springer Berlin Heidelberg. [https://doi.org/10.1007/978-3-540-32210-8\\_7](https://doi.org/10.1007/978-3-540-32210-8_7)
- Berger, W. H., & Parker, F. L. (1970). Diversity of planktonic foraminifera in deep-sea sediments. *Science*, *168*(3937), 1345–1347. <https://doi.org/10.1126/science.168.3937.1345>
- Berry, M. A., White, J. D., Davis, T. W., Jain, S., Johengen, T. H., Dick, G. J., Sarnelle, O., & Deneff, V. J. (2017). Are oligotypes meaningful ecological and phylogenetic units? A case study of *Microcystis* in Freshwater lakes. *Frontiers in Microbiology*, *8*(MAR), 365. <https://doi.org/10.3389/fmicb.2017.00365>
- Bickford, D., Lohman, D. J., Sodhi, N. S., Ng, P. K. L., Meier, R., Winker, K., Ingram, K. K., & Das, I. (2007). Cryptic species as a window on diversity and conservation. *Trends in Ecology and Evolution*, *22*(3), 148–155. <https://doi.org/10.1016/j.tree.2006.11.004>
- Blazewicz, S. J., Barnard, R. L., Daly, R. A., & Firestone, M. K. (2013). Evaluating rRNA as an indicator of microbial activity in environmental communities: Limitations and uses. *ISME Journal*, *7*(11), 2061–2068. <https://doi.org/10.1038/ismej.2013.102>
- Bowers, H. A., Marin, R., Birch, J. M., & Scholin, C. A. (2017). Sandwich hybridization probes for the detection of *Pseudo-nitzschia* (Bacillariophyceae) species: An update to existing probes and a description of new probes. *Harmful Algae*, *70*(November), 37–51. <https://doi.org/10.1016/j.hal.2017.10.005>
- Bowers, H. A., Ryan, J. P., Hayashi, K., Woods, A. L., Marin, R., Smith, G. J., Hubbard, K. A., Doucette, G. J., Mikulski, C. M., Gellene, A. G., Zhang, Y., Kudela, R. M., Caron, D. A., Birch, J. M., & Scholin, C. A. (2018). Diversity and toxicity of *Pseudo-*

- nitzschia* species in Monterey Bay: Perspectives from targeted and adaptive sampling. *Harmful Algae*, 78(January), 129–141. <https://doi.org/10.1016/j.hal.2018.08.006>
- Bradley, I. M., Pinto, A. J., & Guest, J. S. (2016). Gene-Specific Primers for Improved Characterization of Mixed Phototrophic Communities. *Applied and Environmental Microbiology*, 82(19), 5878–5891. <https://doi.org/10.1128/AEM.01630-16>. Editor
- Brunson, J. K., McKinnie, S. M. K., Chekan, J. R., McCrow, J. P., Miles, Z. D., Bertrand, E. M., Bielinski, V. A., Luhavaya, H., Obornik, M., Smith, G. J., Hutchins, D. A., Allen, A. E., & Moore, B. S. (2018). Biosynthesis of the neurotoxin domoic acid in a bloom-forming diatom. *Science*, 361(6409), 1356–1358. <https://doi.org/10.1126/science.aau0382>
- Burić, Z., Viličić, D., Mihalić, K. C., Carić, M., Kralj, K., & Ljubešić, N. (2008). *Pseudo-nitzschia* blooms in the Zrmanja river estuary (Eastern Adriatic Sea). *Diatom Research*, 23(1), 51–63. <https://doi.org/10.1080/0269249X.2008.9705736>
- Burki, F., Roger, A. J., Brown, M. W., & Simpson, A. G. B. (2020). *The New Tree of Eukaryotes*. <https://doi.org/10.1016/j.tree.2019.08.008>
- Cabrini, M., Fornasaro, D., Cossarini, G., Lipizer, M., & Virgilio, D. (2012). Phytoplankton temporal changes in a coastal northern Adriatic site during the last 25 years. *Estuarine, Coastal and Shelf Science*, 115, 113–124. <https://doi.org/10.1016/j.ecss.2012.07.007>
- Callahan, B. J., McMurdie, P. J., & Holmes, S. P. (2017). Exact sequence variants should replace operational taxonomic units in marker-gene data analysis. *The ISME Journal*, 11, 2639–2643. <https://doi.org/10.1038/ismej.2017.119>
- Callahan, B. J., McMurdie, P. J., Rosen, M. J., Han, A. W., Johnson, A. J. A., & Holmes, S. P. (2016). DADA2: High-resolution sample inference from Illumina amplicon data. *Nature Methods*, 13(7), 581–583. <https://doi.org/10.1038/nmeth.3869>
- Carlson, M. C. G., McCary, N. D., Leach, T. S., & Rocap, G. (2016). *Pseudo-nitzschia* challenged with co-occurring viral communities display diverse infection phenotypes. *Frontiers in Microbiology*, 7(APR), 1–11. <https://doi.org/10.3389/fmicb.2016.00527>
- Caroppo, C., Congestri, R., Bracchini, L., & Albertano, P. (2005). On the presence of *Pseudo-nitzschia calliantha* Lundholm, Moestrup et Hasle and *Pseudo-nitzschia delicatissima* (Cleve) Heiden in the Southern Adriatic Sea (Mediterranean Sea, Italy). *Journal of Plankton Research*, 27(8), 763–774. <https://doi.org/10.1093/plankt/fbi050>
- Casabianca, S., Penna, A., Pecchioli, E., Jordi, A., Basterretxea, G., & Vernesi, C. (2011). Population genetic structure and connectivity of the harmful dinoflagellate *Alexandrium minutum* in the Mediterranean Sea. *Proceedings of the Royal Society B: Biological Sciences*, 279(1726), 129–138. <https://doi.org/10.1098/rspb.2011.0708>
- Casteleyn, G., Adams, N. G., Vanormelingen, P., Debeer, A.-E., Sabbe, K., & Vyverman, W. (2009). Natural Hybrids in the Marine Diatom *Pseudo-nitzschia pungens* (Bacillariophyceae): Genetic and Morphological Evidence. *Protist*, 160(2), 343–354. <https://doi.org/10.1016/J.PROTIS.2008.11.002>
- Casteleyn, G., Leliaert, F., Backeljau, T., Debeer, A. E., Kotaki, Y., Rhodes, L., Lundholm, N., Sabbe, K., & Vyverman, W. (2010). Limits to gene flow in a cosmopolitan marine planktonic diatom. *Proceedings of the National Academy of Sciences of the United States of America*, 107(29), 12952–12957. <https://doi.org/10.1073/pnas.1001380107>

- Cerino, F., Bernardi Aubry, F., Coppola, J., La Ferla, R., Maimone, G., Socal, G., & Totti, C. (2012). Spatial and temporal variability of pico-, nano- and microphytoplankton in the offshore waters of the southern Adriatic Sea (Mediterranean Sea). *Continental Shelf Research*, *44*, 94–105. <https://doi.org/10.1016/j.csr.2011.06.006>
- Cerino, F., Fornasaro, D., Kralj, M., Giani, M., & Cabrini, M. (2019). Phytoplankton temporal dynamics in the coastal waters of the north-eastern Adriatic Sea (Mediterranean Sea) from 2010 to 2017. *Nature Conservation*, *34*, 343–372. <https://doi.org/10.3897/natureconservation.34.30720>
- Cerino, F., Orsini, L., Sarno, D., Dell’Aversano, C., Tartaglione, L., & Zingone, A. (2005). The alternation of different morphotypes in the seasonal cycle of the toxic diatom *Pseudo-nitzschia galaxiae*. *Harmful Algae*, *4*(1), 33–48. <https://doi.org/10.1016/j.hal.2003.10.005>
- Chekan, J. R., McKinnie, S. M. K., Noel, J. P., & Moore, B. S. (2020). Algal neurotoxin biosynthesis repurposes the terpene cyclase structural fold into an N-prenyltransferase. *Proceedings of the National Academy of Sciences of the United States of America*, *117*(23), 12799–12805. <https://doi.org/10.1073/pnas.2001325117>
- Ciminiello, P., Dell’Aversano, C., Fattorusso, E., Forino, M., Magno, G. S., Tartaglione, L., Quilliam, M. A., Tubaro, A., & Poletti, R. (2005). Hydrophilic interaction liquid chromatography/mass spectrometry for determination of domoic acid in Adriatic shellfish. *Rapid Communications in Mass Spectrometry*, *19*(14), 2030–2038. <https://doi.org/10.1002/rcm.2021>
- Ciminiello, P., Dell’aversano, C., Iacovo, E. Dello, Fattorusso, E., Forino, M., Tartaglione, L., Benedettini, G., Onorari, M., Serena, F., Battocchi, C., Casabianca, S., & Penna, A. (2014). *First Finding of Ostreopsis cf. ovata Toxins in Marine Aerosols*. <https://doi.org/10.1021/es405617d>
- Clayden, J., Read, B., & R. Hebditch, K. (2005). Chemistry of Domoic Acid, Isodomoic Acids, and Their Analogues. In *Cheminform* (Vol. 36). <https://doi.org/10.1002/chin.200536253>
- Cristescu, M. E. (2019). Can Environmental RNA Revolutionize Biodiversity Science? *Trends in Ecology and Evolution*, *34*(8), 694–697. <https://doi.org/10.1016/j.tree.2019.05.003>
- Commission Regulation (EC) No 2074/2005 of 5 December 2005 laying down implementing measures for certain products under Regulation (EC) No 853/2004 of the European Parliament and of the Council*, (2005). <https://eur-lex.europa.eu/LexUriServ/LexUriServ.do?uri=OJ:L:2005:338:0027:0059:EN:PDF>
- Croft, M. T., Warren, M. J., & Smith, A. G. (2006). Algae need their vitamins. In *Eukaryotic Cell* (Vol. 5, Issue 8, pp. 1175–1183). American Society for Microbiology (ASM). <https://doi.org/10.1128/EC.00097-06>
- D’Alelio, D., Amato, A., Kooistra, W. H. C. F., Procaccini, G., Casotti, R., & Montresor, M. (2009). Internal Transcribed Spacer Polymorphism in *Pseudo-nitzschia multistriata* (Bacillariophyceae) in the Gulf of Naples: Recent Divergence or Intraspecific Hybridization? *Protist*, *160*(1), 9–20. <https://doi.org/10.1016/j.protis.2008.07.001>
- D’Alelio, D., d’Alcalà, M. R., Dubroca, L., Diana Sarn, Zingone, A., & Montresor, M.

- (2010). The time for sex: A biennial life cycle in a marine planktonic diatom. *Limnology and Oceanography*, *55*(1), 106–114. <https://doi.org/10.4319/lo.2010.55.1.0106>
- D’Alelio, D., Hay Mele, B., Libralato, S., Ribera d’Alcalà, M., & Jordán, F. (2019). Rewiring and indirect effects underpin modularity reshuffling in a marine food web under environmental shifts. *Ecology and Evolution*, *ece3.5641*. <https://doi.org/10.1002/ece3.5641>
- D’Alelio, D., & Ruggiero, M. V. (2015). Interspecific plastidial recombination in the diatom genus *Pseudo-nitzschia*. *Journal of Phycology*, *51*(6), 1024–1028. <https://doi.org/10.1111/jpy.12350>
- De Vargas, C., Audic, S., Henry, N., Decelle, J., Mahe, F., Logares, R., Lara, E., Berney, C., Le Bescot, N., Probert, I., Carmichael, M., Poulain, J., Romac, S., Colin, S., Aury, J.-M., Bittner, L., Chaffron, S., Dunthorn, M., Engelen, S., ... Velayoudon, D. (2015). Eukaryotic plankton diversity in the sunlit ocean. *Science*, *348*(6237), 1261605–1261605. <https://doi.org/10.1126/science.1261605>
- DeGange, A. R., & Vacca, M. M. (1989). Sea Otter Mortality at Kodiak Island, Alaska, during Summer 1987. *Journal of Mammalogy*, *70*(4), 836–838. <https://doi.org/10.2307/1381723>
- Diercks, S., Medlin, L. K., & Metfies, K. (2008a). Colorimetric detection of the toxic dinoflagellate *Alexandrium minutum* using sandwich hybridization in a microtiter plate assay. *Harmful Algae*, *7*(2), 137–145. <https://doi.org/10.1016/j.hal.2007.06.005>
- Diercks, S., Metfies, K., & Medlin, L. K. (2008b). Molecular probe sets for the detection of toxic algae for use in sandwich hybridization formats. *Journal of Plankton Research*, *30*(4), 439–448. <https://doi.org/10.1093/plankt/fbn009>
- Dittami, S. M., & Edvardsen, B. (2012). Culture conditions influence cellular rna content in ichthyotoxic flagellates of the genus *Pseudochattonella* (Dictyochophyceae). *Journal of Phycology*, *48*(4), 1050–1055. <https://doi.org/10.1111/j.1529-8817.2012.01183.x>
- Downes-Tettmar, N., Rowland, S., Widdicombe, C., Woodward, M., & Llewellyn, C. (2013). Seasonal variation in *Pseudo-nitzschia* spp. and domoic acid in the Western English Channel. *Continental Shelf Research*, *53*, 40–49. <https://doi.org/10.1016/j.csr.2012.10.011>
- Edvardsen, B., Dittami, S. M., Groben, R., Brubak, S., Escalera, L., Rodríguez, F., Reguera, B., Chen, J., & Medlin, L. K. (2013). Molecular probes and microarrays for the detection of toxic algae in the genera *Dinophysis* and *Phalacrocoma* (Dinophyta). *Environmental Science and Pollution Research*, *20*(10), 6733–6750. <https://doi.org/10.1007/s11356-012-1403-1>
- Falkowski, P. G., Barber, R. T., & Smetacek, V. (1998). Biogeochemical controls and feedbacks on ocean primary production. *Science*, *281*(5374), 200–206. <https://doi.org/10.1126/science.281.5374.200>
- Falkowski, P. G., Katz, M. E., Knoll, A. H., Quigg, A., Raven, J. A., Schofield, O., & Taylor, F. J. R. (2004). The evolution of modern eukaryotic phytoplankton. *Science*, *305*(5682), 354–360. <https://doi.org/10.1126/science.1095964>
- Farrell, H., Gentien, P., Fernand, L., Lunven, M., Reguera, B., González-Gil, S., & Raine,

- R. (2012). Scales characterising a high density thin layer of *Dinophysis acuta* Ehrenberg and its transport within a coastal jet. *Harmful Algae*, *15*, 36–46. <https://doi.org/10.1016/j.hal.2011.11.003>
- Fehling, J., Davidson, K., Bolch, C., & Tett, P. (2006). Seasonality of *Pseudo-nitzschia* spp. (Bacillariophyceae) in western Scottish waters. *Marine Ecology Progress Series*, *323*, 91–105. <https://doi.org/10.3354/meps323091>
- Field, C. B., Behrenfeld, M. J., Randerson, J. T., & Falkowski, P. (1998). Primary production of the biosphere: Integrating terrestrial and oceanic components. *Science*, *281*(5374), 237–240. <https://doi.org/10.1126/science.281.5374.237>
- Fire, S. E., & Dolah, F. M. Van. (2012). Marine Biotoxins: Emergence of Harmful Algal Blooms as Health Threats to Marine Wildlife. In A. A. Aguirre, R. S. Ostfield, & P. Daszak (Eds.), *New Directions in Conservation Medicine: Applied Cases in Ecological Health* (pp. 374–383). Oxford University Press.
- Flewelling, L. J., Naar, J. P., Abbott, J. P., Baden, D. G., Barros, N. B., Bossart, G. D., Bottein, M. Y. D., Hammond, D. G., Haubold, E. M., Heil, C. A., Henry, M. S., Jacocks, H. M., Leighfield, T. A., Pierce, R. H., Pitchford, T. D., Rommel, S. A., Scott, P. S., Steidinger, K. A., Truby, E. W., ... Landsberg, J. H. (2005). Brevetoxicosis: Red tides and marine mammal mortalities. *Nature*, *435*(7043), 755–756. <https://doi.org/10.1038/nature435755a>
- Flynn, K. J., Raven, J. A., Rees, T. A. V., Finkel, Z., Quigg, A., & Beardall, J. (2010). Is the growth rate hypothesis applicable to microalgae? *Journal of Phycology*, *46*(1), 1–12. <https://doi.org/10.1111/j.1529-8817.2009.00756.x>
- Forster, D., Lentendu, G., Filker, S., Dubois, E., Wilding, T. A., & Stoeck, T. (2019). Improving eDNA-based protist diversity assessments using networks of amplicon sequence variants. *Environmental Microbiology*, *21*(11), 4109–4124. <https://doi.org/10.1111/1462-2920.14764>
- Francé, J., Varkitzi, I., Stanca, E., Cozzoli, F., Skejić, S., Ungaro, N., Vascotto, I., Mozetič, P., Ninčević Gladan, Ž., Assimakopoulou, G., Pavlidou, A., Zervoudaki, S., Pagou, K., & Basset, A. (2021). Large-scale testing of phytoplankton diversity indices for environmental assessment in Mediterranean sub-regions (Adriatic, Ionian and Aegean Seas). *Ecological Indicators*, *126*, 107630. <https://doi.org/10.1016/j.ecolind.2021.107630>
- Franchini, A., Malagoli, D., & Ottaviani, E. (2010). Targets and Effects of Yessotoxin, Okadaic Acid and Palytoxin: A Differential Review. *Marine Drugs*, *8*(3), 658–677. <https://doi.org/10.3390/md8030658>
- Franks, P. J. S., & Keafer, B. A. (2003). Sampling techniques and strategies for coastal phytoplankton blooms. *Manual on Harmful Marine Microalgae*, *2*, 51–76.
- Fu, F. X., Tatters, A. O., & Hutchins, D. A. (2012). Global change and the future of harmful algal blooms in the ocean. *Marine Ecology Progress Series*, *470*, 207–233. <https://doi.org/10.3354/meps10047>
- Funk, J. A., Janech, M. G., Dillon, J. C., Bissler, J. J., Siroky, B. J., Bell, P. D., & Johnson, R. H. (2014). Characterization of Renal Toxicity in Mice Administered the Marine Biotoxin Domoic Acid. *J Am Soc Nephrol*, *25*, 1187–1197. <https://doi.org/10.1681/ASN.2013080836>

- Gaudin, C., & De Young, C. (2007). Recreational Fisheries In The Mediterranean Countries: A Review Of Existing Legal Frameworks. <http://www.fao.org/3/a1500e/a1500e00.htm>
- Geraci, J. R. (1989). Humpback whales (*Megaptera novaeangliae*) fatally poisoned by dinoflagellate toxin. *Canadian Journal of Fisheries and Aquatic Sciences*, *46*(11), 1895–1898. <https://doi.org/10.1139/f89-238>
- Giulietti, S., Romagnoli, T., Siracusa, M., Bacchiocchi, S., Totti, C., & Accoroni, S. (2021). Integrative taxonomy of the *Pseudo-nitzschia* (Bacillariophyceae) populations in the NW Adriatic Sea, with a focus on a novel cryptic species in the *P. delicatissima* species complex. *Phycologia*, *00*(00), 1–18. <https://doi.org/10.1080/00318884.2021.1899733>
- Gleason, F. H., Jephcott, T. G., Küpper, F. C., Gerphagnon, M., Sime-Ngando, T., Karpov, S. A., Guillou, L., & van Ogtrop, F. F. (2015). Potential roles for recently discovered chytrid parasites in the dynamics of harmful algal blooms. *Fungal Biology Reviews*, *29*(1), 20–33. <https://doi.org/10.1016/j.fbr.2015.03.002>
- Glibert, P. M. (2020). Harmful algae at the complex nexus of eutrophication and climate change. *Harmful Algae*. <https://doi.org/10.1016/j.hal.2019.03.001>
- Glibert, P. M., Berdalet, E., Burford, M. A., Pitcher, G. C., & Zhou, M. (2018). *Introduction to the Global Ecology and Oceanography of Harmful Algal Blooms (GEOHAB) Synthesis* (pp. 3–7). [https://doi.org/10.1007/978-3-319-70069-4\\_1](https://doi.org/10.1007/978-3-319-70069-4_1)
- Glibert, P. M., & Burford, M. (2017). Globally Changing Nutrient Loads and Harmful Algal Blooms: Recent Advances, New Paradigms, and Continuing Challenges. *Oceanography*, *30*(1), 58–69. <https://doi.org/10.5670/oceanog.2017.110>
- Glibert, P. M., & Burkholder, J. A. M. (2011). Harmful algal blooms and eutrophication: “strategies” for nutrient uptake and growth outside the Redfield comfort zone. *Chinese Journal of Oceanology and Limnology*, *29*(4), 724–738. <https://doi.org/10.1007/s00343-011-0502-z>
- Glibert, P. M., & Burkholder, J. M. (2006). The Complex Relationships Between Increases in Fertilization of the Earth, Coastal Eutrophication and Proliferation of Harmful Algal Blooms. In *Ecology of Harmful Algae* (pp. 341–354). Springer Berlin Heidelberg. [https://doi.org/10.1007/978-3-540-32210-8\\_26](https://doi.org/10.1007/978-3-540-32210-8_26)
- Godhe, A., Asplund, M. E., Härnström, K., Saravanan, V., Tyagi, A., & Karunasagar, I. (2008). Quantification of diatom and dinoflagellate biomasses in coastal marine seawater samples by real-time PCR. *Applied and Environmental Microbiology*, *74*(23), 7174–7182. <https://doi.org/10.1128/AEM.01298-08>
- Godhe, A., & Härnström, K. (2010). Linking the planktonic and benthic habitat: Genetic structure of the marine diatom *Skeletonema marinoi*. *Molecular Ecology*, *19*(20), 4478–4490. <https://doi.org/10.1111/j.1365-294X.2010.04841.x>
- Granéli, E., & Hansen, P. J. (2006). Allelopathy in Harmful Algae: A Mechanism to Compete for Resources? In *Ecology of Harmful Algae* (pp. 189–201). Springer Berlin Heidelberg. [https://doi.org/10.1007/978-3-540-32210-8\\_15](https://doi.org/10.1007/978-3-540-32210-8_15)
- Greenfield, D. I., Marin, R., Jensen, S., Massion, E., Roman, B., Feldman, J., & Scholin, C. a. (2006). Application of Environmental Sample Processor (ESP) methodology for quantifying *Pseudo-nitzschia australis* using ribosomal RNA-targeted probes in

- sandwich and fluorescent in situ hybridization formats. *Limnology and Oceanography: Methods*, 4, 426–435. <https://doi.org/10.4319/lom.2006.4.426>
- Griffith, A. W., & Gobler, C. J. (2020). Harmful algal blooms: A climate change co-stressor in marine and freshwater ecosystems. In *Harmful Algae*. <https://doi.org/10.1016/j.hal.2019.03.008>
- Guéret, S. M., & Brimble, M. A. (2010). Spiroimine shellfish poisoning (SSP) and the spirolide family of shellfish toxins: Isolation, structure, biological activity and synthesis. In *Natural Product Reports* (Vol. 27, Issue 9, pp. 1350–1366). The Royal Society of Chemistry. <https://doi.org/10.1039/c005400n>
- Guillard, R. R., & Ryther, J. H. (1962). Studies of marine planktonic diatoms. I. *Cyclotella nana* Hustedt, and *Detonula confervacea* (Cleve) Gran. *Canadian Journal of Microbiology*, 8, 229–239. <https://doi.org/10.1139/m62-029>
- Guillou, L., Bachar, D., Audic, S., Bass, D., Berney, C., Bittner, L., Boutte, C., Burgaud, G., De Vargas, C., Decelle, J., Del Campo, J., Dolan, J. R., Dunthorn, M., Edvardsen, B., Holzmann, M., Kooistra, W. H. C. F., Lara, E., Le Bescot, N., Logares, R., ... Christen, R. (2013). The Protist Ribosomal Reference database (PR2): A catalog of unicellular eukaryote Small Sub-Unit rRNA sequences with curated taxonomy. *Nucleic Acids Research*, 41(D1), 597–604. <https://doi.org/10.1093/nar/gks1160>
- Guiry, M. D. (2012). How many species of algae are there? *Journal of Phycology*, 48(5), 1057–1063. <https://doi.org/10.1111/j.1529-8817.2012.01222.x>
- Guo, L., Sui, Z., & Liu, Y. (2016). Quantitative analysis of dinoflagellates and diatoms community via Miseq sequencing of actin gene and v9 region of 18S rDNA. *Scientific Reports*, 6(1), 1–9. <https://doi.org/10.1038/srep34709>
- HAEDAT. (2021). *Harmful Algae Event Database*. <http://haedat.iode.org/eventSearch.php?searchtext%5BcountryID%5D=58>
- Hallegraeff, G. M. (1998). *Transport of toxic dinoflagellates via ships' ballast water: bioeconomic risk assessment and efficacy of possible ballast water management strategies*. 168, 297–309. <http://www.int-res.com/articles/meps/168/m168p297.pdf>
- Hallegraeff, G. M., Anderson, D. M., Belin, C., Bottein, M.-Y. D., Bresnan, E., Chinain, M., Enevoldsen, H., Iwataki, M., Karlson, B., McKenzie, C. H., Sunesen, I., Pitcher, G. C., Provoost, P., Richardson, A., Schweibold, L., Tester, P. A., Trainer, V. L., Yñiguez, A. T., & Zingone, A. (2021). Perceived global increase in algal blooms is attributable to intensified monitoring and emerging bloom impacts. *Communications Earth & Environment*, 2(1), 117. <https://doi.org/10.1038/s43247-021-00178-8>
- Hallegraeff, G. M., Anderson, D. M., Cembella, A. D., & Enevoldsen, H. O. (2003). *Manual on harmful marine microalgae*. Unesco.
- Hanic, L. A., Sekimoto, S., & Bates, S. S. (2009). Oomycete and chytrid infections of the marine diatom *Pseudo-nitzschia pungens* (Bacillariophyceae) from Prince Edward Island. *Botany*, 87(11), 1096–1105. <https://doi.org/10.1139/B09-070>
- Haroardóttir, S., Wohlrab, S., Hjort, D. M., Krock, B., Nielsen, T. G., John, U., & Lundholm, N. (2019). Transcriptomic responses to grazing reveal the metabolic pathway leading to the biosynthesis of domoic acid and highlight different defense strategies in diatoms. *BMC Molecular Biology*, 20(1), 1–14. <https://doi.org/10.1186/s12867-019-0124-0>

- Hasegawa, M., Kishino, H., & Yano, T. (1985). Dating of the human-ape splitting by a molecular clock of mitochondrial DNA. *Journal of Molecular Evolution*, *22*(2), 160–174. <http://www.ncbi.nlm.nih.gov/pubmed/3934395>
- Hasle, G. R., & Fryxell, G. A. (1970). Diatoms: Cleaning and Mounting for Light and Electron Microscopy. *Transactions of the American Microscopical Society*, *89*(4), 469. <https://doi.org/10.2307/3224555>
- Hernández, M., Robinson, I., Aguilar, A., González, L. M., López-Jurado, L. F., Reyero, M. I., Cacho, E., Franco, J., López-Rodas, V., & Costas, E. (1998). Did algal toxins cause monk seal mortality? In *Nature* (Vol. 393, Issue 6680, pp. 28–29). CRC. <https://doi.org/10.1038/29906>
- Hoagland, P., Kirkpatrick, B., Jin, D., Kirkpatrick, G., Fleming, L. E., Ullmann, S. G., Beet, A., Hitchcock, G., Harrison, K. K., Li, Z. C., Garrison, B., Diaz, R. E., & Lovko, V. (2020). Lessening the Hazards of Florida Red Tides: A Common Sense Approach. *Frontiers in Marine Science*, *7*, 538. <https://doi.org/10.3389/fmars.2020.00538>
- Hoagland, P., & Scatasta, S. (2006). The Economic Effects of Harmful Algal Blooms. In *Ecology of Harmful Algae* (pp. 391–402). Springer Berlin Heidelberg. [https://doi.org/10.1007/978-3-540-32210-8\\_30](https://doi.org/10.1007/978-3-540-32210-8_30)
- Honsell, G., Dell'Aversano, C., Vuerich, F., Sosa, S., Tartaglione, L., & Tubaro, A. (2008). *Pseudo-nitzschia* and ASP in the northern Adriatic Sea. In Ø. Moestrup, G. J. Doucette, A. Godhe, & G. M. Hallegraeff (Eds.), *Proceedings of the 12th International Conference On Harmful Algae* (pp. 193–195). International Society for the Study of Harmful Algae and Intergovernmental Oceanographic Commission of UNESCO,.
- Hu, S. K., Campbell, V., Connell, P., Gellene, A. G., Liu, Z., Terrado, R., & Caron, D. A. (2016). Protistan diversity and activity inferred from RNA and DNA at a coastal ocean site in the eastern North Pacific. *FEMS Microbiology Ecology*, *92*(4), fiw050. <https://doi.org/10.1093/femsec/fiw050>
- Hutchins, D. A., & Bruland, K. W. (1998). Iron-limited diatom growth and Si:N uptake ratios in a coastal upwelling regime. *Nature*, *393*, 561. <http://dx.doi.org/10.1038/31203>
- Hutchinson, G. E. (1961). The Paradox of the Plankton. *The American Naturalist*, *95*(882), 137–145. <https://doi.org/10.1086/282171>
- Jessup, D. A., Miller, M. A., Ryan, J. P., Nevins, H. M., Kerkering, H. A., Mekebri, A., Crane, D. B., Johnson, T. A., & Kudela, R. M. (2009). Mass stranding of marine birds caused by a surfactant-producing red tide. *PLoS ONE*, *4*(2). <https://doi.org/10.1371/journal.pone.0004550>
- John, U., Litaker, R. W., Montresor, M., Murray, S., Brosnahan, M. L., & Anderson, D. M. (2014). Formal revision of the *Alexandrium tamarense* species complex (Dinophyceae) taxonomy: The introduction of five species with emphasis on molecular-based (rDNA) classification. *Protist*, *165*(6), 779–804. <https://doi.org/10.1016/j.protis.2014.10.001>
- Johnson, S., Harrison, K., & Turner, A. D. (2016). Application of rapid test kits for the determination of Amnesic Shellfish Poisoning in bivalve molluscs from Great Britain. *Toxicon*, *117*, 76–83. <https://doi.org/10.1016/j.toxicon.2016.03.017>
- Jones, H. M., Simpson, G. E., Stickle, A. J., & Mann, D. G. (2005). Life history and

- systematics of *Petronis* (Bacillariophyta), with special reference to British waters. *European Journal of Phycology*, 40(1), 61–87. <https://doi.org/10.1080/09670260400024675>
- Jørgensen, K., & Andersen, P. (2007). Relation between the concentration of *Dinophysis acuminata* and diarrhetic shellfish poisoning toxins in blue mussels (*Mytilus edulis*) during a toxic episode in the Limfjord (Denmark), 2006. *Journal of Shellfish Research*, 26(4), 1081–1087. [https://doi.org/10.2983/0730-8000\(2007\)26\[1081:RBTCOD\]2.0.CO;2](https://doi.org/10.2983/0730-8000(2007)26[1081:RBTCOD]2.0.CO;2)
- Jukes, T. H., & Cantor, C. R. (1969). Evolution of Protein Molecules. In *Mammalian Protein Metabolism* (pp. 21–132). Elsevier. <https://doi.org/10.1016/B978-1-4832-3211-9.50009-7>
- Kegel, J. U., Amo, Y. Del, Costes, L., & Medlin, L. K. (2011). *Testing a Microarray to Detect and Monitor Toxic Microalgae in Arcachon Bay in France. 2*, 1–23. <https://doi.org/10.3390/microarrays2010001>
- Kelley, L. A., Mezulis, S., Yates, C. M., Wass, M. N., & Sternberg, M. J. E. (2015). The Phyre2 web portal for protein modeling, prediction and analysis. *Nature Protocols*, 10(6), 845–858. <https://doi.org/10.1038/nprot.2015.053>
- Kelly, R. P., Shelton, A. O., & Gallego, R. (2019). Understanding PCR Processes to Draw Meaningful Conclusions from Environmental DNA Studies. *Scientific Reports*, 9(1), 1–14. <https://doi.org/10.1038/s41598-019-48546-x>
- Kim, J. H., Park, B. S., Kim, J. H., Wang, P., & Han, M. S. (2015). Intraspecific diversity and distribution of the cosmopolitan species *Pseudo-nitzschia pungens* (Bacillariophyceae): Morphology, genetics, and ecophysiology of the three clades. *Journal of Phycology*, 51(1), 159–172. <https://doi.org/10.1111/jpy.12263>
- Kodama, M., Doucette, G. J., & Green, D. H. (2006). Relationships Between Bacteria and Harmful Algae. In *Ecology of Harmful Algae* (pp. 243–255). Springer Berlin Heidelberg. [https://doi.org/10.1007/978-3-540-32210-8\\_19](https://doi.org/10.1007/978-3-540-32210-8_19)
- Leblanc, K., Quéguiner, B., Diaz, F., Cornet, V., Michel-Rodriguez, M., Durrieu De Madron, X., Bowler, C., Malviya, S., Thyssen, M., Grégori, G., Rembauville, M., Grosso, O., Poulain, J., De Vargas, C., Pujo-Pay, M., & Conan, P. (2018). Nanoplanktonic diatoms are globally overlooked but play a role in spring blooms and carbon export. *Nature Communications*, 9(1). <https://doi.org/10.1038/s41467-018-03376-9>
- Lefebvre, K. A., Kendrick, P. S., Ladiges, W., Hiolski, E. M., Ferriss, B. E., Smith, D. R., & Marcinek, D. J. (2017). Chronic low-level exposure to the common seafood toxin domoic acid causes cognitive deficits in mice. *Harmful Algae*, 64, 20–29. <https://doi.org/10.1016/j.hal.2017.03.003>
- Legrand, C., Rengefors, K., Fistarol, G. O., & Granéli, E. (2003). Allelopathy in phytoplankton - Biochemical, ecological and evolutionary aspects. *Phycologia*, 42(4), 406–419. <https://doi.org/10.2216/i0031-8884-42-4-406.1>
- Lelong, A., Hégaret, H., Soudant, P., & Bates, S. S. (2012). *Pseudo-nitzschia* (Bacillariophyceae) species, domoic acid and amnesic shellfish poisoning: revisiting previous paradigms. *Phycologia*, 51(2), 168–216. <https://doi.org/10.2216/11-37.1>
- Lema, K. A., Metegnier, G., Quéré, J., Latimier, M., Youenou, A., Lambert, C., Fauchot,

- J., Le Gac, M., & Costantini, M. (2019). Inter- and Intra-Specific Transcriptional and Phenotypic Responses of *Pseudo-nitzschia* under Different Nutrient Conditions. *Genome Biology and Evolution*, *11*(3), 731–747. <https://doi.org/10.1093/gbe/evz030>
- Leonilde, R., Elena, L., Elena, S., Francesco, C., & Alberto, B. (2017). Individual trait variation in phytoplankton communities across multiple spatial scales. *Journal of Plankton Research*, *39*(3), 577–588. <https://doi.org/10.1093/plankt/fbx001>
- Lim, H. C., Tan, S. N., Teng, S. T., Lundholm, N., Orive, E., David, H., Quijano-Scheggia, S., Leong, S. C. Y., Wolf, M., Bates, S. S., Lim, P. T., & Leaw, C. P. (2018). Phylogeny and species delineation in the marine diatom *Pseudo-nitzschia* (Bacillariophyta) using *cox1*, LSU, and ITS2 rRNA genes: A perspective in character evolution. *Journal of Phycology*, *54*(2), 234–248. <https://doi.org/10.1111/jpy.12620>
- Litchman, E., de Tezanos Pinto, P., Klausmeier, C. A., Thomas, M. K., & Yoshiyama, K. (2010). Linking traits to species diversity and community structure in phytoplankton. *Hydrobiologia*, *653*(1), 15–28. <https://doi.org/10.1007/s10750-010-0341-5>
- Ljubešić, Z., Bosak, S., Viličić, D., Borojević, K. K., Marić, D., Godrijan, J., Ujević, I., Peharec, P., & Dakovac, T. (2011). Ecology and taxonomy of potentially toxic *Pseudo-nitzschia* species in Lim Bay (north-eastern Adriatic Sea). *Harmful Algae*, *10*(6), 713–722. <https://doi.org/10.1016/j.hal.2011.06.002>
- Lundholm, N., Hasle, G. R., Fryxell, G. A., & Hargraves, P. E. (2002). Morphology, phylogeny and taxonomy of species within the *Pseudo-nitzschia americana* complex (Bacillariophyceae) with descriptions of two new species, *Pseudo-nitzschia brasiliiana* and *Pseudo-nitzschia linea*. *Phycologia*, *41*(5), 480–497. <https://doi.org/10.2216/i0031-8884-41-5-480.1>
- Lundholm, N., Krock, B., John, U., Skov, J., Cheng, J., Pančić, M., Wohlrab, S., Rigby, K., Nielsen, T. G., Selander, E., & Harðardóttir, S. (2018). Induction of domoic acid production in diatoms—Types of grazers and diatoms are important. *Harmful Algae*, *79*(July), 64–73. <https://doi.org/10.1016/j.hal.2018.06.005>
- Lundholm, N., Moestrup, Ø., Hasle, G. R., & Hoef-Emden, K. (2003). A study of the *Pseudo-nitzschia pseudodelicatissima/cuspidata* complex (Bacillariophyceae): What is *P. pseudodelicatissima*? *Journal of Phycology*, *39*(4), 797–813. <https://doi.org/10.1046/j.1529-8817.2003.02031.x>
- Lundholm, N., Moestrup, Ø., Kotaki, Y., Hoef-Emden, K., Scholin, C. A., & Miller, P. (2006). Inter- and intraspecific variation of the *Pseudo-nitzschia delicatissima* complex (Bacillariophyceae) illustrated by rRNA probes, morphological data and phylogenetic analyses. *Journal of Phycology*, *42*(2), 464–481. <https://doi.org/10.1111/j.1529-8817.2006.00211.x>
- Luo, Z., Yang, W., Leaw, C. P., Pospelova, V., Bilien, G., Liow, G. R., Lim, P. T., & Gu, H. (2017). Cryptic diversity within the harmful dinoflagellate *Akashiwo sanguinea* in coastal Chinese waters is related to differentiated ecological niches. *Harmful Algae*, *66*, 88–96. <https://doi.org/10.1016/J.HAL.2017.05.008>
- MacGillivray, M. L., & Kaczmarska, I. (2011). Survey of the efficacy of a short fragment of the *rbcL* gene as a supplemental DNA barcode for diatoms. *Journal of Eukaryotic Microbiology*, *58*(6), 529–536. <https://doi.org/10.1111/j.1550-7408.2011.00585.x>
- Maldonado, M. T., Hughes, M. P., Rue, E. L., & Wells, M. L. (2002). The effect of Fe and

- Cu on growth and domoic acid production by *Pseudo-nitzschia multiseriis* and *Pseudo-nitzschia australis*. *Limnology and Oceanography*, 47(2), 515–526. <https://doi.org/10.4319/lo.2002.47.2.0515>
- Malviya, S., Scalco, E., Audic, S., Vincent, F., Veluchamy, A., Poulain, J., Wincker, P., Iudicone, D., De Vargas, C., Bittner, L., Zingone, A., & Bowler, C. (2016). Insights into global diatom distribution and diversity in the world's ocean. *Proceedings of the National Academy of Sciences of the United States of America*, 113(11), E1516–E1525. <https://doi.org/10.1073/pnas.1509523113>
- Marchetti, A., Parker, M. S., Moccia, L. P., Lin, E. O., Arrieta, A. L., Ribalet, F., Murphy, M. E. P., Maldonado, M. T., & Armbrust, E. V. (2009). Ferritin is used for iron storage in bloom-forming marine pennate diatoms. *Nature*, 457(7228), 467–470. <https://doi.org/10.1038/nature07539>
- Marić, D., Ljubešić, Z., Godrijan, J., Viličić, D., Ujević, I., & Precali, R. (2011). Blooms of the potentially toxic diatom *Pseudo-nitzschia calliantha* Lundholm, Moestrup & Hasle in coastal waters of the northern Adriatic Sea (Croatia). *Estuarine, Coastal and Shelf Science*, 92(3), 323–331. <https://doi.org/10.1016/j.ecss.2011.01.002>
- Marić Pfannkuchen, D., Godrijan, J., Smodlaka Tanković, M., Baričević, A., Kužat, N., Djakovac, T., Pustijanac, E., Jahn, R., & Pfannkuchen, M. (2018). The Ecology of One Cosmopolitan, One Newly Introduced and One Occasionally Advected Species from the Genus *Skeletonema* in a Highly Structured Ecosystem, the Northern Adriatic. *Microbial Ecology*, 75(3), 674–687. <https://doi.org/10.1007/s00248-017-1069-9>
- Massa, F., Onofri, L., & Fezzardi, D. (2017). Aquaculture in the Mediterranean and the Black Sea: A Blue Growth perspective. *Handbook on the Economics and Management of Sustainable Oceans, March*, 93–123. <https://doi.org/10.4337/9781786430724.00013>
- Massana, R., Del Campo, J., Sieracki, M. E., Audic, S., & Logares, R. (2014). Exploring the uncultured microeukaryote majority in the oceans: Reevaluation of ribogroups within stramenopiles. *ISME Journal*, 8(4), 854–866. <https://doi.org/10.1038/ismej.2013.204>
- McCabe, R. M., Hickey, B. M., Kudela, R. M., Lefebvre, K. A., Adams, N. G., Bill, B. D., Gulland, F. M. D., Thomson, R. E., Cochlan, W. P., & Trainer, V. L. (2016). An unprecedented coastwide toxic algal bloom linked to anomalous ocean conditions. *Geophysical Research Letters*, 43(19), 10,366–10,376. <https://doi.org/10.1002/2016GL070023>
- McMurdie, P. J., & Holmes, S. (2013). phyloseq: An R Package for Reproducible Interactive Analysis and Graphics of Microbiome Census Data. *PLoS ONE*, 8(4), e61217. <https://doi.org/10.1371/journal.pone.0061217>
- Medlin, L. K., & Kegel, J. U. (2014). Validation of the detection of *Pseudo-nitzschia* spp. using specific RNA probes tested in a microarray format: Calibration of signal based on variability of RNA content with environmental conditions. *Harmful Algae*, 37(1), 183–193. <https://doi.org/10.1016/j.hal.2014.05.016>
- Medlin, L. K., & Orozco, J. (2017). Molecular techniques for the detection of organisms in aquatic environments, with emphasis on harmful algal bloom species. *Sensors (Switzerland)*, 17(5). <https://doi.org/10.3390/s17051184>

- Mercado, J. M., Ramírez, T., Cortés, D., Sebastián, M., & Vargas-Yáñez, M. (2005). Seasonal and inter-annual variability of the phytoplankton communities in an upwelling area of the Alborán Sea (SW Mediterranean Sea). *Scientia Marina*, *69*(4), 451–465. <https://doi.org/10.3989/scimar.2005.69n4451>
- Mitra, A., Flynn, K. J., Burkholder, J. M., Berge, T., Calbet, A., Raven, J. A., Granéli, E., Glibert, P. M., Hansen, P. J., Stoecker, D. K., Thingstad, F., Tillmann, U., Våge, S., Wilken, S., & Zubkov, M. V. (2014). The role of mixotrophic protists in the biological carbon pump. *Biogeosciences*, *11*(4), 995–1005. <https://doi.org/10.5194/bg-11-995-2014>
- Mitra, A., Flynn, K. J., Tillmann, U., Raven, J. A., Caron, D., Stoecker, D. K., Not, F., Hansen, P. J., Hallegraeff, G., Sanders, R., Wilken, S., McManus, G., Johnson, M., Pitta, P., Våge, S., Berge, T., Calbet, A., Thingstad, F., Jeong, H. J., ... Lundgren, V. (2016). Defining Planktonic Protist Functional Groups on Mechanisms for Energy and Nutrient Acquisition: Incorporation of Diverse Mixotrophic Strategies. *Protist*, *167*(2), 106–120. <https://doi.org/10.1016/j.protis.2016.01.003>
- Moore, J. K., Doney, S. C., Glover, D. M., & Fung, I. Y. (2002). Iron cycling and nutrient-limitation patterns in surface waters of the world ocean. *Deep-Sea Research Part II: Topical Studies in Oceanography*, *49*(1–3), 463–507. [https://doi.org/10.1016/S0967-0645\(01\)00109-6](https://doi.org/10.1016/S0967-0645(01)00109-6)
- Moore, S. K., Dreyer, S. J., Ekstrom, J. A., Moore, K., Norman, K., Klinger, T., Allison, E. H., & Jardine, S. L. (2020). Harmful algal blooms and coastal communities: Socioeconomic impacts and actions taken to cope with the 2015 U.S. West Coast domoic acid event. *Harmful Algae*, *96*, 101799. <https://doi.org/https://doi.org/10.1016/j.hal.2020.101799>
- Moriarty, M. E., Tinker, M. T., Miller, M. A., Tomoleoni, J. A., Staedler, M. M., Fujii, J. A., Batac, F. I., Dodd, E. M., Kudela, R. M., Zubkousky-White, V., & Johnson, C. K. (2021). Exposure to domoic acid is an ecological driver of cardiac disease in southern sea otters. *Harmful Algae*, *101*, 101973. <https://doi.org/10.1016/j.hal.2020.101973>
- Moschandreou, K. K., Baxevanis, A. D., Katikou, P., Papaefthimiou, D., Nikolaidis, G., & Abatzopoulos, T. J. (2012). Inter- and intra-specific diversity of *Pseudo-nitzschia* (Bacillariophyceae) in the northeastern Mediterranean. *European Journal of Phycology*, *47*(3), 321–339. <https://doi.org/10.1080/09670262.2012.713998>
- Moschandreou, K. K., & Nikolaidis, G. (2010). The genus *Pseudo-nitzschia* (Bacillariophyceae) in Greek coastal waters. *Botanica Marina*, *53*(2), 159–172. <https://doi.org/10.1515/BOT.2010.014>
- Mozetič, P., Cangini, M., Francé, J., Bastianini, M., Bernardi Aubry, F., Bužančić, M., Cabrini, M., Cerino, F., Čalić, M., D'Adamo, R., Drakulović, D., Finotto, S., Fornasaro, D., Grilli, F., Kraus, R., Kužat, N., Marić Pfannkuchen, D., Ninčević Gladan, Ž., Pompei, M., ... Skejić, S. (2019). Phytoplankton diversity in Adriatic ports: Lessons from the port baseline survey for the management of harmful algal species. *Marine Pollution Bulletin*, *October*. <https://doi.org/10.1016/j.marpolbul.2017.12.029>
- Mozetič, P., Francé, J., Kogovšek, T. Š., Talaber, I., & Malej, A. (2012). Plankton trends

- and community changes in a coastal sea (northern Adriatic): Bottom-up vs. top-down control in relation to environmental drivers. *Estuarine, Coastal and Shelf Science*, *115*, 138–148. <https://doi.org/10.1016/j.ecss.2012.02.009>
- Mozetič, P., Solidoro, C., Cossarini, G., Socal, G., Precali, R., Francé, J., Bianchi, F., De Vittor, C., Smolaka, N., & Fonda Umani, S. (2010). Recent trends towards oligotrophication of the northern adriatic: Evidence from chlorophyll a time series. *Estuaries and Coasts*, *33*(2), 362–375. <https://doi.org/10.1007/s12237-009-9191-7>
- Mysara, M., Vandamme, P., Props, R., Kerckhof, F. M., Leys, N., Boon, N., Raes, J., & Monsieurs, P. (2017). Reconciliation between operational taxonomic units and species boundaries. *FEMS Microbiology Ecology*, *93*(4). <https://doi.org/10.1093/femsec/fix029>
- Nearing, J. T., Douglas, G. M., Comeau, A. M., & Langille, M. G. I. (2018). Denoising the Denoisers: An independent evaluation of microbiome sequence error- correction approaches. *PeerJ*, *2018*(8), e5364. <https://doi.org/10.7717/peerj.5364>
- Neuendorf, J. (2020). Cell Counting in the Fuchs-Rosenthal Counting Chamber. In *Urine Sediment* (pp. 49–52). Springer International Publishing. [https://doi.org/10.1007/978-3-030-15911-5\\_9](https://doi.org/10.1007/978-3-030-15911-5_9)
- NMFS. (2016). *The Fisheries of the United States, 2015*. <https://www.st.nmfs.noaa.gov/Assets/commercial/fus/fus15/documents/FUS2015.pdf>
- Nunn, G. B., Theisen, B. F., Christensen, B., & Arctander, P. (1996). Simplicity-correlated size growth of the nuclear 28S ribosomal RNA D3 expansion segment in the crustacean order isopoda. *Journal of Molecular Evolution*, *42*(2), 211–223. <https://doi.org/10.1007/BF02198847>
- Olenina, I. (2006). *Biovolumes and size-classes of phytoplankton in the Baltic Sea*. HELCOM Balt.Sea Environ. Proc. No. 106, 144pp.
- Orive, E., Pérez-Aicua, L., David, H., García-Etxebarria, K., Laza-Martínez, A., Seoane, S., & Miguel, I. (2013). The genus *Pseudo-nitzschia* (Bacillariophyceae) in a temperate estuary with description of two new species: *Pseudo-nitzschia plurisecta* sp. nov. and *Pseudo-nitzschia abrensis* sp. nov. *Journal of Phycology*, *49*(6), 1192–1206. <https://doi.org/10.1111/jpy.12130>
- Orozco, J., Villa, E., Manes, C. L., Medlin, L. K., & Guillebault, D. (2016). Electrochemical RNA genosensors for toxic algal species: enhancing selectivity and sensitivity. *Talanta*, *161*, 560–566. <https://doi.org/10.1016/j.talanta.2016.08.073>
- Orsini, L., Procaccini, G., Sarno, D., & Montresor, M. (2004). Multiple rDNA ITS-types within the diatom *Pseudo-nitzschia delicatissima* (Bacillariophyceae) and their relative abundances across a spring bloom in the Gulf of Naples. *Marine Ecology Progress Series*, *271*(May), 87–98. <https://doi.org/10.3354/meps271087>
- Orsini, L., Sarno, D., Procaccini, G., Poletti, R., Dahlmann, J., & Montresor, M. (2002). Toxic *Pseudo-nitzschia multistriata* (Bacillariophyceae) from the Gulf of Naples: morphology, toxin analysis and phylogenetic relationships with other *Pseudo-nitzschia* species. *European Journal of Phycology*, *37*(02), 247–257. <https://doi.org/10.1017/S0967026202003608>
- Paradis, E., & Schliep, K. (2019). ape 5.0: an environment for modern phylogenetics and

- evolutionary analyses in R. *Bioinformatics*, *35*(3), 526–528. <https://doi.org/10.1093/bioinformatics/bty633>
- Patwardhan, A., Amit, R., & Ray, S. (2014). Molecular Markers in Phylogenetic Studies—A Review. *Journal of Phylogenetics & Evolutionary Biology*, *02*(02), 1–9. <https://doi.org/10.4172/2329-9002.1000131>
- Penna, A., Casabianca, S., Guerra, A. F., Vernesi, C., & Scardi, M. (2017). Analysis of phytoplankton assemblage structure in the Mediterranean Sea based on high-throughput sequencing of partial 18S rRNA sequences. *Marine Genomics*, *36*, 49–55. <https://doi.org/10.1016/j.margen.2017.06.001>
- Penna, A., Casabianca, S., Perini, F., Bastianini, M., Riccardi, E., Pigozzi, S., & Scardi, M. (2013). Toxic *Pseudo-nitzschia* spp. in the northwestern Adriatic Sea: Characterization of species composition by genetic and molecular quantitative analyses. *Journal of Plankton Research*, *35*(2), 352–366. <https://doi.org/10.1093/plankt/fbs093>
- Perl, T. M., Bédard, L., Kosatsky, T., Hockin, J. C., Todd, E. C. D., & Remis, R. S. (1990). An Outbreak of Toxic Encephalopathy Caused by Eating Mussels Contaminated with Domoic Acid. *New England Journal of Medicine*, *322*(25), 1775–1780. <https://doi.org/10.1056/nejm199006213222504>
- Pielou, E. C. (1966). The measurement of diversity in different types of biological collections. *Journal of Theoretical Biology*, *13*(C), 131–144. [https://doi.org/10.1016/0022-5193\(66\)90013-0](https://doi.org/10.1016/0022-5193(66)90013-0)
- Piredda, R., Claverie, J. M., Decelle, J., de Vargas, C., Dunthorn, M., Edvardsen, B., Eikrem, W., Forster, D., Kooistra, W. H. C. F., Logares, R., Massana, R., Montresor, M., Not, F., Ogata, H., Pawlowski, J., Romac, S., Sarno, D., Stoeck, T., & Zingone, A. (2018). Diatom diversity through HTS-metabarcoding in coastal European seas. *Scientific Reports*, *8*(1), 1–12. <https://doi.org/10.1038/s41598-018-36345-9>
- Piredda, R., Tomasino, M. P., D’Erchia, A. M., Manzari, C., Pesole, G., Montresor, M., Kooistra, W. H. C. F., Sarno, D., & Zingone, A. (2017). Diversity and temporal patterns of planktonic protist assemblages at a Mediterranean Long Term Ecological Research site. *FEMS Microbiology Ecology*, *93*(1). <https://doi.org/10.1093/femsec/fiw200>
- Pistocchi, R., Guerrini, F., Pezzolesi, L., Riccardi, M., Vanucci, S., Ciminiello, P., Dell’Aversano, C., Forino, M., Fattorusso, E., Tartaglione, L., Milandri, A., Pompei, M., Cangini, M., Pigozzi, S., & Riccardi, E. (2012). Toxin levels and profiles in microalgae from the North-Western Adriatic Sea - 15 Years of studies on cultured species. In *Marine Drugs* (Vol. 10, Issue 1, pp. 140–162). Multidisciplinary Digital Publishing Institute (MDPI). <https://doi.org/10.3390/md10010140>
- Pitcher, G. C., Krock, B., & Cembella, A. D. (2011). Accumulation of diarrhetic shellfish poisoning toxins in the oyster *Crassostrea gigas* and the mussel *Choromytilus meridionalis* in the southern Benguela ecosystem. *African Journal of Marine Science*, *33*(2), 273–281. <https://doi.org/10.2989/1814232X.2011.600372>
- Pochon, X., Zaiko, A., Fletcher, L. M., Laroche, O., & Wood, S. A. (2017). Wanted dead or alive? Using metabarcoding of environmental DNA and RNA to distinguish living assemblages for biosecurity applications. *PLoS ONE*, *12*(11), e0187636.

- <https://doi.org/10.1371/journal.pone.0187636>
- Pocklington, R., Milley, J. E., Bates, S. S., Bird, C. J., De Freitas, A. S. W., & Quilliam, M. A. (1990). Trace Determination of Domoic Acid in Sea Water and Phytoplankton by High-Performance Liquid Chromatography of the Fluorenylmethoxycarbonyl (FMOC) Derivative. *International Journal of Environmental Analytical Chemistry*, *38*(3), 351–368. <https://doi.org/10.1080/03067319008026940>
- Posada, D. (2008). jModelTest: Phylogenetic Model Averaging. *Molecular Biology and Evolution*, *25*(7), 1253–1256. <https://doi.org/10.1093/molbev/msn083>
- Potapova, M., & Hamilton, P. B. (2007). Morphological and ecological variation within the *Achnantheidium minutissimum* (Bacillariophyceae) species complex. *Journal of Phycology*, *43*(3), 561–575. <https://doi.org/10.1111/j.1529-8817.2007.00332.x>
- Pulido, O. M. (2008). Domoic acid toxicologic pathology: a review. *Marine Drugs*, *6*(2), 180–219. <https://doi.org/10.3390/md20080010>
- Quijano-Scheggia, S., Garcés, E., Andree, K. B., de la Iglesia, P., Diogène, J., Fortuño, J. M., & Camp, J. (2010). Especies *Pseudo-nitzschia* en la costa Catalana: Caracterización y contribución al conocimiento actual de la distribución del género en el mar Mediterráneo. *Scientia Marina*, *74*(2), 395–410. <https://doi.org/10.3989/scimar.2010.74n2395>
- Quijano-Scheggia, S., Garcés, E., Flo, E., Fernandez-Tejedor, M., Diogène, J., & Camp, J. (2008). Bloom dynamics of the genus *Pseudo-nitzschia* (Bacillariophyceae) in two coastal bays (NW Mediterranean Sea). *Scientia Marina*, *72*(3), 577–590. <https://doi.org/10.3989/scimar.2008.72n3577>
- Quijano-Scheggia, S., Garcés, E., Sampedro, N., Van Lenning, K., Flo, E., Andree, K., Fortuño, J. M., & Camp, J. (2008). Identification and characterisation of the dominant *Pseudo-nitzschia* species (Bacillariophyceae) along the NE Spanish coast (Catalonia, NW Mediterranean). *Scientia Marina*, *72*(2), 343–359. <https://doi.org/10.3989/scimar.2008.72n2343>
- Quilliam, M. a. (2003). Chemical methods for domoic acid, the amnesic shellfish poisoning (ASP) toxin. *Manual on Harmful Marine Microalgae*, *11*(June 2003), 247–266.
- R Core Team. (2019). *R: A Language and Environment for Statistical Computing*. <https://www.r-project.org/>
- Ramsey, U. P., Douglas, D. J., Walter, J. A., & Wright, J. L. C. (1998). Biosynthesis of domoic acid by the diatom *Pseudo-nitzschia multiseries*. *Natural Toxins*, *6*(3–4), 137–146. [https://doi.org/10.1002/\(SICI\)1522-7189\(199805/08\)6:3/4<137::AID-NT28>3.0.CO;2-L](https://doi.org/10.1002/(SICI)1522-7189(199805/08)6:3/4<137::AID-NT28>3.0.CO;2-L)
- Rhodes, L. L., Adamson, J., & Scholin, C. A. (2000). *Pseudo-nitzschia multistriata* (Bacillariophyceae) in New Zealand. *New Zealand Journal of Marine and Freshwater Research*, *34*(3), 463–467. <https://doi.org/10.1080/00288330.2000.9516948>
- Ribera d'Alcalà, M., Conversano, F., Corato, F., Licandro, P., Mangoni, O., Marino, D., Mazzocchi, M. G., Modigh, M., Montresor, M., Nardella, M., Saggiomo, V., Sarno, D., & Zingone, A. (2004). Seasonal patterns in plankton communities in a pluriannual time series at a coastal Mediterranean site (Gulf of Naples): an attempt to discern recurrences and trends. *Scientia Marina*, *68*(S1), 65–83. <https://doi.org/10.3989/scimar.2004.68s165>

- Richlen, M. L., Erdner, D. L., McCauley, L. A. R., Liberal, K., & Anderson, D. M. (2012). Extensive genetic diversity and rapid population differentiation during blooms of *Alexandrium fundyense* (Dinophyceae) in an isolated salt pond on cape cod, MA, USA. *Ecology and Evolution*, *2*(10), 2588–2599. <https://doi.org/10.1002/ece3.373>
- Rimet, F., Chaumeil, P., Keck, F., Kermarrec, L., Vasselon, V., Kahlert, M., Franc, A., & Bouchez, A. (2016). R-Syst::diatom: An open-access and curated barcode database for diatoms and freshwater monitoring. *Database*, *2016*, baw016. <https://doi.org/10.1093/database/baw016>
- Ritzman, J., Brodbeck, A., Brostrom, S., McGrew, S., Dreyer, S., Klinger, T., & Moore, S. K. (2018). Economic and sociocultural impacts of fisheries closures in two fishing-dependent communities following the massive 2015 U.S. West Coast harmful algal bloom. *Harmful Algae*, *80*(May), 35–45. <https://doi.org/10.1016/j.hal.2018.09.002>
- Ronquist, F., Teslenko, M., van der Mark, P., Ayres, D. L., Darling, A., Höhna, S., Larget, B., Liu, L., Suchard, M. A., & Huelsenbeck, J. P. (2012). MrBayes 3.2: efficient Bayesian phylogenetic inference and model choice across a large model space. *Systematic Biology*, *61*(3), 539–542. <https://doi.org/10.1093/sysbio/sys029>
- Round, F. E., Crawford, R. M., & Mann, D. G. (1990). *The Diatoms : biology & morphology of the genera*. Cambridge University Press.
- Ruggiero, M. V., Sarno, D., Barra, L., Kooistra, W. H. C. F., Montresor, M., & Zingone, A. (2015). Diversity and temporal pattern of *Pseudo-nitzschia* species (Bacillariophyceae) through the molecular lens. *Harmful Algae*, *42*(1), 15–24. <https://doi.org/10.1016/j.hal.2014.12.001>
- Saeed, A. F. U. H., Ling, S., Yuan, J., & Wang, S. (2017). The Preparation and Identification of a Monoclonal Antibody against Domoic Acid and Establishment of Detection by Indirect Competitive ELISA. *Toxins*, *9*(8). <https://doi.org/10.3390/toxins9080250>
- Satake, M., Ofuji, K., Naoki, H., James, K. J., Furey, A., McMahon, T., Silke, J., & Yasumoto, T. (1998). Azaspiracid, a new marine toxin having unique spiro ring assemblies, isolated from irish mussels, *Mytilus edulis* [14]. In *Journal of the American Chemical Society* (Vol. 120, Issue 38, pp. 9967–9968). UTC. <https://doi.org/10.1021/ja981413r>
- Savage, T. J., Smith, G. J., Clark, A. T., & Saucedo, P. N. (2012). Condensation of the isoprenoid and amino precursors in the biosynthesis of domoic acid. *Toxicon*, *59*(1), 25–33. <https://doi.org/10.1016/J.TOXICON.2011.10.010>
- Schliep, K. P. (2011). phangorn: phylogenetic analysis in R. *Bioinformatics*, *27*(4), 592–593. <https://doi.org/10.1093/bioinformatics/btq706>
- Scholin, C. A., Buck, K. R., Britschgi, T., Cangelosi, G., & Chavez, F. P. (1996). Identification of *Pseudo-nitzschia australis* (Bacillariophyceae) using rRNA-targeted probes in whole cell and sandwich hybridization formats. *Phycologia*, *35*(3), 190–197. <https://doi.org/10.2216/i0031-8884-35-3-190.1>
- Scholin, C. A., Herzog, M., Sogin, M., & Anderson, D. M. (1994). Identification of group- and strain-specific genetic markers for globally distributed *Alexandrium* (Dinophyceae). *Journal of Phycology*, *30*(6), 999–1011. <https://doi.org/10.1111/j.0022-3646.1994.00999.x>

- Scholin, C. A., Marin, R., Miller, P. E., Doucette, G. J., Powell, C. L., Haydock, P., Howard, J., & Ray, J. (1999). DNA probes and a receptor-binding assay for detection of *Pseudo-nitzschia* (Bacillariophyceae) species and domoic acid activity in cultures and natural samples. *Journal of Phycology*, 35(6), 1356–1367. <https://doi.org/10.1046/j.1529-8817.1999.3561356.x>
- Scholin, C. A., Miller, P., Buck, K., Chavez, F., Harris, P., Haydock, P., Howard, J., & Cangelosi, G. (1997). Detection and quantification of *Pseudo-nitzschia australis* in cultured and natural populations using LSU rRNA-targeted probes. *Limnology and Oceanography*, 42(5), 1265–1272. [https://doi.org/10.4319/lo.1997.42.5\\_part\\_2.1265](https://doi.org/10.4319/lo.1997.42.5_part_2.1265)
- Selander, E., Kubanek, J., Hamberg, M., Andersson, M. X., Cervin, G., & Pavia, H. (2015). Predator lipids induce paralytic shellfish toxins in bloom-forming algae. *Proceedings of the National Academy of Sciences of the United States of America*, 112(20), 6395–6400. <https://doi.org/10.1073/pnas.1420154112>
- Shannon, C. E. (1948). A Mathematical Theory of Communication. *Bell System Technical Journal*, 27(3), 379–423. <https://doi.org/10.1002/j.1538-7305.1948.tb01338.x>
- Silver, M. W., Bargu, S., Coale, S. L., Benitez-Nelson, C. R., Garcia, A. C., Roberts, K. J., Sekula-Wood, E., Bruland, K. W., & Coale, K. H. (2010). Toxic diatoms and domoic acid in natural and iron enriched waters of the oceanic Pacific. *Proceedings of the National Academy of Sciences*, 107(48), 20762–20767. <https://doi.org/10.1073/pnas.1006968107>
- Smida, D. B., Lundholm, N., Kooistra, W. H. C. F., Sahraoui, I., Ruggiero, M. V., Kotaki, Y., Ellegaard, M., Lambert, C., Mabrouk, H. H., & Hlaili, A. S. (2014). Morphology and molecular phylogeny of *Nitzschia bizertensis* sp. nov.-A new domoic acid-producer. *Harmful Algae*, 32, 49–63. <https://doi.org/10.1016/j.hal.2013.12.004>
- Smith, E. A., Papapanagiotou, E. P., Brown, N. A., Stobo, L. A., Gallacher, S., & Shanks, A. M. (2006). Effect of storage on amnesic shellfish poisoning (ASP) toxins in king scallops (*Pecten maximus*). *Harmful Algae*, 5(1), 9–19. <https://doi.org/10.1016/j.hal.2005.02.002>
- Smith, M. W., Maier, M. A., Suciu, D., Peterson, T. D., Bradstreet, T., Nakayama, J., & Simon, H. M. (2012). High resolution microarray assay for rapid taxonomic assessment of *Pseudo-nitzschia* spp. (Bacillariophyceae) in the field. *Harmful Algae*, 19, 169–180. <https://doi.org/10.1016/j.hal.2012.07.003>
- Sournia, A., Chrétiennot-Dinet, M.-J., & Ricard, M. (1991). Marine phytoplankton: how many species in the world ocean? *Journal of Plankton Research*, 13(5), 1093–1099. <https://doi.org/10.1093/plankt/13.5.1093>
- Stefanni, S., Stanković, D., Borme, D., de Olazabal, A., Juretić, T., Pallavicini, A., & Tirelli, V. (2018). Multi-marker metabarcoding approach to study mesozooplankton at basin scale. *Scientific Reports*, 8(1), 1–13. <https://doi.org/10.1038/s41598-018-30157-7>
- Steidinger, K. A., & Garcés, E. (2006). Importance of Life Cycles in the Ecology of Harmful Microalgae. In *Ecology of Harmful Algae* (pp. 37–49). Springer Berlin Heidelberg. [https://doi.org/10.1007/978-3-540-32210-8\\_4](https://doi.org/10.1007/978-3-540-32210-8_4)
- Stern, R., Kraberg, A., Bresnan, E., Kooistra, W. H. C. F., Lovejoy, C., Montresor, M., Morán, X. A. G., Not, F., Salas, R., Siano, R., Vulot, D., Amaral-Zettler, L., Zingone,

- A., & Metfies, K. (2018). Molecular analyses of protists in long-term observation programmes - Current status and future perspectives. *Journal of Plankton Research*, *40*(5), 519–536. <https://doi.org/10.1093/plankt/fby035>
- Stern, R., Moore, S. K., Trainer, V. L., Bill, B. D., Fischer, A., & Batten, S. (2018). Spatial and temporal patterns of *Pseudo-nitzschia* genetic diversity in the North Pacific Ocean from the Continuous Plankton Recorder survey. *Marine Ecology Progress Series*, *606*, 7–28. <https://doi.org/10.3354/meps12711>
- Sterner, R. W., & Elser, J. J. (2002). *Ecological Stoichiometry*. Princeton University Press. <https://doi.org/10.2307/j.ctt1jktrp3>
- Stivala, C. E., Benoit, E., Aráoz, R., Servent, D., Novikov, A., Molgó, J., & Zakarian, A. (2015). Synthesis and biology of cyclic imine toxins, an emerging class of potent, globally distributed marine toxins. In *Natural Product Reports* (Vol. 32, Issue 3, pp. 411–435). Royal Society of Chemistry. <https://doi.org/10.1039/c4np00089g>
- Sunda, W. G. (2006). Trace Metals and Harmful Algal Blooms. In *Ecology of Harmful Algae* (pp. 203–214). Springer Berlin Heidelberg. [https://doi.org/10.1007/978-3-540-32210-8\\_16](https://doi.org/10.1007/978-3-540-32210-8_16)
- Takemoto, T., Daigo, K., Kondo, Y., & Kondo, K. (1966). Studies on the Constituents of *Chondria armata*. VIII.: On the Structure of Domoic Acid. (1). *YAKUGAKU ZASSHI*, *86*(10), 874–877. [https://doi.org/10.1248/yakushi1947.86.10\\_874](https://doi.org/10.1248/yakushi1947.86.10_874)
- Talaber, I., Francé, J., Flander-Putrlle, V., & Mozetič, P. (2018). Primary production and community structure of coastal phytoplankton in the Adriatic Sea: Insights on taxon-specific productivity. *Marine Ecology Progress Series*, *604*, 65–81. <https://doi.org/10.3354/meps12721>
- Talaber, I., Francé, J., & Mozetič, P. (2014). How phytoplankton physiology and community structure adjust to physical forcing in a coastal ecosystem (northern Adriatic Sea). *Phycologia*, *53*(1), 74–85. <https://doi.org/10.2216/13-196.1>
- Tan, S. N., Teng, S. T., Lim, H. C., Kotaki, Y., Bates, S. S., Leaw, C. P., & Lim, P. T. (2016). Diatom *Nitzschia navis-varingica* (Bacillariophyceae) and its domoic acid production from the mangrove environments of Malaysia. *Harmful Algae*, *60*, 139–149. <https://doi.org/10.1016/j.hal.2016.11.003>
- Tavare, S. (1986). *Some probabilistic and statistical problems in the analysis of DNA sequences* (F. A. O. of the UN (ed.)).
- Templeton, A. R., Crandall, K. A., & Sing, C. F. (1992). A cladistic analysis of phenotypic associations with haplotypes inferred from restriction endonuclease mapping and DNA sequence data. III. Cladogram estimation. *Genetics*, *132*(2), 619–633. <http://www.ncbi.nlm.nih.gov/pubmed/1385266>
- Teng, S. T., Leaw, C. P., Lim, H. C., & Lim, P. T. (2013). The genus *Pseudo-nitzschia* (Bacillariophyceae) in Malaysia, including new records and a key to species inferred from morphology-based phylogeny. *Botanica Marina*, *56*(4), 375–398. <https://doi.org/10.1515/bot-2012-0194>
- Tesson, S. V. M., Legrand, C., van Oosterhout, C., Montresor, M., Kooistra, W. H. C. F., & Procaccini, G. (2013). Mendelian Inheritance Pattern and High Mutation Rates of Microsatellite Alleles in the Diatom *Pseudo-nitzschia multistriata*. *Protist*, *164*(1), 89–100. <https://doi.org/10.1016/J.PROTIS.2012.07.001>

- Tesson, S. V. M., Montresor, M., Procaccini, G., & Kooistra, W. H. C. F. (2014). Temporal changes in population structure of a marine planktonic diatom. *PLoS ONE*, *9*(12), 1–23. <https://doi.org/10.1371/journal.pone.0114984>
- Thorel, M., Claquin, P., Schapira, M., Le Gendre, R., Riou, P., Goux, D., Le Roy, B., Raimbault, V., Deton-Cabanillas, A.-F., Bazin, P., Kientz-Bouchart, V., & Fauchot, J. (2017). Nutrient ratios influence variability in *Pseudo-nitzschia* species diversity and particulate domoic acid production in the Bay of Seine (France). *Harmful Algae*, *68*, 192–205. <https://doi.org/10.1016/j.hal.2017.07.005>
- Tillmann, U., & John, U. (2002). Toxic effects of *Alexandrium* spp. on heterotrophic dinoflagellates: An allelochemical defence mechanism independent of PSP-toxin content. *Marine Ecology Progress Series*, *230*(May 2014), 47–58. <https://doi.org/10.3354/meps230047>
- Totti, C., Romagnoli, T., Accoroni, S., Coluccelli, A., Pellegrini, M., Campanelli, A., Grilli, F., & Marini, M. (2019). Phytoplankton communities in the northwestern Adriatic Sea: Interdecadal variability over a 30-years period (1988–2016) and relationships with meteorological drivers. *Journal of Marine Systems*, *193*, 137–153. <https://doi.org/10.1016/J.JMARSYS.2019.01.007>
- Tragin, M., Zingone, A., & Vaultot, D. (2018). Comparison of coastal phytoplankton composition estimated from the V4 and V9 regions of the 18S rRNA gene with a focus on photosynthetic groups and especially Chlorophyta. *Environmental Microbiology*, *20*(2), 506–520. <https://doi.org/10.1111/1462-2920.13952>
- Trainer, V. L., Bates, S. S., Lundholm, N., Thessen, A. E., Cochlan, W. P., Adams, N. G., & Trick, C. G. (2012). *Pseudo-nitzschia* physiological ecology, phylogeny, toxicity, monitoring and impacts on ecosystem health. *Harmful Algae*, *14*(February 2012), 271–300. <https://doi.org/10.1016/j.hal.2011.10.025>
- Trainer, V. L., Hickey, B. M., & Horner, R. A. (2002). Biological and physical dynamics of domoic acid production off the Washington coast. *Limnology and Oceanography*, *47*(5), 1438–1446. <https://doi.org/10.4319/lo.2002.47.5.1438>
- Turk Dermastia, T., Cerino, F., Stanković, D., Francé, J., Ramšak, A., Žnidarič Tušek, M., Beran, A., Natali, V., Cabrini, M., & Mozetič, P. (2020). Ecological time series and integrative taxonomy unveil seasonality and diversity of the toxic diatom *Pseudo-nitzschia* H. Peragallo in the northern Adriatic Sea. *Harmful Algae*, *93*, 101773. <https://doi.org/10.1016/j.hal.2020.101773>
- Ujević, I., Ninčević-Gladan, Ž., Roje, R., Skejić, S., Arapov, J., & Marasović, I. (2010). Domoic Acid - A New Toxin in the Croatian Adriatic Shellfish Toxin Profile. *Molecules*, *15*(10), 6835–6849. <https://doi.org/10.3390/molecules15106835>
- Utermöhl, H. (1958). Zur Vervollkommnung der quantitativen Phytoplankton-Methodik. *SIL Communications*, *1953-1996*, *9*(1), 1–38. <https://doi.org/10.1080/05384680.1958.11904091>
- Vasselon, V., Domaizon, I., Rimet, F., Kahlert, M., & Bouchez, A. (2017). Application of high-throughput sequencing (HTS) metabarcoding to diatom biomonitoring: Do DNA extraction methods matter? *Freshwater Science*, *36*(1), 162–177. <https://doi.org/10.1086/690649>
- Vasselon, V., Rimet, F., Tapolczai, K., & Bouchez, A. (2017). Assessing ecological status

- with diatoms DNA metabarcoding: Scaling-up on a WFD monitoring network (Mayotte island, France). *Ecological Indicators*, 82(March), 1–12. <https://doi.org/10.1016/j.ecolind.2017.06.024>
- Viličić, D., Djakovac, T., Burić, Z., & Bosak, S. (2009). Composition and annual cycle of phytoplankton assemblages in the northeastern Adriatic Sea. In *Botanica Marina* (Vol. 52, Issue 4, pp. 291–305). <https://doi.org/10.1515/BOT.2009.004>
- Walter, J. A., Falk, M., Wright, J. L., & Wright, Y. L. (1994). Chemistry of the shellfish toxin domoic acid: characterization of related compounds1. *Can. J. Chem*, 72(430). <http://www.nrcresearchpress.com/doi/pdfplus/10.1139/v94-064>
- Wang, Q., Garrity, G. M., Tiedje, J. M., & Cole, J. R. (2007). Naïve Bayesian classifier for rapid assignment of rRNA sequences into the new bacterial taxonomy. *Applied and Environmental Microbiology*, 73(16), 5261–5267. <https://doi.org/10.1128/AEM.00062-07>
- Wang, Z., Maucher-Fuquay, J., Fire, S. E., Mikulski, C. M., Haynes, B., Doucette, G. J., & Ramsdell, J. S. (2012). Optimization of solid-phase extraction and liquid chromatography-tandem mass spectrometry for the determination of domoic acid in seawater, phytoplankton, and mammalian fluids and tissues. *Analytica Chimica Acta*, 715, 71–79. <https://doi.org/10.1016/j.aca.2011.12.013>
- WDFW. (2021). *Razor clam seasons and beaches*. <https://wdfw.wa.gov/fishing/shellfishing-regulations/razor-clams>
- Weigand, H., Beermann, A. J., Čiampor, F., Costa, F. O., Csabai, Z., Duarte, S., Geiger, M. F., Grabowski, M., Rimet, F., Rulik, B., Strand, M., Szucsich, N., Weigand, A. M., Willassen, E., Wyler, S. A., Bouchez, A., Borja, A., Čiamporová-Zatovičová, Z., Ferreira, S., ... Ekrem, T. (2019). DNA barcode reference libraries for the monitoring of aquatic biota in Europe: Gap-analysis and recommendations for future work. In *Science of the Total Environment* (Vol. 678, pp. 499–524). Elsevier B.V. <https://doi.org/10.1016/j.scitotenv.2019.04.247>
- White, T., Bruns, T., Lee, S., & Taylor, J. (1990). Amplification and direct sequencing of fungal ribosomal RNA genes for phylogenetics. In M. Innis, D. Gelfand, J. Shinsky, & T. White (Eds.), *PCR Protocols: A Guide to Methods and Applications* (pp. 315–322). Academic Press. citeulike-article-id:671166
- Wolfe, K. H., Li, W. H., & Sharp, P. M. (1987). Rates of nucleotide substitution vary greatly among plant mitochondrial, chloroplast, and nuclear DNAs. *Proceedings of the National Academy of Sciences of the United States of America*, 84(24), 9054–9058. <https://doi.org/10.1073/pnas.84.24.9054>
- Wood, S. A., Biessy, L., Latchford, J. L., Zaiko, A., von Ammon, U., Audrezet, F., Cristescu, M. E., & Pochon, X. (2020). Release and degradation of environmental DNA and RNA in a marine system. *Science of the Total Environment*, 704(June 2020), 135314. <https://doi.org/10.1016/j.scitotenv.2019.135314>
- Zetsche, E. M., & Meysman, F. J. R. (2012). Dead or alive? Viability assessment of micro- and mesoplankton. *Journal of Plankton Research*, 34(6), 493–509. <https://doi.org/10.1093/plankt/fbs018>
- Zhang, S., Zheng, T., Lundholm, N., Huang, X., Jiang, X., Li, A., & Li, Y. (2021). Chemical and morphological defenses of *Pseudo-nitzschia multiseriis* in response to zooplankton

- grazing. *Harmful Algae*, 104, 102033. <https://doi.org/10.1016/j.hal.2021.102033>
- Zingone, A., Licandro, P., & Sarno, D. (2003). Revising paradigms and myths of phytoplankton ecology using biological time series. *Mediterranean Biological Time Series. CIESM Workshop Monographs*, 22, 109–114.
- Zingone, A., Escalera, L., Aligizaki, K., Fernández-Tejedor, M., Ismael, A., Montresor, M., Mozetič, P., Taş, S., & Totti, C. (2021). Toxic marine microalgae and noxious blooms in the Mediterranean Sea: A contribution to the Global HAB Status Report. *Harmful Algae*, 102(August), 101843. <https://doi.org/10.1016/j.hal.2020.101843>



# Bibliography

## Journal Articles Related to the Thesis

Turk Dermastia, T., Cerino, F., Stanković, D., Francé, J., Ramšak, A., Žnidarič Tušek, M., Beran, A., Natali, V., Cabrini, M., & Mozetič, P. (2020). Ecological time series and integrative taxonomy unveil seasonality and diversity of the toxic diatom *Pseudo-nitzschia* H. Peragallo in the northern Adriatic Sea. *Harmful Algae*, *93*, 101773. <https://doi.org/10.1016/j.hal.2020.101773>

## Conference Proceedings Related to the Thesis

Ph. Hess [Ed]. 2020. Harmful Algae 2018 – from ecosystems to socioecosystems. *Proceedings of the 18th Intl. Conf. on Harmful Algae. Nantes. International Society for the Study of Harmful Algae.* pp 72-75. ISBN: 978-87-990827-7-3. Diversity of *Pseudo-nitzschia* H. Pergallo, 1900 along the Slovenian coast, Adriatic Sea, with insights into seasonality, toxicity and potential introductions. Available from: <https://archimer.ifremer.fr/doc/00651/76285/>

## Book of Abstracts Related to the Thesis

Turk Dermastia, T., Stanković, D., Francé, J., Tušek-Žnidarič, M., Ramšak, A., Mozetič, P. (2018). Diversity and seasonal distribution of *Pseudo-nitzschia* from the Gulf of Trieste with insights in toxicity and potential introductions. In: Abstract book : from ecosystems to socio-ecosystems. *18th international conference on harmful algae*, 21-26 October 2018, Nantes, France. pp. 51. [https://www.icha2018.com/medias/content/files/ICHA\\_2018\\_Abstract\\_Book\\_v7.pdf](https://www.icha2018.com/medias/content/files/ICHA_2018_Abstract_Book_v7.pdf).

Turk Dermastia, T., Mozetič, P., Močnik, A., & Dolenc, J. (2019). First report of domoic acid in *Pseudo-nitzschia multistriata* and *Pseudo-nitzschia delicatissima* strains isolated in the Gulf of Trieste, Adriatic Sea. *European Journal of Phycology*, *54*(sup1), 1–27. <https://doi.org/10.1080/09670262.2019.1626610>

Turk Dermastia, T., Villa, E., Francé, J., Gauillebault, D., Mozetič, P. (2019). Development and validation of a sandwich hybridization-based biosensor for toxic marine diatoms from the *Pseudo-nitzschia* genus. In: Topole, M. (Ed.), et al. Book of Abstracts : Science of the future how to stay up-to-date with your research! *11th*

*Jožef Stefan International Postgraduate School Students' Conference and 13th Young Researchers' Day*, 15th and 16th May 2019, Planica, Slovenia. Ljubljana: Jožef Stefan International Postgraduate School 2019.  
pp. 24. <http://ipssc.mps.si/Proceedings/Proceedings2019.pdf>.

## **Book Chapters Related to the Thesis**

Turk Dermastia, Timotej. Pregled metod za določanje glavnih fiktotoksinov v morskih organizmih in proizvodih. In: Turk, Tom (Ed.), et al. *Dinoflagelati, diatomeje, njihovi toksini in zastrupitve z morskno hrano*. Ljubljana: Nacionalni inštitut za biologijo, 2018. Str. 131-144. Vse živo, zv. 5. ISBN 978-961-93486-9-7.

## **Expert Articles Related to the Thesis**

Turk Dermastia, T.. Z genetiko do popolnejšega vedenja o ekologiji morja. *Alternator : misliti znanost*. 25. 6. 2020, [1] str., ilustr. ISSN 2712-3510.  
<https://doi.org/10.3986/alternator.2020.30>

# Biography

The author of this thesis Timotej Turk Dermastia was born on 23 November 1992. Upon finishing elementary (OŠ Riharda Jakopiča) and high schools (Gimnazija Poljane) with dignity in Slovenia he enrolled to the undergraduate course of biology at the University of Ljubljana. During his studies, he joined the Australian-European Network exchange program and spent half a year in Perth, Australia, at Edith Cowan University. When he returned, he started to intern at the Marine Biology Station (MBS) of the National Institute of Biology for one year, while collaborating with Biosistemika on the development of qPCR probes for the detection of fish in fisheries products. This sparked his interest in marine science and the application to the Master's programme Ecosystem-based Management of Marine Systems at the University of St Andrews, Scotland UK, where his application was successfully received. Immediately after obtaining his MSc working on a project on population genetics of New Caledonian humpback whales, he applied and secured the position as a PhD student at MBS in Piran and enrolled to the Jožef Stefan International Postgraduate School. His PhD job was to determine the local diversity and ecology of toxic algae, particularly the harmful diatoms from the genus *Pseudo-nitzschia*. During his doctoral studies he attended two workshops dealing with analysis of metagenomic data, namely the hackathon EMOSE (2017) – Inter-Comparison of Marine Plankton Metagenomic Analysis Methods in Porto, and the International Course in Microbial Ecology: Hands-on training in Prokaryotic and Eukaryotic metagenomics (ICME10). He was the Vice-Chair of the Euromarine Network Young Scientists Working Group and a member of the Student Council of the Jožef Stefan International Postgraduate School with which he organized annual conferences for students to share their work, meet colleagues and listen to renowned Slovenian researchers. During his PhD work he attended several international conferences and workshops including the 52th European Marine Biology Symposium, the 18th international conference on harmful algae (ICHA2018) and the 7th European Phycological Congress. He has spent two months of his research work in Banyuls-sur-Mer, France, where he collaborated with a spinoff specializing in environmental monitoring for harmful phytoplankton. Therefore, he has also gained experience on the business side of work.

His time away from strict science includes being a vocal science communicator, through many channels, including videos, theatre, and newspaper articles. This is a way for him to express his inherent creative potential. This has led him to the Prometej Award for Science Communication awarded by the Slovenian Science Foundation, as well as the best Science Slam award awarded by Znanost na Cesti. Apart from science communication, his creativity is also channeled through active participation in improvisation theatre, where he is a long-time member of the Gverila Teater theater group.